

DI<sup>in</sup> Helene Hopper

## Identification of odour-active compounds in polyolefins

DISSERTATION

zur Erlangung des akademischen Grades einer Doktorin der technischen  
Wissenschaften

erreicht an der

Technischen Universität Graz



Diese Arbeit wurde am Institut für Analytische Chemie und Lebensmittelchemie in der Arbeitsgruppe "Lebensmittelchemie und Humansensorik" unter der Betreuung von ao.Univ.-Prof. DI Dr.techn. Erich Leitner durchgeführt. März 2010

*Equipped with the five senses, (wo)man explores the universe around her/him and calls the  
adventure Science.* Edwin Powell Hubble

## **Statutory Declaration**

I declare that I have authored this thesis independently, that I have not used other than the declared sources / resources, and that I have explicitly marked all material which has been quoted either literally or by content from the used sources.

.....

date

.....

(signature)

## Table of Contents

<b>1.</b>	<b>INTRODUCTION .....</b>	<b>1</b>
1.1.	AIMS AND TARGETS .....	3
<b>2.</b>	<b>BACKGROUND AND BASICS .....</b>	<b>4</b>
2.1.	ODOUR AND ODOUR PERCEPTION .....	4
2.2.	ODOUR ANALYSIS.....	5
2.3.	POLYOLEFINS (PROCESS CHAIN) .....	7
2.4.	DEGRADATION AND OXIDATION OF POLYOLEFINS.....	14
2.4.a.	<i>Degradation mechanisms of PE<sup>17</sup></i> .....	14
2.4.b.	<i>Degradation mechanisms of PP<sup>17</sup></i> .....	17
2.5.	ODOUR-ACTIVE COMPOUNDS IDENTIFIED IN POLYOLEFINS.....	20
2.5.a.	<i>Identification of odour-active compounds in polyolefins with Retention Indices (RI)</i> .....	26
<b>3.</b>	<b>MATERIALS AND METHODS.....</b>	<b>29</b>
3.1.	POLYOLEFIN SAMPLES .....	29
3.2.	SAMPLE PREPARATION TECHNIQUES .....	40
3.2.a.	<i>Simultaneous Distillation/Extraction (SDE)</i> .....	40
3.2.b.	<i>Solid Phase Extraction (SPE)</i> .....	41
3.2.c.	<i>Solid Phase Microextraction (SPME)</i> .....	43
3.2.d.	<i>Derivatization</i> .....	44
3.3.	GAS CHROMATOGRAPHY (GC) .....	48
3.3.a.	<i>GC-MS of pellets and plaques with SPME</i> .....	49
3.3.b.	<i>GC-MS of fractioned extracts</i> .....	51
3.3.c.	<i>GC-MS measurements of derivatised samples</i> .....	52
3.3.d.	<i>GC-FID-Olfactometry and GC-NPD-Olfactometry (GC-O)</i> .....	54
3.3.e.	<i>Comprehensive Gas Chromatography with time of flight mass spectrometry (GCxGC-TOF-MS) measurements at LECO</i> .....	55
3.3.f.	<i>Quantification of 2-acetyl-1-pyrroline in a PP sample by a standard addition procedure using HS-SPME-GC-NPD</i> .....	56
3.4.	OTHERS .....	58
3.4.a.	<i>Fourier-Transform Infrared Spectroscopy (FTIR)</i> .....	58
3.4.b.	<i>Near Infrared Spectroscopy (NIR) with multivariate calibration</i> .....	59
3.5.	MULTIVARIATE DATA ANALYSIS (MVDA) .....	59
3.5.a.	<i>MasStat©</i> .....	60
3.5.b.	<i>The Unscrambler©</i> .....	61

3.6.	SENSORY EVALUATION .....	61
3.6.a.	<i>Best Estimate Threshold (BET) determination</i> .....	61
3.6.b.	<i>Detection Frequency (SNIF)<sup>64</sup> x Aroma Extract Dilution Analysis (AEDA)</i> .....	64
<b>4.</b>	<b>RESULTS AND DISCUSSION .....</b>	<b>66</b>
4.1.	ANALYSIS METHOD PARAMETERS .....	66
4.1.a.	<i>Recovery for the sample preparation</i> .....	66
4.1.b.	<i>Need and Quality of the fractionation process</i> .....	66
4.2.	COMPARATIVE STUDY – INFLUENCE OF COMPOUNDING CONDITIONS AND INJECTION MOULDING MASS TEMPERATURES (T <sub>M</sub> ).....	68
4.3.	REFERENCE MATERIALS .....	71
4.3.a.	<i>Results of the MVDA of the Detection Frequency results.</i> .....	73
4.3.b.	<i>Results of BF970MO samples using GC-O with Detection Frequency</i> .....	74
4.3.c.	<i>Results of EE188AI samples(EE188AI-9530 from Schwechat and EE188AI-9524 from Beringen) and their base polymers using GC-O with Detection Frequency</i> .....	79
4.3.d.	<i>Results of the FB2230 samples from Schwechat PE4 and Porvoo PE2 using GC-O with Detection Frequency</i> .....	94
4.3.e.	<i>Results of ME3440 samples from Porvoo, Stenungsund and Borouge using GC-O with Detection Frequency</i> .....	100
4.4.	THE INTERACTION OF PHENOLIC ANTIOXIDANTS AND TALC AND THEIR INFLUENCE ON THE GENERATION OF ODOUR- ACTIVE COMPOUNDS .....	107
4.5.	THE INFLUENCE OF ADDITIVES ON THE GENERATION OF ODOUR-ACTIVE COMPOUNDS .....	109
4.6.	ODOUR POTENTIAL OF 2-ETHYL-1-HEXANOL .....	115
4.7.	THE INFLUENCE OF VIS-BREAKING REAGENTS (PEROXIDES) ON THE GENERATION OF ODOUR-ACTIVE COMPOUNDS 117	
4.8.	AUTOXIDATION OF PE AND PP .....	121
4.8.a.	<i>Results of the PP (HD120MO) samples</i> .....	122
4.8.b.	<i>Results of PE (ME3440) samples</i> .....	129
4.9.	QC METHOD (HS-SPME-GC-PID) .....	136
4.10.	SENSORY THRESHOLD DETERMINATION APPLYING THE BET PROCEDURE .....	138
4.11.	THE INFLUENCE OF COLOUR MASTERBATCHES (CMB) ON THE GENERATION OF ODOUR-ACTIVE COMPOUNDS...140	
4.12.	EVALUATION OF THE ODOUR POTENTIAL OF MONOMERS.....	147
4.13.	2-ACETYL-1-PYRROLINE IN POLYOLEFINS .....	152
4.14.	BJ368MO CLAIM .....	154
4.14.a.	<i>Results of HS-SPME-GC-MS measurements</i> .....	154
4.14.b.	<i>Results of the HS-SPME-GC-O measurements</i> .....	156

4.15.	THE INFLUENCE OF THE CATALYST TYPE - METALLOCENE-PP (M-PP) COMPARED TO CONVENTIONAL ZIEGLER-NATTA-PP (ZN-PP) .....	158
<b>5.</b>	<b>CONCLUSION AND OUTLOOK .....</b>	<b>161</b>
5.1.	IDENTIFIED ODOUR-ACTIVE COMPOUNDS DETECTED IN PE AND PP SAMPLES .....	161
5.2.	THE INFLUENCE OF PROCESSING ON THE GENERATION OF ODOUR-ACTIVE COMPOUNDS – IS AN ODOUR EVALUATION ON PELLETS VALID FOR THE JUDGEMENT OF PROCESSED PARTS?.....	161
5.3.	THE INFLUENCE OF PROCESSING LOCATIONS ON THE GENERATION OF ODOUR-ACTIVE COMPOUNDS – IS THERE A TYPICAL PLANT SMELL? .....	162
5.4.	THE INFLUENCE OF ADDITIVES ON THE GENERATION OF ODOUR-ACTIVE COMPOUNDS – WHAT DO TALC, UV STABILIZATION AND COLOUR CONTRIBUTE TO THE ODOUR? .....	163
5.5.	THE INFLUENCE OF THE CATALYST ON THE GENERATION OF ODOUR-ACTIVE COMPOUNDS – WHAT DOES 2-ETHYL-1-HEXANOL CONTRIBUTE TO THE ODOUR? .....	163
5.6.	THE INFLUENCE OF VISBREAKING ON THE GENERATION OF ODOUR-ACTIVE COMPOUNDS – DO PEROXIDES ALWAYS SMELL BAD? 164	
5.7.	THE CRUX WITH MEASURING “NOTHING” – HOW WELL DO DIFFERENT METHODS MEASURE THE THINGS WE WANT TO KNOW? 164	
	<b>REFERENCES .....</b>	<b>IV</b>
	<b>APPENDIX .....</b>	<b>X</b>
	<b>PUBLICATIONS DURING PHD.....</b>	<b>XII</b>
	<b>CURRICULUM VITAE .....</b>	<b>XIV</b>

## List of Figures

Figure 1.	Human odour perception takes place in the olfactory bulb. _____	4
Figure 2.	Schematic Gas Chromatography-Olfactometry (GC-O) instrument. _____	6
Figure 3.	Molecular structure of metallocene catalysts used for PE and PP polymerization (taken from ). The zirconium atom is bound to two chlorines and to a bridged alkyl group which forms a cleft where the $ZrCl_2$ complex is situated and where the polymerization occurs. _____	9
Figure 4.	PP structures resulting from (1) head-to-tail, (2) tail-to-tail and (3) head-to-head reactions (taken from ). _____	9
Figure 5.	Configurational structures in PP (taken from <sup>10</sup> ). _____	10
Figure 6.	HS-SPME-GC-MS chromatograms of mixtures of BHT and talc heated at 200 °C for 1, 5, 10 and 20 min showing the subsequent degradation of the di-tert.-butylphenol (DTBP) to the mono- tert.-butylphenol (MTBP) and the phenol and the formation of 2-methyl-1-propene (2-MP) as predicted by C. Sauer <sup>14</sup> shown in Scheme 1 (taken from <sup>14</sup> ). _____	11
Figure 7.	Kinetics of the main processes in polyolefin degradation. (a) absorption of $O_2$ , formation of end products; (b) intermediates, mass change; (c) molecular mass <sup>17</sup> . _____	14
Figure 8.	SDE apparatus according to. <sup>38</sup> _____	40
Figure 9.	SPME device, annotation see text (adapted from <sup>44</sup> ). _____	43
Figure 10.	Total ion chromatogram (TIC) of a PP fraction I (top) and fraction II (bottom) with marked homologous series of n-alkanes and n-alkanals. _____	67
Figure 11.	MasStat© cluster obtained from fraction I and fraction II data of WG140AI and L140WG samples (pellets and injection moulded plaques moulded at $T_M$ 200 °C, 230 °C and 260 °C). _____	67
Figure 12.	MasStat© Cluster of pellets and injection moulded plaques at three mass temperatures (200 °C, 230 °C, 260 °C); Labels: “L” ... L140WG pellets; “W” ... WG140AI-05 pellets; “200L, 230L, 260L” ... plaques from L140WG compounded at 200°C, 230°C and 260°C; “200W, 230W, 260W” ... plaques from WG140AI-05 compounded at 200 °C, 230 °C and 260 °C). _____	70
Figure 13.	MasStat© Cluster of pellets and injection moulded plaques at three $T_M$ (200 °C, 230 °C, 260 °C) with a differentiation in pellets and plaques. _____	71
Figure 14.	MasStat© cluster from fraction II data of all the samples (pellets and plaques at three $T_M$ from L140WG-06 (L140), WG140AI-05 (WG140) and WG140AI-06 (WG140-06)). _____	71
Figure 15.	MVDA of representative detection frequency results (G ... pellets, P ... plaques). _____	74
Figure 16.	Detection Frequency (SNIF) Diagram of the extract obtained from BF907MO pellets. _____	76
Figure 17.	Detection Frequency (SNIF) Diagram of the 1:100 diluted extract obtained from BF907MO pellets. _____	76
Figure 18.	Detection Frequency (SNIF) Diagram of the extract obtained from BF907MO plaques. _____	77
Figure 19.	Detection Frequency (SNIF) Diagram of 1:100 diluted extract of BF907MO plaques. _____	77

Figure 20.	Detection Frequency (SNIF) Diagram of extract obtained from EE188AI-9530 (Schwechat) pellets. _____	82
Figure 21.	Detection Frequency (SNIF) Diagram of 1:100 diluted extract obtained from EE188AI (Schwechat) pellets. _____	83
Figure 22.	Detection Frequency (SNIF) Diagram of extract obtained from EE188AI (Schwechat) plaques. _____	83
Figure 23.	Detection Frequency (SNIF) Diagram of 1:100 diluted (in green) and 1:1000 diluted (in red) extract obtained from EE188AI (Schwechat) plaques. _____	84
Figure 24.	Detection Frequency (SNIF) Diagram of extract obtained from EE188AI (Beringen) pellets. _____	84
Figure 25.	Detection Frequency (SNIF) Diagram of 1:100 diluted extract obtained from EE188AI (Beringen) pellets. _____	85
Figure 26.	Detection Frequency (SNIF) Diagram of extract obtained from EE188AI (Beringen) plaques. _____	85
Figure 27.	Detection Frequency (SNIF) Diagram of 1:100 diluted (in green) and 1:1000 diluted (in red) extract obtained from EE188AI (Beringen) plaques. _____	86
Figure 28.	SNIF diagram comparison of the EE188AI pellets from Schwechat (on top in green) and Beringen (at the bottom in blue). _____	86
Figure 29.	Detection Frequency (SNIF) Diagram of extract obtained from BS2581 pellets. _____	87
Figure 30.	Detection Frequency (SNIF) diagram of extract obtained from BS2581 plaques. _____	87
Figure 31.	Detection Frequency (SNIF) diagram of extract obtained from BE677AI pellets. _____	88
Figure 32.	Detection Frequency (SNIF) diagram of extract obtained from BE677AI plaques. _____	88
Figure 33.	Detection Frequency (SNIF) diagram of extract obtained from EF015AE pellets. _____	89
Figure 34.	Detection Frequency (SNIF) diagram of extract obtained from EF015AE plaques. _____	89
Figure 35.	Detection Frequency (SNIF) diagram of the extract obtained from FB2230 (Schwechat) pellets. _____	95
Figure 36.	Detection Frequency (SNIF) diagram of the 1:100 diluted extract obtained from FB2230 (Schwechat) pellets. _____	95
Figure 37.	Detection Frequency (SNIF) diagram of the extract obtained from FB2230 (Schwechat) plaques. _____	96
Figure 38.	Detection Frequency (SNIF) diagram of the 1:100 diluted extract obtained from FB2230 (Schwechat) plaques. _____	96
Figure 39.	Detection Frequency (SNIF) diagram of the extract obtained from FB2230 (Porvoo) pellets. _____	97
Figure 40.	Detection Frequency (SNIF) diagram of the 1:100 diluted extract obtained from FB2230 (Porvoo) pellets. _____	97
Figure 41.	Detection Frequency (SNIF) diagram comparison of the FB2230 pellets from Schwechat (on top in green) and Porvoo (at the bottom in blue). _____	98
Figure 42.	MasStat© Cluster Analysis using the HS-SPME-GC-MS data from the three ME3440 samples from Provoo, Stenungsund and Borouge (Note: y-axis scale is 1/10 of x-axis!! (0.05 vs. 0.5). _____	101



Figure 43.	HS-SPME-GC-MS chromatograms for the ME3440 samples with marked compounds which are responsible for the differentiation in the MasStat© cluster. _____	101
Figure 44.	Detection Frequency (SNIF) diagram of the extract obtained from ME3440 (Porvoo) pellets. _____	102
Figure 45.	Detection Frequency (SNIF) diagram of the 1:10 diluted extract obtained from ME3440 (Porvoo) pellets. _____	102
Figure 46.	Detection Frequency (SNIF) diagram of the extract obtained from ME3440 (Stenungsund) pellets. _____	103
Figure 47.	Detection Frequency (SNIF) diagram of the 1:10 diluted extract obtained from ME3440 (Stenungsund) pellets. _____	103
Figure 48.	Detection Frequency (SNIF) diagram of the extract obtained from ME3440 (Borouge) pellets. _____	104
Figure 49.	Detection Frequency (SNIF) diagram of the 1:10 diluted extract obtained from ME3440 (Borouge) pellets. _____	104
Figure 50.	Detection Frequency (SNIF) diagram comparison of the ME3440 pellets from Porvoo (at the bottom in blue), Stenungsund (in the middle in blue) and Borouge (on top in red). _____	105
Figure 51.	GC-FID chromatogram (in blue) with overlaid O-signal (in red) indicating the high odour activity of the unknown compound in MB471WG-9014 extract between 11.5 – 12.7min retention time. _____	109
Figure 52.	GC-MS chromatogram of the MB471WG-9014 sample extract with the labelled tert.-butylphenols (6 and 7) and the area of interest (red circle) analyzed on the non-polar HP-5 column. _____	109
Figure 53.	MasStat© Cluster from HS-SPME-GC-MS data analyzing the influence of additives on odour generation. _____	112
Figure 54.	Cluster of the reference pellets and plaques produced thereof. The direction of Injection moulding is indicated. _____	112
Figure 55.	Cluster of the references from Linz and Monza with differing influence of the Injection moulding. _____	112
Figure 56.	Cluster of the reference and the samples with increased compounding temperature ( $T_c=260$ °C). Note that the influence of the Injection moulding is lost for the $T_c=260$ °C samples. _____	113
Figure 57.	Cluster of the reference and the samples with changed base polymer. Note that the influence of the Injection moulding is the same. _____	113
Figure 58.	Cluster of the reference and the samples without talc. Note that the influence of the Injection moulding is lost for the samples without talc. _____	113
Figure 59.	Cluster of the reference and the samples without colour masterbatch (CMB). Note that the influence of the Injection moulding is lost for the samples without CMB. _____	113

Figure 60.	Cluster of the reference and the samples without epicote. Note that the influence of the Injection moulding is the same for both samples. _____	114
Figure 61.	Cluster of the reference and the samples with reduced heat stabilization. Note that the influence of the Injection moulding is the same for both samples. _____	114
Figure 62.	Cluster of the reference and the samples without scratch resistance additives. Note that the influence of the Injection moulding is the same for both samples. _____	114
Figure 63.	Cluster of the reference and the samples without UV stabilization. Note that the influence of the Injection moulding is lost for the samples without UV stabilization. _____	114
Figure 64.	GC-MS chromatograms of the four samples. The upper two show significant amounts of 2-ethyl-1-hexanol (2-EH) due to the use of the new catalyst RCL05P, the lower two were produced with the old catalyst BCF20P. _____	116
Figure 65.	Chemical structure of Tx101. _____	117
Figure 66.	Chemical structure of Tx301. _____	117
Figure 67.	MasStat© Cluster of HS-SPME-GC-MS data obtained from the peroxide samples. Samples with TX101 in red, samples with Tx301 in green and the reference without peroxide in brown. __	119
Figure 68.	HS-SPME-GC-MS chromatograms of the analyzed data showing clear differences between the two peroxide systems Tx101 and Tx301. _____	120
Figure 69.	Summary of Detection Frequency (SNIF) diagrams for HD120MO without peroxide (in green), with Tx101 and a MFR of 50g/10min (in red) and with Tx301 and a MFR of 50g/10min (in blue). _____	121
Figure 70.	MasStat© Cluster obtained from the HS-SPME-GC-MS data of the unstabilized (unstab.) and stabilized PP samples stored for 0 (ref), 1 (1d), 3 (3d) and 7 (7d) days at 80 °C in normal atmosphere (air) or in reduced oxygen atmosphere (N <sub>2</sub> ). _____	124
Figure 71.	HS-SPME-GC-MS chromatograms of unstabilized PP samples stored @80 °C up to 7 days in normal atmosphere. _____	124
Figure 72.	HS-SPME-GC-MS chromatograms of stabilized PP samples stored @80 °C up to 7 days in normal atmosphere. _____	125
Figure 73.	Detection Frequency (SNIF) diagrams of unstabilized PP samples stored @80 °C in air for (a) 0 days, (b) 1 day (top right) and (c) 3 days (bottom left). _____	125
Figure 74.	Detection Frequency (SNIF) diagrams of unstabilized PP samples stored @80 °C in reduced oxygen atmosphere for (a) 0 days, (b) 1 day, (c) 3 days and (d) 7 days. _____	126
Figure 75.	Detection Frequency (SNIF) diagrams of stabilized PP samples stored @ 80 °C in air for (a) 0 days, (b) 1 day, (c) 3 days and (d) 7 days. _____	126
Figure 76.	Detection Frequency (SNIF) diagrams of stabilized PP samples stored @ 80 °C in reduced oxygen atmosphere for (a) 0 days, (b) 1 day, (c) 3 days and (d) 7 days. _____	127

Figure 77.	Multivariate calibration and cross-validation curves for (a) all PP (HD120MO) samples, (b) stabilized samples in a reduced oxygen atmosphere, (c) stabilized samples in air, (d) unstabilized samples in a reduced oxygen atmosphere and (e) unstabilized samples in air. _____	128
Figure 78.	MasStat© Cluster obtained from the HS-SPME-GC-MS data of the unstabilized (unstab.) and stabilized (stab.) PE samples stored for 0 (ref), 1 (1d), 3 (3d) and 7 (7d) days at 80 °C in normal atmosphere (air) or in reduced oxygen atmosphere (N <sub>2</sub> ). _____	131
Figure 79.	HS-SPME-GC-MS chromatograms of unstabilized PE samples stored @80 °C up to 7 days in normal atmosphere (air). _____	131
Figure 80.	HS-SPME-GC-MS chromatograms of stabilized PE samples stored @80 °C up to 7 days in normal atmosphere (air). _____	132
Figure 81.	Detection Frequency (SNIF) diagrams of unstabilized PE samples stored @ 80 °C in air for (a) 0 days, (b) 1 day, (c) 3 days and (d) 7 days. _____	132
Figure 82.	Detection Frequency (SNIF) diagrams of unstabilized PE samples stored @ 80 °C in a reduced oxygen atmosphere for (a) 0 days, (b) 1 day, (c) 3 days and (d) 7 days. _____	133
Figure 83.	Detection Frequency (SNIF) diagrams of stabilized PE samples stored @ 80 °C in air for (a) 0 days, (b) 1 day, (c) 3 days and (d) 7 days. _____	133
Figure 84.	Detection Frequency (SNIF) diagrams of stabilized PE samples stored @ 80 °C in a reduced oxygen atmosphere for (a) 0 days, (b) 1 day, (c) 3 days and (d) 7 days. _____	134
Figure 85.	Multivariate calibration and cross-validation curves for (a) all PE (ME3440) samples, (b) stabilized samples in reduced oxygen atmosphere, (c) stabilized samples in air, (d) unstabilized samples in a reduced oxygen atmosphere and (e) unstabilized samples in air. _____	135
Figure 86.	Proposed HS-SPME-GC-PID set-up. _____	136
Figure 87.	ChromStat© Cluster of QC samples separated by the material _____	137
Figure 88.	ChromStat© Cluster of QC samples showing separation of different lots of the same material ME3440-05. _____	138
Figure 89.	MasStat© cluster from the HS-SPME-GC-MS data of the coloured (RA130E-8427), the non-coloured (RA130E natural) and the CMB (CMB126 grey) samples. _____	141
Figure 90.	HS-SPME-GC-MS chromatograms of the coloured (RA130E-8427), the non-coloured (RA130E natural) and the CMB (CMB126 grey) samples. _____	142
Figure 91.	Detection Frequency (Total SNIF) diagrams of the CMB126 (in red) and the natural RA130E pellets (in brown) using the 2 g and the 500 mg GC-O results. _____	142
Figure 92.	Detection Frequency (Total SNIF) diagrams of the coloured RA130E pellets (in blue) using the 2 g and the 500 mg GC-O results. _____	143
Figure 93.	MasStat© cluster from the HS-SPME-GC-MS data of the coloured (EE188HP-1048), the non-coloured (EE188HP natural) and the CMB (CMB347 beige) pellet and plaque samples. _____	145

Figure 94.	HS-SPME-GC-MS chromatograms of the coloured (EE188HP-1048), the non-coloured (EE188HP natural) and the CMB (CMB347 beige) pellets and plaque samples.	145
Figure 95.	Detection Frequency (Total SNIF) diagrams of the CMB126 (in red) and the natural RA130E pellets (in brown) using the 2 g and the 500 mg GC-O results.	146
Figure 96.	Detection Frequency (Total SNIF) diagrams of the coloured RA130E pellets (in blue) using the 2 g and the 500 mg GC-O results.	146
Figure 97.	HS-SPME-GC-MS chromatograms of monomer sample 63001 (before purification) and 63103 (after purification) from Kallo and the air sample from Linz.	149
Figure 98.	Mean areas and standard deviations for selected compounds calculated from 5 measurements for the 63001 and the 63103 samples.	149
Figure 99.	GC-MS measurements with extracted m/z 44 typical for the odour-active saturated aldehydes for the 63001 and 63103 samples.	150
Figure 100.	HS-SPME-GC-NPD chromatograms for the 63001 and 63103 samples.	150
Figure 101.	Detection Frequency (SNIF) diagram of the propylene monomer sample 63001 (before purification; in blue) and 63103 (after purification; in red) from Kallo.	151
Figure 102.	Detection Frequency (SNIF) diagram of the 1 <sup>st</sup> propylene monomer sample before purification (in blue) and after purification (in red) from Kallo.	151
Figure 103.	HS-SPME-GC-NPD chromatograms of the PP pellet, the PP box and the standard addition samples.	153
Figure 104.	MasStat© cluster from all samples (labels as described in Table 3).	155
Figure 105.	HS-SPME-GC-MS chromatograms of BJ368MO pellets (BO168) (in black), competitor box with label from France (BO170) (in blue) and BJ368MO box without label from Belgium (BO172) (in red).	156
Figure 106.	HS-SPME-GC-MS chromatograms of the air measurements during the injection moulding of the BJ368MO and the competitor material at cavity 10.	156
Figure 107.	Detection Frequency (SNIF) diagrams of BJ368MO pellets (in red), BJ368MO injection moulded and labelled box from France (in blue) and the injection moulded and labelled competitor box from France (in green). Blue markings show differences in the odour pattern of the two boxes.	158
Figure 108.	Detection Frequency (SNIF) diagram of the metallocene-PP (m-PP) pellets (in blue on top) and plaques (in green, at the bottom).	159
Figure 109.	Extracted HS-SPME-GC-MS chromatogram with the m/z of 44, a typical m/z for saturated aldehydes of the metallocene-PP (m-PP) pellets (in black, on top) and plaques (in green, at the bottom).	159

Figure 110. HS-SPME-GC-MS chromatograms of the metallocene-PP (m-PP) pellets (in black) and plaques (in green) compared to the Ziegler-Natta PP (ZN-PP) EE188AI-9530 pellets (in turquoise) and plaques (in lilac). . \_\_\_\_\_ 160

## List of Tables

Table 1.	Typical mass temperatures ( $T_M$ ) for processing of PE and PP materials. _____	13
Table 2.	List of identified odour-active compounds in PE and PP samples in numerous publications with their sensory threshold values determined in water taken from <sup>32</sup> . _____	21
Table 3.	List of all polyolefin samples which were analyzed during the thesis. _____	30
Table 4.	Apparatus parameter for the SPME-GC-MS measurements using the GC-GCD system. _____	49
Table 5.	Apparatus parameter for the SPME-GC-MS measurements using the 7890 GC-MS system. _____	50
Table 6.	Apparatus parameter for the GC-MS measurements of the liquid fractioned extracts using the GC-MS system. _____	51
Table 7.	Apparatus parameter for the GC-MS measurements of the NMH derivatised liquid fractioned extracts using the GC-MS system. _____	52
Table 8.	Apparatus parameter for the GC-MS measurements of the PFBHA derivatised liquid fractioned extracts using the GC-MS system. _____	53
Table 9.	Apparatus parameter for the GC-O measurements of the liquid extracts. _____	54
Table 10.	GCxGC-TOF-MS parameters for measurements of the liquid fraction II samples. _____	56
Table 11.	Parameter for the quantification of 2-acetyl-1-pyrroline in a PP sample. _____	57
Table 12.	Odour descriptors and odour thresholds in water and oil from the literature <sup>32</sup> for the compounds which sensory threshold values were determined. _____	63
Table 13.	Composition of the test mixture for the GC-O system. _____	65
Table 14.	Detailed recipe for the L140WG-06 and the WG140AI-05 samples. _____	68
Table 15.	Material data sheets for the representative grades. _____	72
Table 16.	Odour-active compounds in BF907MO pellets (pel) and plaques (pla) ( $RI_{exp}$ ... experimental Retention Indices, s.d. ... standard deviation, $RI_{lit}$ ... literature Retention Indices determined with pure standards (om) or taken from literature sources <sup>67,68</sup> ). _____	78
Table 17.	List of identified odour-active compounds detected in EE188AI samples from Beringen and Schwechat in extract obtained from pellets(pel) and plaques(pla). ( $RI_{exp}$ ... experimental Retention Indices, s.d. ... standard deviation, $RI_{lit}$ ... literature Retention Indices determined with pure standards (om) or taken from literature sources <sup>67,68</sup> ). _____	90
Table 18.	List of odour-active compounds present in the base polymers BS2581, BE677AI, EF015AE and in the corresponding compound PP EE188AI from Beringen in pellets (pel) and plaques (pla) ( $RI_{exp}$	

	... experimental Retention Indices, s.d. ... standard deviation, RI <sub>lit</sub> ... literature Retention Indices determined with pure standards (om) or taken from literature sources <sup>67,68</sup> ). _____	92
Table 19.	List of odour-active compounds present in the FB2230 from Schwechat and Porvoo (pel ... pellets; pla ... plaques; RI <sub>exp</sub> ... experimental Retention Indices, s.d. ... standard deviation, RI <sub>lit</sub> ... literature Retention Indices determined with pure standards (om) or taken from literature sources <sup>68</sup> ). _____	98
Table 20.	List of odour-active compounds present in the ME3440 pellets from Porvoo (Po), Stenungsund (St) and Bourouge (Bo). (RI <sub>exp</sub> ... experimental Retention Indices, s.d. ... standard deviation, RI <sub>lit</sub> ... literature Retention Indices determined with pure standards (om) or taken from literature sources <sup>67,68</sup> ). _____	105
Table 21.	2-Ethyl-1-hexanol mean concentrations and standard deviation in the samples determined by GC-MS. _____	116
Table 22.	List of peroxide samples analyzed in the study. Samples in italic were used in the GC-O analyses. _____	118
Table 23.	Differences in selected compounds representative for the use of Tx301 and Tx101. Tx101 was used as reference, values are expressed as difference to the use of Tx101. _____	120
Table 24.	Sensory threshold values determined as group BET in water (s.d. ... standard deviation). ____	139
Table 25.	Sensory threshold values determined as group BET in miglyol (s.d. ... standard deviation). ____	139
Table 26.	Limits of Detection (LOD) and Limit of Quantification (LOQ) and the standard deviation of regression (SDR) for the 2-acetyl-1-pyrroline quantification with HS-SPME-GC-NPD and standard addition. _____	153
Table 27.	2-acetyl-1-pyrroline concentration in the BJ368MO pellets and the injection moulded box determined by standard addition and HS-SPME-GC-NPD (n=3). _____	153

## List of Schemes

Scheme 1.	Reaction pathway of phenolic antioxidant degradation in the presence of talc proposed by Sauer <sup>14</sup> . _____	12
Scheme 2.	Reaction mechanism of carbonyls with PFBHA. _____	46
Scheme 3.	Mechanism of hydrazone formation from carbonyls and NMH. _____	47
Scheme 4.	Mechanism of the catalytic activity of BF <sub>3</sub> on the cyclization of hydrazones to pyrazolines (according to <sup>17</sup> ). _____	47

## Abbreviations

AED	atomic emission detector
amu	atomic mass units
<i>at</i>	atactic
BF <sub>3</sub>	Boron trifluoride
BSTFA	<i>N,O</i> -bis(trimethylsilyl)trifluoroacetamide
DCM	dichloromethane
DEE	diethyl ether
DVB/CAR/PDMS	Divinylbenzene/Carboxen/Polydimethylsiloxane
ECD	electron-capture detector
FID	flame ionisation detector
FPD	flame photometric detector
FT	film thickness of the GC column
GC	gas chromatography
ID	inner diameter of the GC column
IS	Internal Standard
<i>it</i>	isotactic
MS	mass spectrometry
MWD	molecular weight distribution
MVDA	multivariate data analysis
NMH	<i>N</i> -methylhydrazine
NPD	nitrogen phosphorus detector
ODP	olfactory detection port
OR	odour receptor
PAHs	polycyclic aromatic hydrocarbons
PCA	principal component analysis
PE-HD	high density polyethylene
PE-LD	low density polyethylene
PE-LLD	linear low density polyethylene
PFBHA	<i>O</i> -(2,3,4,5,6-Pentafluorobenzyl)hydroxylamine hydrochloride
PP	polypropylene
SDE	simultaneous distillation/extraction
SIM	selected ion monitoring
SPE	solid phase extraction
SPME	Solid Phase Microextraction

<i>st</i>	syndiotactic
$T_c$	compounding temperature
$T_M$	mass temperature
$T_{Melt}$	melting temperature
TMH	3,5,5-trimethyl-1-hexanal



## **Kurzfassung**

Im Rahmen dieser Dissertation wurden geruchsaktive Verbindungen in Polyolefinen (Polyethylen (PE) und Polypropylen (PP)) mit Hilfe der Gaschromatographie (GC) gekoppelt mit Massenspektrometrie (MS) und Olfaktometrie (O), wo die menschliche Nase als Detektor verwendet wird, identifiziert.

Untersucht wurden sowohl PE und PP Materialien aus jenen Anwendungsbereichen, in denen Geruch eine wichtige Materialeigenschaft darstellt. Dazu zählen Lebensmittelverpackungen, Trinkwasserrohre und Komponenten des Automobilinnenraums.

Für die Bildung von geruchsaktiven Verbindungen in Polyolefinen wurden zahlreiche Einflussfaktoren identifiziert. Den größten Einfluss auf die Bildung von Geruchskomponenten in PE und PP haben Verarbeitungsschritte wie Compoundierung, Extrusion und Spritzguß.

Einen weiteren wichtigen Faktor stellen die verwendeten Additive dar. Hier konnten v.a. Füllstoffe, Farb-Masterbatches und Antioxidantien als Geruchstreiber identifiziert werden.

Weiters wurde durch Untersuchungen an Monomeren, Comonomeren und Verdünnern auch für diese Prozessstoffe ein zum Teil erhebliches Geruchspotential ermittelt.

Die Mehrheit der identifizierten Substanzen besitzt eine funktionelle Carbonylgruppe. Dabei handelt es sich sowohl um gesättigte als auch ein- und mehrfach ungesättigte aliphatische Aldehyde und Ketone, die alle sehr niedrige sensorische Geruchsschwellenwerte im ppb Bereich oder darunter aufweisen.

Neben diesen Carbonylverbindungen wurden auch diverse niedersiedende Alkohole, Karbonsäuren, Laktone und aromatische Substanzen wie Kresol und 2-Acetyl-1-pyrrolin als geruchsaktive Komponenten bestimmt.

In einem weiteren Teil der Arbeit wurden die sensorischen Geruchsschwellenwerte der am häufigsten identifizierten Verbindungen mit einem Sensorikpanel in Wasser und Öl bestimmt.

Erst durch diese Schwellenwerte ist es möglich die identifizierten Verbindungen aufgrund ihres Beitrags zum Gesamtgeruch zu reihen.

Dadurch konnte festgestellt werden, dass der Geruch von Polyolefinen v.a. durch die 1-Alken-3-one und die einfach ungesättigten Aldehyde mit einer Kettenlänge zwischen 6 und 10 C-Atomen bestimmt wird. Diese Verbindungen sind bekannte Oxidationsprodukte von PE and PP Materialien.

## **Abstract**

In this work odour-active compounds were identified in polyolefins (namely polyethylene (PE) and polypropylene (PP)) by means of gas chromatography (GC) coupled to different detection systems such as mass spectrometry (MS) and olfactometry (O) where the human nose acts as the detector. The majority of the odour-active compounds are carbonyls, i.e. both saturated and mono- and diunsaturated aldehydes and ketones showing very low sensory odour threshold values in the lower and sub- $\mu\text{g}$  per kg range.

Other identified odour-active compounds include alcohols, carboxylic acids, lactones and aromatic compounds such as cresol and 2-acetyl-1-pyrroline.

Various PE and PP materials were investigated from different application areas, where odour is an important material property. This is the case for food packaging materials, drinking water pipes and the automotive interior.

The formation of odour-active compounds in polyolefins is strongly influenced by various process steps; the biggest influencing factor is the processing including compounding, extrusion and injection moulding.

Next, additives are also influencing the odour of the polyolefinic product; especially fillers, antioxidants and colour master batches contribute to the odour of polyolefinic products.

Last, also monomers, co-monomers and diluents show an odour potential.

Sensory odour threshold values of the most abundant odour-active compounds in polyolefins were determined with a sensory panel in water and oil. With these values it is possible to rank the many compounds for their contribution to the overall odour.

Finally, the 1-alken-3-ones and the mono-unsaturated aldehydes with chain lengths between 5 and 10 C-atoms were identified as major contributors to the odour of polyolefins. These compounds are known oxidation products of PE and PP materials.

## Acknowledgements

Completing a PhD is truly a marathon event, and I would not have been able to complete this journey without the aid and support of countless people over the past four years.

I must first express my sincere gratitude towards my supervisor, Professor Erich Leitner: I started as a novice in Analytical Chemistry and thanks to him and his never-ending support, ability to teach and collegiality I am here today.

I would like to thank my second examiner, Professor Reinhold W. Lang, who immediately accepted my inquiry although I switched my field of research and who supported and accompanied me through my master studies.

I am deeply grateful to Wolfgang Stockreiter: Providing samples is one thing, but sharing thoughts and being present for countless discussions and meetings, often on short notice, is definitely beyond a typical business cooperation – many thanks for this great support!

My acknowledgements to Nina Haar: Nina, it was a real pleasure and honour to work with you. I will definitely miss your attitude and many thanks for keeping me on track!

A special mention of my fellow PhD student and office mate Dr<sup>in</sup> Eva Schrampf who made our conference trips memorable and daily office life a real pleasure and who introduced me to MVDA.

To all the other colleagues of the research group I am deeply indebted: Univ.Do<sup>z</sup><sup>in</sup> Dr<sup>in</sup> Barbara Siegmund for sharing her ideas and thoughts and for having a role model at hand; Claudia Koraiman, Sigrid Hager and DI<sup>in</sup> Lilli Zefferer for helping out with GC-O analyses and highly appreciated coffee breaks.

A special thank you to the students I was able to work with; their work is part of this thesis: Edith Renöckl, who looked into monomer purity, Hanne Furbo working on derivatization of carbonyls during her IAESTE internship and Josefine Mohlin, who determined sensory threshold values with GC-O.

Finally, I would like to thank my parents for having confidence in me. And for the one who was there for me and still is after all these years – Thomas, this is for you!

This work was funded by the Austrian Promotion Agency (FFG) in a BRIDGE project (no. 814233/11968) and was carried out in cooperation with Borealis Polyolefine GmbH.

## 1. Introduction

Nowadays, plastics are used in nearly every aspect of our daily lives. They are used for packaging, in the mobility area for automotive interior and exterior parts, in the building and construction area for transportation of drinking and waste water and natural gas, for products such as toys, computers and cutlery, personal hygiene and medical devices (infusion hose, ...).

The group of polyolefins is the largest group of plastics used nowadays. The most prominent members of polyolefins are polyethylene of various densities (PE) and polypropylene (PP) which account to nearly 50% of all plastics produced in Europe according to recent numbers<sup>1</sup>.

The increased application of plastics materials in all areas of the daily life is mostly determined by their properties in combination with their light weight. Besides mechanical strength, Young's Modulus and chemical stability, additional requirements have to be met in applications where the plastics are in direct contact with the end consumer (food contact materials, interior automotive parts and drinking water pipes), especially as consumers become more and more aware and sensitive. These additional requirements include low/no migration, low/no emission or a low odour rating.

In the context of Food Safety this is a topic of enormous relevance and importance not only for legislative bodies but also for consumers as shown for the discussion about endocrine disruptors present in plastics.

Especially volatiles are of interest as those substances have the possibility to migrate out of the plastic and being emitted to the environment. These volatiles can be formed (a) during processing and use due to the non-inert nature of polymers which are affected by the environment (oxygen, temperature, UV-light, mechanical stress), (b) derive from the polymerization from solvents and/or process additives or (c) from interactions of the polymer with additives and/or printings and labels.

One special sub-group of volatiles are odour-active compounds which are not necessarily harmful to the human health but always irritating and annoying.

Odour-active compounds show a large variety in their type of functional group (including acids, esters, alcohols, carbonyls, thiols, amines, aromatics, ...), in their sensory thresholds (i.e. that concentration where a compound becomes noticeable) ranging from sub-ng per litre up to several

---

<sup>1</sup> Plastics Europe, 2009: The Compelling Facts About Plastics 2009 - An analysis of European plastics production, demand and recovery for 2008. Available on [www.plasticseurope.org](http://www.plasticseurope.org) (accessed 12-14-2009).

mg per litres and in their odour quality (fruity, fatty, pungent, musty, roasty, ...), which is determined mostly at which odour receptor(s) the compound binds to.

Odour-active compounds in plastics are problematic as they do not only smell but more important they can also modify or change the odour and/or flavour of the product which are in contact with the plastic (e.g. packaged food and beverages, drinking water stored in plastic drinking water pipes).

Some plastics are more sensitive in terms of the generation of volatiles and odour-active compounds either due to their type of production (the use of solvents and/or process additives which might cause odour problems e.g. rest urethane in PUR foams) or their chemical structure.

Currently, odour is measured mostly by the use of sensory panels consisting of a group of persons which are constantly trained to evaluate and judge the odour of products.

However, in many cases of material development the evaluation of odour quality and intensity is not sufficient. For understanding and further avoiding the formation of odour-active compounds during the production, an identification of the single odour causing substances is necessary.

Answers to these questions a sensory panel cannot give, and an analytical method is needed.

However, when working with analytical methods such as gas chromatography (GC) coupled to conventional detectors such as mass spectrometry (MS) or flame ionization detector (FID) one needs to overcome the problem that these detectors cannot tell whether a compound is odour-active or not. This information always has to come from a human being.

In this work the results of a three year project about the identification of odour-active compounds in PE and PP materials are presented. By combining the sensory approach using a panel and analytical methods as gas chromatography it is possible to determine which compounds make up the overall odour of polyolefins and to what extent each individual substance contributes to the overall odour.

After establishing a basic knowledge about what kind of odour-active compounds are present in the polyolefins the question arises where these compounds come from and how they are generated.

For this, a look at the whole process chain of polyolefins is needed to identify the possible origins including the raw material-the comonomers and monomers, the polymerization step, the additivation, the compounding and the processing step.

### **1.1. Aims and targets**

This work was carried out in cooperation with Borealis Polyolefine GmbH as business partner.

Borealis mid- and long-term visions and missions deal with the reduction of impurities within their products. One critical impurity for several business areas within the company is odour.

Together with the cooperation partner several targets and aims were set:

- status-quo evaluation of today's Borealis PE and PP products for odour-active compounds present.
- study of influencing parameters on the odour generation along the whole polyolefin process chain including the raw materials, polymerization techniques, additives and processing.
- classification of the odour-active compounds in terms of their odour relevancy by determination of their sensory thresholds.
- identification of the crucial steps in the production of PE and PP on the odour formation.
- establishment of a basic knowledge and awareness of odour-active compounds present in PE and PP.
- establishment of analytical methods for odour measurement.

Answering these questions basic knowledge about the problematic of odour and its measurement should be established. Further, one should be able to work on odour reduction measures.

## 2. Background and basics

### 2.1. Odour and odour perception

To call a substance odour-active several prerequisites have to be met:

- an odour-active compound needs to be volatile at atmospheric pressure
- the compound needs to bind to one or more odour receptor cell types
- compounds with a molecular mass over 300 g/mol do not show odour-activity as they are not able to bind to odour receptor cells.

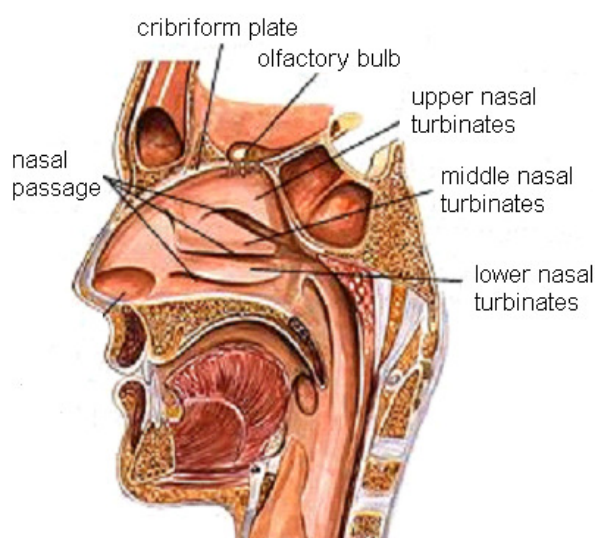


**Figure 1. Human odour perception takes place in the olfactory bulb.**

that in both locations they are activated in the same way<sup>3,4</sup>.

Two different ways of odour perception in the nose can be distinguished: (a) the direct so called *nasal* impression where the odour-active compounds is “travelling” up in the nose to the receptors and (b) the indirect so called *retronasal* impression where odour-active compounds are released in the mouth by chewing, warming and/or contact with the saliva and get to the *regio olfactoria* passing through the palate.

It is possible that nasal and retronasal odour impressions differ due to temperature differences between the environment and in the mouth, availability of saliva and enzyme actions during chewing and swallowing as well as microbial activity in the oral cavity<sup>5</sup>.

Human odour perception takes place in the olfactory bulb or *regio olfactoria* located in the upper nasal cavity. On 2 x 2 cm<sup>2</sup> up to 350 different odour receptor (OR) types are located (see Figure 1).

Axel and Buck discovered that over 1000 genes are responsible for the receptors accounting to approx. 3% of the total genome<sup>2</sup>. Most of the OR are located in the *regio olfactoria*, but lately, researchers showed that in human sperm the same OR can be found as in the human nose and

<sup>2</sup> Buck L.B., Axel R. (1991) Cell 65:175–187.

<sup>3</sup> Vosshall L.B. (2004) Curr. Biol. 14:R918-920.

<sup>4</sup> Spehr M., Schwane K., Heilmann S., Gisselmann G., Hummel T., Hatt H. (2004) Curr. Biol. 14:R832-833.

## 2.2. Odour analysis

Currently, odour is measured mostly by the use of sensory panels consisting of a group of persons which are constantly trained to evaluate and judge the odour of products. To overcome the subject statement of a single panellist it is required (a) to always work with a group of people where all of them fulfil certain requirements in terms of their sensitivity and ability to describe odours, (b) to use objective test questions (no asking for personal preferences but whether there are differences) and (c) to apply appropriate test procedures to ensure a statistically secured result.

Members of sensory panels do not necessarily smell “better” than normal people; during the training sessions they train their ability to describe odours in a objective way (instead of “I don’t like it” they say “This has a green and rotten odour”).

In this work the sensory panel was used for the determination of sensory threshold values in a polyolefin-like matrix.

There are different definitions of sensory threshold values<sup>5</sup>; the *detection threshold* is the lowest concentration at which a panellist detects an odour compared to a blank sample, but cannot further describe the odour. At higher concentrations one is able to describe the odour, that concentration is called the *recognition threshold*. At a certain concentration one is not able to detect a difference in the intensity any more; this concentration is the *terminal threshold*.

In the literature one finds many sensory thresholds values but in most cases these values are either determined in air or water. Sensory threshold values are strongly dependent on the matrix, as it is easy to understand that from a polar matrix non-polar compounds are more easily released than from a non-polar one. As water is a rather polar matrix and PE and PP are non-polar the sensory threshold values for the identified odour-active compounds were determined in a polyolefin-like matrix.

The work of sensory panels is useful for many areas in the food industry, however, this approach has also major some drawbacks:

- A certain amount of people is needed for a statistically approved result

---

<sup>5</sup> Starkenmann C., Le Calv B., Niclass Y., Cayeux I., Beccucci S., Troccaz M. (2008) J. Agric. Food Chem. 56:9575-9580.

<sup>6</sup> ASTM E679 - 04 (2004) Standard Practice for Determination of Odor and Taste Thresholds By a Forced-Choice Ascending Concentration Series Method of Limits.



- A constant and regular training at the start-up and during the work of the panel is needed comparable to the constant calibration of an analytical instrument to be able to work with the analytical instrument “human sensory panel”.
- Sensory tests and trainings are time and personnel consuming; a minimum of one training session per week is recommended.
- As sensory panels can only judge the overall odour of a product no further information about the composition of the odour and the concentration of each odour-active compound in this mixture can be determined.

As the needed information whether a compound is odour-active or not, only a human is able to give, humans need to act as a detector, but instead of judging the overall odour of the product, the panellist detects single odour-active compounds after a separation of the mixture facilitated by a chromatographic technique. Due to the volatile nature of odour-active compounds, gas chromatography (GC) is the method of choice. The coupling of a GC with a human panellist acting as the detector is called gas chromatography-olfactometry (GC-O) shown in Figure 2. A sample is injected into the GC column where the analytes are separated. At the end of the analytical GC column a splitter (e.g. 1:1 as used in our laboratory) divides the effluent between a conventional Flame ionization detector (FID) and the olfactory detection port. The FID signal can be used for calculation of the retention indices (RI) and thus enables an identification of the compound and also to check whether a compound is present in cases the panellist indicates an odour impression.

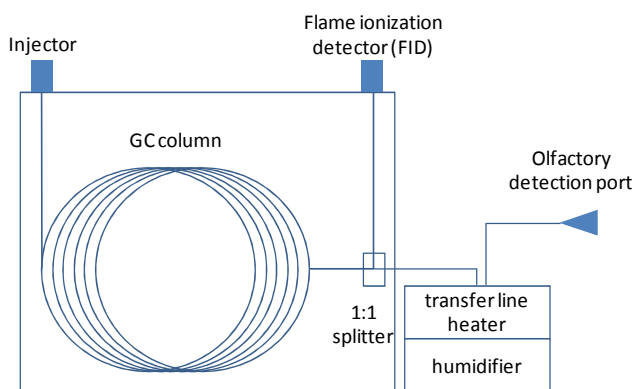


**Figure 2. Schematic Gas Chromatography-Olfactometry (GC-O) instrument.**

As the olfactory detection port is located outside of the GC oven a transfer line, for the transport of the effluent from the end of the GC column to the sniffing port, needs to be heated to avoid condensation of the effluent before the sniffing port. Additionally, the effluent is humidified to prevent the panellists of dry noses during the sniffing sessions.

As it is not advisable to sniff longer than 30 min, but it is necessary to give the panellists enough time for the detection of the single compounds, the GC oven program and the GC column are optimized to achieve the best separation of the analytes in the shortest time feasible. In our

analyses we used a 30 m long GC column with a film thickness of 0.25  $\mu\text{m}$  in combination with a heating rate of 10  $^{\circ}\text{C}/\text{min}$ . With these parameters the odour-active analytes elute within the first 20 min.

### 2.3. Polyolefins (process chain)

The group of polyolefins (i.e. polymers with repeating units having only C- and H-atoms) is one of the most important one among the commercial plastics. When looking at the whole process chain in polyolefin production it is possible to separate the whole process in several steps:

- (1) monomer generation and treatment
- (2) polymerization
- (3) post-polymerization process including additivation
- (4) processing (i.e. injection moulding, extrusion, blow-moulding, ...).

Looking into these different steps one is able to identify several parameters which influence the properties of the polyolefin end product.

(1) When it comes to monomers, for ethylene and propylene mainly petroleum sources are used.

Either natural gas is used in a high temperature cracking process to produce the ethylene from ethane and propane or the gasoline fraction from the primary oil distillation is cracked and further distilled to purify the ethylene from lower alkanes and olefins<sup>7</sup>. For the propylene the C<sub>3</sub> fraction (propylene and propane) is separated from other gases by fractional distillation. Later propane is separated from the propylene in an additional distillation step.

Prior to the monomer entering the polymerization reactor it needs to be purified from impurities which deteriorate the polymerization process and/or the catalytic activity (e.g. carbon monoxide, acetylene, methyl acetylene, oxygen and water)<sup>7</sup>.

(2) For the PE polymerization 4 different processes exist. While PE with low density (PE-LD) is produced in a catalyst-free process at high pressures, three processes exist for the production of PE with high density (PE-HD) working at reduced pressures using the Ziegler-Natta process with highly active  $\text{MgCl}_2$  supported Ti catalysts, the Philips process with metal oxides catalysts and the metallocene process where the catalysts consist of a transition metal compound, usually zirconium or titanium, incorporated into a cyclopentadiene-based structure.

---

<sup>7</sup> Brydson J.A. (1999) *Polyethylene* in: *Plastics Materials: Seventh Edition*, Elsevier Butterworth-Heinemann, Oxford, UK, 205-246.

PP is produced by Ziegler-Natta and metallocene processes, a free radical process would lead to only amorphous PP lacking the desired properties of PP.

The high pressure process for PE-LD is initiated by benzyl peroxides or azodi-isobutyronitril at high pressure (100 – 300 MPa) and temperatures (80 – 300 °C). The obtained polymer contains both short and long chain branches. Special attention must be given to the process control to prevent a runaway reaction. Typically, 10 to 30 % of the monomer is converted into the polymer in a continuous (narrow-bore tubes or stirred reactors) or batch process (autoclave). PE-LD densities are between 0.915 to 0.94 g/cm<sup>3</sup> with about 40 to 50 % crystallinity<sup>8</sup>.

PE-HD (densities 0.942 - 0.965 g/cm<sup>3</sup> and 60 to 80 % crystallinity) and PP are produced by Ziegler-Natta catalysts at low pressures (0.1 to 5 MPa) and temperature below 100°C in the absence of oxygen, water, ethanol and alkali. Ziegler-Natta catalysts enable multi-site reactions leading to a broad molecular weight distribution (MWD). Today's Ziegler-Natta catalysts are highly active with conversion rates of 95 %. These catalysts are MgCl<sub>2</sub> supported heterogeneous TiCl<sub>3</sub> types which are present in a different phase from the reactor mixture. The fixation on the inert support material enables a feeding into the reactor and a better process control. In combination with a Lewis base (e.g. benzoic acid) as an electron donor and a second Lewis base (e.g. methyl-p-toluate) as an external donor the catalyst activity and the stereospecificity are dramatically increased and the post reactor removal of catalyst residues is eliminated<sup>10</sup>.

Another catalyst for production of PE-HD is the Phillips' type: The supported metal oxide (typically 5 % CrO<sub>3</sub> on finely divided silica-alumina) catalysts works between 130 to 160 °C between 3 and 4 MPa. The process shows a high stereo-specificity<sup>7</sup>.

The most modern catalyst systems are metallocenes for the production of linear low density PE (PE-LLD) and syndiotactic PP<sup>9</sup>. Metallocenes are single-site catalysts, i.e. the monomer only reacts at a single site on the catalysts molecule. Metallocenes are compounds in which two cyclopentadienyl or substituted cyclopentadienyl ligands are π-bonded to a metal atom. The stereochemistry of such compounds resembles a distorted tetrahedron. The metal centre can be a zirconium, hafnium or titanium (see Figure 3)<sup>10</sup>. For the formation of the active centre on the metal atom in the cleft between the bridged alkyl groups cocatalysts are needed (e.g.

---

<sup>8</sup> Oberbach K. (2001) Saechtling Kunststoff Taschenbuch, 28th edition, Hanser, Munich, Germany.

<sup>9</sup> Imuta J.-I., Kashiwa N. (2000) Recent Progress on single-site catalysts, in: Handbook of polyolefins (Vasile C., ed.) Marcel Dekker, New York, USA, 71-88.

aluminoxane, boron compounds). A typical example is given in Figure 3 showing a  $\text{Cp}_2\text{ZrCl}_2$  with works with methyl aluminoxane (MAO) as cocatalyst.

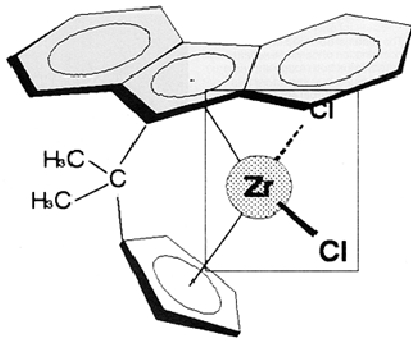


Figure 3. Molecular structure of metallocene catalysts used for PE and PP polymerization (taken from <sup>10</sup>). The zirconium atom is bound to two chlorines and to a bridged alkyl group which forms a cleft where the  $\text{ZrCl}_2$  complex is situated and where the polymerization occurs.

By using this type of catalyst a greater control of the composition distribution, the MWD, the comonomer incorporation and stereo-regularity is achieved. With metallocenes PE and PP types can be realised which are not possible with Ziegler-Natta such as PE-LLD by using 1-octene as comonomer, syndiotactic PP, long chain branched polyolefins and cycloolefin polymers.

Comonomers are used both for PE and PP to control the degree of short chain branches and to retard the growth of large crystal structures<sup>7</sup>. For PE propylene, 1-butene and 1-octene are used to enhance the creep,

environmental stress cracking and thermal cracking properties compared to the corresponding homopolymer. For PP usually ethylene is used as comonomer.

PP is available as syndiotactic and isotactic homopolymer, random, impact and block-copolymer depending on the catalyst used and on the comonomer. Its densities vary between  $0.855 \text{ g/cm}^3$  for the amorphous type and  $0.946 \text{ g/cm}^3$  for a crystalline type.

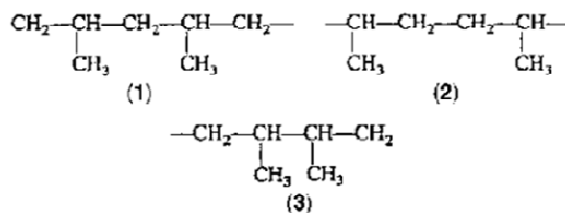


Figure 4. PP structures resulting from (1) head-to-tail, (2) tail-to-tail and (3) head-to-head reactions (taken from <sup>11</sup>).

For PP due to its methyl side chain during polymerization two monomer units can combine (a) head-to-head, (b) tail-to-tail or (c) head-to-tail with the latter one being the most usual one (see Figure 4).

For the configuration three different

structures are possible: (i) syndiotactic (*st*) (i.e. the methyl groups are located *on the opposite side* of the polymer backbone), (ii) isotactic (*it*) (i.e. the methyl groups are located *on the same side* of the polymer backbone) and (iii) atactic (*at*) (i.e. the methyl groups are located *randomly on both sides* of the polymer backbone) (see Figure 5).

<sup>10</sup> Maier C., Haber T. (1998) Polypropylene: The Definitive User's Guide and Databook (Plastics Design Library), William Andrew, Norwich, USA.

<sup>11</sup> Schneider B., Doscocilova D. (2000) Structures of polyolefins, in: Handbook of polyolefins (Vasile C., ed.) Marcel Dekker, New York, USA, 161-222.

Most commercial PPs are predominantly *it* (90 – 95 %) with only small amounts of *st* and *at* segments. Isotactic PP produced with Ziegler-Natta catalysts shows the highest degree of crystallinity and stiffness and tensile strength due to its regular, repeating arrangement.

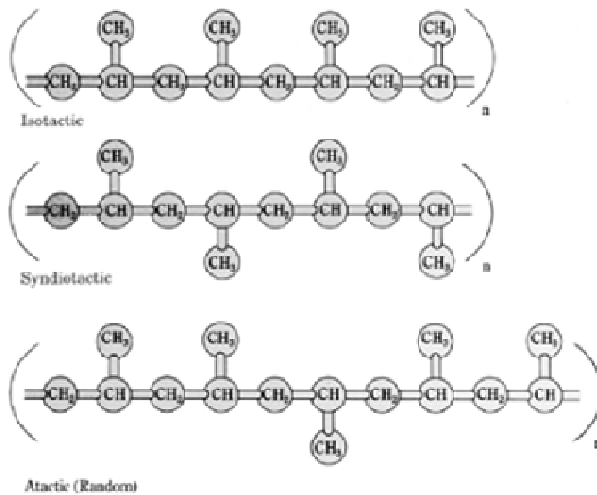


Figure 5. Configurational structures in PP (taken from <sup>10</sup>).

Isotactic PP is quite similar to PE-HD, however, it has a lower density (0.9 g/cm<sup>3</sup>), a higher maximum service temperature and is more susceptible to oxidation.

Syndiotactic PP is produced with metallocene catalysts and shows lower crystallinity but better impact strength and clarity values. Due to its irregular structure *at* PP is sticky and amorphous and used for adhesives and roofing tars<sup>10</sup>.

(3) Additivation of PE and PP is necessary to protect the polymer from degradation through oxidation and/or to influence the processability, structure and properties. Additives can be classified according to their application area in processing additives (slip agents etc.), stabilizers (antioxidants, UV stabilizers), static inhibitors, flame retardants, colour, plasticizers, nucleating agents and fibres and fillers.

It is known that the combination of several additives can have some antagonistic effects. For example, report Barrett et al.<sup>12</sup> that sterically hindered phenols used as antioxidants are rapidly consumed by hindered amine light stabilizers (HALS) and therefore is no longer available for catching radicals formed from the polymer degradation.

Bertin and his coworkers<sup>13</sup> could show that talc as filler material induces a decomposition of a sterically hindered phenol used as antioxidants in polymers. Further they showed that by addition of the talc not only the antioxidant is degraded but also absorbed onto the talc surface and therefore not longer available for an antioxidative effect in the PP matrix. During this work this described phenomena was observed for a talc filled PP material. The highly odour-active unknown compound which turned up is most probably correlated to this degradation of the

<sup>12</sup> Barret J., Gijsman P., Swagten J., Lange R.F.M. (2002) Polym. Degrad. Stab. 76:441–448.

<sup>13</sup> Bertin D., Boutevin B., Rigal G., Fourty G. (1998) Eur. Polym. J. 34:163-170.

phenolic antioxidant in the presence of talc. Sauer<sup>14</sup> proposed a reaction pathway as shown in Scheme 1.

All phenolic based antioxidants were screened and similar behaviour was found for all of them in the presence of talc. In Scheme 1 the general pathway is shown for the easiest phenolic antioxidants 2,6-ditert.-butyl-4-methyl phenol (BHT). His findings were supported by HS-SPME-GC-MS measurements carried out at the Institute with mixtures of talc and BHT, which was heated to 200°C for 1, 5, 10 and 20 min leading to the stepwise degradation of the BHT and the formation of mono-tert.-butyl phenol (MTBP) and the pure phenol by a dealkylation step as shown in Scheme 1 and Figure 6.

Additionally, various unsaturated alkenes as multiples of C<sub>4</sub> are generated by cationic polymerization of the 2-methyl-1-propene (2-MP) as shown in step (5). 2-MP is generated by the release of the tert.-butyl groups from the phenolic antioxidants.

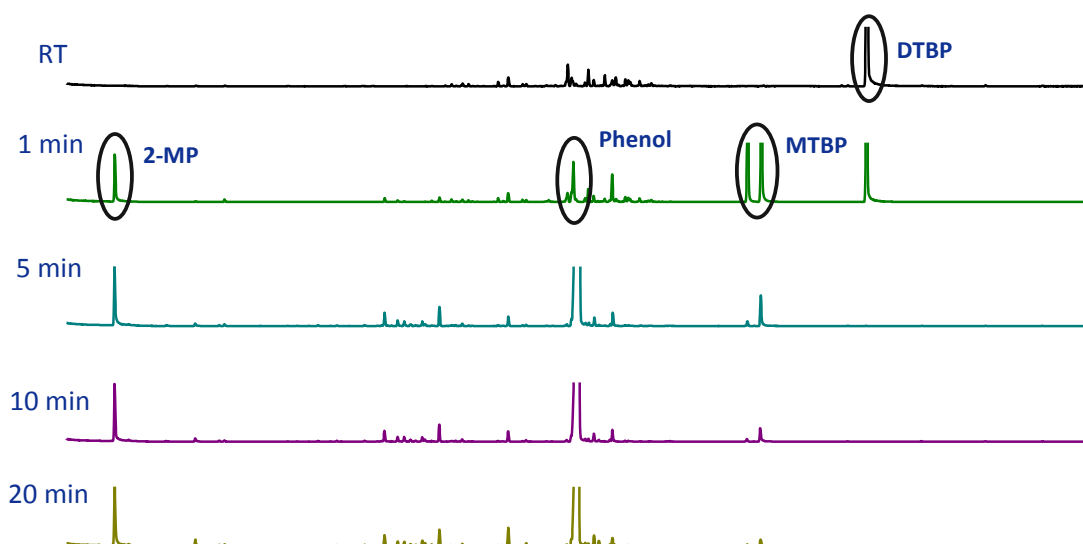
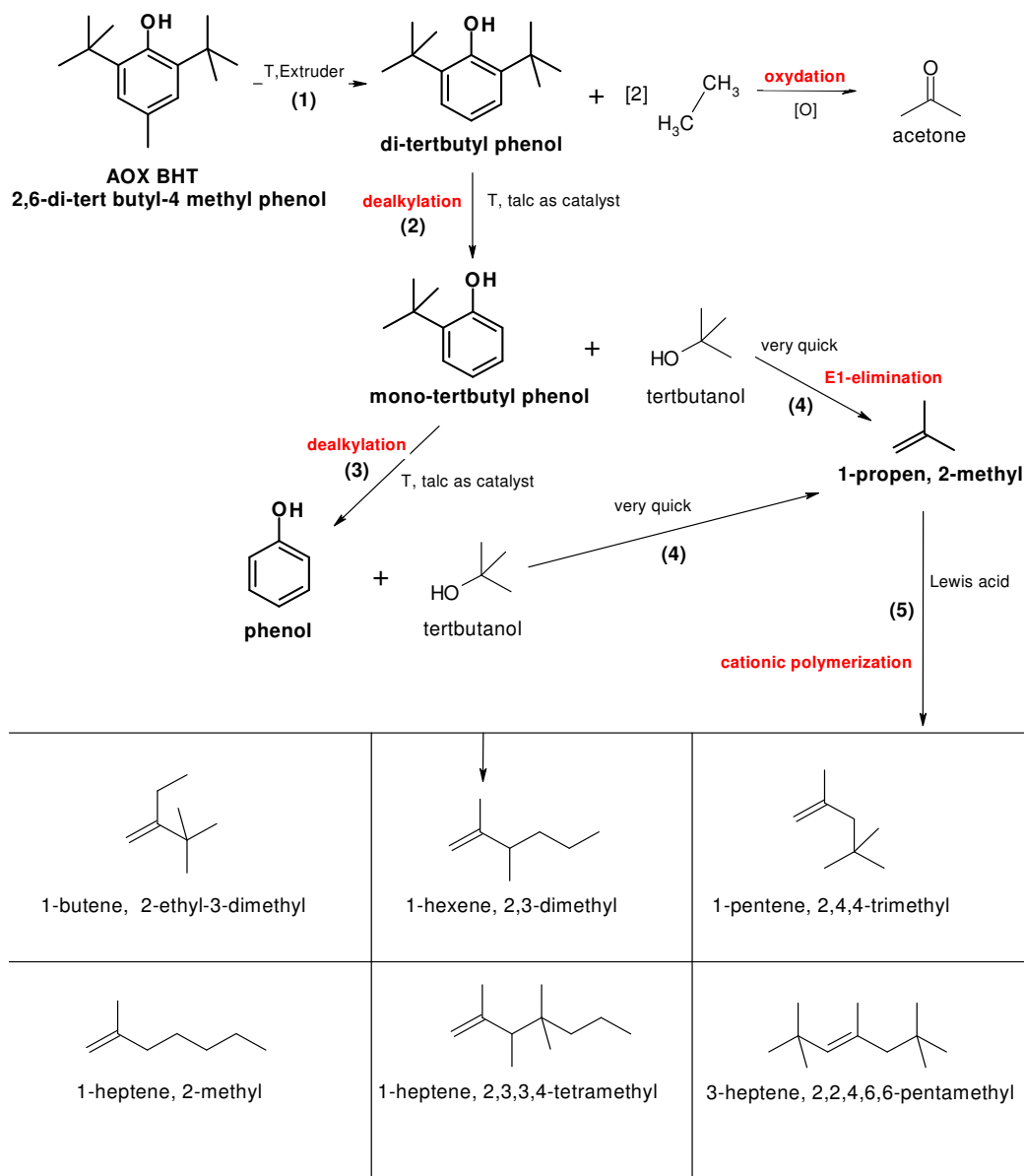


Figure 6. HS-SPME-GC-MS chromatograms of mixtures of BHT and talc heated at 200 °C for 1, 5, 10 and 20 min showing the subsequent degradation of the di-tert.-butylphenol (DTBP) to the mono-tert.-butylphenol (MTBP) and the phenol and the formation of 2-methyl-1-propene (2-MP) as predicted by C. Sauer<sup>14</sup> shown in Scheme 1 (taken from <sup>14</sup>).

<sup>14</sup> Sauer C. (2007) Internal Technical report, Borealis Polyolefine GmbH.



Scheme 1. Reaction pathway of phenolic antioxidant degradation in the presence of talc proposed by Sauer<sup>14</sup>.

(4) PE and PP can be processed by extrusion, including injection moulding and blow moulding. Typical processing temperatures (mass temperatures  $T_M$ ) are given in Table 1. Due to the high temperatures during the processing in the presence of oxygen degradation of the polymer occurs. Although during the processing the amount of oxygen is reduced as the extrusion or injection moulding screw is completely filled with molten polymer, oxidation reactions take place characterized by chain scission and chain extension.

**Table 1. Typical mass temperatures ( $T_M$ ) for processing of PE and PP materials.**

typical $T_M$ <sup>8</sup> [°C]	injection moulding	blow moulding	film and pipe extrusion	cable coatings
PE-LD	160 – 260	140	210	230
PE-HD	260 – 300	160 – 190	230 – 250	250 – 270
PE-LLD	-	-	250 – 380	210 – 235
PP	250 – 270	220 - 270		-

During the processing the availability of the oxygen is restricted and only two ways are known how oxygen is entering the machine: (a) oxygen is absorbed onto the polymer surface where more oxygen is absorbed on powder than on granules due to the higher specific surface area. (b) oxygen is dissolved in the amorphous phase of the polymer<sup>15</sup>. Epacher<sup>15</sup> investigated the process stability of PE-HD depending on the oxygen content. The group showed by polarography measurements that about 20 – 25 ppm oxygen is absorbed and more oxygen was estimated to be dissolved in the polymer (40 – 70 ppm). Different oxygen levels in the processing machine were realised by working in (a) inert atmosphere realized by degassing of the polymer powder and replacing the oxygen by argon and (b) changing the oxygen content in a wide range realized by increasing the number of degassing cycles and exchanging the atmosphere.

It could be proven that the amount of absorbed oxygen can be controlled by the number of degassing cycles or by introducing oxygen into the hopper of the machine. In their final findings they concluded that the stability of the PE-HD (measured as the degree of yellowness and the viscosity) decreases with increasing oxygen content and therefore processing must be excluded from all processing steps to the highest degree possible. It was also shown that the stabilization of the PE-HD is not able to completely eliminate the deterioration of the oxygen on the polymer.

A similar conclusion is drawn by Andersson and his group<sup>16</sup>. They analyzed the degradation of PE-LD, PE-LLD and PE-HD during film extrusion and found out that the antioxidants were not able to prevent the oxidation of the polymer in the air gap (in film extrusion the polymer is vertically extruded through a orifice into a water bath; the distance between the exit of the orifice and the water bath is called the air gap and is the place where the molten polymer is exposed to atmospheric oxygen and oxidation takes place).

Both publications prove that processing is a significant contributor to the formation of oxygen species and therefore oxygen related odour-active compounds could be reduced by reducing the oxidation reactions during processing.

<sup>15</sup> Epacher E., Tolveth J., Kröhnke C., Pukansky B. (2000) *Polymer* 41:8401-8409.

<sup>16</sup> Andersson T., Stalbmom B., Wesslen B. (2004) *J. Appl. Polym. Sci.* 91:1525-1537.



## 2.4. Degradation and oxidation of polyolefins

Degradation of polyolefins is a radical initiated chain reaction with degenerated branching. Tüdös and Iring<sup>17</sup> summarized the kinetics of thermal polyolefin degradation in one diagram (see Figure 7) including an autocatalytic type for the absorption of oxygen as well as for the formation of end-products (a), reaching-a-maximum type as seen for the concentration of intermediates (propagating radicals, hydroperoxides) as well as for the mass of the polymer (b), and a decreasing type for the average length of the macromolecules due to fragmentation (c).

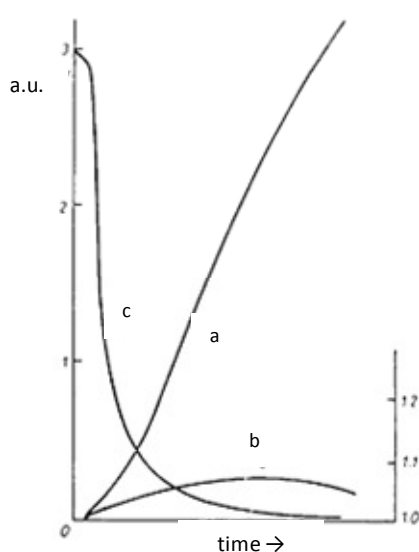


**Figure 7.** Kinetics of the main processes in polyolefin degradation. (a) absorption of  $O_2$ , formation of end products; (b) intermediates, mass change; (c) molecular mass<sup>17</sup>.

Generally, two different types of reactions occur during oxidation as shown by Albertsson<sup>18</sup>: (i) solid state reactions which add oxidation species to the polymer backbone (e.g. formation of hydroperoxide groups on the polymer chain) and (ii) reactions which lead to the formation of volatile products described by Bernstein<sup>19</sup> as “...two chain cleavage events need to liberate a volatile molecule ...”.

Three pathways for the oxidation product formation are known including hydroperoxide decomposition, where the majority of the products derive from, the transformation of peroxy radicals and the radical termination reactions.

About 80% of the end products result from PE hydroperoxides and about 90% of the end products derive from PP hydroperoxides.

### 2.4.a. Degradation mechanisms of PE<sup>17</sup>

The mechanisms of polyolefin degradation in the absence of additives can be described by well-known sequences of reactions<sup>20</sup>. The first step - the initiation or starting reaction, is the formation of free radicals as shown in reaction (1). Here, the  $R^*$  backbone radical plays an important role for the propagation of the oxidation. The  $R^*$  further reacts in several prolongation steps with oxygen

<sup>17</sup> Tüdös F., Iring M. (1988) Acta Polymerica 39:19-26.

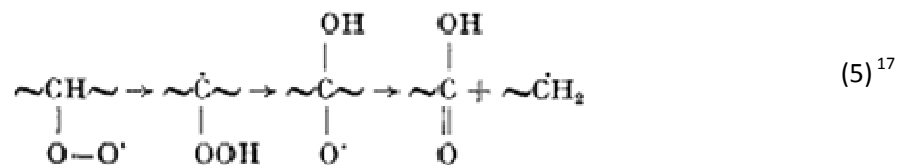
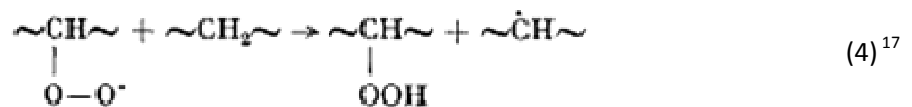
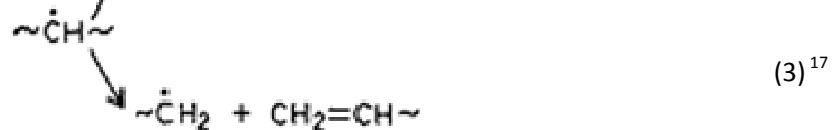
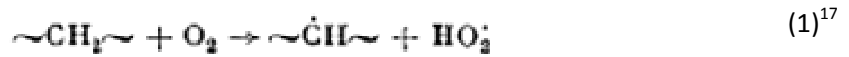
<sup>18</sup> Albertsson A.-C., Gröning M., Hakkarainen M. (2006) J. Polym. Environ. 14:9-13.

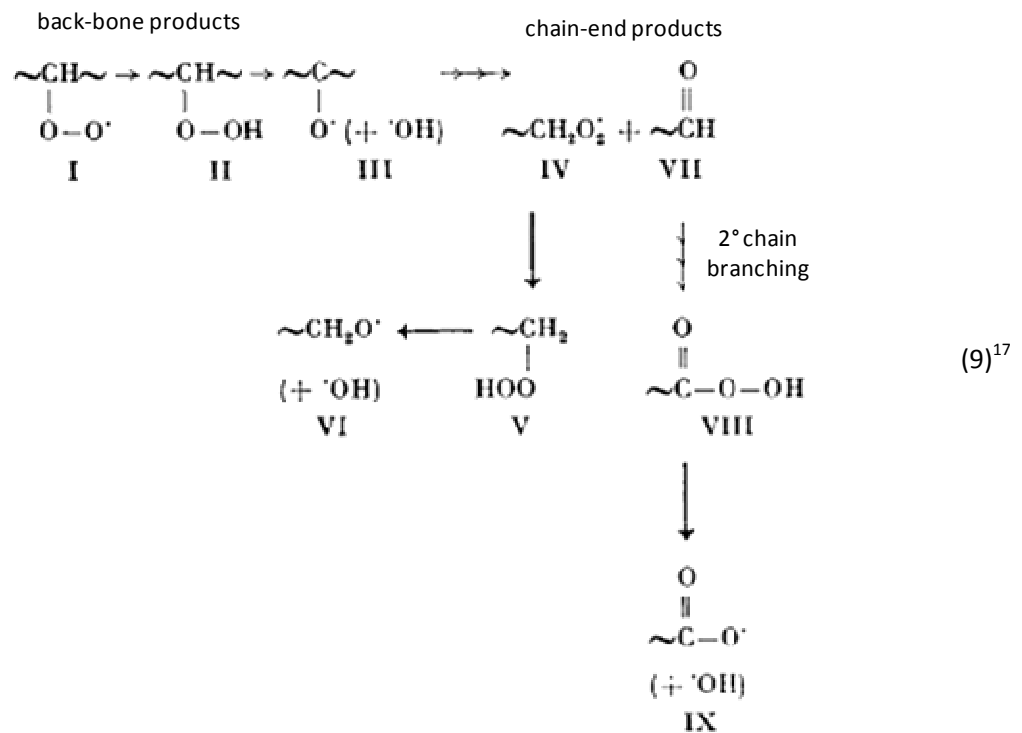
<sup>19</sup> Bernstein R., Thornberg S.M., Assink R.A., Irwin A.N., Hochrein J.M., Brown J.R., Derzon D.K., Klamo S.B., Clough R.L. (2007). Polym. Degrad. Stab. 92:2076-2094.

<sup>20</sup> Hoff A., Jacobsson S. (1981) J. Appl. Polym. Sci. 26:3409-3423.

(2), is transformed to a vinyl end group and a chain-end hydrocarbon radical (3). Reactions (2) and (3) are competitive depending on the oxygen supply. From reaction (2) the hydroperoxide is most likely formed by the attack at the tertiary C-atom of another polymer chain (4). The transformation of  $RO_2^*$  radicals leads to the formation of a carbonyl group and a chain-end hydrocarbon radical (5). The chain-end hydrocarbon radical is further oxidized to a chain-end peroxy radical (6) or reacts to low molecular hydrocarbons (e.g. ethylene) (7). By hydrogen abstraction the chain-end peroxy radical forms a hydroperoxide group and a backbone radical (8).

The further reactions of the hydroperoxides yield the end products aldehydes (acetaldehydes is the dominating product), carboxylic acids, ketones,  $\gamma$ -lactones and esters (9).





It is reported<sup>20</sup> that during the processing two different conditions are present for the formation of oxidized volatiles: (1) partially on and under the surface of the polymer melt with restricted oxygen amount and (2) partially in the gas phase, rich in oxygen, where already volatile decomposition fragments are further oxidized.

The gas phase is most probably contributing more to the formation of short chain oxidized compounds.

Hoff and Jacobssen<sup>20</sup> studied the thermo-oxidation of PE between 264 and 289°C and were able to identify alcohols, aldehydes, ketones, carboxylic acids, cyclic ethers and cyclic esters. The oxygen-containing products were found in a majority compared to the hydrocarbons; the most abundant compounds were fatty acids (formic acid, acetic acid, propionic acid, butyric acid, isovaleric acid, crotonic acid, caproic acid, hydroxyvaleric acid) followed by aldehydes (formaldehyde, acetaldehyde, propanal, isobutanal, butanal, pentanal, acrolein) and ketones (acetone, 1-buten-3-one, 2-butanone, 2-pentanone, 2-hexanone) and lactones (butyrolactone and valerolactone). More acids were generated for PE-HD than for PE-LD.

#### **2.4.b. Degradation mechanisms of PP<sup>21,17</sup>**

For degradation of PP the combination of high temperatures and oxygen is needed, as in vacuum PP is stable up to 300°C as shown by Frank<sup>21</sup>. The degradation reaction is autocatalytic and is preceded by an induction period. With increasing degradation hydroperoxides and carbonyls are formed, the molecular mass decreases, the polymer loses the chemical, mechanical, optical and electrical properties. Especially unstabilized PP is more prone to oxidation than unstabilized PE due to the presence of the methyl side chain and the reactive hydrogen at the tertiary C-atom. This circumstance has the following consequences<sup>17</sup>: (1) a high probability of intramolecular chain transfer and (2) the oxidation rate of hydrocarbon radicals can be measured with the probabilities of the other competitive reactions. Compared to PE in PP the number of propagating radicals and active intermediates is higher<sup>17</sup>. PP also evolves more volatiles than PE<sup>17</sup>.

Due to the intramolecular chain transfer, hydroperoxide sequences decompose to several active species; with highest probability dihydroperoxides are formed<sup>17</sup>.

The initiation or starting reaction is the attack on the tertiary C-atom leading to a backbone tertiary peroxy radical, which forms a hydrocarbon radical (see reaction I-II). This radical is further oxidized or forms new macroradical species via chain scission (see reaction III). The primary hydrocarbon macroradical (III a) is oxidized in intra- or intermolecular chain transfer reactions and lead to terminal mono- or dihydroperoxides. These hydroperoxides lead to the formation of the end products in numerous reactions shown in (IV) including ketones, carboxylic acids,  $\gamma$ -lactones and esters. The ketones derive mainly from decomposed secondary backbone hydroperoxides; the carboxylic acids are formed involving chain scission in either a radical decomposition of peroxides via the aldehyde group or via direct transformation of the peroxy radical.

Hoff and Jacobsen<sup>22</sup> summarized their conclusions about thermo-oxidative degradation of PP at processing temperatures between 240 °C and 290 °C as such:

- (1) In the initial phase of PP oxidation the absorbed oxygen is nearly quantitatively used for the formation of hydroperoxides.
- (2) The hydroperoxide concentration depends on the oxygen pressure rather than the temperature.
- (3) The formation of hydroperoxide sequences, mainly dihydroperoxides is observed during PP oxidation.

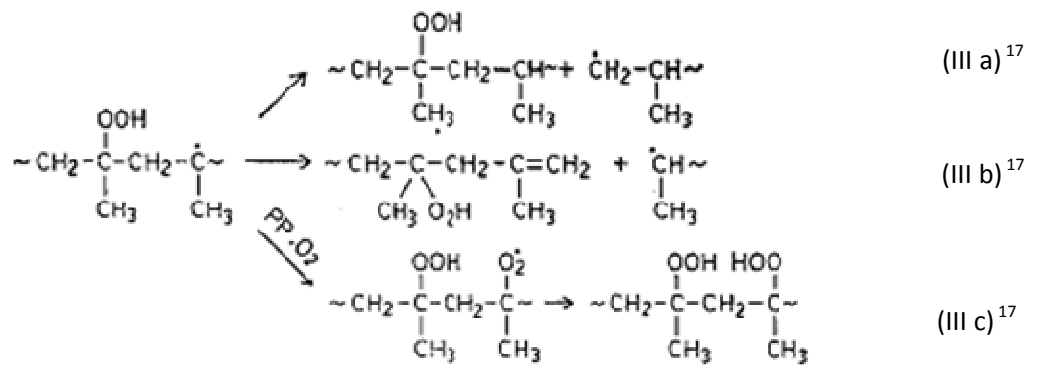
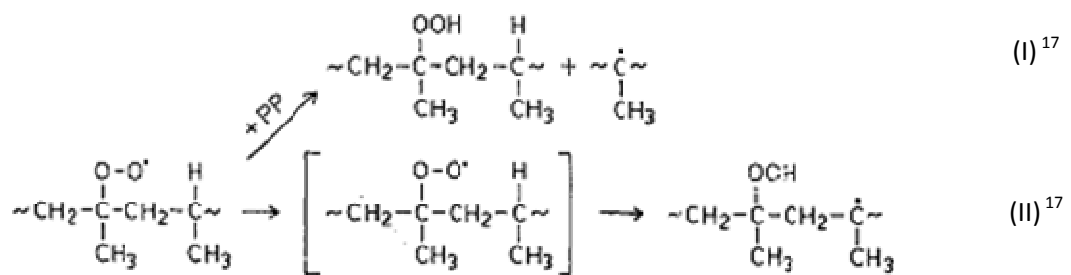
---

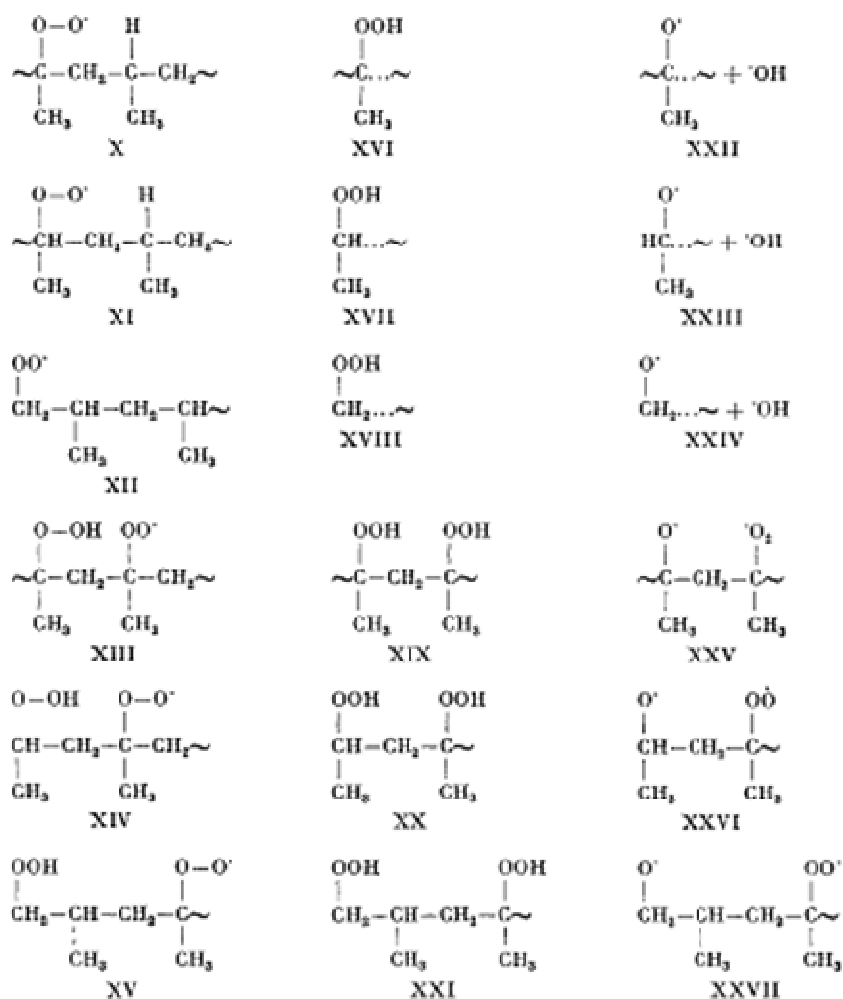
<sup>21</sup> Frank H.P. (1976) J. Polym. Sci. Symp. 57:311-318.

<sup>22</sup> Hoff A., Jacobssen S. (1982) J. Appl. Polym. Sci. 27:2539-2551.

(4) An increase in the temperature leads to an increasing oxygen absorption, and this oxygen uptake is linearly correlated with the volatiles formation.

Further, it could be shown that all the volatile products produced are a result of the decomposition of the PP hydroperoxides. It is believed that the fragmentation of the alkoxy radical is the principal process for lowering the molecular weight of PP by formation of volatile compounds.



(IV)<sup>17</sup>

Similar to PE, the majority of the volatiles are oxygen-containing compounds such as aldehydes (formaldehyde, acetaldehyde, propanal, 2-methylacrolein), ketones (acetone, 2-butanone, 2-pentanone, 1-hydroxy-2-propanone, methyl cyclopropyl ketone, acetylacetone), alcohols (methanol, 2-methyl-2-propen-1-ol), acids (formic acid, acetic acid) and ethers (methyl formiate). Acetic acid was shown not to form directly from the PP hydroperoxide decomposition but from further reactions of oxidized products. Especially ketones are believed to be plausible precursors, as ketones are among the main products of thermal oxidation in PP.

For the formation of carbonyls as final oxidation product from thermal oxidation of PP Richaud et al.<sup>23</sup> performed a kinetic study and were able to prove that carbonyls are the final product in the oxidation process starting with the building-up of hydroperoxides.

<sup>23</sup> Richaud E., Farcas F., Fayolle B., Audouin L., Verdu J. (2007) Polym. Degrad. Stab. 92:118-124.

### 2.5. Odour-active compounds identified in polyolefins

For polyolefins such as PE and PP several authors<sup>25-31</sup> identified the numerous odour-active compounds in the polymer itself formed during processing and compounding. More publications were found dealing with multi-layer samples (e.g. PE-aluminium-cardboard), but these findings were not included as it was not clear which compound comes from the polyolefin layer and which not.

A list of all identified substances including aldehydes, ketones, carboxylic acids, esters, lactones, aromatic compounds, alcohols and hydrocarbons and, if available, the sensory threshold values determined in water for each compound are given in Table 2. Among these reported compounds the aldehydes and ketones show the lowest values. By further differentiation among those two groups the compounds with a chain length of 6 to 8 C-atoms show the lowest threshold values in the homologous series and the 1-alkene-3-ones show the lowest sensory threshold values overall. Normal concentrations of odour-active carbonyls are in the lower  $\mu\text{g}$  per kg range and below, but can dramatically increase after severe thermal treatment as shown by Bravo<sup>26</sup>. In this work PE was heated in glass vessels for 15 min at 250 °C.

Other reported sources for odour problems with plastic products are interactions of the polymer with additives and/or printings where e.g. ink components migrate through the polymer into the product and react there to odour-active compounds<sup>24</sup>.

However, most publications deal only with a qualitative identification and do not give actual concentrations most probably due to the problems associated with the quantification of odour-active compounds in polyolefins such as the low concentration range, co-elution and interferences with non-odour-active compounds and the difficulties to use more selective detection systems. If reported the concentrations of identified compounds are also listed. The concentrations given are taken from three publications, whereas the by Bravo<sup>26</sup> determined concentrations after a heavy degradation of PE samples. The values given by Rebeyrolle-Bernard<sup>29</sup> are marked as g/kg, but after consideration of the sample preparation the values are most probably given as  $\mu\text{g}/\text{kg}$ .

---

<sup>24</sup> Piringer O., Rüter M. (2000) in: Plastic Packaging Materials for Food (Piringer O., Baner A.L., ed.), 407-426, Wiley-VCH, Weinheim.

**Table 2.** List of identified odour-active compounds in PE and PP samples in numerous publications with their sensory threshold values determined in water taken from <sup>32</sup>.

Compound	Amount <sup>#*~</sup> [µg/kg]	found in	Sensory threshold values in water <sup>+</sup> [µg/kg]	Identified by
<b>Aldehydes</b>				
butanal		PE-LD	0.007 – 0.0373	Villberg <sup>25</sup>
pentanal		PE-LD	0.012 – 0.1	Villberg <sup>25</sup>
hexanal	177,000 in PE <sup>26</sup>	PP, PE-HD, PE-LD	0.0025 – 0.75	Bravo <sup>26</sup> , Tyapkova <sup>27</sup> , Villberg <sup>28</sup> , Villberg <sup>25</sup>
heptanal	3.2 in PP <sup>29</sup>	PP, PE-LD	0.03 – 0.06	Rebeyrolle-Bernard <sup>29</sup> , Villberg <sup>25</sup>
octanal	107,000 in PE <sup>26</sup> , 5.4 in PP <sup>29</sup>	PP, PE-LD	0.000 41 – 0.248	Bravo <sup>26</sup> , Rebeyrolle- Bernard <sup>29</sup> , Tyapkova <sup>27</sup> , Villberg <sup>25</sup>
nonanal	97,000 in PE <sup>26</sup> , 12.2 in PP <sup>29</sup>	PP, PE-HD, PE-LD	0.001 – 0.1	Bravo <sup>26</sup> , Rebeyrolle- Bernard <sup>29</sup> , Skjervak <sup>30</sup> , Tyapkova <sup>27</sup> , Villberg <sup>28</sup> , Villberg <sup>25</sup>
decanal	10.3 in PP <sup>29</sup>	PP, PE-HD, PE-LD	0.0001 – 0.0058	Rebeyrolle-Bernard <sup>29</sup> , Skjervak <sup>30</sup> , Villberg <sup>25</sup>
undecanal	10.2 in PP <sup>29</sup>	PP, PE-LD	0.000 41 – 0.01	Rebeyrolle-Bernard <sup>29</sup> , Villberg <sup>25</sup>
dodecanal	12.5 in PP <sup>29</sup>	PP, PE-LD	0.00053 – 0.002	Rebeyrolle-Bernard <sup>29</sup> , Villberg <sup>25</sup>
tridecanal		PE-LD	0.008 – 0.07	Villberg <sup>25</sup>
tetradecanal	9.3 in PP <sup>29</sup>	PP	0.053 – 0.067	Rebeyrolle-Bernard <sup>29</sup>
pentadecanal		PE-LD	0.43 - 1	Villberg <sup>25</sup>
methylhexanal		PE-HD	-	Villberg <sup>28</sup>
2-methylpropanal		PE-LD	0.0004 – 0.01	Villberg <sup>25</sup>
2-methylpropanal		PE-LD	0.0004 – 0.01	Villberg <sup>25</sup>

<sup>25</sup> Villberg K., Veijanen A. (2001) *Anal. Chem.* 73:971-977.

<sup>26</sup> Bravo A., Hotchkiss J.H., Acree T.E. (1992) *J. Agric. Food Chem.* 40:1881-1885.

<sup>27</sup> Tyapkova O., Czerny M., Buettner A. (2009) *Polym. Degrad. Stab.* 94:757-769.

<sup>28</sup> Villberg K., Veijanen A., Gustafsson I., Wickström K. (1997) *J. Chromatogr., A* 791:213-219.

<sup>29</sup> Rebeyrolle-Bernard P., Etievant P. (1993) *J. Appl. Polym. Sci.* 49:1159-1164.

<sup>30</sup> Skjervak I., Due A., Gjerstad K.O., Herikstad H. (2003) *Water Res* 37:1912-1920.



Compound	Amount <sup>#**</sup> [µg/kg]	found in	Sensory threshold values in water <sup>+</sup> [µg/kg]	Identified by
2-methylpropanal		PE-LD	0.0004 – 0.01	Villberg <sup>25</sup>
4-methylpentanal		PE-LD	0.39	Villberg <sup>25</sup>
2,3-dimethylhexanal		PE-LD	-	Villberg <sup>25</sup>
2,3-dimethylpentanal		PE-LD	-	Villberg <sup>25</sup>
2-ethylbutanal		PE-LD	0.041 – 0.081	Villberg <sup>25</sup>
(E)-2-propenal (acrolein)		PE-LD	0.11	Villberg
(E)-2-butenal		PE	0.525	Villberg <sup>25</sup>
(E)-2-pentenal		PE	0.31 – 1.5	Villberg <sup>25</sup>
(E)-2-hexenal		PE	0.03	Villberg <sup>25</sup>
(E)-2-octenal		PE-HD	0.000 34 – 0.02	Villberg <sup>28</sup>
(E)-2-nonenal	11,000 in PE <sup>26</sup>	PE, PP	0.000 08 – 0.000 4	Bravo <sup>26</sup> , Tyapkova <sup>27</sup>
(Z)-2-nonenal		PP	0.000 02	Tyapkova <sup>27</sup>
(Z)-4-nonenal		PP	-	Tyapkova <sup>27</sup>
(E)-2-decenal		PP	0.0003 – 0.25	Tyapkova <sup>27</sup>
2-methyl-2-propenal		PE-LD	-	Villberg <sup>25</sup>
2-ethylpropenal		PE-LD	-	Villberg <sup>25</sup>
8-nonenal		PE-HD	-	Sanders <sup>31</sup>
(E,E)-2,4-heptadienal		PE-HD	0.058 – 0.8	Villberg <sup>28</sup>
2,4-undecadienal		PE-HD	0.000 01	Villberg <sup>28</sup>
(E,Z)-2,6-nonadienal		PP	0.000 0018 – 0.000 14	Tyapkova <sup>27</sup>
(E)-4,5-epoxy-(E)2-decenal		PP	0.00012 – 0.005	Tyapkova <sup>27</sup>
<b>Ketones</b>				
propanone (acetone)		PE, PP	0.832 – 10,000	
2-pentanone		PE-LD	0.01 - 4	Villberg <sup>25</sup>
3-hexanone		PE-LD	0.041 – 0.081	Villberg <sup>25</sup>
2-heptanone		PE-LD	0.001 – 4.6	Villberg <sup>25</sup>
3-heptanone		PE-LD	0.0075 – 0.16	Villberg <sup>25</sup>
2-decanone		PE-HD	0.003 – 0.041	Skjervak <sup>30</sup>

<sup>31</sup> Sanders R.A., Zyzak D.V., Morsch T.R., Zimmerman S.P., Searles P.M., Srothers M.A., Eberhart B.L., Woo A.K. (2005) J. Agric. Food Chem. 53:1713-1716.

Compound	Amount <sup>#*~</sup> [µg/kg]	found in	Sensory threshold values in water <sup>+</sup> [µg/kg]	Identified by
2-undecanone		PE-HD	0.007 – 0.082	Skjervak <sup>30</sup>
2-dodecanone		PE-HD	0.042 – 0.083	Skjervak <sup>30</sup>
3-methyl-2-butanone		PE-LD	0.81 – 1.67	Villberg <sup>25</sup>
5-methyl-3-hexanone		PE-LD	0.040 – 0.081	Villberg <sup>25</sup>
3-methyl-2-hexanone		PE-LD	0.041 – 0.083	Villberg <sup>25</sup>
3-methyl-2-heptanone		PE-LD	-	Villberg <sup>25</sup>
4-methyl-2-heptanone	18.5 in PP <sup>29</sup>	PP	-	Rebeyrolle-Bernard <sup>29</sup>
3,3-dimethyl-2-butanone		PE-LD	-	Villberg <sup>25</sup>
4,4-dimethyl-2-pentanone		PE-LD	0.0081 – 0.040	Villberg <sup>25</sup>
2,3-dimethylcyclobutanone		PE-LD	-	Villberg <sup>25</sup>
4-ethylcyclohexanone		PE-HD, PE-LD	-	Villberg <sup>28</sup> , Villberg <sup>25</sup>
unknown methyl ketone	15.8 in PP <sup>29</sup>	PP	-	Rebeyrolle-Bernard <sup>29</sup>
methylpentenone		PE-HD	-	Villberg <sup>28</sup>
2,3-butandione	n.d. <sup>26</sup>	PE	0.003 – 2.3	Bravo <sup>26</sup>
1-hepten-3-one	< 2,000 in PE <sup>26</sup>	PE	0.00004	Bravo <sup>26</sup>
1-octen-3-one	< 2,000 in PE <sup>26</sup>	PE, PP	0.000 089 – 0.004	Bravo <sup>26</sup> , Tyapkova <sup>27</sup>
1-nonen-3-one	< 2,000 in PE <sup>26</sup>	PE, PP	0.000 000 008	Bravo <sup>26</sup> , Tyapkova <sup>27</sup>
3-buten-2-one		PE-LD	-	Villberg <sup>25</sup>
3-penten-2-one		PE-LD	0.0015 – 1.2	Villberg <sup>25</sup>
7-octen-2-one		PE-LD	-	Villberg <sup>25</sup>
<b>Carboxylic acids</b>				
acetic acid		PP, PE-LD	22 – 1,000	Tyapkova <sup>27</sup> , Villberg <sup>25</sup>
propanoic acid		PE-LD	0.1 – 40.3	Villberg <sup>25</sup>
butanoic acid	91.9 in PP <sup>27</sup>	PP, PE-LD	0.05 - 40	Tyapkova <sup>27</sup> , Villberg <sup>25</sup>
pentanoic acid	102 in PP <sup>27</sup>	PP, PE-LD	0.28 – 4.7	Tyapkova <sup>27</sup> , Villberg <sup>25</sup>
hexanoic acid	230 in PP <sup>27</sup>	PP, PE-LD	0.093 – 10	Tyapkova <sup>27</sup> , Villberg <sup>25</sup>
heptanoic acid		PE-LD	0.64 – 10.4	Villberg <sup>25</sup>

Compound	Amount <sup>#*~</sup> [µg/kg]	found in	Sensory threshold values in water <sup>+</sup> [µg/kg]	Identified by
octanoic acid	159 in PP <sup>27</sup>	PP, PE-LD	0.91 - 19	Tyapkova <sup>27</sup> , Villberg <sup>25</sup>
tetradecanoic acid	69.5 in PP <sup>29</sup>	PP	10	Rebeyrolle-Bernard <sup>29</sup>
hexadecanoic acid	245.7 in PP <sup>29</sup>	PP	-	Rebeyrolle-Bernard <sup>29</sup> , Tyapkova <sup>27</sup>
2-/3-methylbutanoic acid	8.3 in PP <sup>27</sup>	PP	0.01 – 9.3	Tyapkova <sup>27</sup>
2,2-dimethylpropanoic acid		PE-LD	5.0 - 50	Villberg <sup>25</sup>
phenylacetic acid		PP	1	Tyapkova <sup>27</sup>
<b>Esters</b>				
ethyl propanate		PE-HD	0.0089 – 1.9	Villberg <sup>28</sup>
ethyl hexanoate		PE-HD	0.00001 – 0.22	Skjervak <sup>30</sup>
ethyl octanoate		PE-HD	0.005 – 1.0	Skjervak <sup>30</sup>
ethyl (E,Z)-2,4-decadienoate		PE-HD	0.1	Skjervak <sup>30</sup>
propyl hexanoate		PE-HD	-	Skjervak <sup>30</sup>
butyl acetate		PE-HD	0.01 - 38	Skjervak <sup>30</sup>
butyl acrylate		PE-HD	0.002 – 0.02	Villberg <sup>28</sup>
butyl hexanoate		PE-HD	-	Skjervak <sup>30</sup>
hexyl acetate		PE-HD	0.0043 – 8.2	Skjervak <sup>30</sup>
hexamethyl butanoate		PE-HD	-	Skjervak <sup>30</sup>
hexyl hexanoate		PE-HD	6.4	Skjervak <sup>30</sup>
isobornyl acetate		PE-HD	-	Skjervak <sup>30</sup>
2,2,4-trimethyl-1,3-pentenediol-diisobutyrate		PE-HD	-	Skjervak <sup>30</sup>
<b>Lactones</b>				
γ-nonalactone		PP	0.025	Tyapkova <sup>27</sup>
γ-decalactone		PP	0.001 – 0.6	Tyapkova <sup>27</sup>
γ-undecalactone		PP	0.06	Tyapkova <sup>27</sup>
γ-dodecalactone		PP	0.007	Tyapkova <sup>27</sup>

Compound	Amount <sup>#*~</sup> [µg/kg]	found in	Sensory threshold values in water <sup>+</sup> [µg/kg]	Identified by
<b>Terpenoids</b>				
α-pinene		PE-HD	0.006 - 2.08	Skjervak <sup>30</sup>
Δ-carene		PE-HD	0.77	Skjervak <sup>30</sup>
limonene		PE-HD	0.004 - 1	Skjervak <sup>30</sup>
α -terpinolene		PE-HD	0.041 – 0.2	Skjervak <sup>30</sup>
α -farnesene		PE-HD	-	Skjervak <sup>30</sup>
<b>Aromatic compounds</b>				
4-methylphenol (p-cresol)		PP	0.055 – 0.2	Tyapkova <sup>27</sup>
3-ethylphenol		PP	0.8	Tyapkova <sup>27</sup>
toluene		PE-HD	0.024 - 5	Skjervak <sup>30</sup> , Villberg <sup>28</sup>
benzene		PP	0.072 - 111	Skjervak <sup>30</sup>
ethyl benzene		PP	0.0024 – 1.2	Skjervak <sup>30</sup>
2-/ 3-/ 4-dimethylbenzene (o-/ m-/ p-xylene)		PP	1 – 1.8 / 1 – 1.1 / 0.53 - 1	Skjervak <sup>30</sup>
vinylbenzene (styrene)		PP	0.0036 – 0.73	Skjervak <sup>30</sup>
isopropyl benzene		PP	0.07 – 0.1	Skjervak <sup>30</sup>
propyl benzene		PP	-	Skjervak <sup>30</sup>
ethyl methyl benzene		PP	-	Skjervak <sup>30</sup>
1,3,5-trimethyl benzene		PP	0.003 – 0.7	Skjervak <sup>30</sup>
1,2,4-trimethyl benzene		PP	0.26 – 0.5	Skjervak <sup>30</sup>
isopropyl toluene		PP	-	Skjervak <sup>30</sup>
naphthalene		PP	0.0068 – 0.5	Skjervak <sup>30</sup>
vanillin		PP	0.058 – 66.7	Tyapkova <sup>27</sup>
ethylvanillin		PP	0.1	Tyapkova <sup>27</sup>
2,6-di-tert.-butylquinone	142.2 in PP <sup>29</sup>	PP	-	Rebeyrolle-Bernard <sup>29</sup>
2,6-di-tert.-butylbenzoquinone		PE-HD	-	Skjervak <sup>30</sup>

Compound	Amount <sup>#*~</sup> [µg/kg]	found in	Sensory threshold values in water <sup>+</sup> [µg/kg]	Identified by
2,6-di-tert.-butylphenol	446.6 in PP <sup>29</sup>	PP, PE-HD	0.2	Rebeyrolle-Bernard <sup>29</sup> , Skjervak <sup>30</sup>
2,6-di-tert.-butyl-4-methylphenol		PE-HD	1	Skjervak <sup>30</sup>
2,6-di-tert.-butyl-4-ethylphenol	47.3 in PP <sup>29</sup>	PP	-	Rebeyrolle-Bernard <sup>29</sup>
2,6-di-tert.-butyl-4-propylphenol	7.5 in PP <sup>29</sup>	PP	-	Rebeyrolle-Bernard <sup>29</sup>
<b>Alcohols</b>				
1-decanol	12.0 in PP <sup>29</sup>	PP	0.0066 – 0.775	Rebeyrolle-Bernard <sup>29</sup>
1-dodecanol	14.4 in PP <sup>29</sup>	PP	0.016 – 0.158	Rebeyrolle-Bernard <sup>29</sup>
tetradecanol	2.5 in PP <sup>29</sup>	PP	-	Rebeyrolle-Bernard <sup>29</sup>
hexadecanol	9.7 in PP <sup>29</sup>	PP	-	Rebeyrolle-Bernard <sup>29</sup>
octadecanol	199.9 in PP <sup>29</sup>	PP	-	Rebeyrolle-Bernard <sup>29</sup>
<b>Alkanes and Alkenes</b>				
pentamethyl-heptane		PE-HD	-	Villberg <sup>28</sup>
1-dodecene		PE-HD	-	Villberg <sup>28</sup>

<sup>#</sup> Values determined by Bravo<sup>26</sup> were achieved after heavy thermal degradation of PE. <sup>\*</sup> Values taken from Rebeyrolle-Bernard<sup>29</sup> at lowest processing temperatures applied. <sup>~</sup> Values determined by Tyapkova<sup>27</sup> in non-irradiated PP. <sup>+</sup> literature values taken from<sup>32</sup>

### 2.5.a. Identification of odour-active compounds in polyolefins with Retention Indices (RI)

The concept of Retention Indices (RI) was introduced by Kovats<sup>33</sup> and Dool<sup>34</sup> to characterize compounds according to their retention behaviour independent of their actual retention time which depends on the column flow and configuration. The independent normalized RI can then be used for databases and for identification of unknown compounds. In most cases temperature-programmed relative RIs are used<sup>35</sup>.

<sup>32</sup> Van Gemert L.J. (2003) Odour Thresholds, Oliemans Punter&Partners BV, The Netherlands.

<sup>33</sup> Kovats E. (1958) Hel. Chim. Acta 41:1915-1920.

<sup>34</sup> Dool H, Kratz P.(1963) J Chrom. 11:463-471.

<sup>35</sup> Farkas P., Le Quere J.L, Maarse H., Kovac M. (1994) in: Maarse H., van der Heij D.G. (ed.), Trends in Flavour Research, Elsevier Science B.V., The Netherlands.

For this, homologous series of n-alkanes serve as reference compounds which are designated with RIs established from their number of C-atoms times 100 (e.g. n-octane has 8 C-atoms and therefore the RI of 800). For all other compounds the RI is interpolated between the two n-alkanes in which the compound is eluting according to

$$RI = 100 \cdot x + 100 \cdot \frac{(RT_x - RT_z)}{(RT_{z+1} - RT_z)}$$

Other RI concepts uses ethyl esters as reference compounds but the Kovat's RI concept is the most used one.

Farkas et al.<sup>35</sup> defined standard parameter which enable (1) a separation of a wide range of compounds in one run, (2) a retention of low-boiling compounds by applying a start temperature of 35°C, (3) the use of either a split, splitless or on-column injection and (4) use an optimized linear carrier gas velocity for hydrogen carrier gas for a temperature range up to 250°C for establishing a RI database.

Considering all these parameters one is able to determine the RIs of many compounds and to compare these RIs with reference databases such as<sup>65,66,67</sup>.

Given parameters can easily be adapted to other column dimensions based on these equations applying a linear carrier velocity of 36cm/s at 143°C per definition:

$$k = \frac{r \cdot t_0}{\beta}$$

whereas

k ...ratio

r ... temperature ramp

t<sub>0</sub> ... carrier gas hold-up time

β ... phase ratio of used column;  $\beta = \frac{r}{2 \cdot FT} = \frac{ID}{4 \cdot FT}$

For using a column of different dimensions under similar conditions, the equation is expressed for the new temperature ramp r by using the given k, the calculated phase ratio β and after the dead time t<sub>0</sub> was either measured experimentally or by using a flow calculation software (e.g. FlowCalc, Version A.02.07, Hewlett-Packard, Toronto, Canada).

For an identification of odour-active compounds three conditions have to be met<sup>36</sup>

(1) The RI of the unknown compound in the sample is determined on two columns of different polarity and these values match with the RI of a reference standard.

<sup>36</sup> Molyneux R.J., Schieberle P. (2007) J. Agric. Food Chem. 55:4625-4629.

(2) The mass spectra of the compound is clear and matches with the reference spectra

(3) The odour impression of the unknown compound is the same as the impression of the reference in a certain concentration.

Only if all three conditions are met, an odour-active compound is successfully identified.

For this reason, RIs are a valuable and crucial tool for the identification of odour-active compounds, especially in cases where other identification criteria fail e.g. no clear and distinct mass spectra or the lack of a pure reference standard.

### **3. Materials and Methods**

#### **3.1. Polyolefin samples**

In Table 3 a list of all analyzed polyolefin samples with their lot number, type and other information is given together with the corresponding analytical program.



**Table 3. List of all polyolefin samples which were analyzed during the thesis.**

No.	Sample description	Lot no.	Sample form	Type	Additional information	Section
BO29	MB471WG-9014	28006474	pellets	PP	compound PP, with talc	4.4
BO30	MB471WG-9014-01	28006470	pellets	PP	compound PP, with talc	4.4
BO32	L140WG-06	4130003102	plaques ( $T_M=200^\circ\text{C}$ )	PP	compound grade	4.2
BO33	L140WG-06	4130003102	plaques ( $T_M=260^\circ\text{C}$ )	PP	compound grade	4.2
BO34	WG140 AI-06	4080000771	pellets	PP	compound grade	4.2
BO35	WG140 AI-05	4080000770	pellets	PP	compound grade	4.2
BO36	L140WG-06	4130003102	pellets	PP	compound grade	4.2
BO37	L140WG-06	4130003102	plaques ( $T_M=230^\circ\text{C}$ )	PP	compound grade	4.2
BO38	WG140AI-05	4080000770	plaques ( $T_M=200^\circ\text{C}$ )	PP	compound grade	4.2
BO39	WG140AI-05	4080000770	plaques ( $T_M=230^\circ\text{C}$ )	PP	compound grade	4.2
BO40	WG140AI-05	4080000770	plaques ( $T_M=260^\circ\text{C}$ )	PP	compound grade	4.2
BO41	BF970MO	3170005751	pellets	PP	compound grade, PP5, Schwechat	4.3
BO42	BF970MO	3170005751	plaques ( $T_M=230^\circ\text{C}$ )	PP	compound grade, PP5, Schwechat	4.3
BO43	FB2230	2400000618	pellets	PE	reactor grade, PE4, Schwechat	4.3
BO44	FB2230	2400000618	plaques ( $T_M=230^\circ\text{C}$ )	PE	reactor grade, PE4, Schwechat	4.3
BO45	RJ900MO	B6869	pellets	PP	visbroken, catalyst BCF02P, MFI=100 g/10 min	4.6
BO46	RE450MO	B6870	pellets	PP	catalyst BCF02P, MFI=13 g/10 min	4.6

No.	Sample description	Lot no.	Sample form	Type	Additional information	Section
BO47	RE450MO	B6888	pellets	PP	catalyst RCL05P, MFI=13 g/10 min	4.6
BO48	RJ900MO	B6889	pellets	PP	visbroken, catalyst RCL05P, MFI=100 g/10 min	4.6
BO49	EE188AI-9530	4020001484	pellets	PP	compound grade, Schwechat	4.3
BO50	EE188AI-9530	4020001484	plaques (T <sub>M</sub> =230 °C)	PP	compound grade, Schwechat	4.3
BO51	BS2581	2210004326	pellets	PE	Burghausen	4.3
BO52	BS2581	2210004326	plaques (T <sub>M</sub> =230 °C)	PE	Burghausen	4.3
BO53	BE677AI-10	3160006008	pellets	PP	Schwechat	4.3
BO54	BE677AI-10	3160006008	plaques (T <sub>M</sub> =230 °C)	PP	Schwechat	4.3
BO55	EF015AE	7A11EAC3	pellets	PP	Kallo	4.3
BO56	EF015AE	7A11EAC3	plaques (T <sub>M</sub> =230 °C)	PP	Kallo	4.3
BO57	EE188AI-9524	C1-7114	pellets	PP	compound grade, Beringen	4.3
BO58	EE188AI-9524	C1-7114	plaques (T <sub>M</sub> =230 °C)	PP	compound grade, Beringen	4.3
BO59	BS2581	2210004156	pellets		Burghausen	4.3
BO60	BS2581	2210004156	plaques (T <sub>M</sub> =230 °C)		Burghausen	4.3
BO61	BE677AI	3160006008	pellets		Schwechat	4.3
BO62	BE677AI	3160006008	plaques (T <sub>M</sub> =230 °C)		Schwechat	4.3
BO63	EF015AE	7D02EAA1	pellets		Kallo	4.3
BO64	EF015AE	7D02EAA1	plaques (T <sub>M</sub> =230 °C)		Kallo	4.3

No.	Sample description	Lot no.	Sample form	Type	Additional information	Section
BO65	EE188HP-1048	2800	pellets ( $T_C^*=220\text{ }^\circ\text{C}$ )	PP	compound grade, Monza	4.5
BO66	EE188HP-1048	2800 Z025	plaques ( $T_M=230\text{ }^\circ\text{C}$ )	PP	compound grade, Monza	4.5
BO67	72959/1		pellets ( $T_C=220\text{ }^\circ\text{C}$ )	PP	compound grade, reference	4.5
BO68	72959/1		plaques ( $T_M=230\text{ }^\circ\text{C}$ )	PP	compound grade, reference	4.5
BO69	72959/2		pellets ( $T_C=260\text{ }^\circ\text{C}$ )	PP	compound grade, compounding at $260\text{ }^\circ\text{C}$	4.5
BO70	72959/2		plaques ( $T_M=230\text{ }^\circ\text{C}$ )	PP	compound grade, compounding at $260\text{ }^\circ\text{C}$	4.5
BO71	72959/3		pellets ( $T_C=220\text{ }^\circ\text{C}$ )	PP	compound grade, changed base polymer	4.5
BO72	72959/3		plaques ( $T_M=230\text{ }^\circ\text{C}$ )	PP	compound grade, changed base polymer	4.5
BO73	72959/4		pellets ( $T_C=220\text{ }^\circ\text{C}$ )	PP	compound grade, no talc	4.5
BO74	72959/4		plaques ( $T_M=230\text{ }^\circ\text{C}$ )	PP	compound grade, no talc	4.5
BO75	72959/5		pellets ( $T_C=220\text{ }^\circ\text{C}$ )	PP	compound grade, no colour MB	4.5
BO76	72959/5		plaques ( $T_M=230\text{ }^\circ\text{C}$ )	PP	compound grade, no colour MB	4.5
BO77	72959/6		pellets ( $T_C=220\text{ }^\circ\text{C}$ )	PP	compound grade, no epicote	4.5
BO78	72959/6		plaques ( $T_M=230\text{ }^\circ\text{C}$ )	PP	compound grade, no epicote	4.5
BO79	72959/7		pellets ( $T_C=220\text{ }^\circ\text{C}$ )	PP	compound grade, reduced heat stabilization	4.5
BO80	72959/7		plaques ( $T_M=230\text{ }^\circ\text{C}$ )	PP	compound grade, reduced heat stabilization	4.5
BO81	72959/8		pellets ( $T_C=220\text{ }^\circ\text{C}$ )	PP	compound grade, reduced scratch additive	4.5

No.	Sample description	Lot no.	Sample form	Type	Additional information	Section
BO82	72959/8		plaques ( $T_M=230\text{ }^\circ\text{C}$ )	PP	compound grade, reduced scratch additive	4.5
BO83	72959/9		pellets ( $T_C=220\text{ }^\circ\text{C}$ )	PP	compound grade, no UV stabilisation	4.5
BO84	72959/9		plaques ( $T_M=230\text{ }^\circ\text{C}$ )	PP	compound grade, no UV stabilisation	4.5
BO85	ME 3440	20B06217 Nr.2, 9689	pellets	PE	Stenungsund	4.3
BO86	ME 3440-05	20B06438	pellets	PE	Stenungsund	4.3
BO88	RJ370MO (T101)		pellets		RJ370MO + Tx101 (liquid), MFI=45 g/10 min	4.7
BO89	RJ370MO (T301)		pellets		RJ370MO + Tx301 (liquid), MFI=45 g/10 min	4.7
BO90	HD120MO (T101)		pellets		HD120MO +Tx101 (MB5%), MFI=12.5 g/10 min	4.7
BO91	HD120MO (T101)		pellets		HD120MO +Tx101 (MB5%), MFI=50 g/10 min	4.7
BO92	HD120MO (T101)		pellets		HD120MO +Tx101 (MB5%), MFI=100 g/10 min	4.7
BO93	HD120MO (T301)		pellets		HD120MO +Tx301 (MB25%), MFI=50 g/10 min	4.7
BO94	HD120MO		pellets		HD120MO reference, MFI=8 g/10 min	4.7
BO95	FB2230	5080147	pellets	PE	reactor grade, PE2 Porvoo	4.3

No.	Sample description	Lot no.	Sample form	Type	Additional information	Section
BO96	HE3490-07	20B06480	pellets	PE		4.9
BO97	HE3490-07	20B06484	pellets	PE		4.9
BO98	HE3490-07	20B06482	pellets	PE		4.9
BO99	HE3490-07	20B06475	pellets	PE		4.9
BO100	HE3490-07	20B06486	pellets	PE		4.9
BO101	HE3490-07	20B06485	pellets	PE		4.9
BO102	HE3490-07	20B06487	pellets	PE		4.9
BO103	HE3490-07	20B06488	pellets	PE		4.9
BO104	HE3490-07	20B06489	pellets	PE		4.9
BO105	HE3490-1MO2	20B06491	pellets	PE		4.9
BO106	ME3440-05	Test	pellets	PE		4.9
BO107	HE3490-1MO2	20B06492	pellets	PE		4.9
BO108	HE3490-1MO2	20B06494	pellets	PE		4.9
BO109	ME3440-05	20B06500	pellets	PE		4.9
BO110	ME3440-05	20B06497	pellets	PE		4.9
BO111	ME3440-05	20B06501	pellets	PE		4.9
BO112	ME3440-05	20B06503	pellets	PE		4.9

No.	Sample description	Lot no.	Sample form	Type	Additional information	Section
BO113	HE3470-05	20B06529	pellets	PE		4.9
BO114	HE3470-05	20B06531	pellets	PE		4.9
BO115	HE3470-05	20B06534	pellets	PE		4.9
BO116	HE3470-05	20B06535	pellets	PE		4.9
BO117	HE3490-07	20B06536	pellets	PE		4.9
BO118	HE3490-07	20B06537	pellets	PE		4.9
BO119	HE3490-07	20B06538	pellets	PE		4.9
BO120	HE3490-07	20B06539	pellets	PE		4.9
BO121	HE3490-07	20B06540	pellets	PE		4.9
BO122	HE3490-07	20B06541	pellets	PE		4.9
BO123	HE3490-07	20B06543	pellets	PE		4.9
BO124	HE3490-07	20B06544	pellets	PE		4.9
BO125	HE3490-07	20B06546	pellets	PE		4.9
BO126	HE3490-07	20B06545	pellets	PE		4.9
BO127	HE3490-07	20B06548	pellets	PE		4.9
BO128	HE3490-07	20B06549	pellets	PE		4.9
BO129	HE3490-07	20B06550	pellets	PE		4.9

No.	Sample description	Lot no.	Sample form	Type	Additional information	Section
BO130	HE3490-07	20B06551	pellets	PE		4.9
BO131	HE3490-07	20B06552	pellets	PE		4.9
BO132	HE3490-H01	20B06554	pellets	PE		4.9
BO133	HE3490-H01	20B06555	pellets	PE		4.9
BO134	HE3490-H01	20B06557	pellets	PE		4.9
BO135	ME3440-05	20B06569	pellets	PE		4.9
BO136	ME3440-05	20984099	pellets	PE		4.9
BO137	ME3440-05	20984103	pellets	PE		4.9
BO138	ME3440-05	20984155	pellets	PE		4.9
BO139	ME3440-05	20B06572	pellets	PE		4.9
BO140	ME3440-05	20B06574	pellets	PE		4.9
BO153	HD120MO		powder	PP	unstabilized powder, stored cool, dark and under N <sub>2</sub>	4.7
BO154	HD120MO		powder	PP	stabilized powder (compounded and milled from 79676-09)	4.7
BO155	CMB126 7052		pellets		colour MB for RA130E-8427	4.7
BO156	CMB347 3715	413000	pellets		colour MB for EE188AI-HP	4.7
BO65	EE188HP-1048	2800	pellets	PP	compound PP	4.11

No.	Sample description	Lot no.	Sample form	Type	Additional information	Section
BO66	EE188HP-1048	2800 Z025	plaques	PP	compound PP	4.11
BO75	EE188AI-HP natural		pellets	PP	compound PP	4.11
BO76	EE188AI-HP natural		plaques	PP	compound PP	4.11
BO157	RA130E natural	627720	pellets	PP	colour MB for RA130E-8427	4.11
BO158	MB471WG natural	28007687	pellets	PP	compound PP	4.4
BO159	RA130E-8427	626470	pellets	PP	compound PP	4.11
BO160	CMB441 9014	ITNA137561			colour MB for MB471WG-9014 01	4.11
BO161	ME3440		powder	PE	unstabilized powder, stored cool, dark and under N <sub>2</sub>	4.7
BO162	ME3440		powder	PE	stabilized powder, stored cool, dark and under N <sub>2</sub>	4.7
BO158	MB471WG natural	28007687	pellets	PP	compound PP, reference, 1x extruded	4.4
BO163	MB471WG natural	83593-01	pellets	PP	compound PP, 2x extruded	4.4
BO164	MB471WG natural	83593-03	pellets	PP	compound PP, 4x extruded	4.4
BO165	MB471WG natural	83593-06	pellets	PP	compound PP, 7x extruded	4.4
BO166	MB471WG natural	83593-09	pellets	PP	compound PP, 10x extruded	4.4
BO167	MB471WG natural	83593-12	pellets	PP	compound PP, 13x extruded	4.4
	DEHY-63001	63001	propylene		22/6/09 11; sample before purification	4.12



No.	Sample description	Lot no.	Sample form	Type	Additional information	Section
	DEHY-63103	63103	propylene		22/6/09 11, sample after purification	4.12
	Air from lab in Linz					4.12
BO168	BJ368MO	3170007714	pellets	PP		4.13
BO169	BJ368MO	3170007714	boxes	PP	labelled boxes, produced in France (??)	4.13
BO170	Competitor (Total)		boxes	PP	labelled boxes, produced in France (??)	4.13
BO171	11343 PP white MB	Ampacet	pellets		colour MB for boxes from France	4.13
BO172	BJ368MO	3170007714	boxes	PP	unlabelled boxes, produced in Belgium	4.13
BO173	BJ368MO	3170007714	boxes	PP	labelled boxes, produced in Belgium (Becel)	4.13
BO174	Competitor (Total)		boxes	PP	labelled boxes, produced in Belgium (Becel)	4.13
BO175	In-mould Label		label		in-mould label from Belgium (Becel)	4.13
BO178	BJ368MO	3170007714	boxes	PP	labelled boxes, produced in Belgium (Superfors)	4.13
BO179	BJ368MO-03	3170007988	plaques ( $T_M=260\text{ }^\circ\text{C}$ )	PP	sample 1; MFR=77.26 g/10min	4.13
BO180	BJ368MO-03	3170007988	plaques ( $T_M=280\text{ }^\circ\text{C}$ )	PP	sample 1; MFR=77.26 g/10min	4.13
BO181	BJ368MO-03	3170007988	plaques ( $T_M=300\text{ }^\circ\text{C}$ )	PP	sample 1; MFR=77.26 g/10min	4.13
BO182	BJ368MO	3170007985	plaques ( $T_M=260\text{ }^\circ\text{C}$ )	PP	sample 2;	4.13

No.	Sample description	Lot no.	Sample form	Type	Additional information	Section
BO183	BJ368MO	3170007985	plaques ( $T_M=280$ °C)	PP	sample 2	4.13
BO184	BJ368MO	3170007985	plaques ( $T_M=300$ °C)	PP	sample 2	4.13
BO185	BJ368MO;	3170007983	plaques ( $T_M=260$ °C)	PP	sample 3	4.13
BO186	BJ368MO	3170007983	plaques ( $T_M=280$ °C)	PP	sample 3	4.13
BO187	BJ368MO	3170007983	plaques ( $T_M=300$ °C)	PP	sample 3	4.13
BO188	BJ368MO	3170007983	pellet	PP	sample 3	4.13
BO189	BJ368MO	3170007985	pellet	PP	sample 2	4.13
BO190	BJ368MO	3170007988	pellet	PP	sample 1	4.13
BO191	ME 3440	1109149	pellet	PE	reactor grade, PE2 Porvoo	4.3
BO192	ME 3440	5090313	pellet	PE	reactor grade, Borouge	4.3
BO193	ME 3440	20B07066	pellet	PE	reactor grade, PE3 Stenungsund	4.3
BO206	Total m-PP		pellet	PP	competitor material (Total), metallocene-PP	4.15
BO207	Total m-PP		plaques	PP	competitor material (Total), metallocene-PP	4.15

$T_M$  ... mass temperature during injection moulding;  $T_C$  ... mass temperature during compounding

### 3.2. Sample preparation techniques

#### 3.2.a. Simultaneous Distillation/Extraction (SDE)<sup>37</sup>

Simultaneous Distillation/Extraction (SDE) is a well-established technique for isolation or extraction of volatile compounds from a non-volatile matrix. SDE is very useful for isolation of odour-active compounds intended for a GC analysis as water steam works on the one hand as the extraction media purging out the volatiles of the matrix and leaving the non-volatiles back and on the other hand as a selective solvent where non-water soluble compounds such as plasticisers in polymers are not extracted. This is in a big contrast to normal extraction techniques using e.g. n-hexane where also non-volatiles are extracted.

Additionally, in SDE a concentration of the volatiles is facilitated.

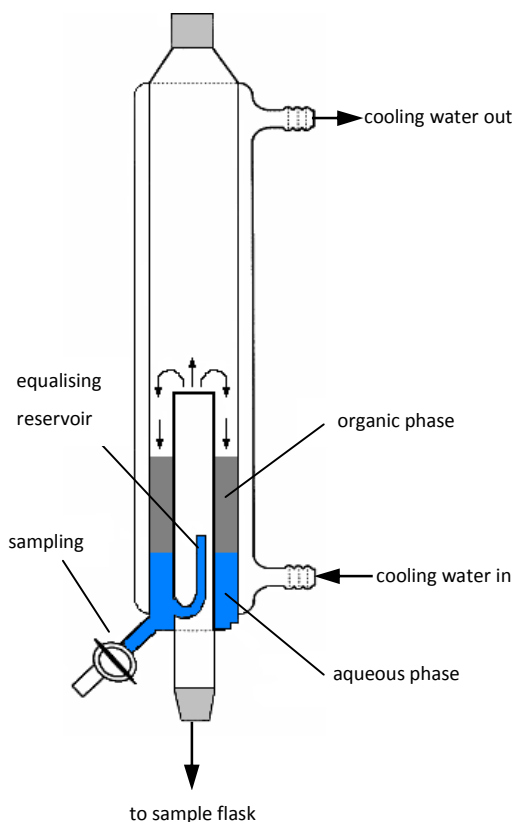


Figure 8. SDE apparatus according to.<sup>38</sup>

In general, an aqueous solution or a water slurry of the solid material is boiled under constant stirring in a round flask connected to a distillation leg. Simultaneously, a water-non-soluble organic solvent is vaporized in another flask or part of the apparatus and distilled in a distillation leg too. Both vapours condense in a cooled leg or cooled part of the apparatus and extraction takes place in between the two liquid phases on the condenser surface. Then water and solvent are collected, decanted and returned to their respective flasks.

For all sample extractions we applied a SDE apparatus according to<sup>38</sup> obtained from a local glass manufacturer (Glasbläserei Bartelt, Graz, Austria). Compared to a conventional Likens-Nickerson SDE<sup>39</sup> and various modifications for example described by Lindner et al.<sup>40</sup> this

<sup>37</sup> Chaintreau A. (2001) *Flav. Frag.* 16:136-138.

<sup>38</sup> Veith G.D., Kiwus L.M. (1977) *Bull. Environ. Contam. Toxicol.* 17:631-636.

<sup>39</sup> Likens S.T., Nickerson G.B. (1964) *Am. Soc. Brew. Chem. Proc.*, 5-13.

<sup>40</sup> Filek G., Bergamini M., Lindner W. (1995) *J. Chromatogr., A*, 712:355-364.

apparatus is easier to handle and to clean. In a previous work Repnegg<sup>41</sup> could show that both apparatus give similar extraction and concentration efficiencies. The apparatus is shown in Figure 8. The apparatus itself is water cooled and directly connected to the tap water supply. On top of the Veith apparatus a Graham condenser is cooled down to -10 °C.

At the bottom, the apparatus is attached to a 2 L round flask filled with 900 ml deionised water, 500 to 750 mg sample material (pellets or moulded parts cut in pieces), 20 µg/kg internal standard (IS) 3,5,5-trimethyl-1-hexanal (TMH) dissolved in n-hexane (picograde, for residue analysis, Promochem, Wesel, Germany) and a Teflon® coated magnetic stir bar. The flask is heated with a magnetic stirring plate until boiling. In the Veith apparatus 25 ml deionized water and 25 ml n-pentane (picograde, for residue analysis, Promochem, Wesel, Germany) are filled whereas the n-pentane serves as collecting solvent. The water constantly drops back into the sample flask during the procedure from the equalising reservoir.

The procedure lasts for 4 hours after the water started to boil. After a cooling period of 30 min the n-pentane extract is collected and stored until use in a deep-freezer.

Each sample is extracted fivefold by using 6 apparatus in parallel, whereas one apparatus is used for a blank experiment to observe the whole sample preparation process. For the blank sample the complete procedure is carried out without the sample material but with the IS. Possible contaminations originating from the water or solvents used can be traced back<sup>37</sup>.

Prior to the sample extractions the whole apparatus is cleaned for 2 hours. For cleaning the system, the same procedure as described above is applied but one uses only 900 ml deionised water in the 2 L round flask. Organic extracts of the cleaning cycles are collected and stored in the deep-freezer.

Changeable glass ware and the stir bars are washed in a laboratory dish washer, rinsed with acetone (Brenntag, Vienna, Austria) and stored at 300 °C (flasks) and 100 °C (stir bars) in a laboratory oven until use.

### **3.2.b. Solid Phase Extraction (SPE)<sup>42</sup>**

Normal phase Solid Phase Extraction (SPE) was used for sample clean-up and separation of the interfering matrix from the odour-active compounds. Normal phase SPE is used to retain the more

---

<sup>41</sup> Repnegg F. (2001) *Geruchsaktive Verbindungen in Polyolefinen*, Dissertation, Graz University of Technology.

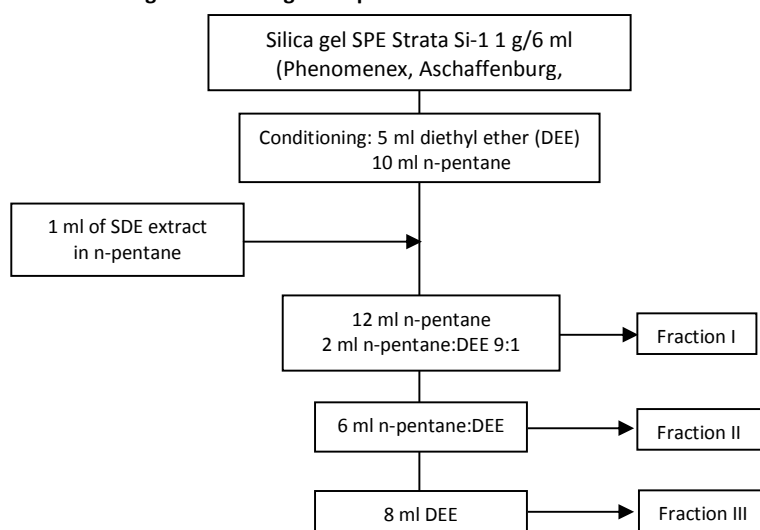
<sup>42</sup> Supelco (2009) *Normal Phase Solid Phase Extraction*, accessed 01/12/2010. <http://www.sigmaaldrich.com/analytical-chromatography/sample-preparation/spe/normalphase-methodology.html>

polar compounds and elute the non-polar compounds first, based on polar interactions such as hydrogen bonding,  $\pi$ - $\pi$ , dipole-dipole, and induced dipole-dipole interactions. For the retention of polar compounds in the SPE cartridge by interaction of the analytes and the sorbent material, the analytes must be introduced onto the SPE cartridge in a non-polar solvent such as n-pentane, n-hexane, diethyl ether (DEE) or chlorinated solvents (dichloromethane (DCM)).

The scheme for all normal phase SPE materials is similar: In a conditioning and equilibrium step the cartridge is loaded first with two to three times of the tube volume of the polar solvent and then with the non-polar solvent. Second, the cartridge is loaded with the sample dissolved in a non-polar solvent. Third, in a washing step the whole sample is brought onto the cartridge, and finally, analytes are eluted with increasingly polar solvents (or solvent mixtures) in succession in multiple compound classes.

The method developed by<sup>41</sup> was adapted to our needs and carried out as described here; all used solvents were of picograde purity (Promochem, Wesel, Germany):

**Scheme 1. Fractionation on silica gel SPE cartridges adapted from<sup>41</sup>.**



The fraction I and III were analyzed as received by GC-MS (3.3.b) whereas the fraction II was concentrated to 2 ml using a TurboVap 500 closed cell concentration evaporator (Caliper Life Sciences GmbH, Rüsselsheim, Germany) prior to the GC-MS measurements (3.3.b).

In previous works (Siegmund<sup>43</sup>, Repnegg<sup>41</sup>) it was shown that in fraction I most of the linear and branched alkanes and alkenes are eluted, in fraction II the odour-active carbonyls are collected and in fraction III all other compounds such as alcohols and acids are eluted.

### 3.2.c. Solid Phase Microextraction (SPME)

Solid Phase Microextraction (SPME) is an alternative approach to sampling and extraction invented by J. Pawliszyn<sup>44</sup>. The SPME device (see Figure 9) looks very similar to a conventional liquid syringe and consists of a thin supporting fibre (a) implemented in a fibre tubing (b) which can be retrieved into the piercing support needle (c) by using a plunger (d).

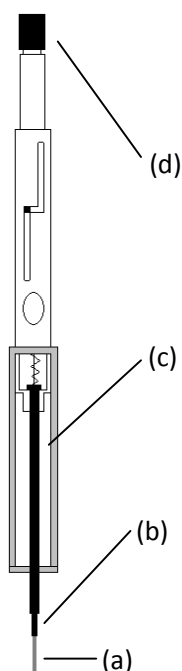


Figure 9. SPME device, annotation see text (adapted from<sup>44</sup>).

The advantages of SPME compared to other sampling techniques are that SPME is (1) solvent-free, (2) time-saving, (3) easy to introduce into the gas chromatography (GC) inlet and (4) able to simultaneously sample, extract and concentrate the analytes on the fibre<sup>44</sup>. In addition, SPME can be used either manually or with an autosampler.

Once, the analytes are ad- or absorbed onto the SPME fibre, the SPME device can be directly injected into the GC.

We used SPME both for GC-MS and GC-O analyses.

In all experiments a 2 cm StableFlex SPME fibre with a 50/30  $\mu\text{m}$  coating of Divinylbenzene and Carboxen on a Polydimethylsiloxane fibre (DVB/CAR/PDMS) from Supelco (Bellafonte, USA) was used. Based on previous analyses and the supplier's information this fibre is useful for [ ... analytes with a molecular mass between 40 and 275 g/mol. ... 2 cm StableFlex fibre is recommended for trace compound analysis.]<sup>45</sup>.

For GC analysis using SPME it is recommended to use an inlet liner with a reduced inner diameter to improve the peaks shape and height<sup>46</sup>. Additionally, the use of the 0.75 mm ID instead of the

<sup>43</sup> Siegmund B. (1997) *Untersuchung und Optimierung der Aromaeigenschaften eines Convenience-Food Produkts*, Dissertation, Graz University of Technology.

<sup>44</sup> Pawliszyn J. (1997) *Solid Phase Microextraction Theory and Practise*, Wiley-VCH, New York, USA.

<sup>45</sup> Supelco (2009) Product information, accessed on 01/12/2010. <http://www.sigmaaldrich.com/analytical-chromatography/analytical-products.html?TablePage=18156565>

<sup>46</sup> Supelco Technical note T397136A (1997) Reduce Inlet Liner ID for Sharper Peaks by SPME/GC, accessed 01/12/2010,

conventional 2 mm ID inlet liner increases the linear velocity through the liner and introduces the analytes in a narrow band onto the analytical column which is of extreme influence for highly volatile compounds.

In all analyses we used the 0.75 mm ID inlet liner (Supelco, Bellafonte, USA) for the SPME measurements. Different temperature programs for the compound extraction were applied ranging from 40 °C to 50 °C with an extraction time between 10 min to 20 min. In all experiments a thermostating time of 5 min and desorption time in the inlet liner of 10 min were used.

### 3.2.d. Derivatization<sup>47</sup>

Derivatization is a common technique in analytical chemistry and here especially for chromatography. For analysis of odour-active compounds in various more or less complicated matrices like foods, beverages or packaging materials it is used due to several reasons:

- to achieve a selective detection of analytes of interest in a more or less complicated matrix.
- to further improve the selectivity by insertion of a heteroatom-containing derivatization group in combination with a heteroatom-sensitive detector like a nitrogen-phosphorus detector (NPD), an electron-capture detector (ECD), a flame photometric detector (FPD), an atomic emission detector (AED) or mass spectrometry in selected ion monitoring mode (MS-SIM).
- to improve and lower detection limits by shifting analytes of interest to another retention area and/or a higher mass area with less interferences.

In contrast to post-chromatographic derivatization in liquid chromatography (i.e. derivatization *after* chromatographic separation and prior to detection) for gas chromatography (GC) pre-chromatographic derivatization (i.e. derivatization *prior* to GC separation) is applied mainly for

- enhancing the volatility of low volatile compounds.
- decreasing the polarity and therefore enhancing the detectability/elution of compounds such as organic acids or sugars.
- increasing the stability of thermal labile compounds which otherwise would be degraded in the gas chromatographic inlet.
- improving the separation of co-eluting compounds by shifting them further apart.

---

[http://www.sigmaaldrich.com/etc/medialib/docs/Supelco/Application\\_Notes/4676.Par.0001.File.tmp/4676.pdf](http://www.sigmaaldrich.com/etc/medialib/docs/Supelco/Application_Notes/4676.Par.0001.File.tmp/4676.pdf)

<sup>47</sup> Knapp D.R. (1979), *Handbook of Analytical Derivatization reactions*, Wiley-Interscience, New York, USA.

- improving the detectability by use of element-specific detectors (NPD, FPD, ECD, AED) by insertion of hetero-atoms (nitrogen, phosphorus, halogens) or using MS in SIM mode as “larger” mass fragments enable easier identification due to less interferences.
- separating optical active isomers by a selective reaction of the derivatization reagent of one of the isomers or by reaction with both enantiomers but giving better resolution of the isomers.
- selectively separating analytes of interest from a complex mixture (e.g. matrix) as shown for partially hydrogenated nitrogen-containing polycyclic aromatic hydrocarbons (PAHs) by derivatization with trifluoroacetyl chloride<sup>48</sup>.

The most common used derivatization reagent for carbonyls is *O*-(2,3,4,5,6-Pentafluorobenzyl)hydroxylamine hydrochloride (PFBHA). PFBHA reacts with carbonyls to the corresponding oximes and forms syn and anti isomers which are usually separated in the GC run (shown in Scheme 2).

A great number of publications about the use of PFBHA for derivatization of carbonyls can be found but most of them deal only with the saturated aldehydes. Schmarr and his group<sup>49</sup> determined alkanals, (E)-2-alkenals, (E,E)-2,4-alkadienals, aromatic aldehydes such as benzaldehyde and others as well as various ketones as their PFBHA derivatives by HS-SPME and GC-MSxMS in wines but admitted problems with the derivatization of unsaturated ketones such as the 1-alken-3-ones due to their prolonged reaction time needed for a quantitatively conversion (personal communication).

We showed<sup>50</sup> that PFBHA is not able to derivatize 1-alken-3-ones in an appropriate time whereas the alkanals, the (E)-2-alkenals and the (E,E)-2,4-alkadienals could be derivatised within 30 min at 80 °C.

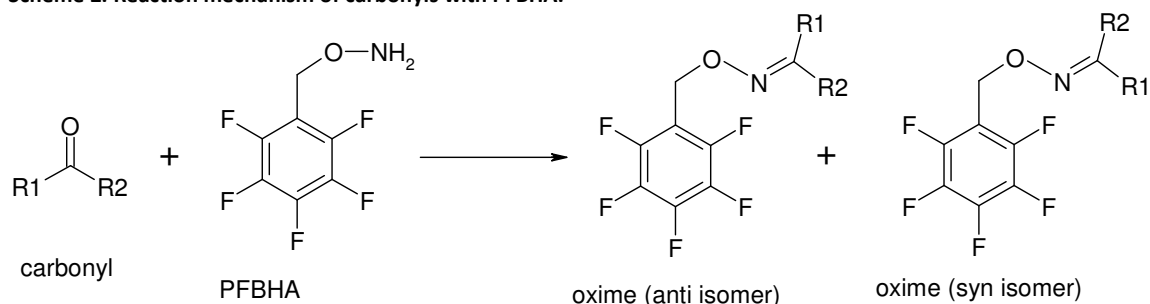
---

<sup>48</sup> Wood K.V., Schmidt C.E., Cooks R.G., Batts B.D. (1984) *Anal. Chem.* 56:1335-1338.

<sup>49</sup> Schmarr H.G., Potouridis T., Ganß S., Sang W., Köpp B., Bokuz U., Fischer U. (2008) *Anal. Chim. Acta* 617:119–131.

<sup>50</sup> Hopfer, H.; Haar, N.; Koraimann C., Leitner, E. (2009) 100 – 103; in: *Proceedings of the EURO FOOD CHEM XV* (H. Sorensen, S. Sorensen, A.D. Sorensen, J.C. Sorensen, K.E. Andersen, C. Bjerregaard, P. Moller, ed.), Faculty of Life Sciences, University of Copenhagen, Denmark



**Scheme 2. Reaction mechanism of carbonyls with PFBHA.**

However, PFBHA was used for derivatization of the fraction II in some programs.

The derivatization routine consists of two parts, in the first one the derivatization reagent is prepared and in the second one the carbonyls react with the reagent.

The derivatization reagent was prepared freshly each time prior to the derivatization.

- 200 µl aqueous PFBHA [50 g/L]
- + 200 µl CH<sub>2</sub>Cl<sub>2</sub> (picograde, for residue analysis, Promochem, Wesel, Germany)
- + 2-3 drops aqueous NaOH 2N
- Thoroughly stirring for 30sec with a vortex mixer (Heidolph, Schwabach, Germany)
- dispose the upper aqueous phase and use the lower halogen phase as derivatization reagent

The derivatization reaction was carried out as described here:

- 50 µl of the concentrated SDE extract in n-pentane
- + 20 µl derivatization reagent
- + 1000 µl n-hexane (picograde, for residue analysis, Promochem, Wesel, Germany)
- Thoroughly stirring for 30 sec with a vortex mixer (Heidolph, Schwabach, Germany)

⇒ reaction for 30 min at 80 °C in a heating block

- Cool down to room temperature
- Use the solution directly for the GC-MS analysis

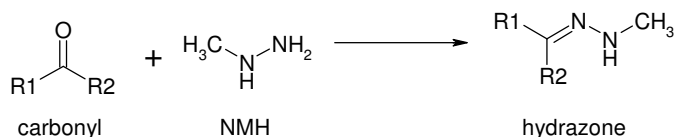
For every derivatization one derivatization blank was made. The same procedure as described above was applied, but instead of 50 µl extract 50 µl n-hexane (picograde, for residue analysis, Promochem, Wesel, Germany) was used.

Looking for alternatives, we tested several other reagents to derivatize carbonyls in trace amounts. In this work we applied derivatization for the selective and sensitive detection of

aldehydes and ketones by the use of *N*-methylhydrazine (NMH). We applied a modified method adapted from Tamura and Shibamoto<sup>51</sup>.

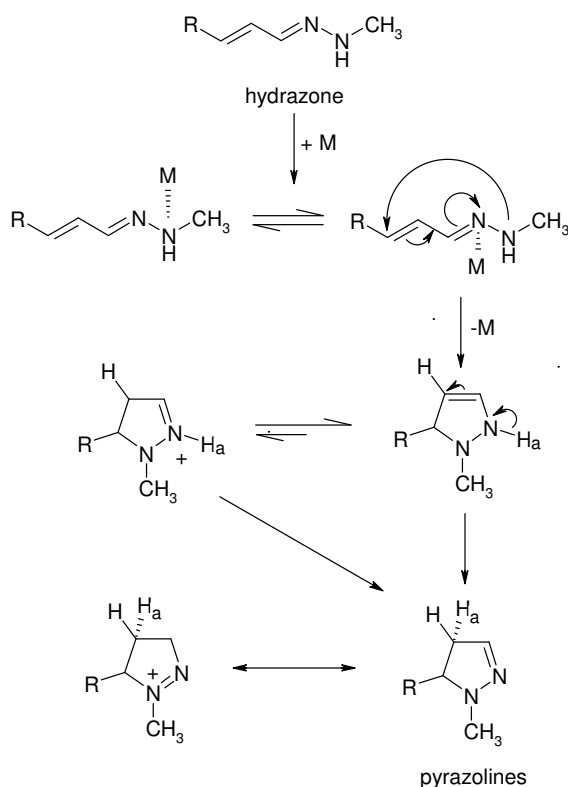
Carbonyls react with hydrazines to their corresponding hydrazones as shown in Scheme 3.

**Scheme 3. Mechanism of hydrazone formation from carbonyls and NMH.**



In case of the presence of a double bond in the carbonyl a further partial cyclization from the hydrazone to the pyrazoline takes place. By addition of Boron trifluoride ( $\text{BF}_3$ ) acting as a catalyst for the adol condensation a complete transfer of the hydrazones into the pyrazolines can be achieved (see Scheme 4).

**Scheme 4. Mechanism of the catalytic activity of  $\text{BF}_3$  on the cyclization of hydrazones to pyrazolines (according to<sup>17</sup>).**



Advantages of this cyclization are (a) a better peak shape as pyrazoline peaks do not show tailing or double peaks whereas the hydrazones do and (b) lower detection limits as the ring structure shows a more unique fragmentation pattern in the MS as the aliphatic hydrazones. In our case this cyclization was observed with the 2-alkenals, the 2,4-alkadienals and most probably also with the 1-alken-3-ones. Based on our investigations and the literature we were able to define characteristic  $m/z$  for the respective group for all investigated homologous series.

For the alkanals which do not cyclize due to their lack of the double bond the characteristic  $m/z$  ion is 72 originating from the  $\cdot\text{CH}_2\text{-CH=N-NH-CH}_3$  rest.

<sup>51</sup> Tamura H., Shibamoto T. (1991), *Anal Chim Acta* 248:619-623.

The (E)-2-alkenals show a characteristic fragment of 83 m/z due to the aromatic 5-ring. We could find the characteristic m/z of 109 for the 2,4-alkadienals and for the 1-alken-3-ones the prominent m/z of 97 but could not clear the structure behind until now.

However, for the analysis of the compounds and for the GC-MS measurements in SIM mode the explicit structure is not needed.

The applied derivatization routine is described here:

- An aliquot of fraction II (1 or 0.5 ml) in n-pentane or 1 ml standard solution
- + NMH (10  $\mu$ l for 0.5 ml or 20  $\mu$ l for 1 ml solution)
- Thoroughly stirring for 30 sec with a vortex mixer (Heidolph, Schwabach, Germany)

⇒ reaction for 60 min at 40 °C in a heating block

- Cool down to room temperature
- + BF<sub>3</sub>-etherate (10  $\mu$ l for 0.5 ml and 20  $\mu$ l for 1 ml solution)
- Thoroughly stirring for 30 sec with a vortex mixer (Heidolph, Schwabach, Germany)

⇒ reaction for 30 min at 40 °C

- Cool down to room temperature
- Use the solution directly for the GC-MS analysis

For every derivatization one derivatization blank was made. The same procedure as described above was applied, but instead of the extract the same volume n-hexane (picograde, for residue analysis, Promochem, Wesel, Germany) was used.

### 3.3. Gas Chromatography (GC)

Gas Chromatography (GC) is the method for the analysis of volatile and odour-active compounds as in the GC the mobile phase is a gas and analytes are separated in their gaseous state. We applied GC with various sample preparation techniques (liquid injection of the organic SPE extract, liquid injection of the fractionated SPE extract, liquid injection of the derivatised fractions, SPME injection of pellets and plaques), separation techniques (HP-5 column, DB-WAX column) and detection systems (flame ionisation detection (FID), nitrogen phosphorous detection (NPD), mass spectroscopy (MS)).

### 3.3.a. GC-MS of pellets and plaques with SPME

Two similar GC-MS systems were used during the thesis. In the results section for each task the used system is indicated. Parameters for the GC-MS measurements with SPME are summarized in Table 4 for the GC-GCD system and in Table 5 for the 7890GC-5975MS system .

**Table 4. Apparatus parameter for the SPME-GC-MS measurements using the GC-GCD system.**

gas chromatograph	Hewlett Packard G 1800 A GCD system (combination of GC and MS)
mass spectrometer	
autosampler	CTC CombiPal
SPME fibre	Supelco DVB/Car/PDMS, 50/30 µm, 2 cm, Stable Flex
SPME parameter	
thermostatting time	5 min
extraction time	10 – 20 min
desorption time	10 min
temperature	40 – 50 °C
sample amount	1 g – 2 g
injection mode	splitless after 2 min
injection temperature	270 °C
interface temperature	280 °C
ionisation mode	electron ionisation with 70 eV
MS mode	Scan
EM voltage	1823 V (atune)
solvent delay	0 min
mass range	20 – 300 amu, Threshold 10, 2.67 scans/sec
carrier gas	helium 5.0
column	Agilent HP-5MS (5% phenyl-95%-methylpolysiloxane) <sup>52</sup>
column dimension	30 m x 0.25 mm ID x 1 µm FT
GC mode	constant flow 0.8 ml/min
carrier gas velocity	32.8 cm/s
temperature program	
start temperature	-10 °C using liquid nitrogen for cooling for 1min

<sup>52</sup> Agilent Technologies Inc. (2008) J&W GC Column Selection Guide.

heating rate	12 °C/min
end temperature	280 °C for 1 min
GC run time	26.17 min
GC method name	PFS_OMIN.m

**Table 5. Apparatus parameter for the SPME-GC-MS measurements using the 7890 GC-MS system.**

gas chromatograph	Agilent 7890 GC
mass spectrometer	Agilent 5975N MS
autosampler	CTC CombiPal (Zwingen, Switzerland)
SPME fibre	Supelco DVB/Car/PDMS, 50/30µm, 2cm, Stable Flex
SPME parameter	
thermostating time	5 min
extraction time	10 – 20 min
desorption time	10 min
temperature	40 – 50 °C
sample amount	250 mg – 2 g
injection mode	splitless after 1 min
injection temperature	270 °C
interface temperature	280 °C
ion source temperature	230 °C
quadrupol temperature	150 °C
ionisation mode	electron ionisation with 70 eV
MS mode	Scan
EM voltage	1847 applying a Gain Factor of 2 (atune)
solvent delay	0 min
mass range	20 – 300 amu, Threshold 50, 4.94 samples/sec
carrier gas	helium 5.0
column	Agilent HP-5MS UI (different phase composition, same selectivity as HP-5MS columns but lower bleeding) <sup>53</sup>
column dimension	30 m x 0.25 mm ID x 0.25 µm FT

<sup>53</sup> Agilent Technologies Inc (2008) NEW Agilent J&W Ultra Inert Capillary GC Columns.

GC mode	constant flow 0.8 ml/min
carrier gas velocity	31.2 cm/sec
temperature program	
start temperature	-10 °C using liquid nitrogen for cooling for 1 min
heating rate	8 °C/min
end temperature	260 °C for 1 min
GC run time	35.75 min
GC method name	PFS_0MIN_SOLVENT.m

### 3.3.b. GC-MS of fractioned extracts

**Table 6. Apparatus parameter for the GC-MS measurements of the liquid fractioned extracts using the GC-MS system.**

Gas chromatograph	Hewlett Packard HP5890A GC
mass spectrometer	Hewlett Packard HP5975 MS
autosampler	Hewlett Packard HP7673 Autosampler
syringe	Hamilton 10 µl
injection volume	1 µl
injection mode	splitless after 1 min
injection temperature	250 °C
interface temperature	280 °C
ionisation mode	electron ionisation with 70 eV
MS mode	Scan
EM voltage	2353 V (atune)
solvent delay	3.5 min
mass range	40 – 290 amu; Threshold 10, 2.98 scans/sec
carrier gas	helium 5.0
column	Agilent HP-5MS (5% phenyl-95%-methylpolysiloxane) <sup>52</sup>
column dimension	30 m x 0.25 mm ID x 0.25 µm FT
GC mode	constant flow 0.8 ml/min
carrier gas velocity	33 cm/s
temperature program	
start temperature	35 °C for 0 min
heating rate	5.3 °C/min

end temperature	250 °C for 0 min
GC run time	40.5 min
GC method name	BORMS.m

### 3.3.c. GC-MS measurements of derivatised samples

**Table 7. Apparatus parameter for the GC-MS measurements of the NMH derivatised liquid fractioned extracts using the GC-MS system.**

Gas chromatograph	Hewlett Packard HP5890A GC
mass spectrometer	Hewlett Packard HP5975 MS
autosampler	Hewlett Packard HP7673 Autosampler
syringe	Hamilton 10 µl
injection volume	1 µl
injection mode	splitless after 1 min
injection temperature	250 °C
interface temperature	280 °C
ionisation mode	electron ionisation with 70 eV
MS mode	SIM
EM voltage	2624 V (maxsens)
solvent delay	7 min
SIM parameters	ion (dwell ... measurement time per ion in milliseconds); start time
group 1	86 (60), 72 (60); 0 min; 6.45 scans/sec
group 2	112 (50), 100 (50), 97 (50), 83 (50), 72 (50); 13.2 min; 3.03 scans/sec
group 3	126 (50), 114 (50), 97 (50), 83 (50), 72 (50); 17.9 min; 3.03 scans/sec
group 4	140 (50), 128 (50), 97 (50), 83 (50), 72 (50); 22.8 min; 3.03 scans/sec
group 5	154 (50), 142 (50), 97 (50), 83 (50), 72 (50); 27.5 min; 3.03 scans/sec
group 6	170 (100), 72 (100); 30 min; 4.26 scans/sec
group 7	168 (50), 156 (50), 97 (50), 83 (50), 72 (50); 32.0 min; 3.03 scans/sec
group 8	182 (50), 170 (50), 97 (50), 83 (50), 72 (50); 36.0 min; 3.03 scans/sec
group 9	196 (50), 184 (50), 97 (50), 83 (50), 72 (50); 41.0 min; 3.03 scans/sec
group 10	210 (50), 198 (50), 97 (50), 83 (50), 72 (50); 45.0 min; 3.03 scans/sec
group 11	224 (50), 212 (50), 97 (50), 83 (50), 72 (50); 48.5 min; 3.03 scans/sec
group 12	238 (50), 226 (50), 97 (50), 83 (50), 72 (50); 52.0 min; 3.03 scans/sec

group 13	252 (50), 240 (50), 97 (50), 83 (50), 72 (50); 55.5 min; 3.03 scans/sec
carrier gas	helium 5.0
column	Agilent HP-5MS (5% phenyl-95%-methylpolysiloxane) <sup>52</sup>
column dimension	30 m x 0.25 mm ID x 0.25 µm FT
GC mode	constant flow 0.8 ml/min
carrier gas velocity	31.4 cm/s
temperature program	
start temperature	-10 °C (using liquid nitrogen for cooling) for 1min
heating rate 1	10 °C/min up to 30 °C
heating rate 2	3 °C/min up to 220 °C
heating rate 3	30 °C/min for 5 min
end temperature	310 °C for
GC run time	76.33 min
GC method name	NMHSIM10.m

**Table 8. Apparatus parameter for the GC-MS measurements of the PFBHA derivatised liquid fractioned extracts using the GC-MS system.**

Gas chromatograph	Hewlett Packard HP5890A GC
mass spectrometer	Hewlett Packard HP5975 MS
autosampler	Hewlett Packard HP7673 Autosampler
syringe	Hamilton 10 µl
injection volume	1 µl
injection mode	splitless after 1 min
injection temperature	250 °C
interface temperature	280 °C
ionisation mode	electron ionisation with 70 eV
MS mode	SIM
EM voltage	2326 (maxsens)
solvent delay	5 min
SIM parameters	ion (dwell ... measurement time per ion in milliseconds); start time
group 1	276 (70), 250 (70), 239 (70), 181 (70); 5 min; 2.9 scans/sec
MS detector	off (12 min), on (13 min)



carrier gas	helium 5.0
column	Agilent HP-5MS (5% phenyl-95%-methylpolysiloxane) <sup>52</sup>
column dimension	30 m x 0.25 mm ID x 0.25 µm FT
GC mode	constant flow 0.86 ml/min
carrier gas velocity	33.3 cm/s
temperature program	
start temperature	35 °C (0 min)
heating rate	5.3 °C/min
end temperature	280 °C (0 min)
GC run time	46.2 min
GC method name	BORMSDER.m

### 3.3.d. GC-FID-Olfactometry and GC-NPD-Olfactometry (GC-O)

For GC-O we used both the liquid extracts and SPME as sample preparation techniques. All analyses were carried out on the same system differing only in the injection parameters for liquid and SPME injection (listed in Table 9). Most GC-O analyses were carried out by using the FID, but some samples were additionally sniffed by using the NPD to selectively detect nitrogen compounds.

**Table 9. Apparatus parameter for the GC-O measurements of the liquid extracts.**

Gas chromatograph	Hewlett Packard HP5890 GC
detectors	Flame ionisation Detector (FID) and olfactory detection port (ODP) (Gerstel, Mülheim an der Ruhr, Germany)
liquid injection parameters	
syringe	Hamilton 10 µl
injection volume	1 µl manual
injection mode	splitless after 1 min
injection temperature	220 °C
SPME injection parameters	
sample amount	250 mg – 2 g
thermostatting time	5 min
extraction time	10 – 15 min
desorption time	10 min

temperature	40-50 °C
injection temperature	270 °C
detector temperature	300 °C
carrier gas	helium 5.0
FID gas flows	
synthetic air 5.0	400 ml/min
nitrogen 5.0	40 ml/min (make-up flow)
hydrogen 5.0	40 ml/min
column	Agilent HP-5 (5% phenyl-95%-methylpolysiloxane) <sup>52</sup>
column dimension	30 m x 0.32 mm ID x 0.25 µm FT
GC mode	constant pressure, 95 kPa column head pressure
carrier gas velocity	35 cm/s at 35°C
splitter	stainless steel fixed 1:1 splitter (SGE, Griesheim, Germany) at the end of the analytical column to separate the effluent between the FID or NPD and the ODP using deactivated fused silica columns (1 m x 0.1 mm ID)
temperature program	
start temperature	35 °C (0 min)
heating rate	5.3 °C/min
end temperature	250 °C (0 min)
ODP parameters	
interface temperature	290 °C
humidification	with deionized water
auxiliary gas	synthetic air 5.0
GC run time	40.5 min
GC method name	Boreafid.m / Borebfid.m / Boreanpd.m / Borebnpd.m

**3.3.e. Comprehensive Gas Chromatography with time of flight mass spectrometry (GCxGC-TOF-MS) measurements at LECO**

For selected samples we carried out measurements of fraction II with a multidimensional gas chromatography system coupled to a TOF-MS. These measurements were carried out at LECO in Mönchengladbach, Germany. Measurement parameters are listed in Table 10.

**Table 10. GCxGC-TOF-MS parameters for measurements of the liquid fraction II samples.**

<b>Hardware Settings</b>	
Injector	Cooled Injection System CIS (Gerstel, Mülheim an der Ruhr, Germany)
GCxGC-TOF-MS system	Pegasus® 4D (LECO, Mönchengladbach, Germany)
columns	
1 <sup>st</sup> dimension	VF-5ms; 30 m x 0.25 mm ID x 0.25 µm FT
2 <sup>nd</sup> dimension	VF-17ms 2 m x 0.18 mm ID x 0.2 µm FT
<b>Method parameters</b>	
injection temperature	220 °C
GC mode	constant flow, 1.5 ml/min
injection volume	1 µl
oven program	
start temperature	40 °C (1 min)
heating rate	10 °C/min
end temperature	280 °C (1 min)
Offset to 2 <sup>nd</sup> oven	5 °C
modulator temperature	30 °C higher than 1 <sup>st</sup> oven
2 <sup>nd</sup> dimension time	5 sec
Hot pulse time	0.6 sec
Acquisition delay	300 sec
mass range	35 – 500 amu
detector voltage	1.8 kV
ion source temperature	200 °C

**3.3.f. Quantification of 2-acetyl-1-pyrroline in a PP sample by a standard addition procedure using HS-SPME-GC-NPD<sup>54</sup>**

2-acetyl-1-pyrroline was quantified in a PP sample by applying a standard addition procedure. For this, 2-acetyl-1-pyrroline diluted in methanol (picograde, for residue analysis, Promochem, Wesel,

<sup>54</sup> Hopfer H., Schrampf E., Leitner E. (2010) J. Chromatogr., A., submitted.

Germany) was added to the PP sample with the concentration of 0 pg, 5 pg, 50 pg, 500 pg and 5 ng. The added volume was fixed to 5  $\mu$ l to keep the matrix constant. This avoids non-linear behaviour of the calibration curve due to solvent-fibre interaction. The quantification was performed by extrapolation using the calibration curve.

The described GC–NPD method is fully validated, including the determination of the limits of detection (LOD) and limits of quantification (LOQ) for the investigated compound using the Validata software<sup>55</sup>. Calibration curves were obtained from six different concentrations (3-fold) versus the peak areas. Linear calibration could be used with a correlation coefficients  $R^2 \geq 0.98$ . The linearity of the calibration curves was checked by linearity tests according to Mandel; the suitability of the linear model was verified by analysis of the residuals<sup>56</sup> and DIN 32645<sup>57</sup>. Furthermore, for the validation of the method the variances were tested for their homogeneity based on the 95 and 99 % confidence interval.

Calculations of the values for the limit of detection (LOD) and the limit of quantification (LOQ) are based on the calibration function. The LOD is defined as the lowest concentration differing significantly from zero; the LOQ is the lowest concentration of the analyte that can be determined with a S.D.  $\leq 5\%$ .

**Table 11. Parameter for the quantification of 2-acetyl-1-pyrroline in a PP sample.**

Gas chromatograph	Agilent 7890 GC
detectors	nitrogen phosphorus detector (NPD)
autosampler	CTC CombiPal (Zwingen, Switzerland)
SPME fibre	Supelco DVB/Car/PDMS, 50/30 $\mu$ m, 2cm, Stable Flex
SPME injection parameters	
sample amount	1 g
thermostatting time	5 min
extraction time	20 min
desorption time	20 min
temperature	50 °C
injection temperature	270 °C

<sup>55</sup> Wegscheider W., Rohrer C., Neuböck R. (1997) Validata - Excel 97 Makro zur Methodvalidierung, Version 3.02.48.

<sup>56</sup> W. Funk, V. Damman, G. Donnevert, Qualitätssicherung in der Analytischen Chemie, VCH, Weinheim, 1992.

<sup>57</sup> DIN 32645 (1994) Chemical analysis - Decision limit, detection limit and determination limit under repeatability conditions - Terms, methods, evaluation.

detector temperature	200 °C
carrier gas	helium 5.0
NPD gas flows	
Detector fuel gas off*	1 – 4 min
synthetic air 5.0	60 ml/min
nitrogen 5.0	2.6 ml/min
hydrogen 5.0	2.8 ml/min
column	Agilent HP-5 (5% phenyl-95%-methylpolysiloxane) <sup>52</sup>
column dimension	30 m x 0.25 mm ID x 0.25 µm FT
GC mode	constant flow of 0.8 ml/min
carrier gas velocity	31.5cm/sec
temperature program	
start temperature	-10 °C (1 min)
heating rate	8 °C/min
end temperature	260 °C (1 min)
GC run time	40.5 min
GC method name	PFS_NPD-ALLES.m

\* The detector was switched off during the elution of the solvent to enhance the lifetime of the NPD pearl.

### 3.4. Others

#### 3.4.a. Fourier-Transform Infrared Spectroscopy (FTIR)

FTIR was applied as a reference analysis method for the autoxidation program (4.7). We used the FTIR system at the Institute for Chemistry of Polymers at the University of Leoben. The carbonyl index as standard method for degradation of polyolefins was chosen according to DIN 53383 part 2<sup>58</sup>. Thin films were produced using a heatable hydraulic press (Perkin Elmer, Waltham, USA) in combination with a constant thickness film maker (Specac Atlas Series Platen Controller) and a cooling Device PN 15515 (Specac Ltd., Orpington, UK). Prior to the IR measurements the film thickness was measured (Ericson Foil Thickness Gauge Model 497). From each sample two independent films were produced and measured.

<sup>58</sup> DIN 53383-2:1983-06 (1983) Testing of plastics; testing of oxidation stability by means of ageing in an oven; polyethylene of high density (PE-HD), infra red spectroscopic (IR) determination of the carbonyl content.

The FTIR system "Spectrum One" was from Perkin Elmer (Waltham, USA).

A blank run was recorded at the beginning of each measurement day. All samples were measured in 20 scans from 4000 to 500  $\text{cm}^{-1}$  with a resolution of 4 $\text{cm}^{-1}$ .

We calculated from all samples the so called Carbonyl Index (CI) according to<sup>58</sup>. The CI is the ratio of the peak height or peak area of the carbonyl  $\nu\text{C}=\text{O}$  peak at 1715  $\text{cm}^{-1}$  to the  $\delta\text{CH}_2$  and  $\delta_{\text{as}}\text{CH}_3$  peak at 1456  $\text{cm}^{-1}$ . The more the polyolefin material is oxidized the higher the amount of carbonyl groups gets and the lower the number of  $\text{CH}_2$  and  $\text{CH}_3$  groups gets. Thus, an increasing CI indicates increasing oxidation.

#### **3.4.b. Near Infrared Spectroscopy (NIR) with multivariate calibration**

For the autoxidation program (4.7) we used the near infrared spectroscopy (NIR) with a subsequent multivariate data analysis after we failed with the IR as a reference method. We used the Thermo FT-NIR Antaris II system with an InGaAs detector. All samples were analysed as powders using a spinning sample cup in a wave number range from 10,000 to 4,000  $\text{cm}^{-1}$  applying diffuse reflectance. 32 scans were recorded with a resolution of 8  $\text{cm}^{-1}$ . The achieved data was used for a multivariate data analysis using the The Unscrambler software (Version 9.7) (Camo, Norway).

#### **3.5. Multivariate data analysis (MVDA)<sup>59</sup>**

Multivariate data analysis (MVDA) is a useful tool for large quantities of data where the actual information is scattered and hidden by non-usable junk, comparable to the background noise in a MS system. Similar to the human brain, MVDA is able to filter the important information and to classify it according to the given question. Additionally, MVDA presents this information in a way which is easier for us to understand. Instead of n-dimensional matrices, data is shown graphically so that similarities and underlying pattern are easier to recognise (e.g. Principal Component Analysis (PCA) or Cluster Analysis).

MVDA is especially applied for analyses where large quantities of data are generated such as spectroscopy. For example, recording a NIR spectrum in a wave number range from 1000 to 1700 nm with a resolution of 1 nm for one measurement 700 data points are recorded. Knowing that for 20 samples at least 3 repeating measurements are normally recorded, one ends with 700 x 20 x 3 = 42,000 data points, a typical data set for MVDA.

---

<sup>59</sup> Kessler W. (2007) Multivariate Datenanalyse für die Pharma-, Bio- und Prozessanalytik, Wiley-VCH, Weinheim, Germany.

So for applying MVDA, one measures  $N$  objects with  $M$  properties or variables and gets a  $N \times M$  matrix.

Based on different data treatment methods one is able to get only qualitatively answers (e.g. how different or how similar are my samples?) or in case of NIR also quantitatively answers can be given by establishing a multivariate calibration model.

### **3.5.a. MasStat©**

In this work we used MVDA solely for quantitative answers. In most cases we used the MasStat© program from Analyt MTC (Version 3.02, Müllheim, Germany) for a qualitative cluster analysis of GC-MS data. Important to mention is that it is recommended to use an automated sampler for the GC-MS system to avoid large deviations in the retention time of the compounds in order to obtain clear separated sample clusters. As the program is looking for differences in the recorded mass ions based on intensity and/or retention time, one is interested to have the replica measurements as similar as possible so that the program really uses only the differences between the samples and not between the replica measurements of one sample. However, to ensure that the depicted differences are really sample-driven, it is important to check if the shown information is really present also in the original data.

For all programs MasStat© was used as described here:

- 1) Load all measured samples into the program
- 2) Indicate in the first run only which samples are replica measurements
- 3) Exclude prominent background and noise ions such as air ( $m/z$  28 and 32) and siloxanes (73, 77, 131, 147, 155, 207, 231, 271, 286)
- 4) Apply “normalized all peaks” instead of “raw data” to normalize all chromatograms and MS spectra.
- 5) Steadily increase the number of ions used for the cluster analysis until no further change can be observed (generally between 5 and 10).
- 6) Ask the system which ions make up the difference between the most extreme samples (those with the biggest distance in between) and do this for all the other samples as well.
- 7) Use these ions for a check in the GC-MS analysis program and see which compounds these ions have.
- 8) If the checked ions bear real sample differences, keep them, otherwise exclude those from the cluster analysis.

In the ideal end one gets a sample cluster and is able to tell which compounds are responsible for the differences.

### **3.5.b. The Unscrambler®**

The software The Unscrambler® from Camo (Version 9.7, Oslo, Norway) was used for the MVDA of the NIR measurements used in the autoxidation program (4.7) for the NIR data analysis.

All data was pre-treated with multiplicative scatter correction to minimise non-specific scatter phenomena. Outlier detection was applied using Principal Component Analysis (PCA).

## **3.6. Sensory evaluation**

### **3.6.a. Best Estimate Threshold (BET) determination**

The question which odour-active compound is more “smelly” is answered by determination of sensory threshold values. The sensory threshold values were determined applying the Best Estimate Threshold (BET) procedure according to ASTM E679<sup>60</sup>.

The used sensory test panel consisted of 13 well trained panellists (26–45 years, 8 females, 5 males), whose ability to recognize the basic tastes sweet, sour, salty, and bitter was tested as a basic requirement to act as panellist according to DIN 10961<sup>60</sup>.

The panellists were trained in several sessions prior to the threshold determination with the substances of interests listed in Table 12 to get the panellists more familiar with the odours. For this purpose, substances listed in Table 12 were first presented on filter paper strips dipped into ethanolic solutions (1 vol%) and panellists were asked to describe the odour. The obtained descriptors were collected and discussed with the panel.

Secondly, substances were presented in water (1 mg/L, 10 µg/L for 1-Hexen-3-one) and panellists were asked again to describe the odour and to evaluate the perceived intensity compared to the previous sample (0 ... no difference in intensity, + ... more intense, - ... less intense than previous sample). Differences between the descriptors obtained from the compounds in ethanolic solution presented on strips and in the water were discussed with the panel.

For the determination of the sensory detection threshold the so called “Best Estimate Threshold” (BET) procedure was applied according to ASTM 679<sup>60</sup>. BET values for each panellist as well as a group BET were determined first in water.

---

<sup>60</sup> DIN 10961:1996-08 (1996) Training of assessors for sensory analysis.



In a second stage, thresholds of those substances with lowest thresholds in water were additionally determined in miglyol, a oil matrix consisting only of saturated fatty acids. The maximum volume added to the matrix for the threshold determination was 50 µl of the appropriate dilution. The threshold determination was carried out for the water values in plastic cups and approx. 50 ml were presented to the panellists. For the values in miglyol blue coloured standard olive oil testing glasses were used and approx. 5 ml of test solution was presented to the panellists. The panellists were informed about the tested compound which was written on the evaluation protocol as this should increase sensitivity according to O'Mahony<sup>61</sup>.

To determine the odour threshold of one compound, a series of six three-alternative forced choice (3-AFC) tests was presented to the panellists at one time. Each triangle test contained two odorant-free samples and one sample spiked with the compound of interest. According to the ASTM standard<sup>6</sup>, the concentration of the odour compound was increased stepwise (factor 4-5) with each triangle test. The panellists were asked to identify the differing sample for each triangle. In addition, they were asked to describe the noticed difference in order to obtain information about differences between detection and recognition threshold levels.

In every test session only one series of six 3-AFC tests was presented to the panellists. The BET for the single panellists was calculated as the geometric mean from the highest concentration that was not recognized as differing from the others and the lowest concentration that was identified as differing from the other samples in the triangle. The group BET was derived by geometrical averaging of the individual BET values. Information about the deviation of the determined BET value was accessed by calculating the standard log deviation.

---

<sup>61</sup> O'Mahony M. (1995) Food Qual. Prefer 6:227–238.

**Table 12. Odour descriptors and odour thresholds in water and oil from the literature<sup>32</sup> for the compounds which sensory threshold values were determined.**

<b>Compound</b>	<b>odour descriptors</b>	<b>previously reported odour threshold in water<sup>b</sup> or oil<sup>c</sup> (µg/L)</b>
(E)-2-heptenal	green, fatty, old oil-rancid, stink bug, nuts, pungent	13 - 51 <sup>b</sup>
heptanal	green, soapy, fatty, fresh, stink bug	3 - 550 <sup>b</sup>
octanal	green, soapy, fatty, cardboard, metallic	0.41 - 250 <sup>b</sup>
decanal	soapy, plastic, green, fruity-orange, cleaning/washing detergent, fatty	0.1 - 245 <sup>b</sup>
nonanal	mouldy-cellar-earthy, cardboard, a bit fruity, dusty, old chair/house, fatty, goat stable	2.53 - 260 <sup>b</sup>
(E)-2-octenal	(smashed) stink bug, green, fatty, rancid, dusty, plastic	0.2 - 20 <sup>b</sup>
γ-octalactone	coconut, sweet	7 - 14 <sup>b</sup>
(E)-2-decenal	soapy, green, stink bug, pungent, rancid, fatty	0.3 - 250 <sup>b</sup>
2,3-butandione	butter, yoghurt, sour cream, milk, fatty, sour milk	0.3 - 2300 <sup>b</sup> ; 3 - 10 <sup>c</sup>
(E)-2-nonenal	green, rancid, cucumber, stink bug, fatty	0.08 - 0.4 <sup>b</sup> ; 45 - 900 <sup>c</sup>
1-octen-3-one	mushroom, forest soil-earthy, green, road painting-zebra crossing	0.005 - 0.01 <sup>b</sup> ; 3 - 10 <sup>c</sup>
1-hexen-3-one	plastic, unpleasant-pungent, warm burnt plastic, (carpet) glue, solvent	0.02 - 0.024 <sup>b</sup> ; 5 <sup>c</sup>

<sup>a</sup> The descriptors were acquired from the panel in the training phase. Descriptors are listed in decreasing number of entries given by the panellists. <sup>b</sup> Odour threshold in water<sup>32</sup>. <sup>c</sup> Odour threshold in different oils if available<sup>32</sup>.

### 3.6.b. *Detection Frequency (SNIF)<sup>64,62</sup> x Aroma Extract Dilution Analysis (AEDA)<sup>63</sup>*

An evaluation of the odour-active compounds was accomplished by 4-6 trained panellists (5 females, 1 male, 25-45 years). All panellists are members of the in-house sensory panel and specially trained for odour evaluation and description. Each sample is sniffed in one run by a single panellist until all odour-active substances are eluted. A maximum of three runs per person and day are carried out. Dilutions (1:100 and 1:1000 if necessary) are evaluated by three and, one judge, respectively. Panellists were asked to state the odour impression which was recorded by activating a microphone via the software (Gerstel ODP, Mülheim an der Ruhr, Germany).

A combination of Detection Frequency (surface of Nasal Impact SNIF) adapted from Linssen<sup>64</sup> and Pollien<sup>62</sup> and the Aroma Extract Dilution Analysis (AEDA) adapted from Ulrich and Grosch<sup>63</sup> has been developed. All obtained olfactory chromatograms are graphically overlaid and normalized. Compounds with SNIF-values of 80% and 100% for the pure extracts and all compounds detected by one judge in the diluted samples are used for identification. The identification of the odour-active compounds is made by comparison of experimental and literature Kováts' Retention Indices (RI)<sup>34,35</sup> with values from institute's own RI database and internet databases<sup>65,66,67</sup>. For the calculation of linear RI an n-alkane mix was analysed the same way as the samples. For comparison and identification the RI of the odour-active compounds were calculated at the beginning of the odour impression. Pre-tests showed that the comparability with reference databases is best when RI are calculated at the starting time of odour impression. This is of enormous influence for highly odour-active compounds eluting for a long time where RI span over 50 indices. A substance was taken into account if the database value did not differ from the experimental value more than  $\pm 5$ . A periodically check of the GC-O system with a test mixture was carried out. With this mixture (1) it was assured that the obtained RI are valid, (2) that the system itself (injector, column) does not have polar sites which absorb analytes, and (3) that the GC is properly heating.

The mix was used both for liquid and SPME injections, where in the first case 1 $\mu$ l of a 10mg/L solution and in the latter one 100ng in a HS vials were injected. In Table 13 the mixture composition is listed together with the literature and measured RI. All values do not differ from

---

<sup>62</sup> Pollien P., Ott A., Montigon F., Baumgartner M., Munoz-Box R., Chaintreau A. (1997) J Agr Food Chem 45:2630-2637.

<sup>63</sup> Grosch W. (1994) Flav. Fragr. 9:147-158.

<sup>64</sup> Linssen J.P.H., Janssens J.L.G.M., Roozen J.P., Posthumus M.A. (1993) Food Chem. 46:367-371.

<sup>65</sup> Acree T., Arn H. (2004) Flavornet and human odor space, www.flavornet.org. Accessed 08/28/2009.

<sup>66</sup> Mottram R., The LRI and Odour Database, www.odour.org.uk. Accessed 08/28/2009.

<sup>67</sup> El-Sayed AM (2009) The Pherobase: Database of Insect Pheromones and Semiochemicals, www.pherobase.com. Accessed 08/28/2009.

the literature ones more than 3 units except for acenaphthen which is extremely sensitive to faster temperature ramps as used for the GC-O runs (10 °C/min instead of 5.3 °C/min).

**Table 13. Composition of the test mixture for the GC-O system.**

Compound	RI (HP-5)	
	literature <sup>68</sup>	measured
n-alkanes from C6-C20	600 - 2000	600 - 2000
$\alpha$ -pinene	932.6	934.5
$\beta$ -pinene	975.6	977.8
p-cymene	1024.3	1026.1
1,8-cineol	1030.8	1032.9
L-menthol	1173.5	1176.3
methyl decanoate	1325.2	1324.9
1-dodecanol	1474.3	1474.8
acenaphthene	1487.0	1495.9

<sup>68</sup> Farkaš P., Sádecká J., Leitner E., Siegmund B., Petka J. (2001) SKAF flavour database.

## 4. Results and Discussion

### 4.1. Analysis method parameters

#### 4.1.a. Recovery for the sample preparation

Due to the use of the IS 3,5,5-trimethylhexanal added to the samples prior to the SDE process we were able to calculate the so called Recovery. According to the CITAC/EURACHEM guide to quality in Analytical Chemistry<sup>69</sup> it is needed to have [...good knowledge of the amount of analyte in the original sample relative to that in the sample presented to the end measurement process ...]. To monitor sample preparation losses, contamination or interferences, the Recovery (R) is defined as is the systematic error of the measuring system and is expressed as the amount/concentration of the IS measured as a percentage to the theoretical amount/concentration present in the matrix.

$$R = \frac{c_{meas}}{c_{theo}} \cdot 100\%$$

whereas

$c_{meas}$  ... measured concentration

$c_{theo}$  ... theoretical concentration determined from beginning concentration

The recovery was calculated from the area of all five extracts and the blank for all samples compared to the area of the IS theoretically present in the samples and was determined for randomly selected samples with 63.20 % ± 13.1.

#### 4.1.b. Need and Quality of the fractionation process

The use of SPE cartridges for fractionation of the obtained SDE extract was necessary as otherwise a separation of the odour-active carbonyls from the non-odorous linear and branched alkanes and alkenes could not be obtained. Additionally, a concentration step for the carbonyls was needed for detection with the GC-MS while the alkanes and alkenes were present in high concentrations (mg/kg). In Figure 10 we show an example of the separation of the non-odorous, non-polar volatiles from the mid-polar, odour-active compounds by fractionation on silica gel SPE cartridges from the PP extract (EE188AI plaques). The homologous series of n-aldehydes from C7-C12 in the concentration range of the IS and above can be found in fraction 2 which would have been heavily interfered by linear and branched alkanes and alkenes without fractionation (n-alkanes from C5-C14 are marked in fraction 1). Additionally, an example is given, which proves that the important

---

<sup>69</sup> CITAC/Eurachem Guide (2002) Guide to Quality in Analytical Chemistry.

information about odour-active compounds is conserved in fraction II: In Figure 12 the MasStat© cluster of fractioned SDE extracts is shown. While the fraction I of the 8 samples (two materials as pellets and at three  $T_M$  (200 °C, 230 °C, 260 °C) injection moulded plaques; see also section 0) fall together in one cluster, the individual fraction II are well separated along one line according to the injection moulding temperature and the material.

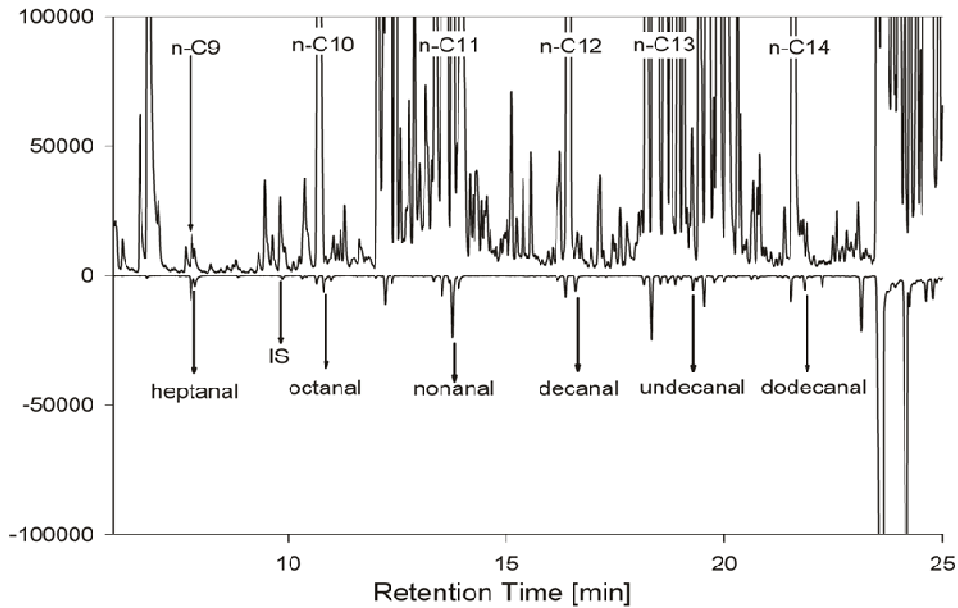


Figure 10. Total ion chromatogram (TIC) of a PP fraction I (top) and fraction II (bottom) with marked homologous series of n-alkanes and n-alkanals.

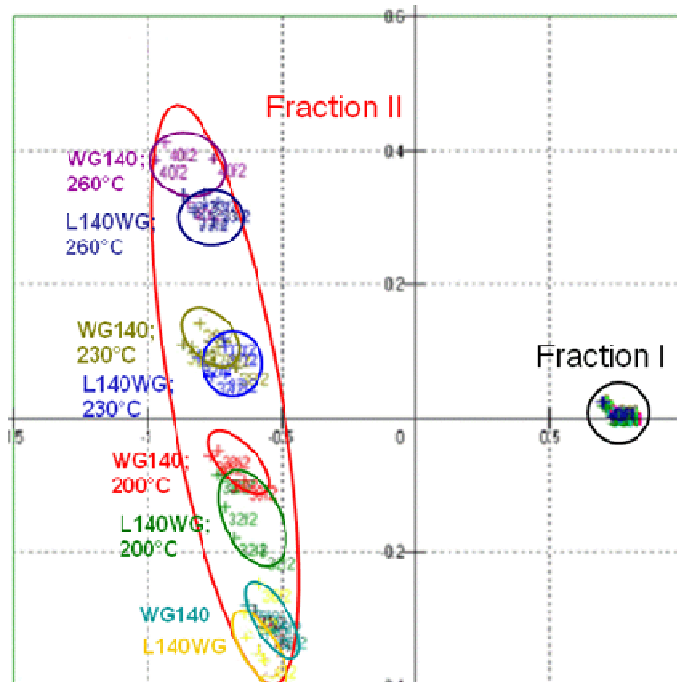


Figure 11. MasStat© cluster obtained from fraction I and fraction II data of WG140AI and L140WG samples (pellets and injection moulded plaques moulded at  $T_M$  200 °C, 230 °C and 260 °C).

#### 4.2. Comparative study – influence of compounding conditions and injection moulding mass temperatures ( $T_M$ )

In the beginning of the project we decided to look at the most obvious influencing parameter in the whole process chain – the injection moulding mass temperature  $T_M$ . Three samples (L140WG-06, WG140AI-06 and WG140AI-05) with only slightly differing recipes (see Table 14) and compounded on different machines (L140WG-06 was compounded on a small lab machine while both WG140AI grades were compounded on a plant machine) (see Table 3, sample BO32 to BO40) were selected and screened. We investigated all three materials as pellets and two materials as injection moulded plaques (WG140AI-05 and L140WG-06) processed at three temperatures (200 °C, 230 °C, 260 °C) in a comparative study. The last pellet sample (WG140AI-06) could not be compounded as there was not enough material available.

SDE extracts were obtained as described in 3.2.a, fractioned according to 3.2.b, and analyzed by GC-MS (3.3.b). Additionally, all samples were analyzed with HS-SPME-GC-MS as described in 3.2.c and 3.3.a. All the samples were evaluated by HS-SPME-GC-O (3.3.d) too. The GC-MS data of both the fractions and the SPME was evaluated with the MVDA tool MasStat© (3.5.a).

**Table 14. Detailed recipe for the L140WG-06 and the WG140AI-05 samples.**

L140WG-06		WG140AI-05
produced on lab scale compounder ZSK40, with HMS	<b>additional information</b>	produced on plant scale compounder ZE90A, with BE50
	<b>polymer composition</b>	
85,15 % (5L2EAB1)	<b>BG055AI</b>	84,784 % (ex Kallo)
6 % WB130HMS	<b>2<sup>nd</sup> polymer</b>	5,6 % BE50
-	<b>additive carrier powder</b>	1 % B-powder
-	<b>chalk</b>	0.1 % Calcitec M/5
8%	<b>talc 3.8 (Tital 15)</b>	7,5%
0.4 % (Irganox PS802)	<b>sulphur stabilizer TPS</b>	0,4 % (Irganox PS802)
0.12 % (Alkanox 240)	<b>phosphate</b>	0,046 % (Hostanox PAR24 FF)
0.07 % (Irganox 1330)	<b>phenolic antioxidant</b>	0,22 % (Ethanox 330 P)
0.2 % (Dimodan HP FF)	<b>antistatic agent</b>	0,23 % (Rikemal AS-005)
0.06 % (calcium stearate)	<b>acid scavenger</b>	0.09 % (calcium stearate)
	<b>acid scavenger</b>	0,03 % (DHT 4A)

The results of the Cluster Analysis using MasStat© for the HS-SPME-GC-MS and the fractioned SPE extracts analyzed with GC-MS can be used for answering these questions:

- 1) What are the differences in between the pellet and injection moulded plaques made thereof? What influence does the processing have on the material?
- 2) What are the differences in between the three samples? Are there differences between the pellets and the injection moulded plaques?
- 3) What influence does the mass temperature during injection moulding have?

In Figure 12 the basic MasStat© cluster of the samples is shown, where we did not specify which samples are pellets or plaques.

Nevertheless, there are noticeable differences (i) in between the two materials coming mostly due to the different composition demonstrated by a clear separation of the sample clusters along the A2-axis (on top the L140WG material, at the bottom the WG140AI-05 material), and (ii) in between the pellets and the injection moulded plaques by a separation along the A1-axis (on the far right side lay the pellets labelled as “L” for the L140WG-06 material and “W” for the WG140AI-05 material, on the far left side the 260 °C mass temperature samples labelled as “260L” and “260W” for the respective material, the 200 °C and 230 °C mass temperature samples are in between). Additionally, one is able to see that the L140WG-06 material is more affected by the injection moulding as the distances in between the individual clusters are larger compared to the WG140AI-05 material, where the 260 °C  $T_M$  sample is approx. at the same vertical position as the 230 °C  $T_M$  sample of the L140WG-06 material. This is an indication that the L140WG material composition is more prone to degradation as the WG140AI samples.

In the second cluster (Figure 13) we labelled the samples with “g” (pellet) or “p” (plaques) to show the differences based on the processing. A similar picture as in Figure 12 is obtained. Again, (i) both materials are clearly separated, (ii) the pellets are separated from the plaques, (iii) the influence of the  $T_M$  during the injection moulding results in separated clusters which lay along a straight line in both materials and (iv) again a larger distance in between the compounding temperatures in the L140WG-06 samples compared to the WG140AI-05 material is found. However, in the latter material the 200 °C and 230 °C samples are closer to each other and more separated from the 260 °C samples.

The same procedure was applied to the GC-MS data of the fractioned extracts as shown in Figure 11 and Figure 14.



In Figure 11 one can clearly see that after the fractionation the compounds which are responsible for the differences in between the samples are collected in fraction II, while in fraction I the substances responsible for the in MVDA called “junk” data are collected. For us this is a proof for the validity of our sample preparation method, as similar evidence is given by both the HS-SPME and the fraction II data.

From Figure 14 the same conclusions as from the HS-SPME clusters can be drawn. The WG140AI-06 pellets lay in between the other two sample pellets, indicating that also the injection moulded plaques would most probably also lay in between the plaques of the L140WG-06 and WG140AI-05 materials.

All pellets and plaques samples were evaluated with HS-SPME-GC-O by one trained panellist with method parameters as described in section 3.3.d.

Due to this single evaluation, no statistical approved results could be obtained; although, six compounds (1-octen-3-one, octanal, 1-nonen-3-one, 6-/8-nonenal, (E)-2-nonenal and (E,E)-2,4-nonadienal) were detected in both pellet and plaque samples.

However, due to the single panellist no trends as seen in the MVDA could be obtained from the GC-O.

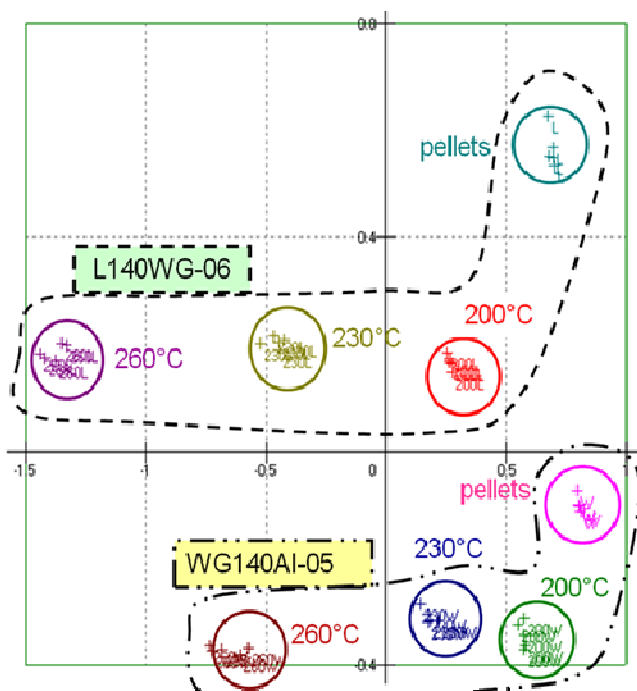


Figure 12. MasStat© Cluster of pellets and injection moulded plaques at three mass temperatures (200 °C, 230 °C, 260 °C); Labels: “L” ... L140WG pellets; “W” ... WG140AI-05 pellets; “200L, 230L, 260L” ... plaques from L140WG compounded at 200°C, 230°C and 260°C; “200W, 230W, 260W” ... plaques from WG140AI-05 compounded at 200 °C, 230 °C and 260 °C).

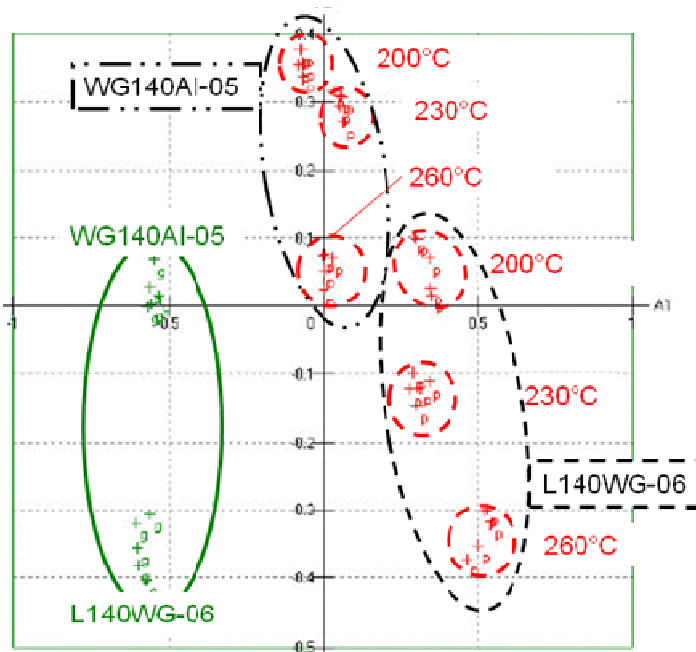


Figure 13. MasStat© Cluster of pellets and injection moulded plaques at three  $T_M$  (200 °C, 230 °C, 260 °C) with a differentiation in pellets and plaques.

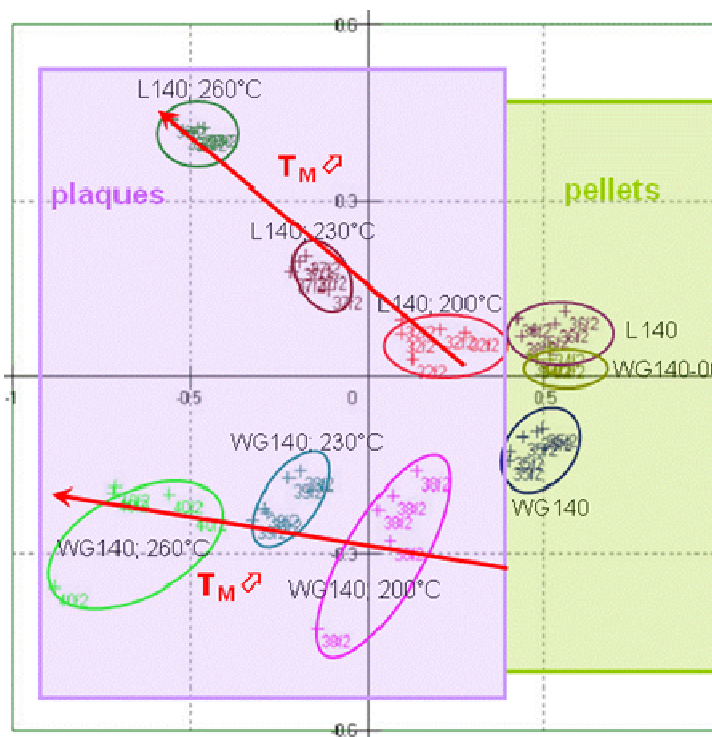


Figure 14. MasStat© cluster from fraction II data of all the samples (pellets and plaques at three  $T_M$  from L140WG-06 (L140), WG140AI-05 (WG140) and WG140AI-06 (WG140-06)).

### 4.3. Reference materials

During this thesis selected grades were screened for odour-active compounds. The selection for these grades was based on following thoughts:

- i) grades that are available from different sources (i.e. different polymerization plants or different compounding sites).
- ii) grades that preferably use the in-house polymerization technology “BorStar”.
- iii) grades that are of high importance for the company in terms of use and sale
- iv) grades that are used in business areas where odour is of importance (i.e. moulding, mobility, packaging, pipe)
- v) PP and PE grades

Based on these considerations four materials were selected (material details are given in Table 15):

- FB2230 ... Borstar PE film grade; available from Porvoo PE2 and Schwechat PE4
- ME3440 ... Borstar PE pipe grade; available from Provoo PE2, Stenungsund PE3 and Borouge
- BF970MO ... Borstar PP moulding grade; available from Schwechat PP5
- EE188AI ... compound PP mobility grade; available from Schwechat (-9530) and Beringen (-9524)

**Table 15. Material data sheets for the representative grades.**

	<b>Borstar © FB2230<sup>70</sup></b>	<b>BorSafe™ ME3440<sup>71</sup></b>	<b>Bormod™ BF970MO<sup>72, 73</sup></b>	<b>Daplen™ EE188AI<sup>73</sup></b>
application	blow film	pipe	moulding, mobility	mobility
type	HMW PE- LLD*	bimodal PE- MD**	heterophasic PP block copolymer	TPO*** compound PP
density [g/cm <sup>3</sup> ]	0.923	0.951	0.905	1.030
MFR* <sup>#</sup> [g/10min]	0.9 (190 °C/5.0 kg)	0.85 (190 °C/5.0 kg)	20 (230 °C/2.16 kg)	11 (230 °C/2.16 kg)
processing temperature [°C]	190-210	200-220 (T <sub>Melt</sub> )	210-260 (T <sub>M</sub> )	220-260 (T <sub>M</sub> )
others	AO <sup>#</sup>		BNT <sup>###</sup> , AS <sup>###</sup>	

\* HMW PE-LLD ... high molecular weight PE linear low density; \*\* PE-MD ... polyethylene medium density; \*\*\* TPO ... thermoplastic polyolefin; \*<sup>#</sup> MFR ... melt flow rate; <sup>#</sup> AO ... antioxidant; <sup>###</sup> BNT ... Borealis nucleation technology; <sup>###</sup> AS ... antistatic agent

<sup>70</sup> Product data sheet Borstar © FB2230 (2008) Borealis AG, Vienna.

<sup>71</sup> Product data sheet BorSafe™ ME3440 (2008) Borealis AG, Vienna.

<sup>72</sup> Product data sheet Bormod™ BF970MO (2008) Borealis AG, Vienna.

<sup>73</sup> Product data sheet Daplen™ EE188AI (2008) Borealis AG, Vienna.

Apart from the ME3440 and one FB2230 grade, for all materials both pellets and plaques were evaluated. For the EE188AI grade also the respective base polymers were screened for odour-active compounds. The FB2230 from Porvoo PE2 arrived in the second year and ME3440 was investigated in year three, while all other samples were evaluated in the first year of the thesis.

In the following sections the results obtained from GC-O with subsequent MVDA and the GC-O with subsequent Detection Frequency (see section 3.6.b) evaluation using the liquid extract are discussed. For the GC-O discussion it must be mentioned that all odour-active compounds could be resolved well with exception of the RI area between 1095 and 1104 due to several reasons:

- (1) In that area several compounds elute very close to each other; namely (E) 4-, (E + Z) 6-, 8-nonenal and nonanal with RI of 1096, 1095.1, 1101.2, 1096.5, 1104.6.
- (2) Additionally, are the odour impressions of these substances similar; all of them are described as fatty, burnt, waxy, plastic
- (3) All the nonenals show very low sensory thresholds as shown in Table 24 and Table 25 resulting in very intense and long-lasting odour impressions. The less intense nonanal was frequently masked by the other compounds. In most cases different odour impressions were not separated but more moved into the next one, thus making a clear separation impossible.

#### **4.3.a. Results of the MVDA of the Detection Frequency results.**

We applied multivariate data analysis (MVDA) with the Unscrambler© program on the detection frequency results (see section 3.6.b) to get a better picture about differences and similarities between the samples. For that we took all the 80 % and 100 % SNIF values together with the corresponding RI for all samples and rated the 100 % values with 2 and the 80 % values with 1, if a sample neither had 80 or 100 % SNIF value for the corresponding RI the values was set to 0. Information about processing type (pellet or plaques) as well as material type (PE or PP) was added as category variables.

The result of the MVDA is shown in Figure 15 a clear distinction between PE (on the left side) and PP (on the right side) can be made as well as a clear separation between pellets (G) and plaques (P) for the same material.

Both E188AI pellets from Beringen and Schwechat are more separated from each other while the plaques are relatively close to each other. The pellets and plaques originating from Schwechat are more separated from each other than the Beringen ones. This is an indicator that the differences in between the pellets and plaques from Schwechat are larger maybe due to a higher amount or

more types of odour-active compounds in the plaques compared to the pellets. Additionally it can be assumed that the pellets from Beringen have more in common with the plaques of both origins than with the pellets from Schwechat.

The BF970MO samples show the smallest difference between pellets and plaques, i.e. small differences in the type and/or amount of odour-active compounds.

For the FB2230 material from Schwechat PE4 a huge difference between pellets and plaques was observed indicating a huge difference in the amount and/or type of odour-active compounds between the pellets and the plaques.

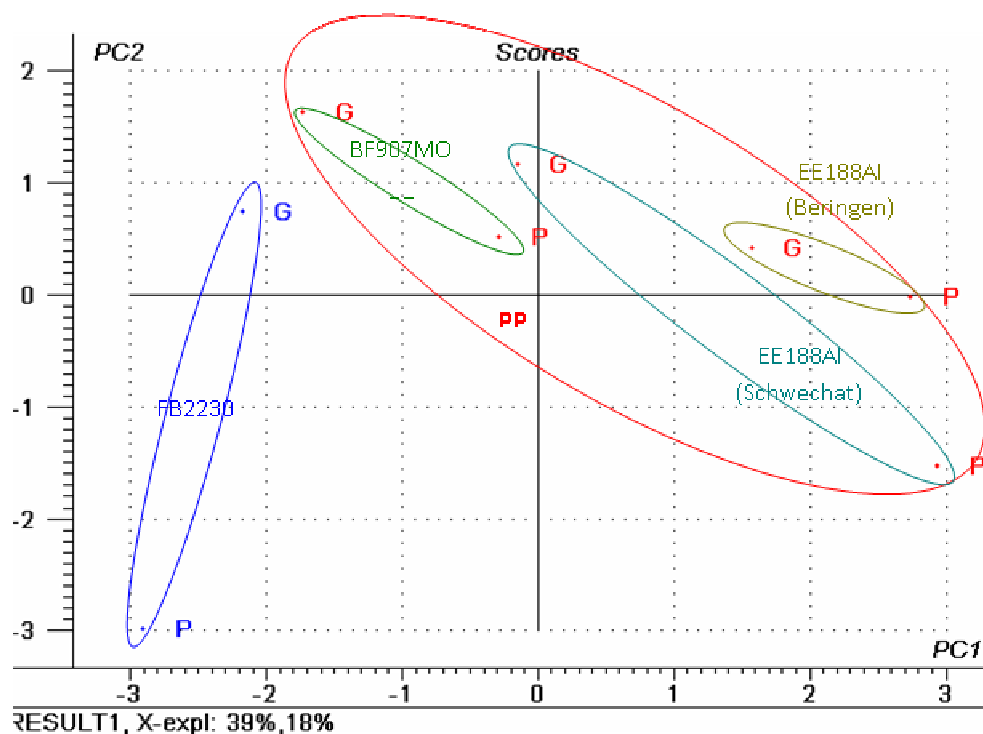


Figure 15. MVDA of representative detection frequency results (G ... pellets, P ... plaques).

#### 4.3.b. Results of BF970MO samples using GC-O with Detection Frequency

In Figure 16 to Figure 19 the Detection Frequency (SNIF) diagrams of the pure and 1:100 diluted extracts (see section 3.2.a) from both the pellets and the plaques are shown. A summary of identified odour-active compounds for the pellets and the plaques is given in Table 16.

The number of odour-active compounds increased after injection moulding; the number of odour-active compounds in the pure extracts with a SNIF value of 100 % (i.e. detection of all panellists) rose from three in the pellets to 7 in the plaques.

A similar picture is given by the 1:100 diluted extracts where no compounds were detected by all panellists in the pellets and three compounds with a SNIF value of 100% were detected after injection moulding.

The sum of compounds with 80 % and 100 % SNIF value doubled from the pellet to the plaque extracts (from 6 to 13).

The three major odour drivers of BF970MO (i.e. those compounds which were detected both in the pellets and plaques extract as well as in the 1:100 plaque extract) were identified as:

- 1-octen-3-one
- 1-nonen-3-one
- (E)-2-nonenal

A complete list of all identified odour-active compounds present in both the pellet and the plaque extracts is given in Table 16. Most of the identified compounds are aldehydes and ketones with a chain length between 5 and 14 C-atoms. Additionally, an aromatic nitrogen compound (2-acetyl-1-pyrroline), some alcohols and lactones were detected.

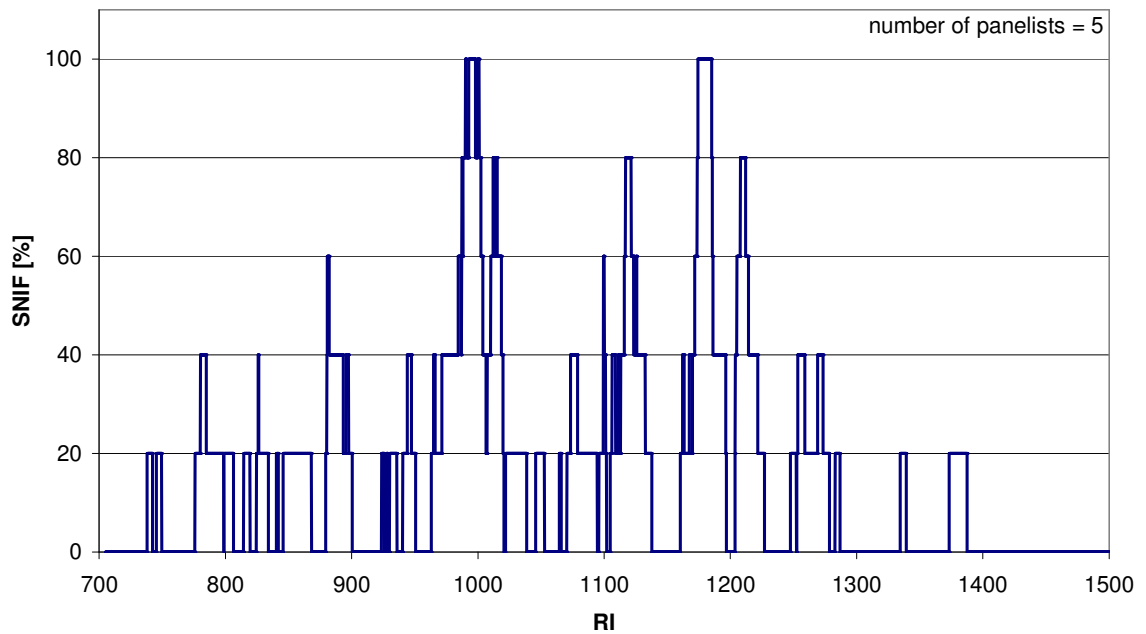


Figure 16. Detection Frequency (SNIF) Diagram of the extract obtained from BF907MO pellets.

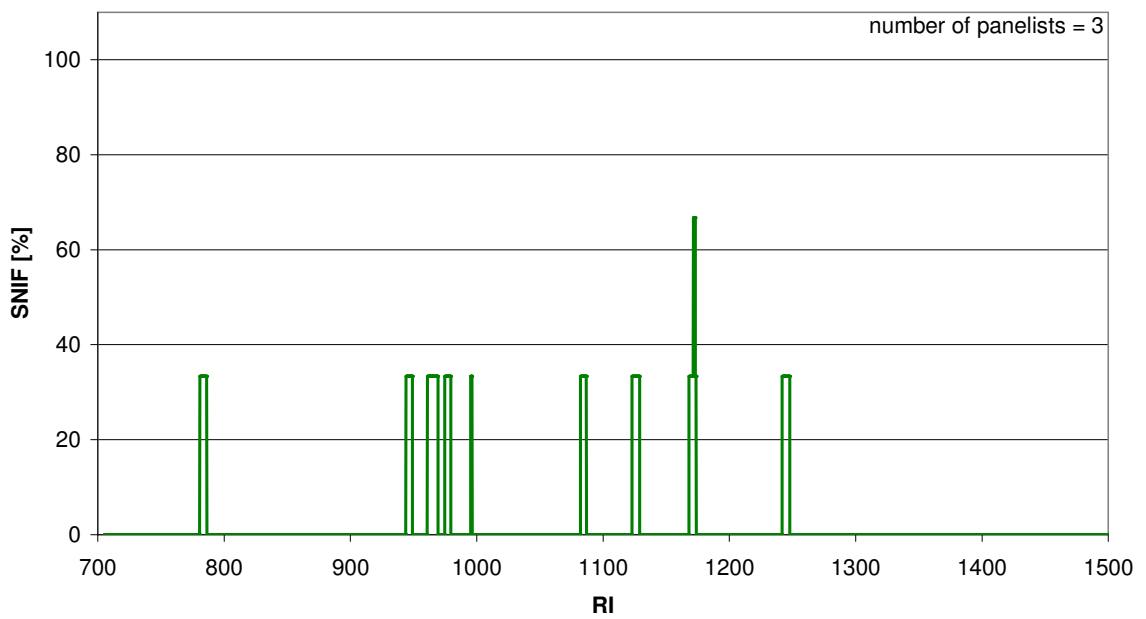


Figure 17. Detection Frequency (SNIF) Diagram of the 1:100 diluted extract obtained from BF907MO pellets.

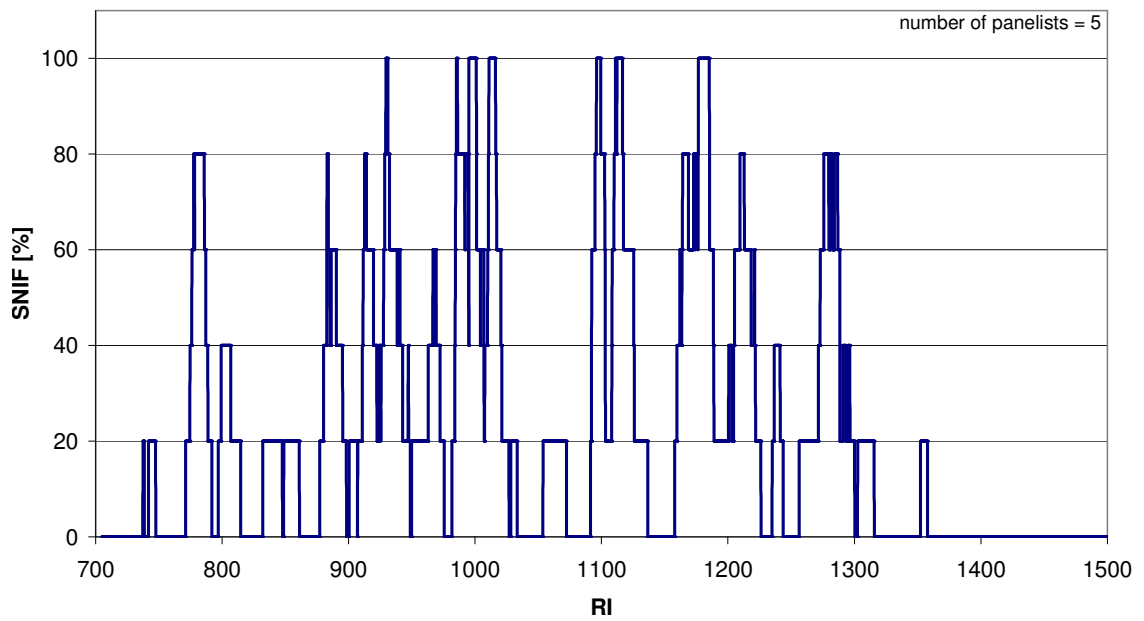


Figure 18. Detection Frequency (SNIF) Diagram of the extract obtained from BF907MO plaques.

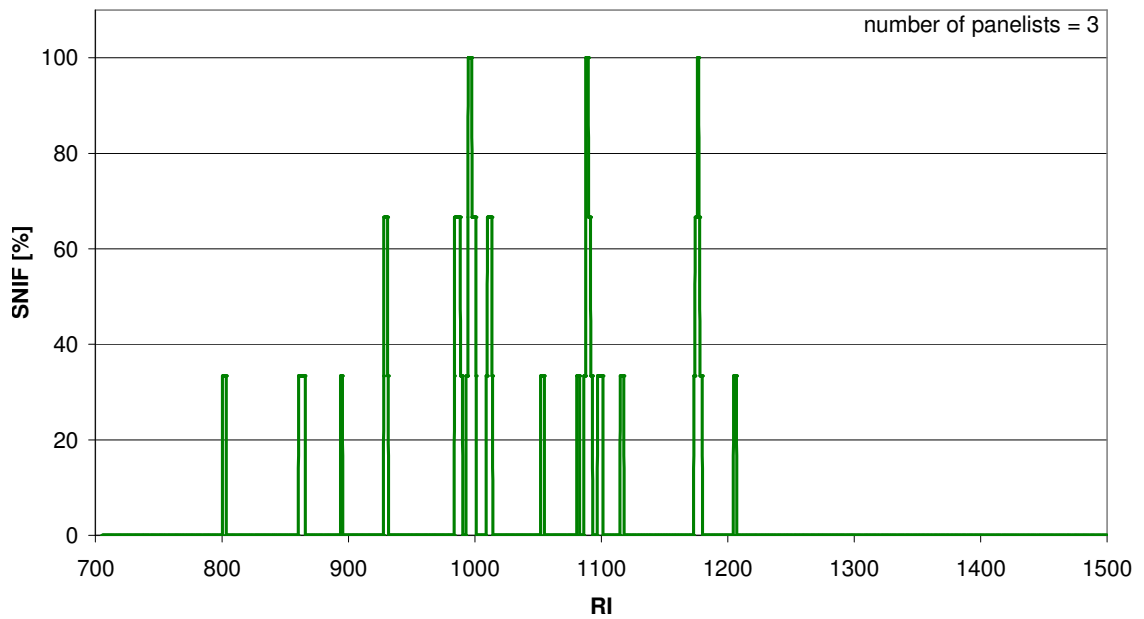


Figure 19. Detection Frequency (SNIF) Diagram of 1:100 diluted extract of BF907MO plaques.



**Table 16. Odour-active compounds in BF907MO pellets (pel) and plaques (pla) ( $RI_{exp}$  ... experimental Retention Indices, s.d. ... standard deviation,  $RI_{lit}$  ... literature Retention Indices determined with pure standards (om) or taken from literature sources<sup>67,68</sup>).**

Compound	Identified in		mean $RI_{exp}$ (HP5) $\pm$ s.d.	$RI_{lit}$ (HP5)	Source
	pel	pla			
(E)-2-pentenal	✓	✓	743.0 $\pm$ 5.7	759.4	om
1-hexen-3-one	✓	✓	776.6 $\pm$ 2.4	770.1	om
hexanal	✓	✓	798.2 $\pm$ 0.0	790.6	om
unknown	✓		814.3		
2-methyl-2-pentenal	✓	✓	828.9 $\pm$ 3.8	823.3	om
(Z)-2-hexenal	✓	✓	846.0 $\pm$ 3.5	843.1	<sup>68</sup>
1-hepten-3-one	✓	✓	881.1 $\pm$ 1.9	872.4	om
heptanal	✓	✓	899.3 $\pm$ 0.8	898.0	om
unknown		✓	909.7		
2-acetyl-1-pyrroline	✓	✓	925.5 $\pm$ 1.1	926	om
unknown	✓		928.8		
3-hepten-2-one	✓	✓	940.0 $\pm$ 3.3	934.4	om
(E)-2-heptenal	✓	✓	955.3 $\pm$	954.8	om
1-octen-3-one	✓	✓	984.4 $\pm$ 0.1	977.1	om
unknown	✓	✓	993.5 $\pm$ 0.5		
octanal	✓	✓	1007.4 $\pm$ 0.6	1002.3	om
(E,E)-2,4-heptadienal	✓		1018.1	1010.4	om
2-ethylhexanol		✓	1027.4	1028.6	om
3-octen-2-one	✓		1044.8	1039.2	om
(E)-2-octenal	✓	✓	1059.4 $\pm$ 11.0	1058.7	om
1-nonen-3-one	✓	✓	1084.2 $\pm$ 9.6	1079.7	om
(E)-6-nonenal				1095.1	
(Z)-6-nonenal	✓	✓	1103.6 $\pm$ 0.0	1101.2	om
8-nonenal				1096.5	
nonanal				1104.6	
(E,E)-2,4-octadienal	✓		1113.3	1110.3	om
(E)-2-nonenal	✓	✓	1164.6 $\pm$ 7.4	1161.4	om
decanal	✓	✓	1202.9 $\pm$ 1.6	1206.8	om

Compound	Identified in		mean RI <sub>exp</sub> (HP5) ± s.d.	RI <sub>lit</sub> (HP5)	Source
	pel	pla			
? 3-decen-2-one ? *	✓	✓	1238.5 ± 6.6	[1239]	
γ-octalactone	✓	✓	1252.7 ± 1.8	1258.8	<sup>68</sup>
(E)-2-decenal	✓	✓	1269.4 ± 3.0	1264.1	om
2-undecanone		✓	1287.4	1294.3	<sup>68</sup>
unknown		✓	1292.6		
? 3-undecen-2-one ?*		✓	1332.2	[1339]	
methyl anthranilate	✓		1349.8	1343.6	<sup>68</sup>
(E)-2-undecenal	✓		1371.6	1366.5	om

\* for compounds marked with questions marks pure standards could not be obtained.

#### 4.3.c. Results of EE188AI samples(EE188AI-9530 from Schwechat and EE188AI-9524 from Beringen) and their base polymers using GC-O with Detection Frequency

In Figure 20 to Figure 27 the Detection Frequency (SNIF) diagrams for the two EE188AI grades from Schwechat and Beringen for the extracts and diluted extracts obtained from the pellets and the plaques are shown.

A summary of identified odour-active compounds in the EE188AI material is given in Table 17.

In comparison to the reactor grade PP BF970MO (see section 4.3.b) for both EE188AI grades a high number of odour-active compounds were already detected in the pellets extract with SNIF values of 80 % and 100 %.

In the Schwechat samples an increase in the number and intensity of odour-active compounds from the pellets to the plaques can be seen (5 additional compounds with 100% SNIF value in the plaques). These additional compounds were already detected in the pellets but with lower SNIF values.

In the 1:100 diluted extracts still 5 and 6 odour-active compounds were detected in the pellets and plaques, respectively. Due to this high number of compounds with SNIF values of 100 % in the 1:100 diluted extracts of the plaques, a further 1:1000 dilution was sniffed by one panellist and revealed 8 remaining main odour drivers:

- 2-acetyl-1-pyrroline
- 1-octen-3-one
- octanal
- (E)-2-octenal

- 1-nonen-3-one
- 6-/ 8-nonenal
- (E)-2-nonenal
- decanal

In the Beringen samples a similar conclusion can be drawn: Again, a high number of odour-active compounds was detected by 80 % and 100 % of the panellists already in the pellets. After injections moulding two additional odour-active compounds with a 100 % SNIF value were detected in the plaque extract compared to the pellet extract (7 compounds with 100 % SNIF value).

In the 1:100 diluted extracts the difference between the pellets and the plaques was more pronounced: instead of two compounds with 100 % SNIF detected in the pellets, 8 compounds with high odour relevancy (i.e. SNIF value of 100 %) could be detected by all panellists in the plaque sample.

This discrepancy between the pure and the 1:100 diluted extract is most probably due to the high odour intensity of the extract: The compounds cannot be fully resolved by the panellist before the next odour-active compound is already eluting; every breath increases the risk of missing out compounds.

By diluting the extract this problem becomes less prone and odour detection is easier due to clearly separated odour impressions.

Evaluation of the 1:1000 diluted extract obtained from the plaque extract by one panellist revealed 6 remaining main odour drivers:

- heptanal
- octanal
- 1-nonen-3-one
- 6-/ 8-nonenal
- (E)-2-nonenal
- decanal

By comparing the two EE188AI materials some dissimilarity can be found:

- (i) although most odour-active compounds are the same, differences in intensity (i.e. concentration) were detected (e.g.: 1-octen-3-one was present in the 1:1000 diluted Schwechat extract while not detected in the Beringen extract).

(ii) For the 1:1000 diluted extracts the Schwechat sample showed one compound more and also their concentration seems to be higher (e.g. 2-acetyl-1-pyrroline vanished in the Beringen sample but not in the Schwechat sample in the 1:1000 diluted extracts).

In Figure 28 a direct comparison of the SNIF diagrams of the pure extracts obtained from the EE188AI pellets from Schwechat and Beringen is shown. The SNIF pattern look very similar, however, some differences can be found. All these compounds are highly odour-active and were all detected in the highest dilution of the extract obtained from the plaques, indicating that (1) these substances survive during the injection moulding,(2) most probably are further generated during the injection moulding of the pellets to the plaques, and (3) are known to be oxidation products and/or generated during elevated temperatures (i.e. 2-acetyl-1-pyrroline is a typical Maillard reaction product in food where during heating the compound forms from a reducing sugar and an amino acid).

- The Schwechat sample shows higher SNIF values (i.e. higher amounts) in
  - hexanal (RI 790)
  - 2-acetyl-1-pyrroline (RI 926)
  - 1-octen-3-one (RI 978)
- The Beringen sample shows higher SNIF values (i.e. higher amounts) in
  - 1-hexen-3-one (RI 779)
  - 1-nonen-3-one (RI 1079)
  - (E)-2-decenal (RI 1255)

During compounding of the EE188AI samples from Beringen the base polymers (i.e. those which are used in the formulation) were collected, injection moulded into plaques and analyzed as well. The samples are BS2581, a PE-HD, BE677AI, a mobility compound PP and EF015AE, a PP.

The samples were extracted and evaluated with GC-O as described in section 3. The resulting Detection Frequency (SNIF) diagrams are shown in Figure 29 – Figure 34.

Similar conclusion as in the EE188AI compound PP can be drawn:

- 1) The same substances turn up in both the pellets and plaques (e.g. compare the SNIF diagrams of BS2581 in Figure 29 - Figure 30).
- 2) These odour-active substances are more intense (i.e. higher concentrated) in the plaques indicated by broader SNIF areas in the SNIF diagrams (see Figure 29 - Figure 30).

3) The highest number of odour-active compounds was detected in the BE677AI material, whose odour pattern is also very similar to that of the EE188AI material (see Figure 26 and Figure 32).

3) Again, mainly aldehydes and ketones were detected, but in one sample (BE677AI plaques) the same nitrogen-containing compound 2-acetyl-1-pyrroline as in the EE188AI samples was identified, indicating that this substance in the EE188AI comes from the BE677AI material. This substance – 2-acetyl-1-pyrroline – possesses a high odour relevancy and contributes significantly to the overall aroma in the EE188AI plaques from Schwechat and Beringen. A comparison of odour-active compounds present in the individual base polymers and the EE188AI material is given in Table 18. Although some compounds turn up in both a base polymer and in the EE188AI compound (e.g. 2-acetyl-1-pyrroline) most substances seem to from during compounding resulting from oxidative processes.

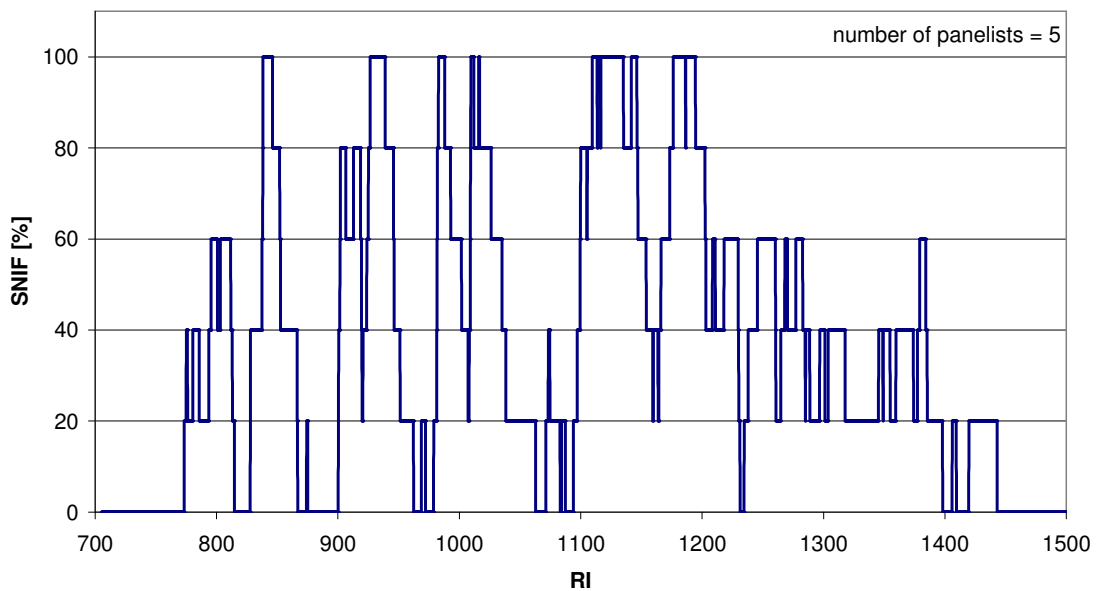


Figure 20. Detection Frequency (SNIF) Diagram of extract obtained from EE188AI-9530 (Schwechat) pellets.

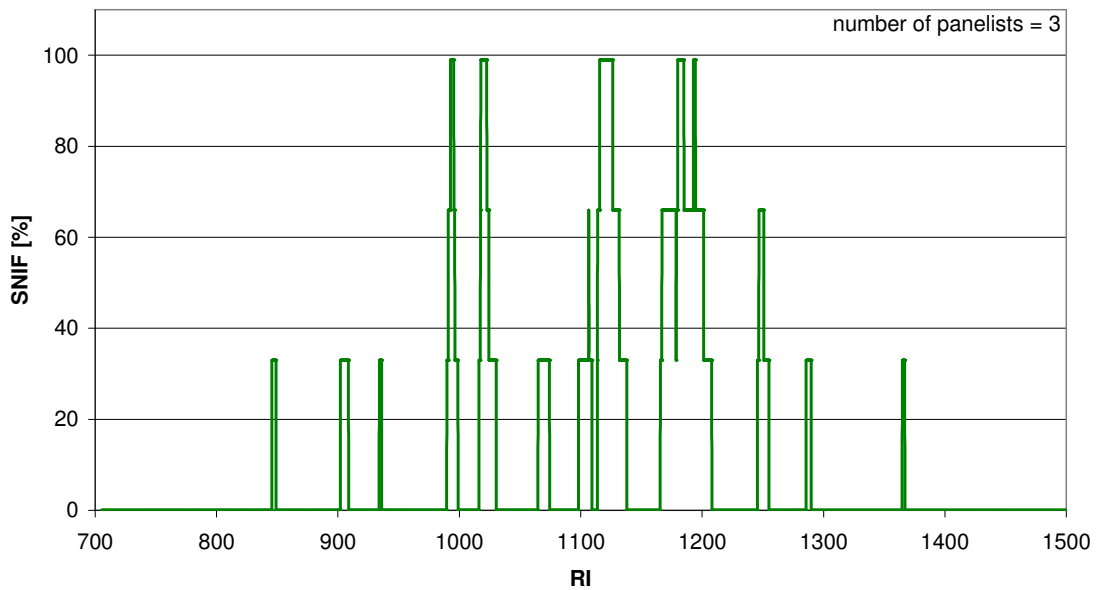


Figure 21. Detection Frequency (SNIF) Diagram of 1:100 diluted extract obtained from EE188AI (Schwechat) pellets.

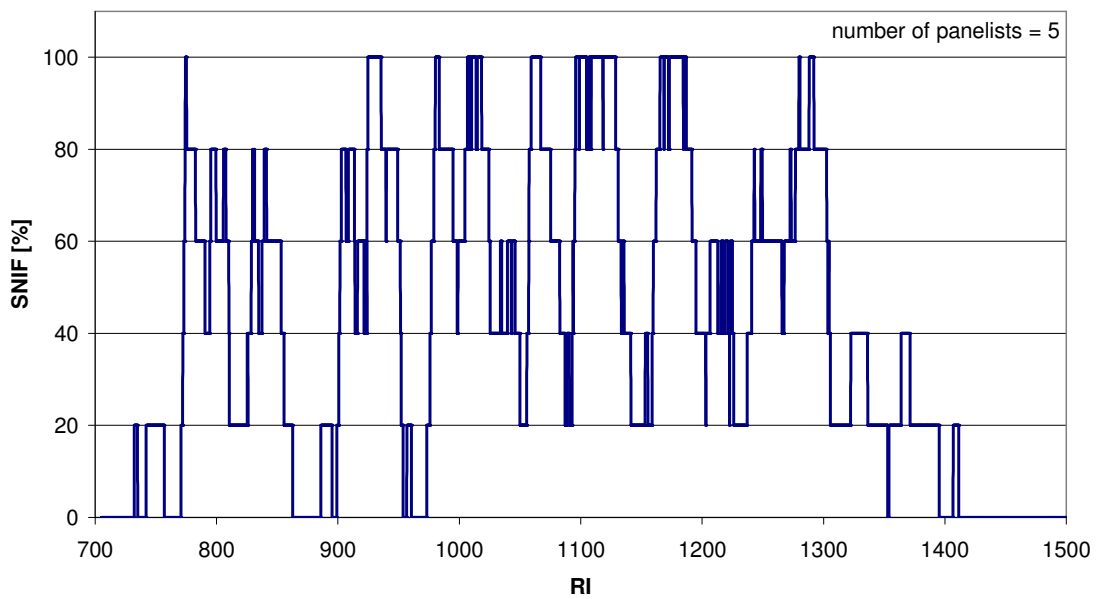


Figure 22. Detection Frequency (SNIF) Diagram of extract obtained from EE188AI (Schwechat) plaques.

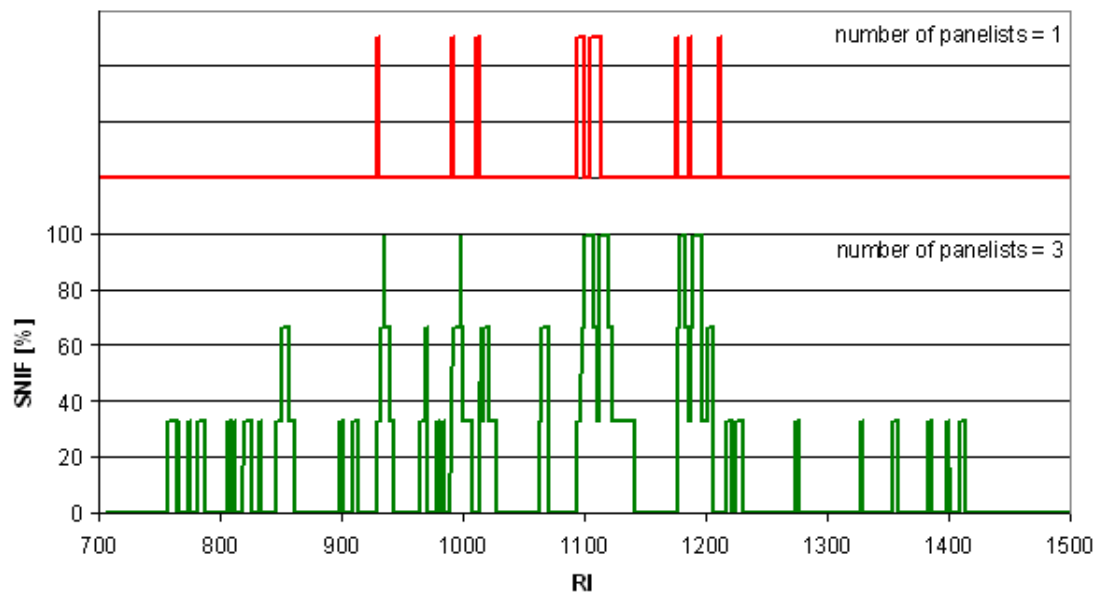


Figure 23. Detection Frequency (SNIF) Diagram of 1:100 diluted (in green) and 1:1000 diluted (in red) extract obtained from EE188AI (Schwechat) plaques.

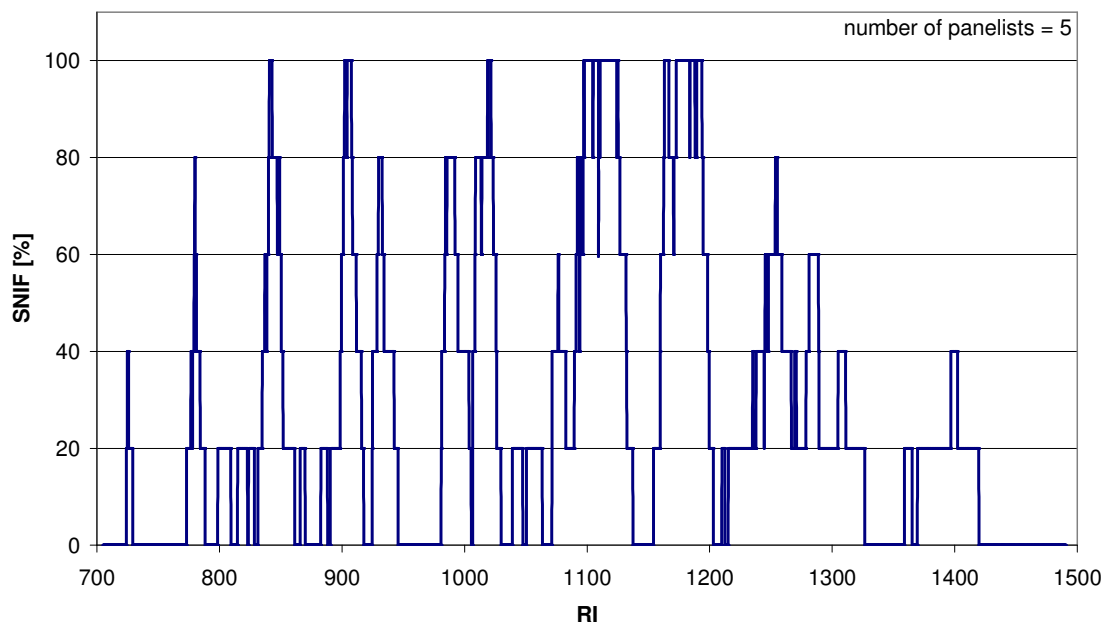


Figure 24. Detection Frequency (SNIF) Diagram of extract obtained from EE188AI (Beringen) pellets.

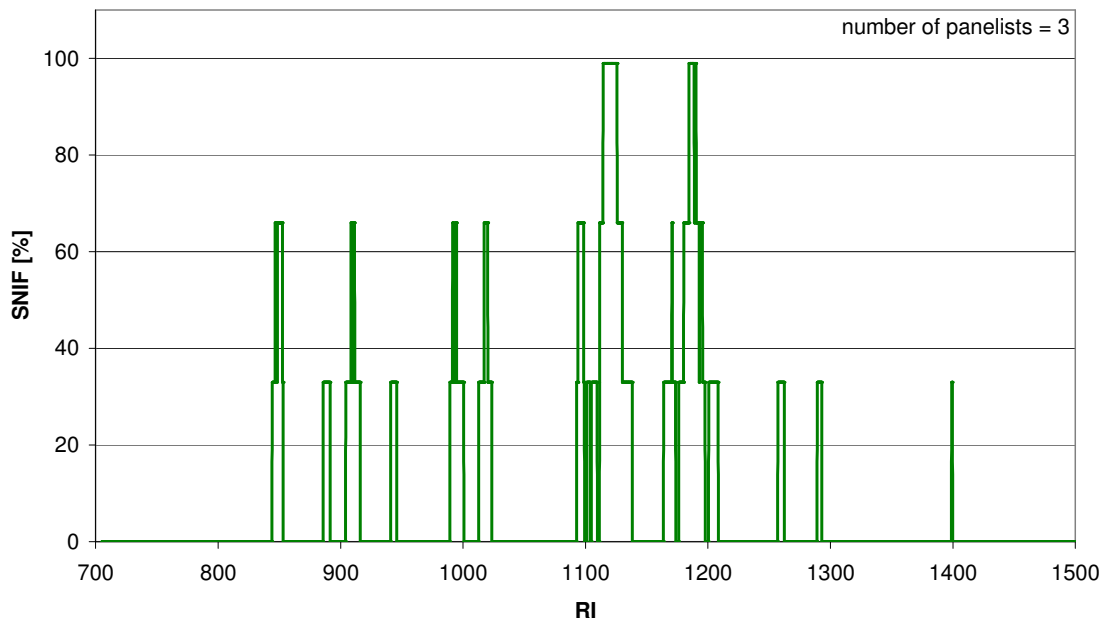


Figure 25. Detection Frequency (SNIF) Diagram of 1:100 diluted extract obtained from EE188AI (Beringen) pellets.

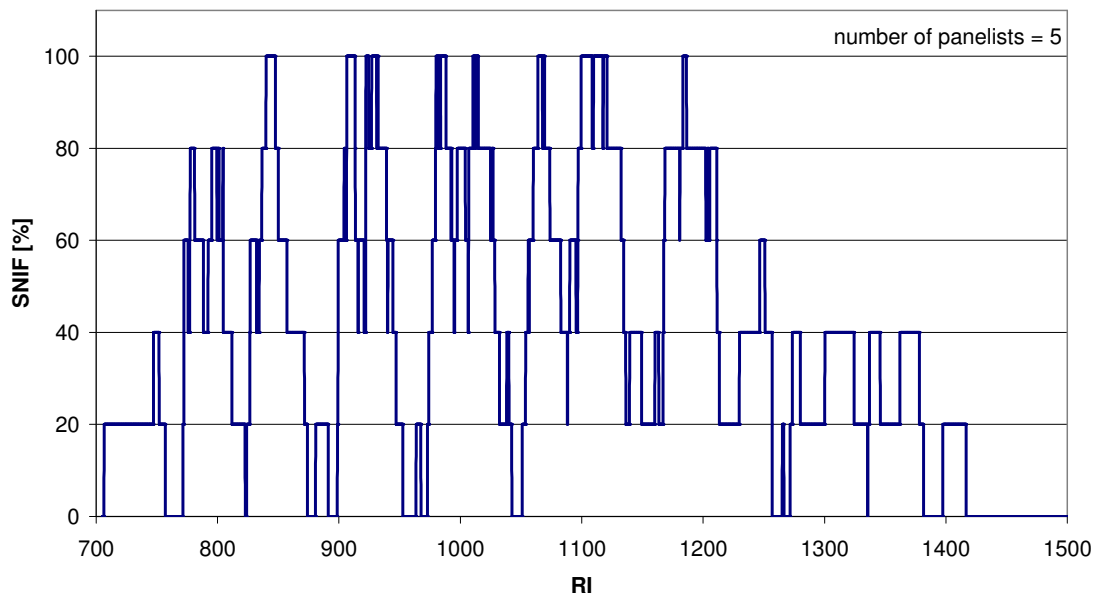


Figure 26. Detection Frequency (SNIF) Diagram of extract obtained from EE188AI (Beringen) plaques.



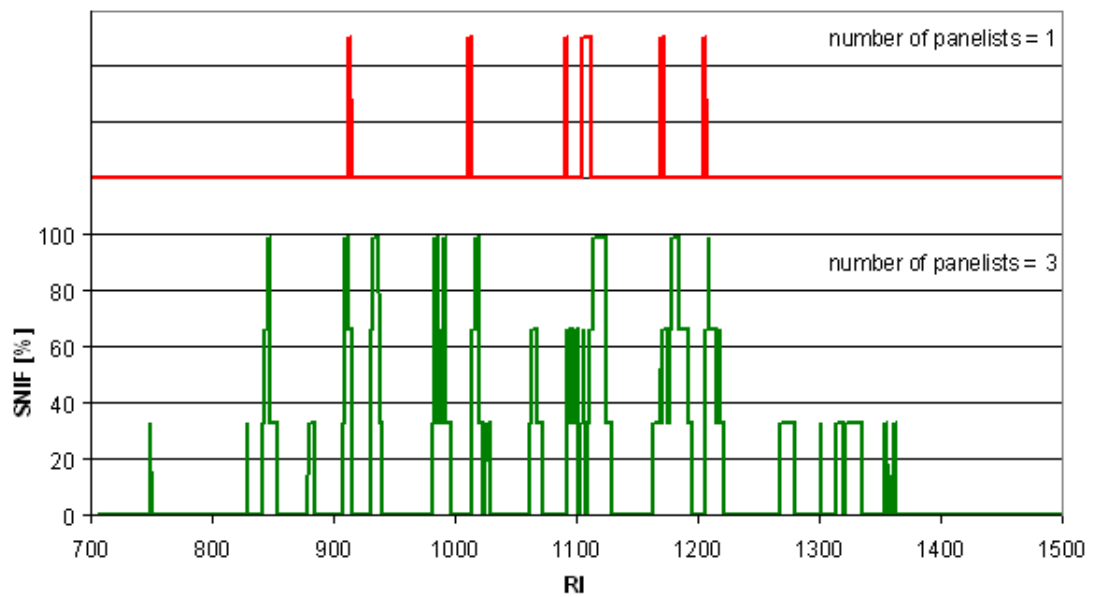


Figure 27. Detection Frequency (SNIF) Diagram of 1:100 diluted (in green) and 1:1000 diluted (in red) extract obtained from EE188AI (Beringen) plaques.

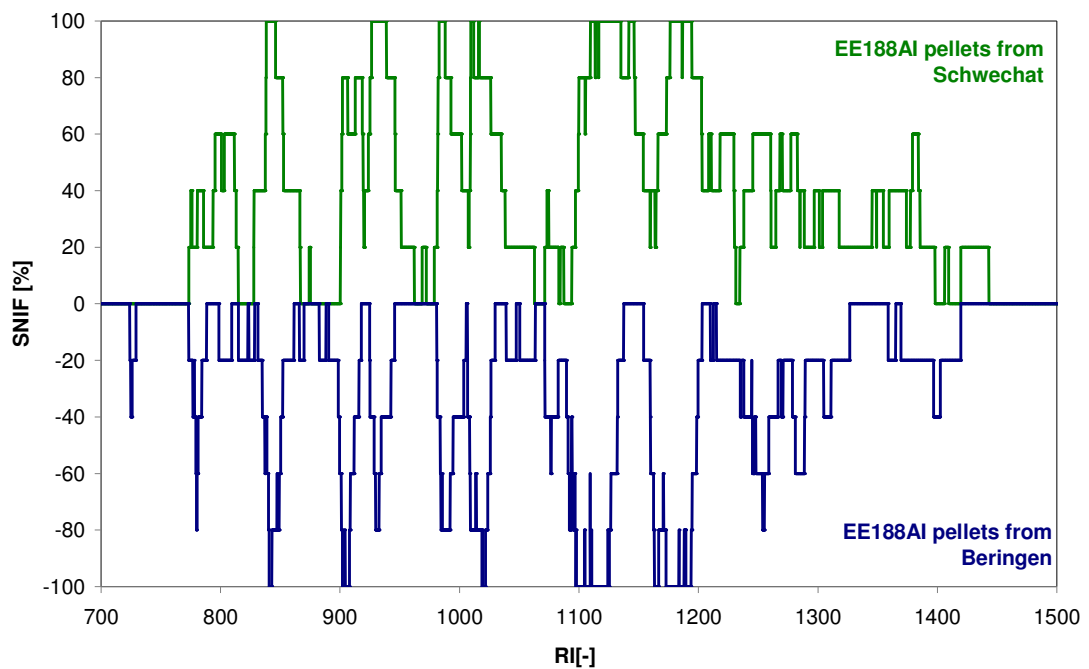


Figure 28. SNIF diagram comparison of the EE188AI pellets from Schwechat (on top in green) and Beringen (at the bottom in blue).

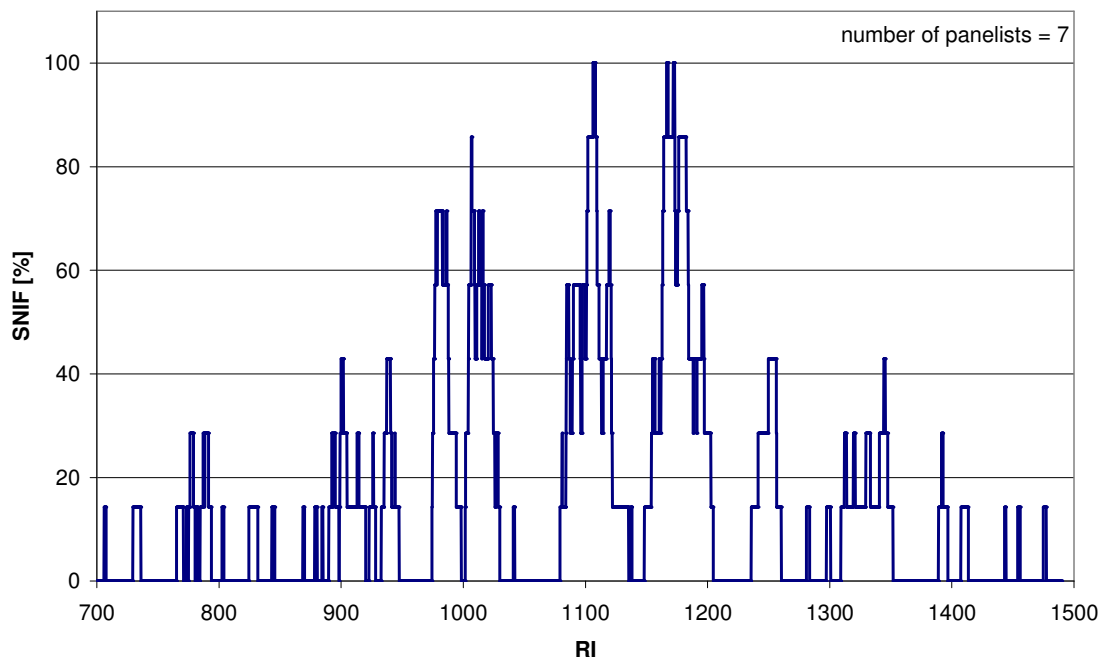


Figure 29. Detection Frequency (SNIF) Diagram of extract obtained from BS2581 pellets.

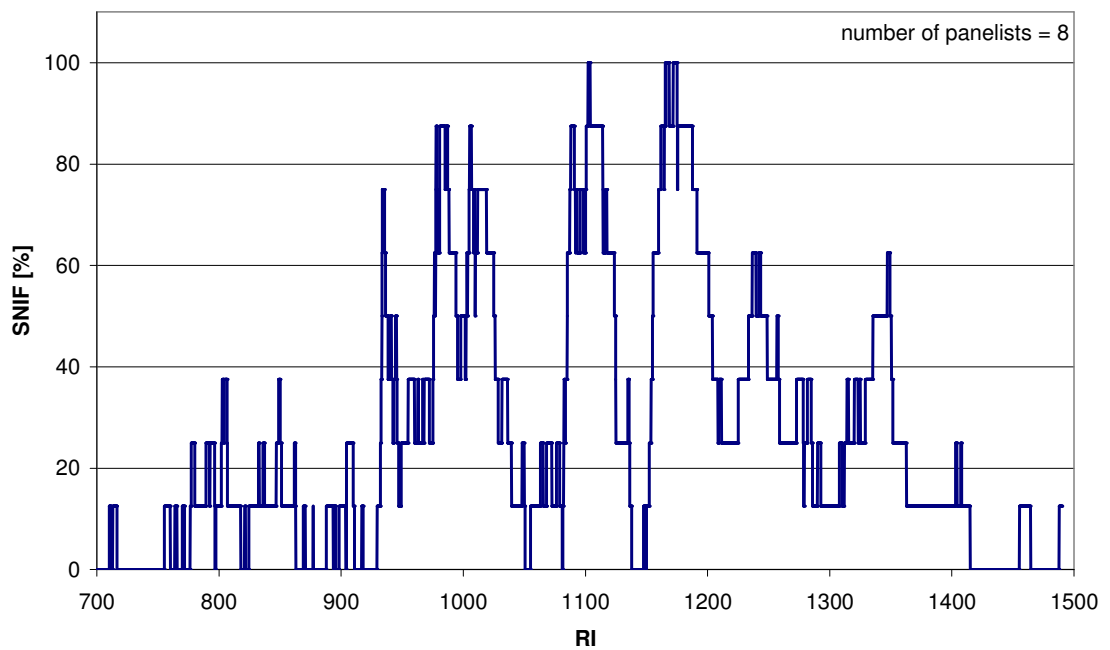


Figure 30. Detection Frequency (SNIF) diagram of extract obtained from BS2581 plaques.

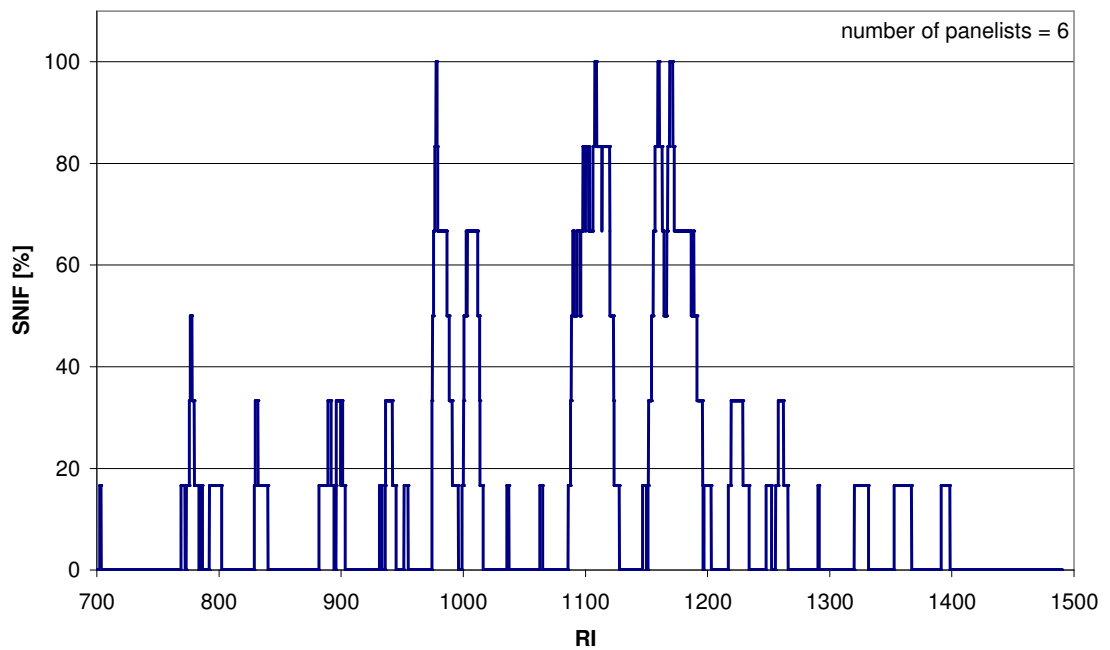


Figure 31. Detection Frequency (SNIF) diagram of extract obtained from BE677AI pellets.

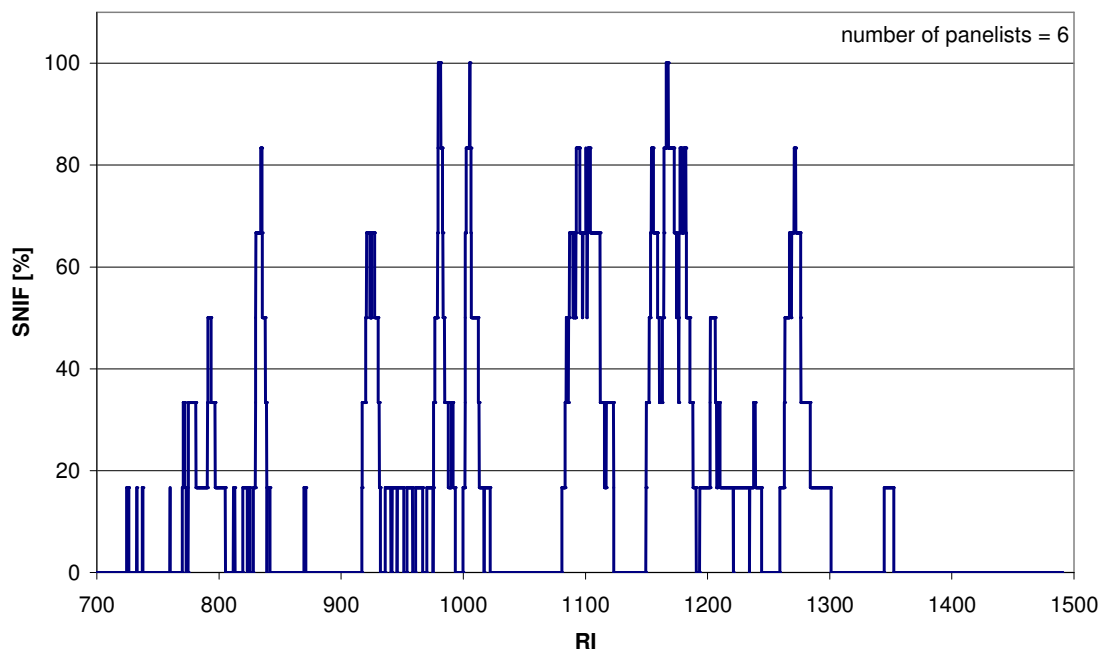


Figure 32. Detection Frequency (SNIF) diagram of extract obtained from BE677AI plaques.

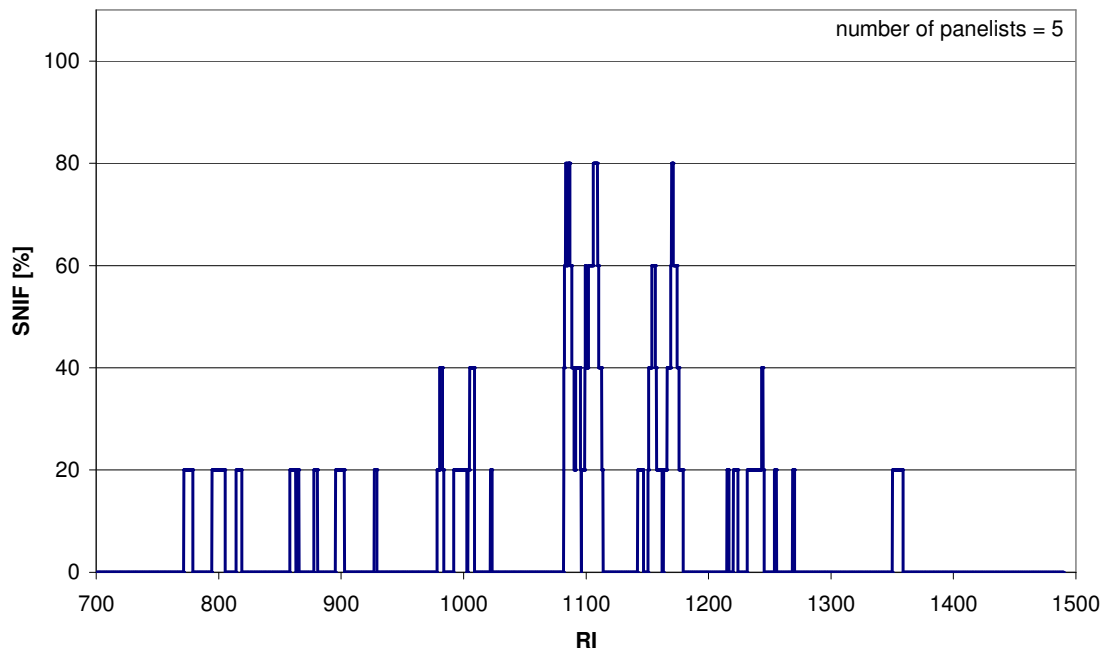


Figure 33. Detection Frequency (SNIF) diagram of extract obtained from EF015AE pellets.

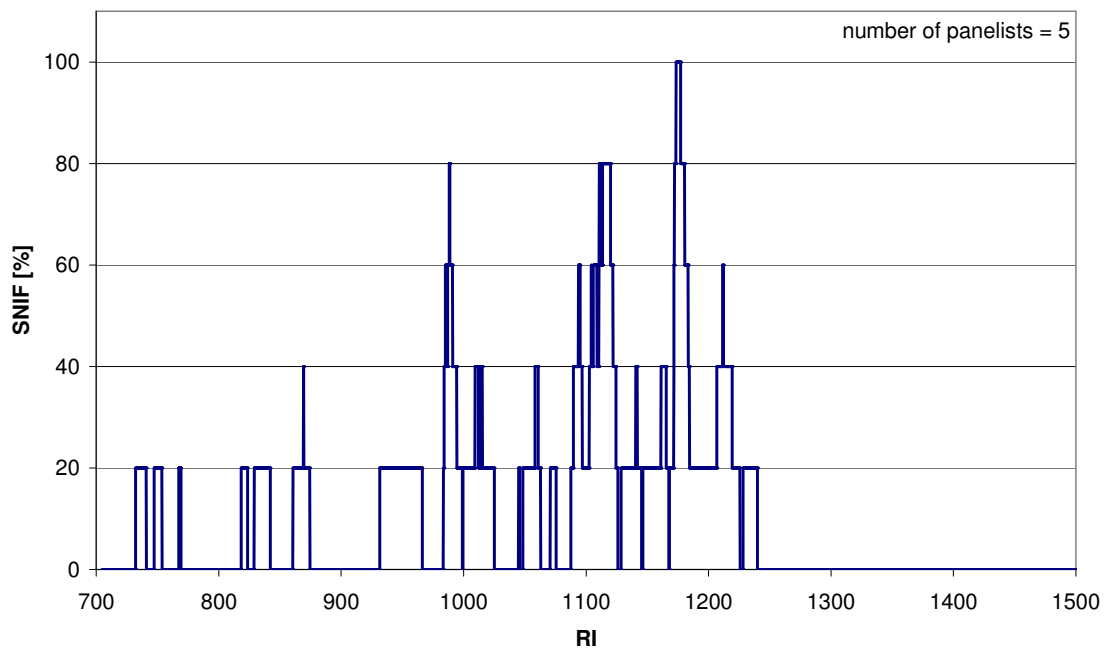


Figure 34. Detection Frequency (SNIF) diagram of extract obtained from EF015AE plaques.

**Table 17.** List of identified odour-active compounds detected in EE188AI samples from Beringen and Schwechat in extract obtained from pellets(pel) and plaques(pla). ( $RI_{exp}$  ... experimental Retention Indices, s.d. ... standard deviation,  $RI_{lit}$  ... literature Retention Indices determined with pure standards (om) or taken from literature sources<sup>67,68</sup>).

Compound	Schwechat		Beringen		mean $RI_{exp}$ $\pm$ s.d.	$RI_{lit}$	Source
	pel	pla	pel	pla			
pentanal				✓	706.3	697.4	<sup>68</sup>
(E)-2-pentenal		✓	✓	✓	738.5 $\pm$ 8.1	759.4	om
1-hexen-3-one	✓	✓	✓	✓	774.7 $\pm$ 2.0	770.1	om
hexanal	✓	✓	✓	✓	797.2 $\pm$ 3.3	790.6	om
unknown			✓		814.9		
2-methyl-2-pentenal	✓	✓	✓	✓	829.3 $\pm$ 4.1	823.3	om
(Z)-2-hexenal		✓	✓	✓	841.0 $\pm$ 2.3	843.1	<sup>68</sup>
1-hepten-3-one	✓	✓	✓	✓	875.9 $\pm$ 8.3	872.4	om
heptanal	✓	✓	✓	✓	902.8 $\pm$ 2.1	898.0	om
(E,E)-2,4-hexadienal	✓	✓	✓	✓	915.4 $\pm$ 0.4	907.2	om
2-acetyl-1-pyrroline	✓	✓	✓	✓	926.6 $\pm$ 0.9	926	om
3-hepten-2-one		✓		✓	937.0 $\pm$ 2.7	934.4	om
(E)-2-heptenal	✓	✓	✓	✓	965.4 $\pm$ 8.5	954.8	om
1-octen-3-one	✓	✓	✓	✓	984.4 $\pm$ 2.0	977.1	om
unknown				✓	994.0		
octanal	✓	✓	✓	✓	1009.6 $\pm$ 1.5	1002.3	om
(E,E)-2,4-heptadienal		✓	✓		1015.7 $\pm$ 1.3	1010.4	om
2-ethylhexanol	✓			✓	1027.2 $\pm$ 3.7	1028.6	om
3-octen-2-one				✓	1037.0	1039.2	om
(E)-2-octenal	✓	✓	✓	✓	1061.6 $\pm$ 4.1	1058.7	om
1-nonen-3-one	✓	✓	✓	✓	1092.5 $\pm$ 3.6	1079.7	om
(E)-6-nonenal						1095.1	
(Z)-6-nonenal	✓	✓	✓	✓	1099.8 $\pm$ 2.1	1101.2	om
8-nonenal						1096.5	
nonanal						1104.6	
(E,E)-2,4-octadienal	✓			✓	1114.8 $\pm$ 1.9	1110.3	om
3-nonen-2-one				✓	1138.1	1139.9	<sup>68</sup>
$\gamma$ -heptalactone			✓		1152.5	1152.7	<sup>68</sup>
(E)-2-nonenal	✓	✓	✓	✓	1163.8 $\pm$ 3.5	1161.4	om
decanal	✓	✓	✓	✓	1208.3 $\pm$ 3.7	1206.8	om

Compound	Schwechat		Beringen		mean $RI_{exp} \pm$ s.d.	$RI_{lit}$	Source
	pel	pla	pel	pla			
? 3-decen-2-one ?*	✓	✓	✓	✓	1226.6 ± 9.1	[1239]	
(E)-2-decenal	✓	✓	✓	✓	1273.4 ± 3.5	1264.1	om
undecanal	✓	✓	✓	✓	1298.3 ± 3.6	1307.8	om
? 3-undecen-2-one ?*		✓		✓	1337.6 ± 5.0	[1339]	
(E)-2-undecenal	✓	✓	✓	✓	1359.2 ± 8.3	1366.5	om
δ-nonalactone			✓	✓	1395.3 ± 0.2	1392.7	<sup>68</sup>
dodecanal		✓			1405.7	1409.7	om

\* for compounds marked with questions marks pure standards could not be obtained.

Table 18. List of odour-active compounds present in the base polymers BS2581, BE677AI, EF015AE and in the corresponding compound PP EE188AI from Beringen in pellets (pel) and plaques (pla) ( $RI_{exp}$  ... experimental Retention Indices, s.d. ... standard deviation,  $RI_{lit}$  ... literature Retention Indices determined with pure standards (om) or taken from literature sources<sup>67,68</sup>).

Compound	BS2581		BE677AI		EF015AE		EE188AI Beringen		mean $RI_{exp}$ +/- s.d.	$RI_{lit}$	Source
	pel	pla	pel	pla	pel	pla	pel	pla			
pentanal	✓	✓						✓	708.1 ± 3.1	697.4	68
unknown	✓	✓		✓		✓			727.7 ± 2.5		
3-penten-2-one				✓		✓	✓	✓	739.1 ± 7.1	734.0	68
(E)-3-pentenal		✓		✓					756.3 ± 1.1	759.4	om
unknown	✓	✓	✓						766.1 ± 2.4		
1-hexen-3-one	✓	✓	✓	✓	✓	✓	✓	✓	773.1 ± 3.7	770.1	om
(Z)-3-hexenal	✓		✓		✓				785.1 ± 0.7	788.1	om
hexanal		✓	✓	✓	✓		✓	✓	795.0 ± 2.6	790.6	om
unknown	✓			✓	✓	✓	✓		812.4 ± 2.3		
2-methyl-2-pentenal	✓	✓		✓		✓			823.2 ± 2.7	823.3	om
unknown			✓	✓			✓	✓	828.4 ± 1.7		
(E)-2-hexenal	✓	✓		✓			✓	✓	841.3 ± 2.4	849.5	68
1-hepten-3-one		✓		✓	✓	✓	✓		865.3 ± 3.4	872.4	om
unknown	✓	✓	✓		✓		✓	✓	883.0 ± 4.1		
heptanal	✓	✓	✓		✓		✓	✓	900.1 ± 3.9	898.0	om
(E,E)-2,4-hexadienal	✓	✓					✓	✓	915.1 ± 1.5	907.2	om
2-acetyl-1-pyrroline				✓	✓	✓	✓	✓	924.5 ± 2.5	926.0	om
3-hepten-2-one	✓	✓	✓	✓					937.4 ± 2.6	934.4	om
(E)-2-heptenal		✓	✓	✓	✓				951.2 ± 2.8	954.8	om
1-heptanol		✓	✓	✓				✓	963.4 ± 2.9	968.4	om
1-octen-3-one	✓	✓	✓	✓	✓	✓	✓	✓	977.3 ± 1.2	977.1	om
unknown	✓			✓	✓	✓	✓	✓	988.4 ± 3.0		
octanal	✓	✓	✓	✓	✓	✓	✓	✓	1004.7 ± 2.8	1002.3	om
(E,E)-2,4-heptadienal				✓		✓	✓		1017.0 ± 0.5	1010.4	om
2-ethylhexanol	✓	✓			✓			✓	1025.7 ± 2.3	1028.6	om
3-octen-2-one			✓			✓	✓	✓	1036.7 ± 1.5	1039.2	om
unknown	✓	✓			✓	✓			1046.2 ± 4.0		
(E)-2-octenal	✓	✓	✓			✓	✓	✓	1061.6 ± 1.6	1058.7	om

Compound	BS2581		BE677AI		EF015AE		EE188AI Beringen		mean $R_{i\text{exp}}$ + s.d.	$R_{i\text{lit}}$	Source
	pel	pla	pel	pla	pel	pla	pel	pla			
unknown	✓	✓							1075.2 ± 1.7		
1-nonen-3-one	✓	✓	✓	✓	✓	✓	✓	✓	1086.3 ± 3.2	1079.7	om
(E)-6-nonenal										1095.1	
(Z)-6-nonenal	✓	✓	✓	✓	✓	✓	✓	✓	1099.0 ± 2.5	1101.2	om
8-nonenal										1096.5	
nonanal						✓	✓	✓	1106.8 ± 3.2	1104.6	om
(E,E)-2,4-octadienal		✓		✓		✓		✓	1117.2 ± 1.8	1110.3	om
3-nonen-2-one	✓			✓		✓		✓	1135.3 ± 3.0	1139.9	68
unknown	✓		✓		✓				1145.0 ± 3.9		
γ-heptalactone		✓	✓	✓	✓	✓	✓		1153.0 ± 1.4	1152.7	68
(E)-2-nonenal	✓	✓	✓	✓	✓	✓	✓	✓	1165.1 ± 2.3	1161.4	om
? 1-decen-3-one ?*		✓	✓					✓	1175.2 ± 2.8	[1178]	
unknown	✓		✓					✓	1187.4 ± 3.2		
(Z)-4-decenal	✓		✓	✓		✓		✓	1199.5 ± 3.0	1197.3	om
decanal		✓						✓	1208.6 ± 0.6	1206.8	om
(E,E)-2,4-nonadienal			✓		✓	✓	✓		1217.6 ± 1.5	1215.9	om
unknown		✓	✓	✓	✓			✓	1224.7 ± 4.2		
?3-decen-2-one?*	✓	✓	✓	✓	✓			✓	1241.9 ± 4.6	[1239]	
γ-octalactone			✓	✓	✓				1257.9 ± 4.9	1251.4	om
(E)-2-decenal		✓		✓	✓			✓	1271.3 ± 3.3	1264.1	om
?1-undecen-3-one?*	✓	✓							1280.7 ± 0.5	[1278]	
undecanal	✓	✓	✓					✓	1308.1 ± 4.7	1308.8	om
(E,E)-2,4-decadienal	✓	✓	✓						1321.5 ± 2.7	1319.4	om
?3-undecen-2-one?*	✓	✓						✓	1332.7 ± 3.0	[1339]	
unknown	✓	✓	✓	✓	✓			✓	1349.9 ± 5.7		
δ-nonalactone	✓		✓					✓	1393.0 ± 2.8	1392.7	om

\* for compounds marked with questions marks pure standards could not be obtained.



#### **4.3.d. Results of the FB2230 samples from Schwechat PE4 and Porvoo PE2 using GC-O with Detection Frequency**

In Figure 34 to Figure 38 the Detection Frequency (SNIF) diagrams of the pure and 1:100 diluted extracts obtained from FB2230 pellets and plaques from Schwechat are shown. The FB2230 material from Porvoo arrived a year after the Schwechat material and only pellets were evaluated. The SNIF diagrams for the pure and 1:100 diluted extract obtained from the FB2230 pellets from Porvoo are shown in Figure 39 and Figure 40. Figure 41 shows a direct comparison of the SNIF diagrams for the two FB2230 pellets from Schwechat and Porvoo.

A complete list of identified odour-active compounds detected in FB2230 pellets and plaques from both plants is given in Table 19.

Injection Moulding of the FB2230 pellets from Schwechat increased the number of odour-active compounds with SNIF values of 100% from 3 to 5 (compare Figure 34 and Figure 37). The sum of compounds with SNIF values of 100% and 80% rose from 7 to 10 compounds.

For the diluted extracts the situation is similar for the plaques, while in the diluted pellet extract no compounds with SNIF values of 100% were identified. In the diluted plaque's extract three main odour drivers with SNIF values of 100% were identified as:

- 1-nonen-3-one
- 6-/8-nonenal/nonanal
- (E)-2-nonenal

For the FB2230 pellets from Porvoo the picture is a bit diverse:

While in the pure extract 5 compounds with high odour relevancy (SNIF values of 100%) were detected, after dilution 4 out of these 5 could be still detected by all panellists; these 4 remaining compounds were identified as main odour drivers in the FB2230 material from Porvoo:

- 1-hexen-3-one
- 2-acetyl-1-pyrroline
- unknown (RI 969)
- 6-/8-nonenal/nonanal

By comparing the SNIF diagrams for the two FB2230 extracts obtained from the pellets several differences can be addressed (see Figure 41):

(1) More odour-active compounds with high relevancy (SNIF = 100%) turn up for the Porvoo material – five for the Porvoo and three for the Schwechat pellets.

(2) The Porvoo material shows more early eluting odorants with high impact between RI 780 and 1500, while for the Schwechat material the odour-active compounds with high impact elute between RI 1500 and 1200.

(3) Some odorants turn up with high impact (100%) either in the in the Porvoo or Schwechat material (e.g. RI 780, 1-Hexen-3-one in Porvoo 100%, in Schwechat 40% ; RI 1166, (E)-2-Nonenal in Porvoo 40%, in Schwechat 100%).

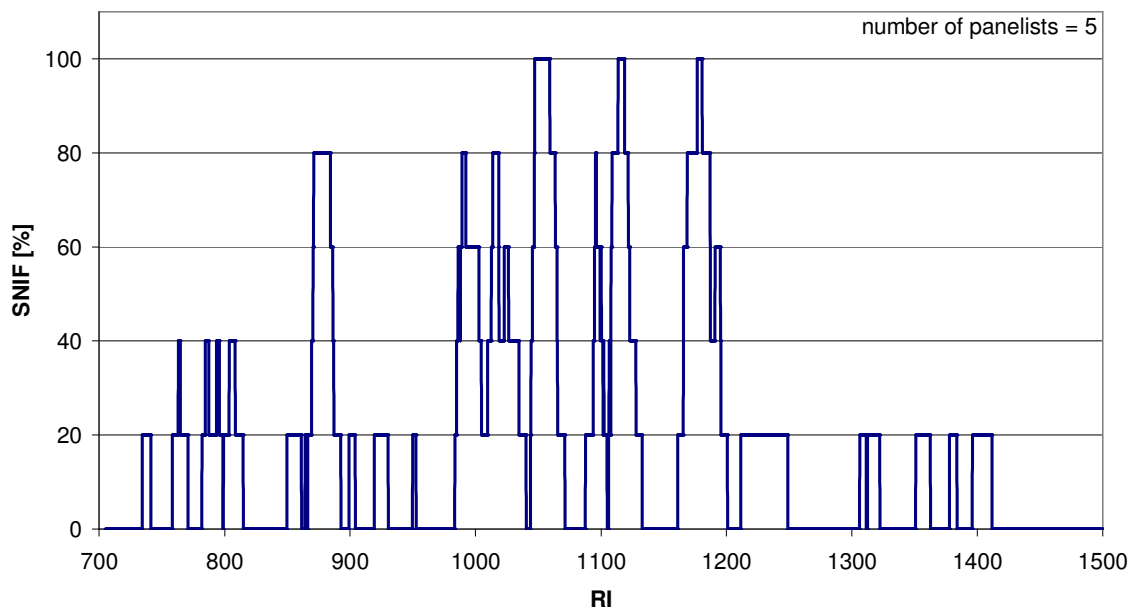


Figure 35. Detection Frequency (SNIF) diagram of the extract obtained from FB2230 (Schwechat) pellets.

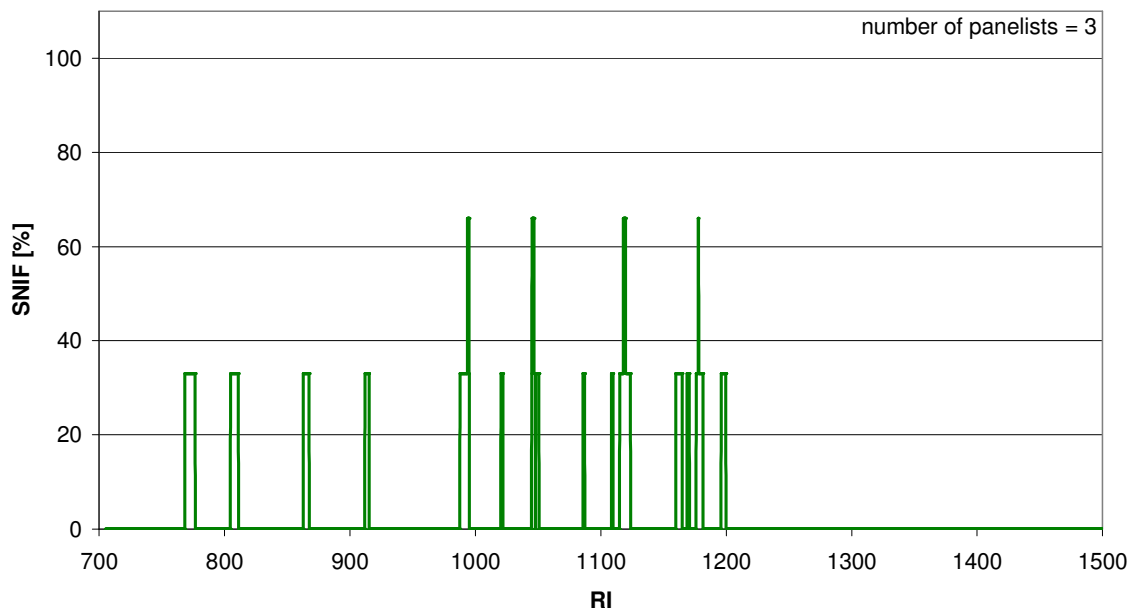


Figure 36. Detection Frequency (SNIF) diagram of the 1:100 diluted extract obtained from FB2230 (Schwechat) pellets.

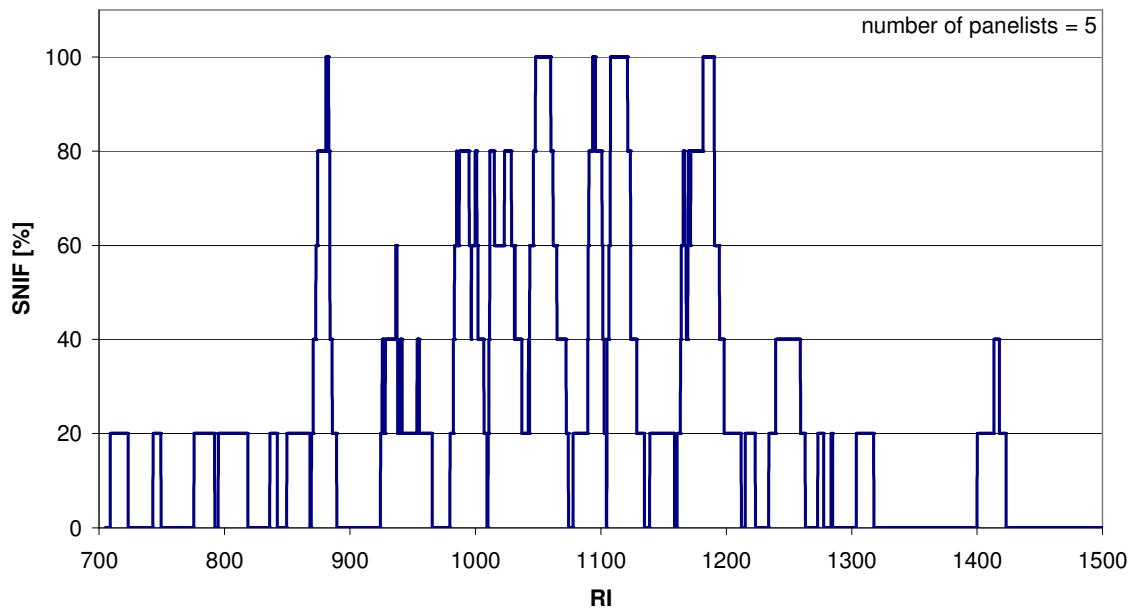


Figure 37. Detection Frequency (SNIF) diagram of the extract obtained from FB2230 (Schwechat) plaques.

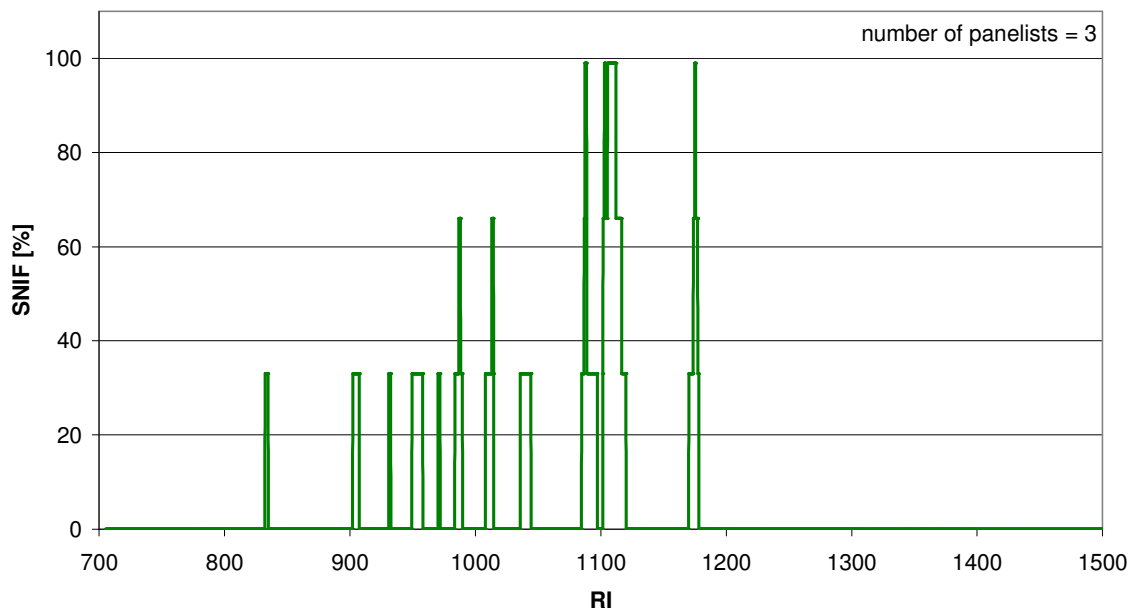


Figure 38. Detection Frequency (SNIF) diagram of the 1:100 diluted extract obtained from FB2230 (Schwechat) plaques.

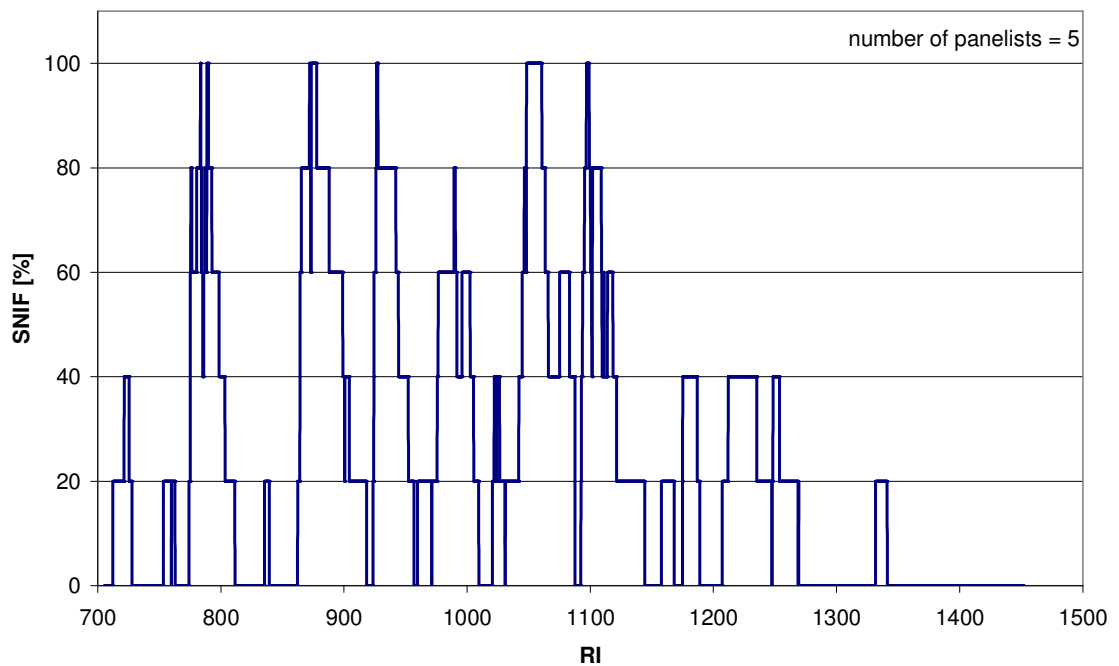


Figure 39. Detection Frequency (SNIF) diagram of the extract obtained from FB2230 (Porvoo) pellets.

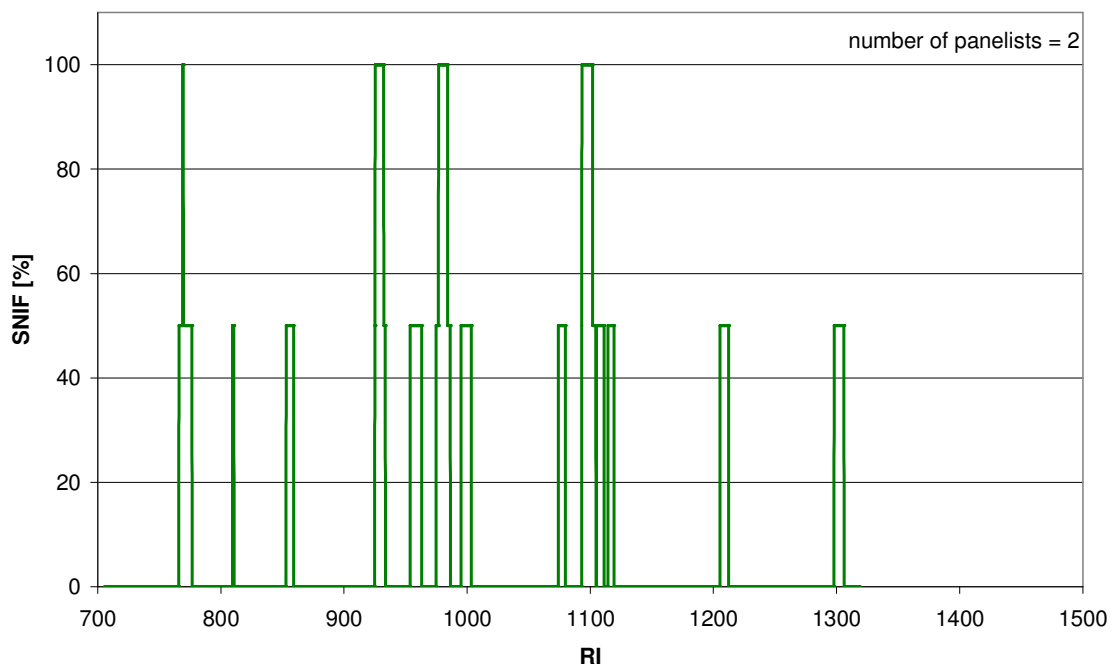


Figure 40. Detection Frequency (SNIF) diagram of the 1:100 diluted extract obtained from FB2230 (Porvoo) pellets.

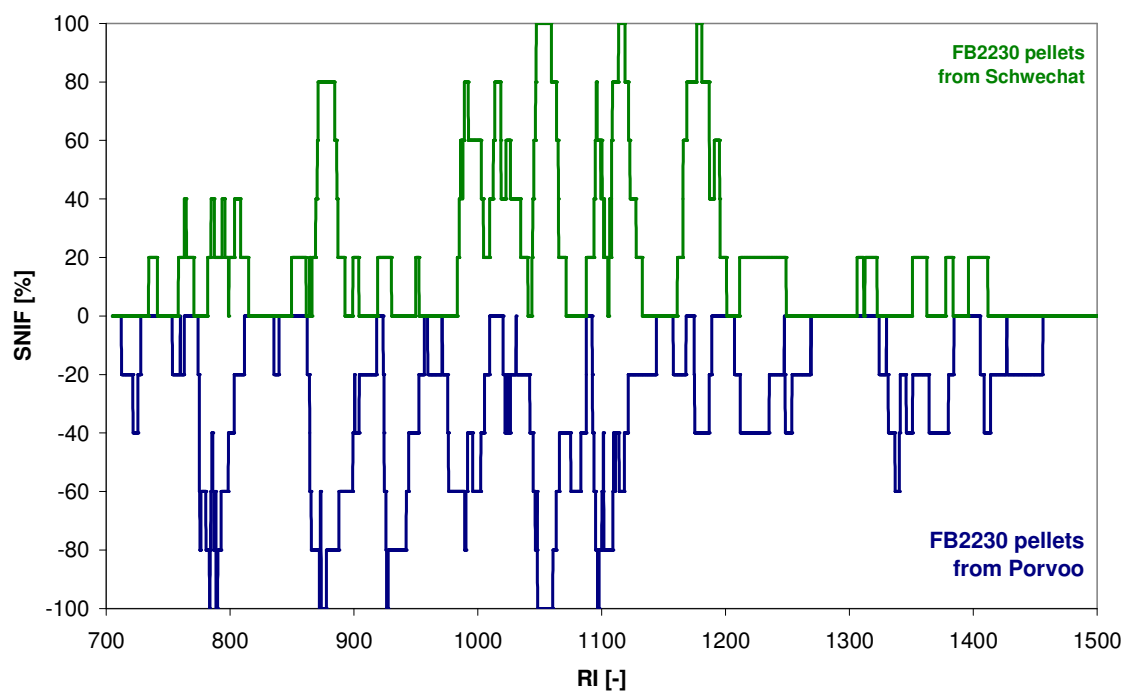


Figure 41. Detection Frequency (SNIF) diagram comparison of the FB2230 pellets from Schwechat (on top in green) and Porvoo (at the bottom in blue).

Table 19. List of odour-active compounds present in the FB2230 from Schwechat and Porvoo (pel ... pellets; pla ... plaques;  $RI_{exp}$  ... experimental Retention Indices, s.d. ... standard deviation,  $RI_{lit}$  ... literature Retention Indices determined with pure standards (om) or taken from literature sources<sup>68</sup>).

Compound	Porvoo	Schwechat		mean $RI_{exp} \pm$ s.d.	$RI_{lit}$	Source
	pel	pel	pla			
pentanal			✓	708.2	697.2	<sup>68</sup>
unknown	✓			718.4		
(E)-2-pentenal	✓	✓	✓	734.5 ± 7.9	759.4	om
unknown	✓	✓		758.2 ± 2.9		
1-hexen-3-one	✓	✓	✓	778.0 ± 4.1	770.1	om
(Z)-3-hexenal	✓			785.9	788.1	om
hexanal		✓	✓	796.1 ± 2.6	790.6	om
?3-hexen-2-one?*	✓		✓	833.3 ± 0.4	823.3	om
(E)-2-hexenal		✓	✓	849.0 ± 0.0	849.5	68
unknown	✓	✓		861.8 ± 2.0		
1-hepten-3-one	✓	✓	✓	870.0 ± 2.4	872.4	om
heptanal	✓	✓		896.5 ± 2.0	898.0	om
2-acetyl-1-pyrroline	✓	✓	✓	922.6 ± 4.1	926.0	om
3-heptene-2-one			✓	941.1	934.4	om

Compound	Porvoo	Schwechat		mean $R_{I_{exp}} \pm$ s.d.	$R_{I_{lit}}$	Source
	pel	pel	pla			
(E)-2-heptenal	✓	✓		951.2 ± 3.1	954.6	om
1-octen-3-one	✓	✓	✓	984.3 ± 1.2	977.1	om
unknown			✓	997.2		
octanal	✓	✓	✓	1011.6 ± 2.4	1002.3	om
3-octen-2-one	✓	✓	✓	1042.2 ± 2.8	1039.2	om
unknown	✓			1067.1		
1-nonen-3-one	✓	✓	✓	1087.9 ± 3.2	1079.7	om
(E)-6-nonenal					1095.1	
(Z)-6-nonenal	✓	✓	✓	1098.4 ± 5.2	1101.2	om
8-nonenal					1096.5	
nonanal	✓	✓		1104.7 ± 1.5	1104.6	om
(E,E)-2,4-octadienal	✓			1112.4	1110.3	om
3-nonen-2-one	✓		✓	1137.5	1139.9	<sup>68</sup>
(E)-2-nonenal	✓	✓	✓	1165.6 ± 1.7	1161.4	om
?1-decen-3-one?*		✓	✓	1175.1 ± 0.0	[1178]	
unknown		✓		1188.9		
(Z)-4-decenal	✓			1199.9	1197.3	om
decanal		✓	✓	1211.5 ± 2.8	1206.8	om
?3-decen-2-one?*	✓		✓	1236.6 ± 2.5	[1239]	
(E)-2-decenal			✓	1275.9	1264.1	om
undecanal	✓	✓	✓	1307.2 ± 5.9	1308.8	om
(E,E)-2,4-decadienal	✓			1322.1	1319.4	om
?3-undecen-2-one?*	✓			1334.5	[1339]	
(E)-2-undecenal	✓			1352.6	1366.5	om
δ-nonalactone	✓	✓	✓	1397.4 ± 6.0	1392.7	om

\* for compounds marked with questions marks pure standards could not be obtained.

#### **4.3.e. Results of ME3440 samples from Porvoo, Stenungsund and Borouge using GC-O with Detection Frequency**

The ME3440 samples were obtained from three different plants (Porvoo (Po), Stenungsund (St) and Borouge (Bo)) and thus a MVDA with the MasStat© program was possible to look for similarities and differences in between the samples. HS-SPME-GC-MS data was used for the differentiation. Only pellets were screened.

In Figure 42. the result of the MVDA is shown: Despite the same composition and similar GC-MS chromatograms the program was able to differentiate between the samples. All three samples lie on a horizontal line when x- and y-axis (respectively PC1 and PC2) are scaled the same and are differentiated along the x-axis (= PC1) with the Stenungsund sample on the left side, followed by the Porvoo sample in the middle and the Borouge sample on the right side. Looking into the details for the differentiation one is able to find compounds which are responsible for differences of the ME3440 samples:

- 2-ethyl-1-hexanol (Bo >> Po ~ St)
- toluene (Bo > Po > St)
- Cyclohexane (Bo)
- 1-ethylcyclohexene (Bo > Po > St)
- Methyl-alkenes (Po ~ St > Bo)

Using GC-O with Detection Frequency, it is able to identify odour-active compounds which contribute to the differences in the odour pattern of the three ME3440 samples.

Due to the general lower odour of the samples, only a 1:10 dilution was evaluated by GC-O. All SNIF diagrams for the pure and the 1:10 diluted extract are shown in Figure 44 to Figure 49. A complete list of the odour-active compounds detected in the three ME3440 samples is given in Table 20.

A comparison of the SNIF diagrams obtained from the pure extract of the three ME3440 samples is shown in Figure 50. Differences can be found for these compounds:

- 1-Hexen-3-one (SNIF 100% in Po; 60% in St and Bo)
- 1-Hepten-3-one (SNIF 80% in St., 60% in Po and Bo)
- 2-Acetyl-1-pyrroline (SNIF 100% in Bo, 60% in Po, 40% in St)
- Octanal (SNIF 100% in St, 60% in Po and Bo)
- 2-Ethylhexanol (SNIF 100% in Bo, 40% in Po and St)

- (E,E)-2,4-Decadienal (SNIF 80% in Po, 40% in St, 20% in Bo)

Overall, the lowest number and/or the lowest SNIF values can be found in the Stenungsund sample, followed by the Provoo sample. Comparing this picture with the one obtained from the MVDA one could speculate that with increasing number and/or increasing odour intensity the samples are shifted to the right side on the cluster shown in Figure 42.

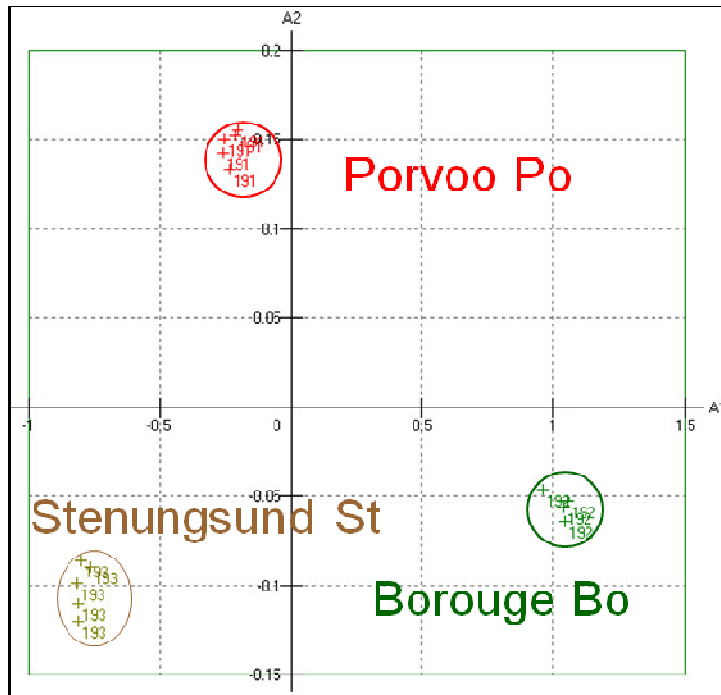


Figure 42. MasStat© Cluster Analysis using the HS-SPME-GC-MS data from the three ME3440 samples from Provoo, Stenungsund and Borouge (Note: y-axis scale is 1/10 of x-axis!! (0.05 vs. 0.5)).

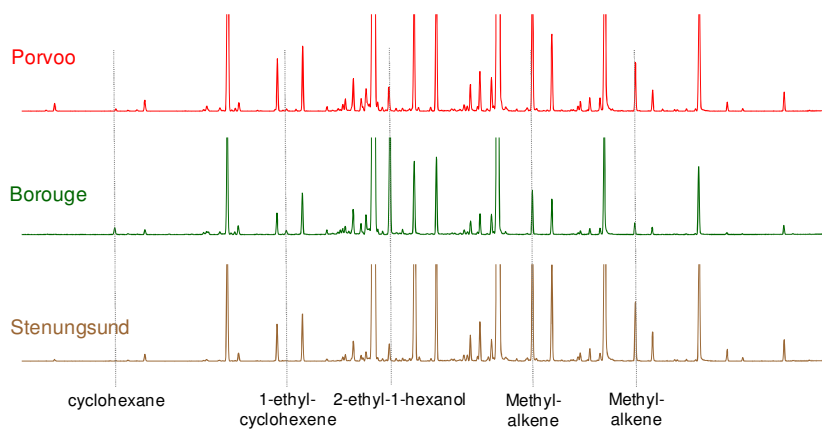


Figure 43. HS-SPME-GC-MS chromatograms for the ME3440 samples with marked compounds which are responsible for the differentiation in the MasStat© cluster.



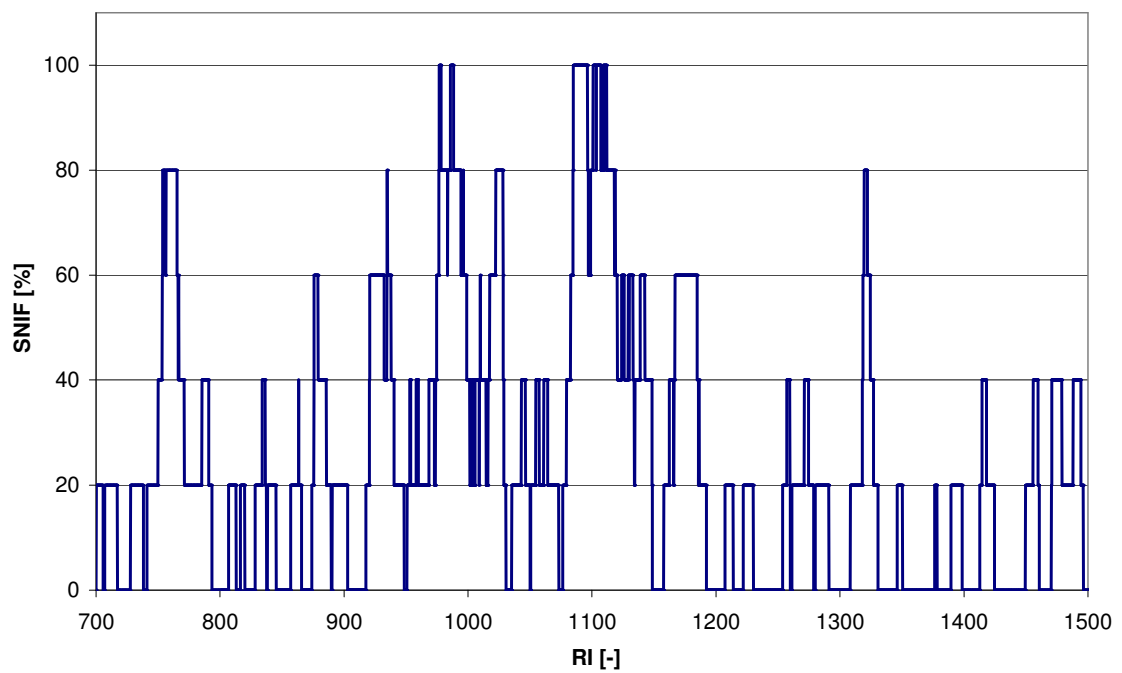


Figure 44. Detection Frequency (SNIF) diagram of the extract obtained from ME3440 (Porvoo) pellets.

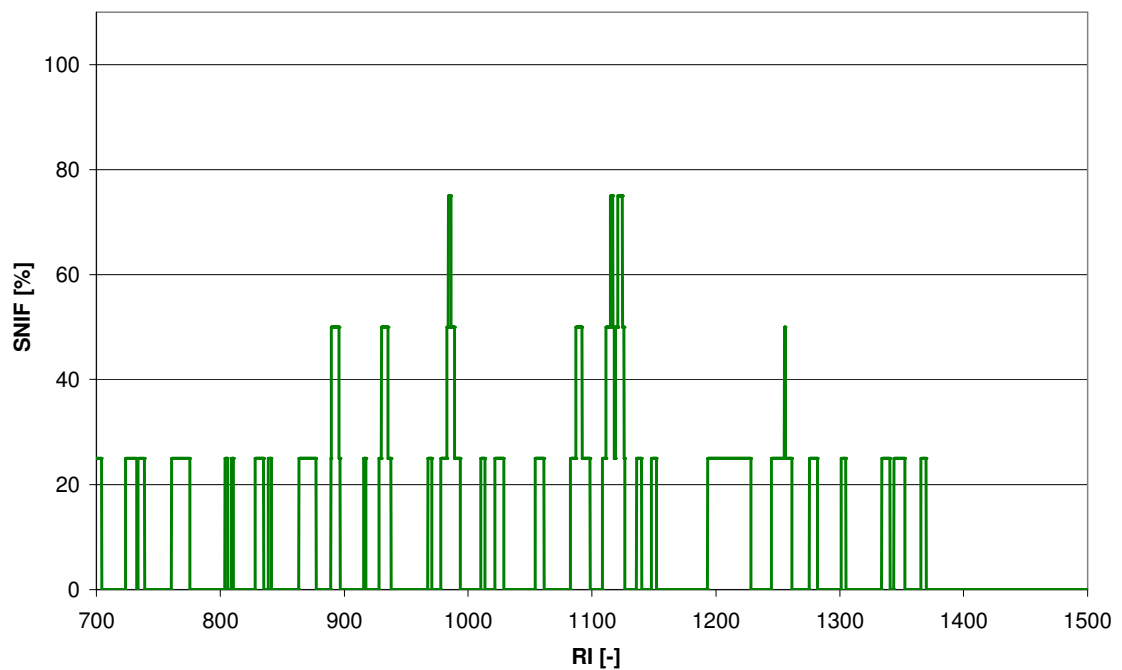


Figure 45. Detection Frequency (SNIF) diagram of the 1:10 diluted extract obtained from ME3440 (Porvoo) pellets.

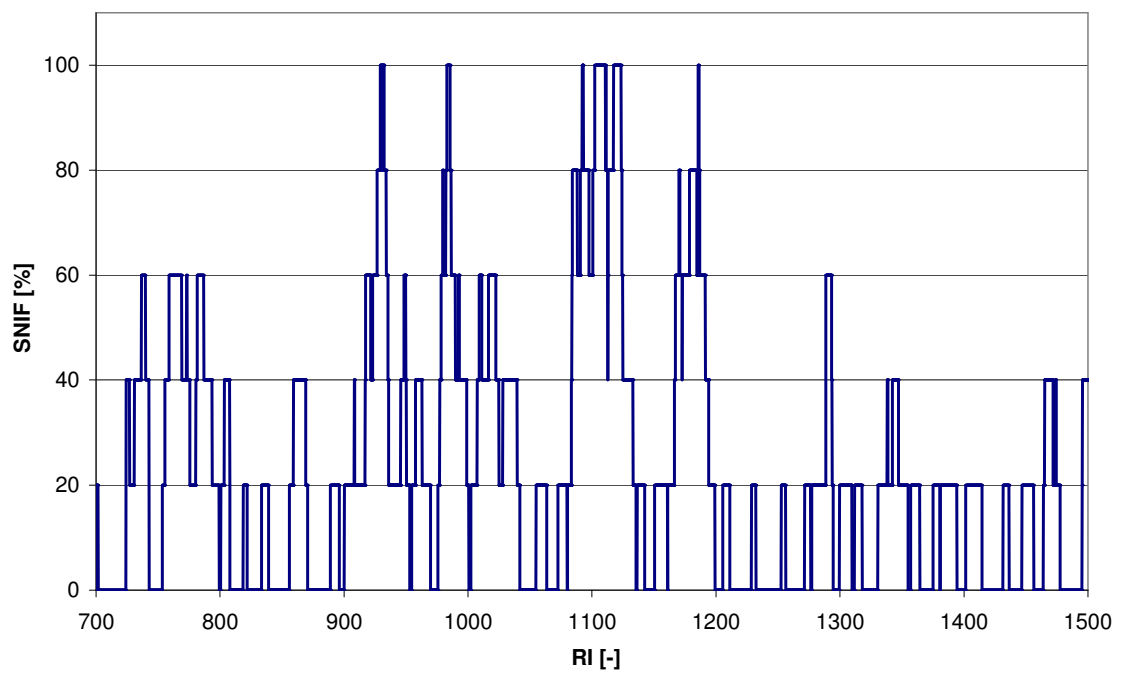


Figure 46. Detection Frequency (SNIF) diagram of the extract obtained from ME3440 (Stenungsund) pellets.

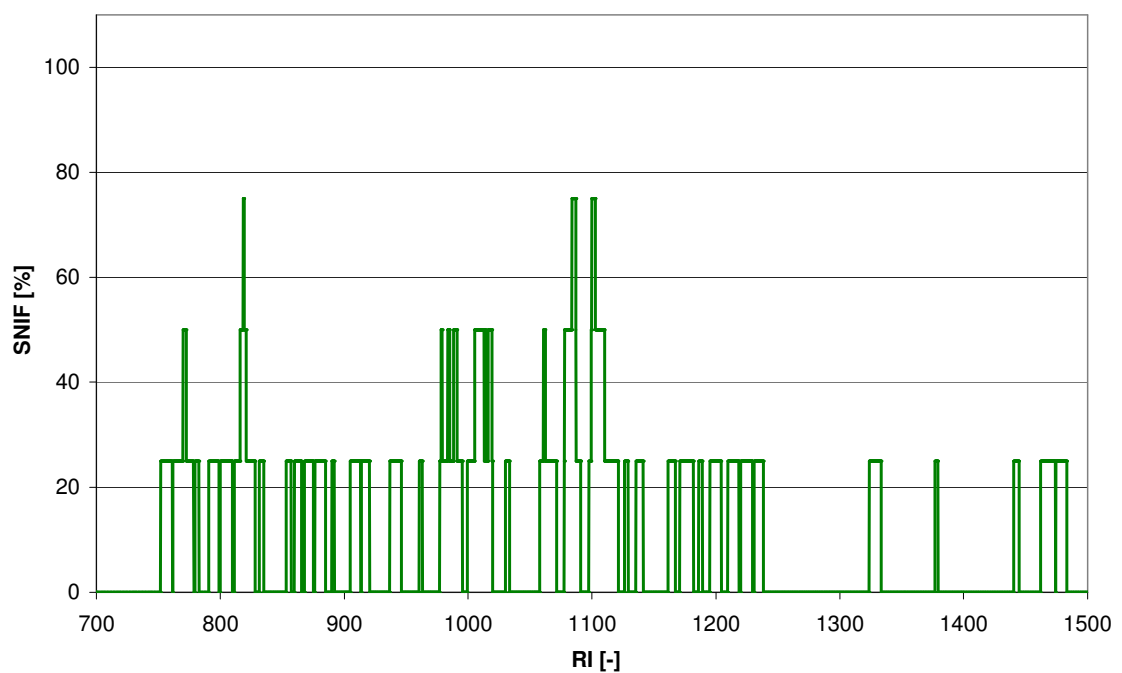


Figure 47. Detection Frequency (SNIF) diagram of the 1:10 diluted extract obtained from ME3440 (Stenungsund) pellets.

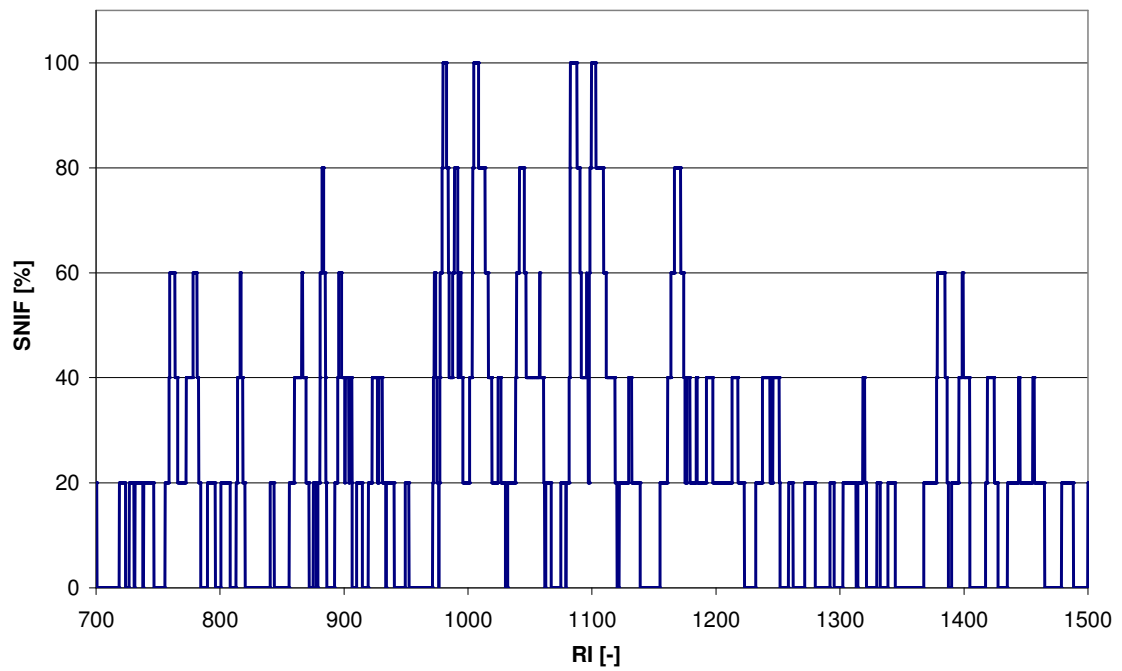


Figure 48. Detection Frequency (SNIF) diagram of the extract obtained from ME3440 (Borouge) pellets.

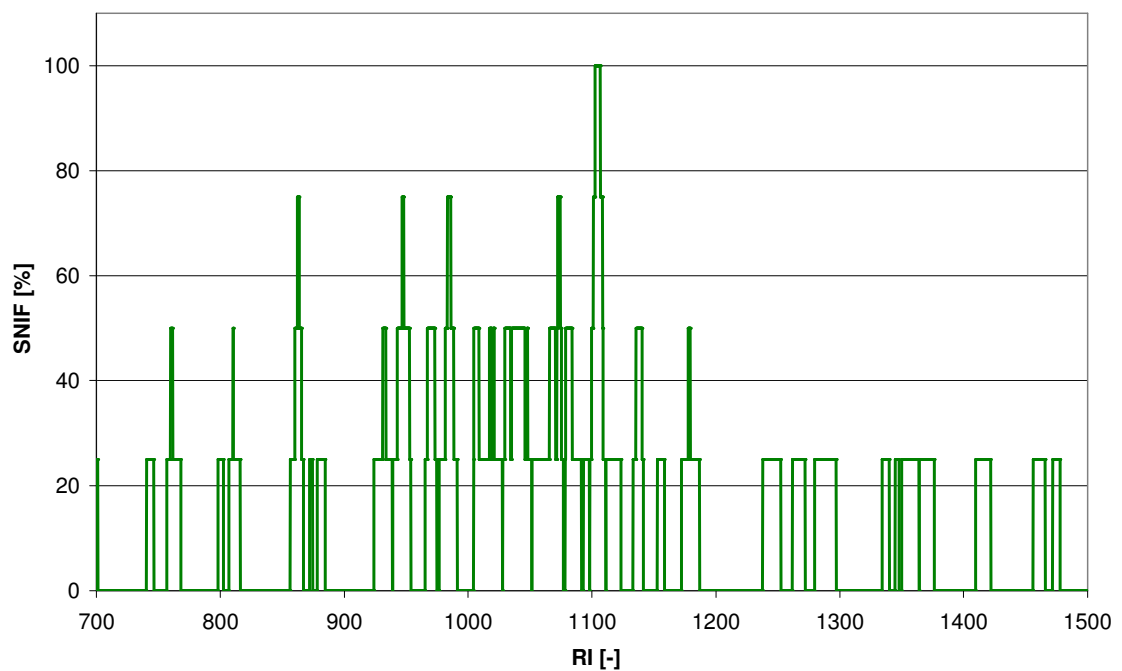


Figure 49. Detection Frequency (SNIF) diagram of the 1:10 diluted extract obtained from ME3440 (Borouge) pellets.

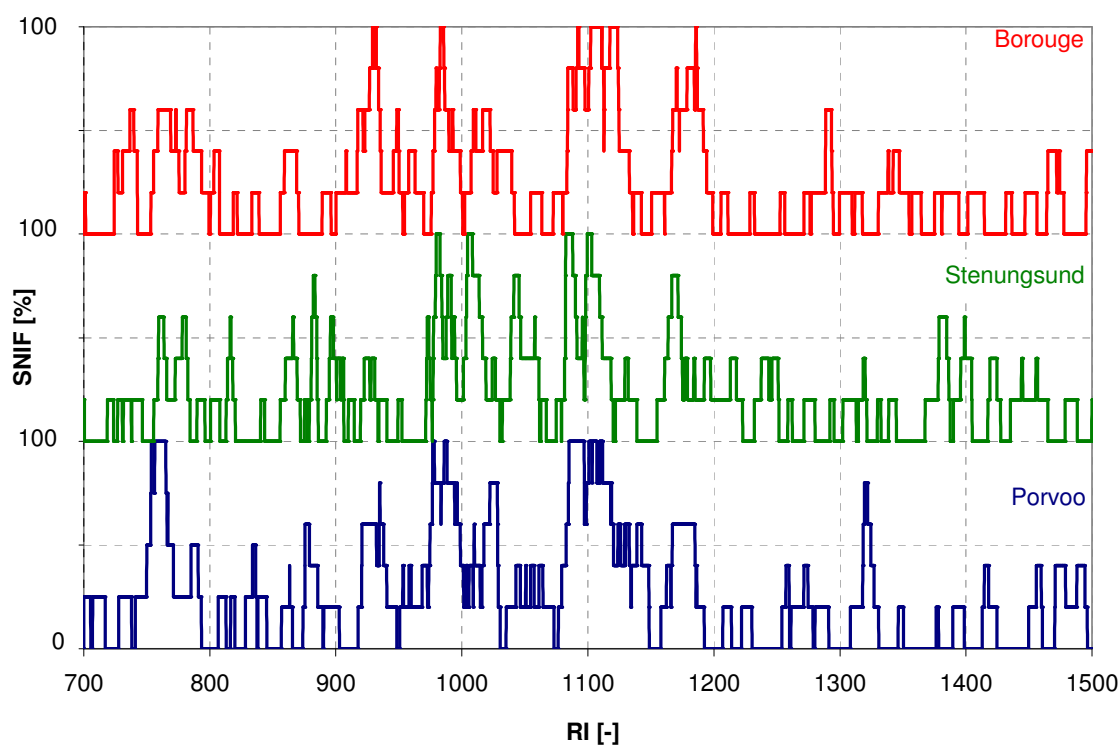


Figure 50. Detection Frequency (SNIF) diagram comparison of the ME3440 pellets from Porvoo (at the bottom in blue), Stenungsund (in the middle in blue) and Borouge (on top in red).

Table 20. List of odour-active compounds present in the ME3440 pellets from Porvoo (Po), Stenungsund (St) and Borouge (Bo). ( $RI_{exp}$  ... experimental Retention Indices, s.d. ... standard deviation,  $RI_{lit}$  ... literature Retention Indices determined with pure standards (om) or taken from literature sources<sup>67,68</sup>).

Compound	Porvoo	Stenungsund	Borouge	mean $RI_{exp} \pm s.d.$	$RI_{lit}$	Source
pentanal	✓	✓	✓	701.0 ± 4.6	697.4	<sup>68</sup>
unknown	✓	✓	✓	724.3 ± 3.4		
3-penten-2-one	✓	✓	✓	735.5 ± 4.3	734.0	<sup>68</sup>
(E)-2-pentenal	✓	✓	✓	755.7 ± 3.2	759.4	om
1-hexen-3-one	✓	✓	✓	778.6 ± 5.0	770.1	om
hexanal	✓	✓	✓	800.3 ± 6.3	790.6	om
unknown	✓	✓	✓	815.8 ± 2.4		
2-methyl-2-pentenal	✓			828.5	823.3	om
unknown	✓	✓		833.9 ± 0.5		
?3-hexen-2-one?*	✓		✓	839.4 ± 1.8	[839]	
unknown	✓	✓	✓	861.7 ± 6.5		
1-hepten-3-one	✓	✓	✓	878.3 ± 3.2	872.4	om
heptanal	✓	✓	✓	894.9 ± 4.4	898.0	om
(E,E)-2,4-hexadienal		✓	✓	907.7 ± 2.7	907.2	om

Compound	Porvoo	Stenungsund	Borouge	mean RI <sub>exp</sub> ±s.d.	RI <sub>lit</sub>	Source
2-acetyl-1-pyrroline	✓	✓	✓	921.4 ± 3.7	926.0	om
3-hepten-2-one	✓	✓	✓	932.8 ± 2.5	934.4	om
(E)-2-heptenal	✓	✓	✓	951.5 ± 4.1	954.8	om
unknown		✓	✓	973.0 ± 1.8		
1-octen-3-one	✓	✓	✓	975.8 ± 3.4	977.1	om
unknown	✓	✓	✓	985.9 ± 2.7		
unknown	✓	✓	✓	993.5 ± 2.4		
octanal	✓	✓	✓	1005.5 ± 3.0	1002.3	om
2-ethylhexanol	✓	✓	✓	1020.2 ± 4.7	1028.6	om
3-octen-2-one	✓		✓	1034.1 ± 2.1	1039.2	om
(E)-2-octenal	✓	✓	✓	1056.0 ± 4.4	1058.7	om
1-nonen-3-one	✓	✓	✓	1082.1 ± 2.3	1079.7	om
(E)-6-nonenal					1095.1	
(Z)-6-nonenal	✓	✓	✓	1098.4 ± 3.6	1101.2	om
8-nonenal					1096.5	
nonanal					1104.6	
(E,E)-2,4-octadienal	✓	✓	✓	1113.1 ± 3.2	1110.3	om
unknown	✓		✓	1122.9 ± 1.3		
unknown	✓		✓	1130.9 ± 2.4		
3-nonen-2-one	✓	✓		1137.9 ± 2.2	1139.9	<sup>68</sup>
γ-heptalactone	✓	✓	✓	1154.5 ± 3.5	1152.7	<sup>68</sup>
(E)-2-nonenal	✓	✓	✓	1164.8 ± 2.5	1161.4	om
?1-decen-3-one?*	✓	✓	✓	1185.2 ± 5.0	[1178]	
decanal	✓	✓	✓	1208.5 ± 3.8	1206.8	om
2-ethylhexanol	✓	✓		1225.3 ± 4.7	1228.6	
? 3-decen-2-one ?			✓	1234.9 ± 3.3	[1239]	
unknown			✓	1245.2 ± 0.9		
γ-octalactone	✓	✓	✓	1256.9 ± 3.8	1258.8	
(E)-2-decenal	✓	✓	✓	1272.7 ± 2.9	1264.1	om
?1-undecen-3-one?*	✓	✓		1285.7 ± 4.6	[1278]	
unknown			✓	1292.3		
undecanal	✓	✓	✓	1303.6 ± 4.7	1308.8	om
(E,E)-2,4-decadienal	✓	✓	✓	1316.8 ± 3.0	1319.4	om

Compound	Porvoo	Stenungsund	Borouge	mean RI <sub>exp</sub> ±s.d.	RI <sub>lit</sub>	Source
unknown		✓	✓	1330.1 ± 0.5		
?3-undecen-2-one?*		✓	✓	1338.6 ± 0.5	[1339]	
unknown	✓	✓		1348.8 ± 7.6		
(E)-2-undecenal			✓	1367.7	1366.5	om
1-dodecen-3-one	✓	✓	✓	1377.2 ± 1.7	1383.0	om
δ-nonalactone	✓	✓	✓	1392.8 ± 7.4	1392.7	om
dodecanal	✓		✓	1416.2 ± 2.8	1410.6	om
?3-dodecen-2-one?*		✓	✓	1436.9 ± 6.3	[1439]	
unknown	✓	✓	✓	1454.6 ± 6.8		
(E)-2-dodecenal	✓	✓	✓	1473.4 ± 4.0	1467.6	<sup>68</sup>
unknown	✓	✓		1493.1 ± 4.2		
unknown	✓		✓	1505.0 ± 5.0		
tridecanal			✓	1510.4	1511.7	<sup>68</sup>
unknown		✓	✓	1521.8 ± 1.1		
unknown		✓	✓	1534.3 ± 1.6		
unknown		✓	✓	1547.7 ± 3.2		
unknown		✓	✓	1565.2 ± 1.1		

\* for compounds marked with questions marks pure standards could not be obtained.

#### 4.4. The interaction of phenolic antioxidants and talc and their influence on the generation of odour-active compounds

One mobility grade MB471WG-9014 was claimed due to its intensive odour and the questions whether the responsible compound could be the 2-methyl-1-propene found in huge amounts in the HS-GC-MS analyses according to VDA277<sup>74</sup> was raised.

Two samples (the claimed lot and a grade with a slightly different formulation) were analyzed as described in sections 3.2.a, 3.2.b, 3.3.b, 3.3.d and 3.3.e.

GC-O analyses of the fractioned extract were carried out for both samples and a highly odour-active compound described as “waxy, burnt, suffocating” was detected in both samples but with different intensities: While in the claimed MB471WG-9014 the odour was very intense, in the second grade MB471WG-9014-01 the compound was less pronounced.

<sup>74</sup> Verband der Automobilindustrie, 1995, VDA 277 - Nichtmetallische Werkstoffe der KFZ Innenausstattung-Bestimmung der Emission organischer Verbindungen.

In Figure 51 GC-FID-O chromatograms of both samples are shown. Although the odour-active compound gave a very intense signal and at the same retention time a large peak was detected, this peak is not responsible for the odour as proven by GC-O of the pure reference; furthermore these huge peaks in the relevant area are the three stereoisomers of tert.-butylphenols (2-, 3-, 4-) which are coeluting with the odour-active compound of interest (see Figure 52). A rough estimation of the concentration of the analyte was carried out giving a concentration of the analyte of interest of less than 1 µg/kg.

A change of the analytical GC-column from the standard HP-5 to a more polar DB-WAX and applying the same GC parameters should according to literature help to separate coeluting peaks. In this case it did not: On the HP-5 column the unknown compound coeluted with 3-tert.-butylphenol and on the DB-WAX column the 2-tert.-butylphenol overlaid the analyte of interest.

A check whether the unknown compound has nitrogen- or sulphur-containing functional groups was carried out with NPD (in N-mode) and FPD, but no signal was observed in the relevant area.

Applying derivatization using *O*-(2,3,4,5,6-Pentafluorobenzyl)-hydroxylamine (PFBHA) to transfer an possibly carbonyl group into the corresponding oxime thus eliminating the odour function of the analyte did not work – during the subsequent GC-O of the derivatized extract the odour was still detectable and did not change.

A second derivatization reagent – *N,O*-bis(trimethylsilyl)trifluoroacetamide) (BSTFA) – which trimethylsilylates alcohols, amines, carboxylic acids and phenols, followed by GC-O was successful; the odour could not be detected.

Summarizing the results, the unknown compound which odour is described as pungent, intense, dusty, burnt, waxy and suffocating, is

- (1) most likely a phenolic compound indicated by the coelution with the tert.-butylphenols and the reaction with BSTFA,
- (2) is not 2-, 3-, or 4-tert.-butylphenol due to their lack of the characteristic odour in the relevant concentration range which was checked by GC-O of pure references and
- (3) does not have functional groups containing N or S due to the lack of response to the element-specific detectors NPD ( in N-mode) and FPD.

However, a chemical name and/or structure is yet unknown. It is assumed that the unknown compound derive from the degradation of the phenolic antioxidants in presence of the talc as described by Sauer (see Scheme 1).

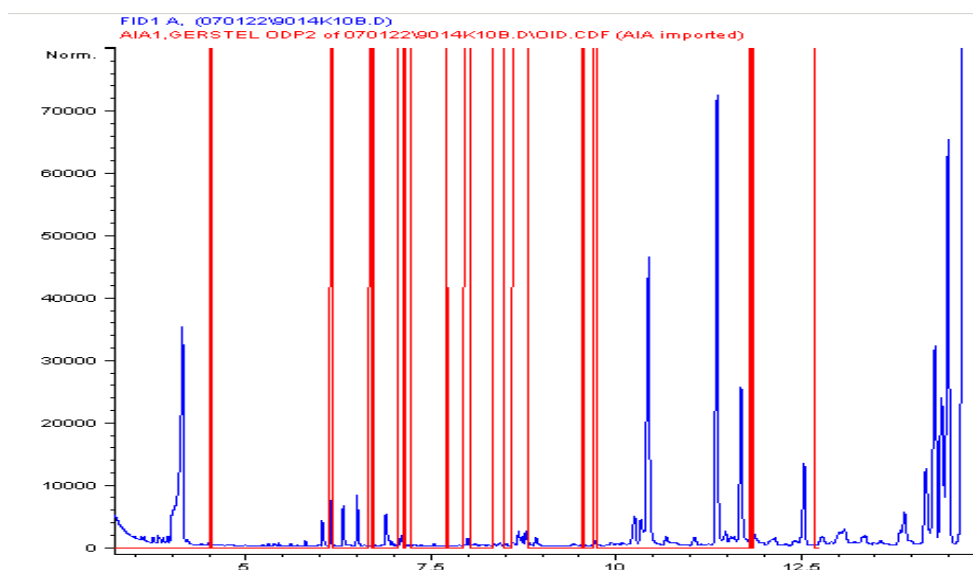


Figure 51. GC-FID chromatogram (in blue) with overlaid O-signal (in red) indicating the high odour activity of the unknown compound in MB471WG-9014 extract between 11.5 – 12.7min retention time.

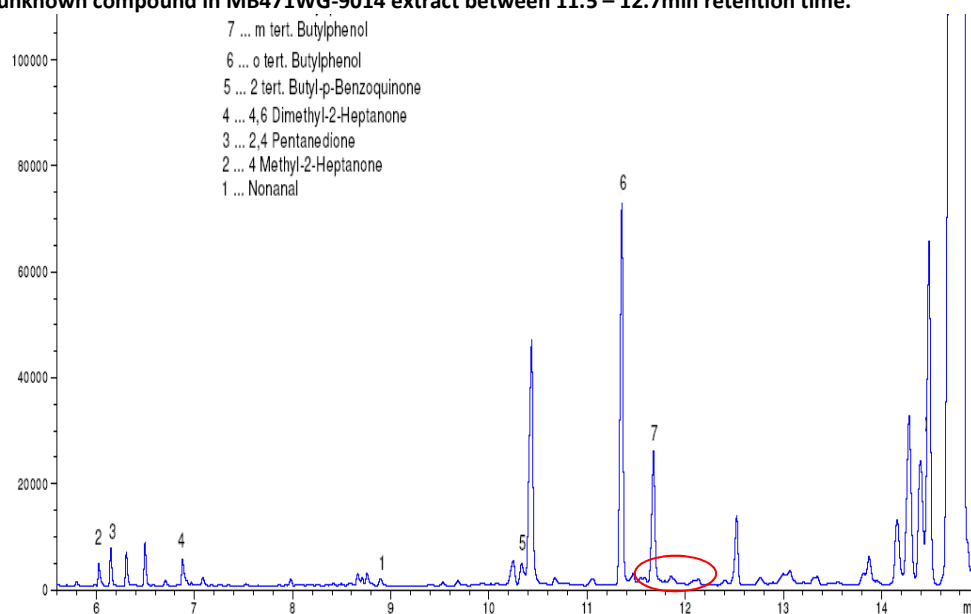


Figure 52. GC-MS chromatogram of the MB471WG-9014 sample extract with the labelled tert.-butylphenols (6 and 7) and the area of interest (red circle) analyzed on the non-polar HP-5 column.

#### 4.5. The influence of additives on the generation of odour-active compounds

For an overview of the contribution of various additives to the odour of polyolefin products a SPME study was performed. 20 samples consisting of both pellets and thereof produced plaques were investigated with HS-SPME-GC-MS and HS-SPME-GC-O to determine critical additives in terms of odour generation. The approach was rather simple: the same formulation was used for all



samples, but each time a different additive was left out. All pellets were compounded at 200 °C, all plaques were injection moulded with a  $T_M$  of 230 °C.

The samples were:

- reference grade containing all additives (EE188HP-1048 in beige)
- reference grade from a different site (Monza) and storage time
- reference grade compounded at 260 °C instead of 220 °C
- grade with a change of the base polymer
- grade without talc
- grade without colour masterbatch (CMB)
- grade without epicote (antioxidants for processing)
- grade with reduced heat stabilization
- grade without scratch additives
- grade without UV stabilization

The HS-SPME-GC-O analyses were carried out by two trained panellists; one of them evaluated all pellet samples, the second one all plaque samples.

In all samples similar odour-active compounds were identified including saturated and unsaturated aldehydes with chain lengths from 6 to 12 C-atoms described as “fatty, green, orange, plastic-like, waxy, stink bug”, ketones with chain lengths from 5 to 9 C-atoms with “plastic, glue-like, mushroom, butter” descriptors, terpenes originating from an additive of plant origin (GMS) described as “terpene-like, woody, fresh” and the aromatic nitrogen compound 2-acetyl-1-pyrroline detected in all compounds.

In case of leaving out the epicote more intense odour-active compounds were detected including some unknown compounds described as “Onion-like” and “gin, juniper berry, fresh-cut wood”.

The HS-SPME-GC-MS analysis with a subsequent MVDA using MasStat© led to the cluster shown in Figure 53. In the next figures (Figure 54 - Figure 63) this cluster is successively discussed due to its complexity. Samples are always compared to the reference.

Based on the cluster analysis one is able to that

- 1) injection moulding influences the generation of volatiles and odour-active compounds in a certain way indicated by a movement of the cluster to the upper left.
- 2) the reference ex Monza differs significantly from the reference from Linz. Additionally, the injection moulding influence is more pronounced than for the reference ex Linz. This could be

explained by a longer storage period of the Monza material (pellets more to the right than those ex Linz).

3) a change in the base polymer does not change much; the influence of the injection moulding is the same as for the reference, indicating that the additives have a larger influence on the injection moulding than the polymer itself.

4) an increase in the compounding temperature from 220 °C to 260°C is (a) a similar process as injection moulding ( = shifting the cluster to the upper left) and (b) is more severe than injection moulding at 230 °C ( = larger distance between pellets and plaques) and (c) by the subsequent injection moulding step of the at 260 °C compounded pellets no significant change can be observed as in the reference.

5) two different types of additives can be classified: those which react in any kind during the injection moulding and those which do not react during compounding; when leaving out talc, UV stabilization or CMB the pellets' and plaques' cluster fall together, indicating that these additives contribute to the volatile and odour generation during injection moulding. When leaving out the other additives (scratch resistance, epicote) or reducing the heat stabilization, the remaining additives can still react during the processing step.

Knowing that (a) injection moulding leads to an increase in odour-active oxidation products such as aldehydes and ketones and (b) the samples without talc, colour MB and UV stabilization showed less odour-active compounds in the GC-O analyses, one is able to further classify the MasStat© cluster as such: the more the samples are located on the left side the more volatiles and odour-active compounds are present.

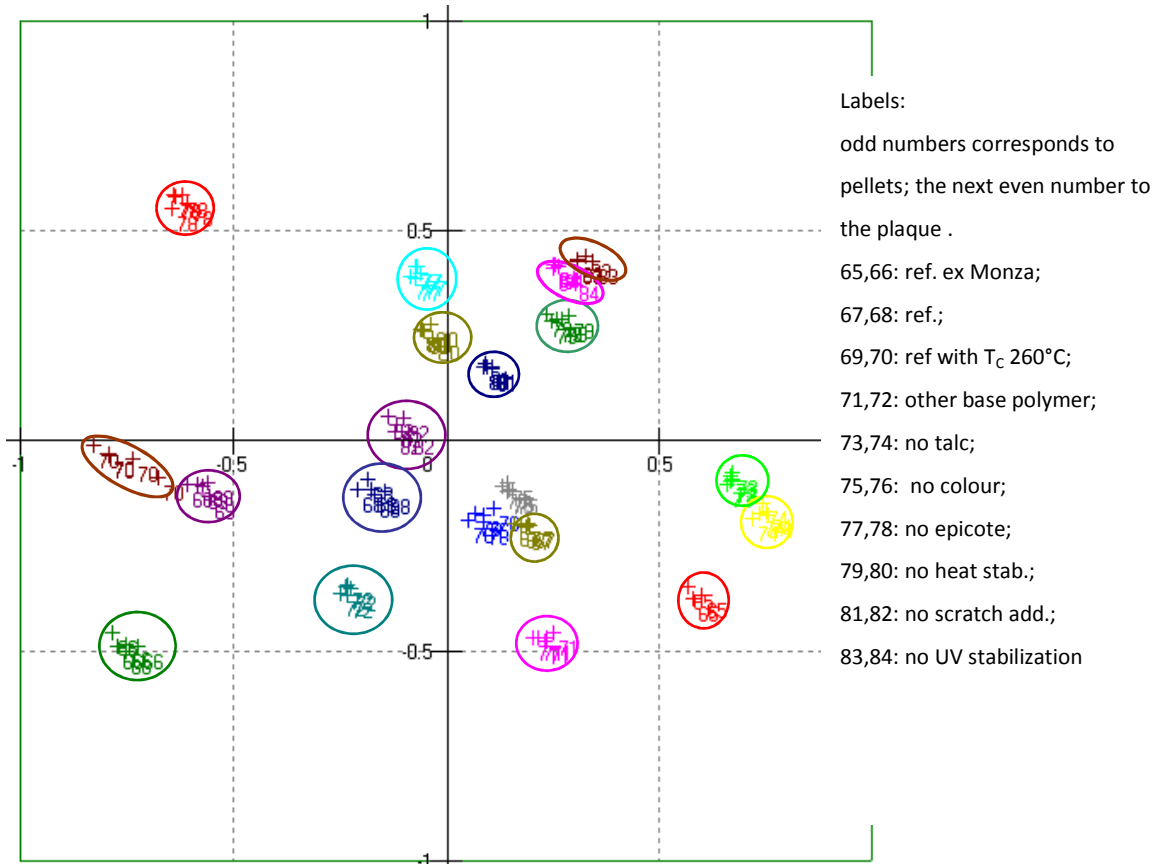


Figure 53. MasStat© Cluster from HS-SPME-GC-MS data analyzing the influence of additives on odour generation.

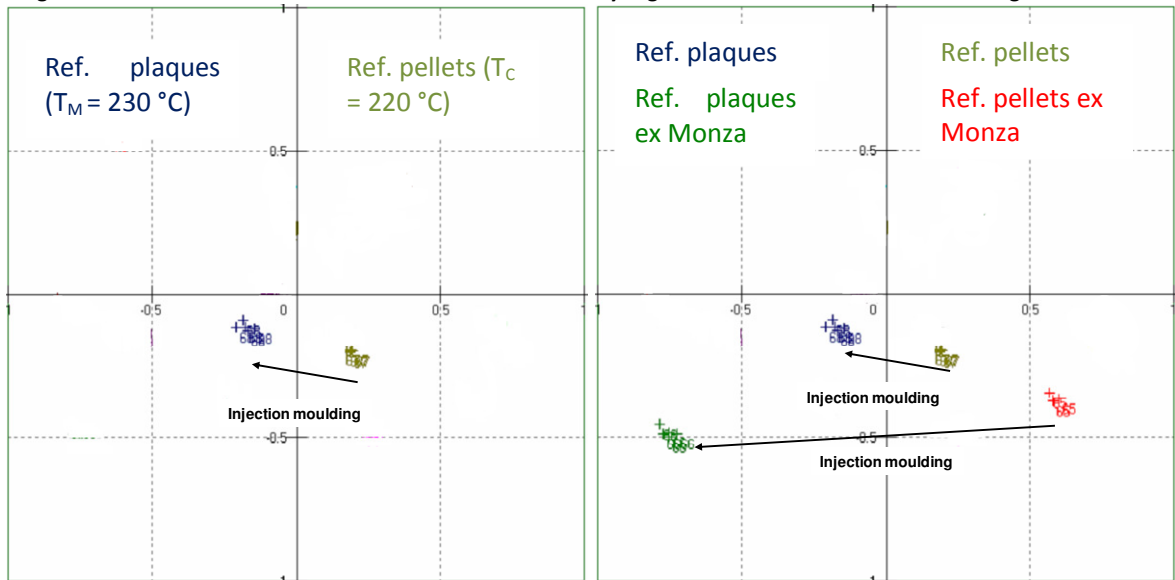


Figure 54. Cluster of the reference pellets and plaques produced thereof. The direction of Injection moulding is indicated.

Figure 55. Cluster of the references from Linz and Monza with differing influence of the Injection moulding.

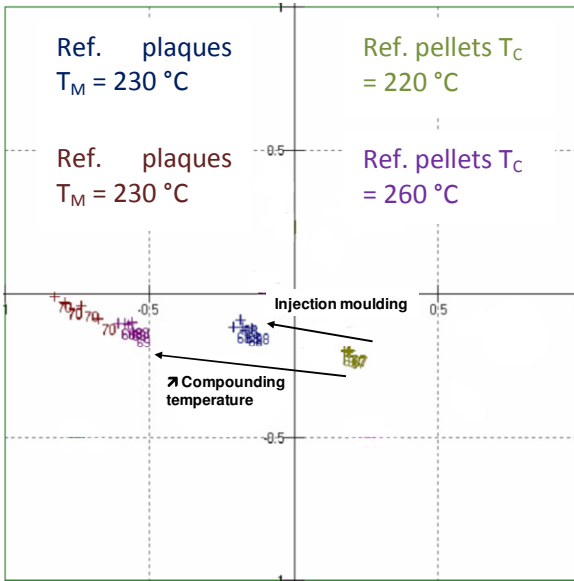


Figure 56. Cluster of the reference and the samples with increased compounding temperature ( $T_C=260\text{ }^\circ\text{C}$ ). Note that the influence of the Injection moulding is lost for the  $T_C=260\text{ }^\circ\text{C}$  samples.

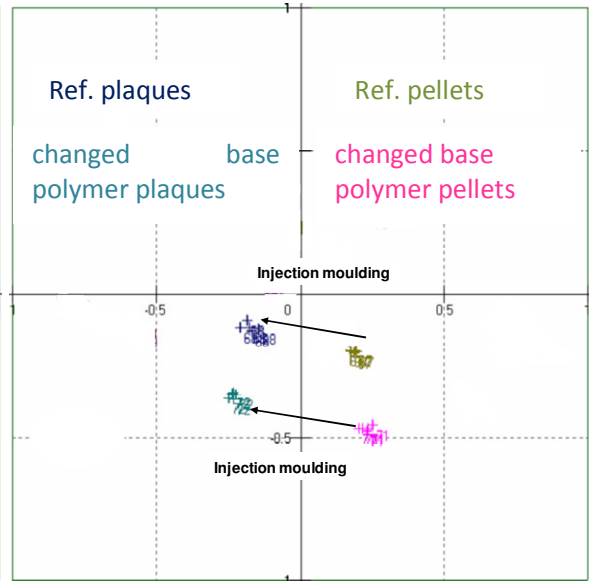


Figure 57. Cluster of the reference and the samples with changed base polymer. Note that the influence of the Injection moulding is the same.

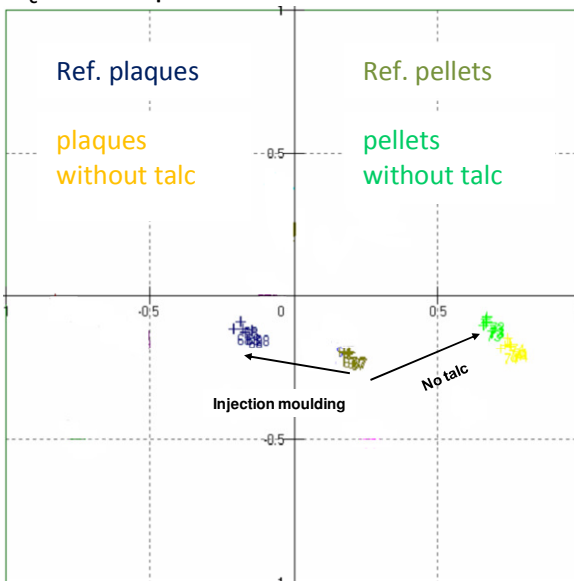


Figure 58. Cluster of the reference and the samples without talc. Note that the influence of the Injection moulding is lost for the samples without talc.

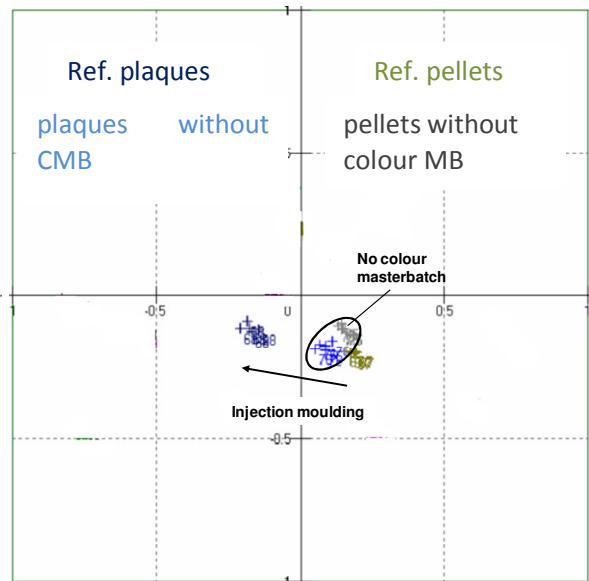


Figure 59. Cluster of the reference and the samples without colour masterbatch (CMB). Note that the influence of the Injection moulding is lost for the samples without CMB.

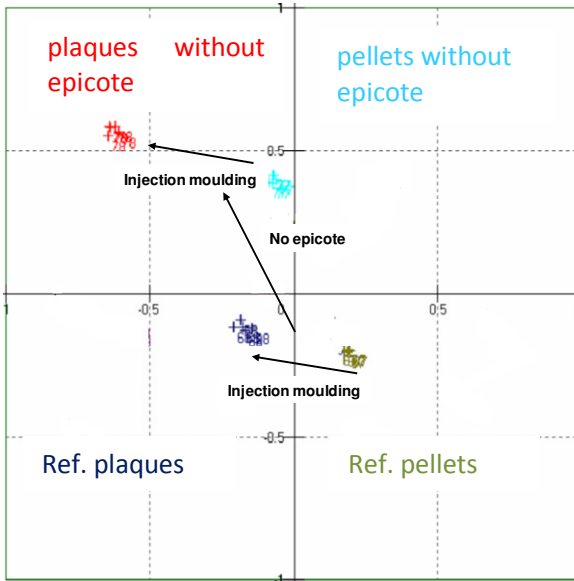


Figure 60. Cluster of the reference and the samples without epicote. Note that the influence of the Injection moulding is the same for both samples.

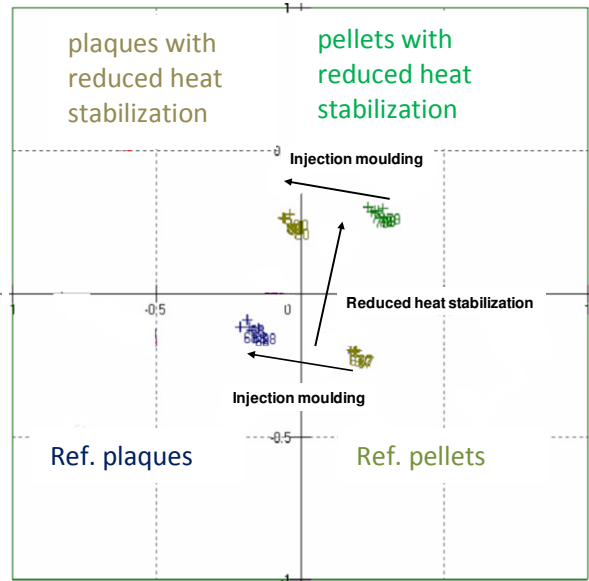


Figure 61. Cluster of the reference and the samples with reduced heat stabilization. Note that the influence of the Injection moulding is the same for both samples.

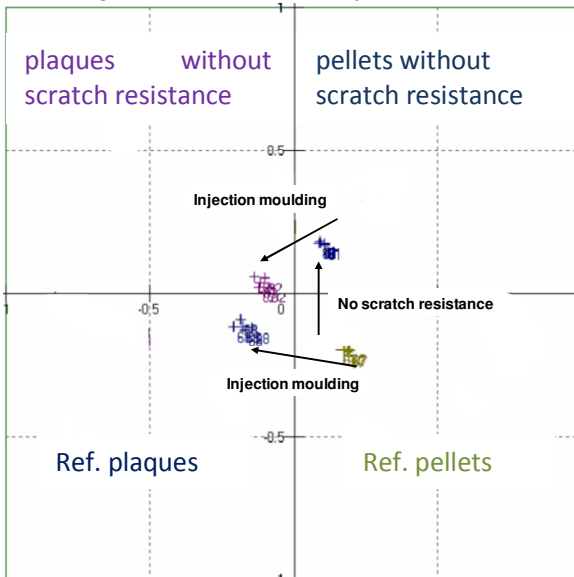


Figure 62. Cluster of the reference and the samples without scratch resistance additives. Note that the influence of the Injection moulding is the same for both samples.

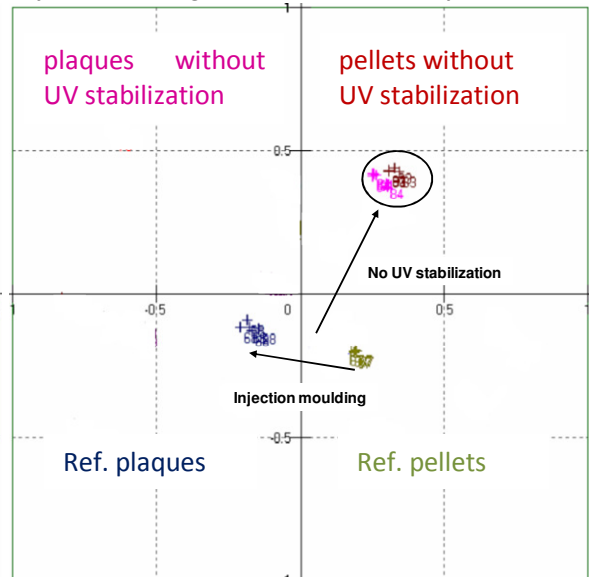


Figure 63. Cluster of the reference and the samples without UV stabilization. Note that the influence of the Injection moulding is lost for the samples without UV stabilization.

#### 4.6. Odour potential of 2-ethyl-1-hexanol

An evaluation of the odour potential of the alcohol 2-ethyl-1-hexanol (2-EH) was carried out. The background to this evaluation was the development of a new catalyst (RCL05P) which emits significant higher amounts of 2-EH than the old catalysts (BCF02P). Additionally, increased odour was determined by the Borealis sensory panel when using the new catalyst in the polyolefin grades.

We got four samples for the evaluation (two with the new catalyst, two with the old one) and determined the amount of 2-EH in those samples and determined the odour threshold for 2-EH in the pellets.

Samples were extracted as described in section 3.2.a, fractioned as described in section 3.2.b and the obtained fractions were analysed by GC-MS as described in section 3.3.c.

GC-O analyses of the extracts were carried out as described in section 3.3.d with 3 panellists.

Quantification of the 2-EH was carried out in the fraction II applying an external calibration with a reference 2-EH obtained from Schuchardt (purity  $\geq$  99%, Munich, Germany).

In Figure 64 a comparison of the GC-MS chromatograms is given for the samples, in Table 21 the determined concentrations of 2-EH in the samples are listed. The concentrations were determined with 3.4 mg/kg and 3.6 mg/kg for the RCL50P samples and were below the limit of detection of 0.05 mg/kg in the BCF02P samples.

No differences in the 2-EH concentration between the visbroken and the non-visbroken sample could be found.

The odour threshold was determined by GC-O using dilution analysis: the extract was diluted 1:2 and 1:3 and evaluated with 2 trained panellists until no odour was perceived. The threshold for 2-EH was determined in the range of 1-2 mg/kg pellets. This threshold value is a 1000-fold higher than those of the aldehydes and ketones in the lower  $\mu\text{g}/\text{kg}$  range as shown in Table 25.

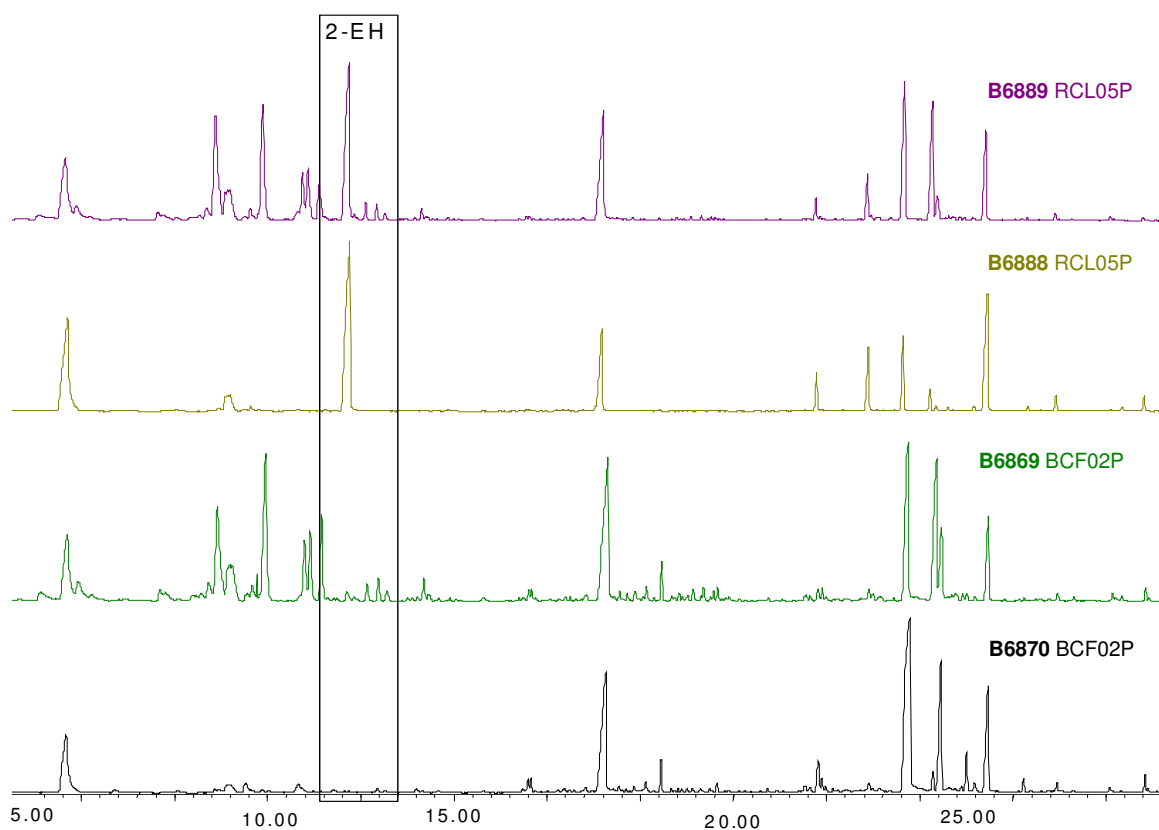


Figure 64. GC-MS chromatograms of the four samples. The upper two show significant amounts of 2-ethyl-1-hexanol (2-EH) due to the use of the new catalyst RCL05P, the lower two were produced with the old catalyst BCF20P.

Table 21. 2-Ethyl-1-hexanol mean concentrations and standard deviation in the samples determined by GC-MS.

Sample	2-Ethyl-1-hexanol in pellets [mg/kg] (n=5)
B6889 with RCL05P RJ900MO; MFR = 100g/10min; visbroken	$3.4 \pm 0.3$
B6888 with RCL05P RE450MO; MFR = 13g/10min	$3.6 \pm 0.5$
B6869 with BCF02P RJ900MO; MFR = 100g/10min; visbroken	< 0.05
B6870 with BCF02P RE450MO; MFR = 13g/10min	< 0.05

#### 4.7. The influence of vis-breaking reagents (peroxides) on the generation of odour-active compounds

Based on the results from the additive screening (see section 4.5) in the second year of the thesis the influence of peroxides on the generation of odour-active compounds was investigated. Peroxides are used for a controlled decrease of the average molecular mass of the PP in combination with a narrower molecular weight distribution (MWD) for production of the so called visbroken (VB-PP) or controlled rheology PP (CR-PP) grades. A narrower MWD results in less wrapage, more uniform shrinkage and better drawdown during extrusion; on the other hand less stiffness and the loss of melt strength occur.

We evaluated the influence of two different peroxide systems on the odour by HS-SPME-GC-MS with subsequent MVDA using MasStat© and by GC-O using extracts obtained from selected grades (HD120MO with no peroxide as reference, HD120MO + Tx101 and HD120MO + Tx301) as shown in Table 23.

Samples were selected to evaluate various aspects of the peroxide visbreaking and the influence on the generation of odour-active compounds:

- two peroxide systems (2,5-dimethyl-2,5-di(tert-butylperoxy)hexane (Tx101) and 3,6,9-triethyl-3,6,9-trimethyl-1,4,7-triperoxonane (Tx301))
- used in two polymers (HD120MO and RJ370MO) from different sites (Linz and Schwechat)
- applying different peroxide concentrations measured by MFR [g/10min] from 8 (reference without peroxide), 12.5, ..., 100
- applying different peroxide dosing (masterbatch (MB) and liquid)

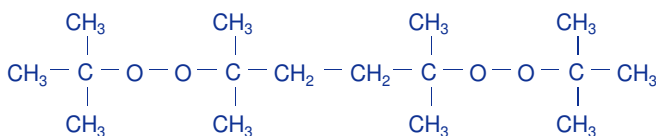


Figure 65. Chemical structure of Tx101.

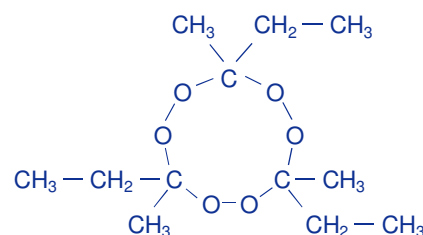


Figure 66. Chemical structure of Tx301.



**Table 22. List of peroxide samples analyzed in the study. Samples in italic were used in the GC-O analyses.**

peroxide dosing	Polymer	MFR [g/10min]	peroxide system	
MB	HD120MO	<i>8 (reference)</i>	-	
		12.5	Tx101	
		50	Tx101	Tx 301
		100	Tx101	
liquid	RJ370MO	45	Tx101	Tx301

In Figure 67 the MasStat© cluster obtained from the HS-SPME-GC-MS data is shown:

- samples are clearly separated indicating a different volatile pattern
- separation of the samples is based on the peroxide system rather than the polymer as the Tx101 samples are located on the right side and the Tx301 samples are located on the left side of the cluster irrespective what polymer (HD120MO or Rj370MO) is used.
- HD120MO samples containing increasing amounts of Tx101 fall together on a straight line indicating the generation of the same volatiles in increasing amounts.
- different types of dosage lead to similar results as the RJ370MO samples (liquid dosage) and the HD120MO samples (MB dosage) are close to each other.

A deeper look into the HS-SPME-GC-MS data shows a total different volatile composition for the two different peroxide systems (see Figure 68). Table 23 summarizes the differences in both polymer materials for selected compounds calculated with Tx101 as reference (=100%). For most cases the same results can be found for both polymers except for the methyl-tert.-butyl ether which appeared only in the RJ370MO with both peroxide systems. Due to the different molecular structure of the Tx101 and Tx301 the different volatile pattern are easily explained; e.g. lack Tx301-containing samples acetone and tert.-butanol while Tx101-containing samples do not show the presence of acetates.

In terms of odour a summary of the SNIF diagrams is given in Figure 69 where the odour pattern for the HD120MO reference is compared to the HD120MO with Tx101 (MFR 50 g/10min) and to the HD120MO with Tx301 (MFR 50 g/10min).

By addition of peroxide the number of odour-active compounds with a high impact (SNIF=100 %) is increased (from 8 for the reference to 12 for the Tx101 and 10 for the Tx301 material). These odour-active compounds can be grouped in

- odour-active aldehyde and ketones which are present in the reference as well but in smaller concentrations

or

- additional odour-active compounds which are generated in the presence of peroxides such as 2-methyl-3-furanthiol (RI(HP5) = 855; roasty, meat-like, sweet, spicy), 3-hepten-2-one (RI(HP5) = 936; chewing-gum, sweet, roasty, faecal, plastic, fatty) and an unknown compound (RI(HP5) = 1220; musty, phenolic, burnt plastic, sweet).

Additionally, these following compounds were only detected in the sample with Tx101:

- 2-methyl-2-pentenal (RI(HP5) = 831); plastic, roasty, green
- not yet identified (RI(HP5) = 1034); mouldy, green, chemical, plastic

These compounds turned up only in the Tx301 sample:

- methyl butanoate (RI(HP5) = 729); sweet, alcoholic, fruity, chemical
- hexanal (RI(HP5) = 801); sweet, fruity, green apple
- not yet identified (RI(HP5) = 895); black currant, sweet, rotten, sour, faecal
- (E)-p-mentha-6,8-dien-2-hydroperoxide (RI(HP5) = 1368); alcoholic, pungent, intense, chemical, ethereal

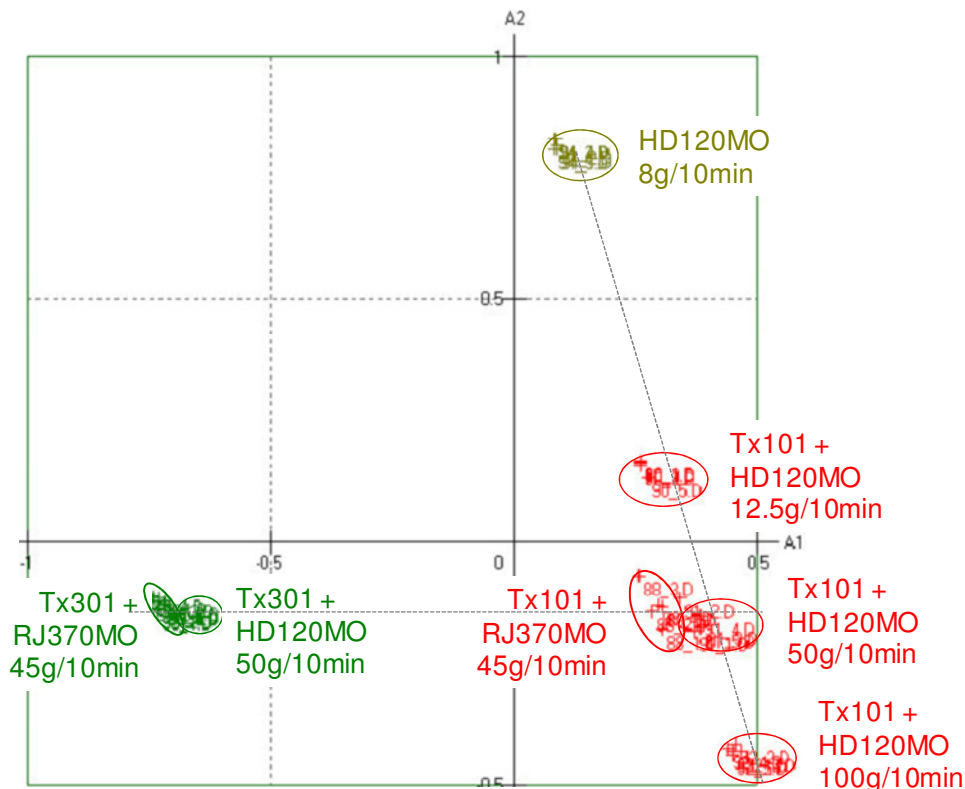


Figure 67. MasStat© Cluster of HS-SPME-GC-MS data obtained from the peroxide samples. Samples with TX101 in red, samples with Tx301 in green and the reference without peroxide in brown.

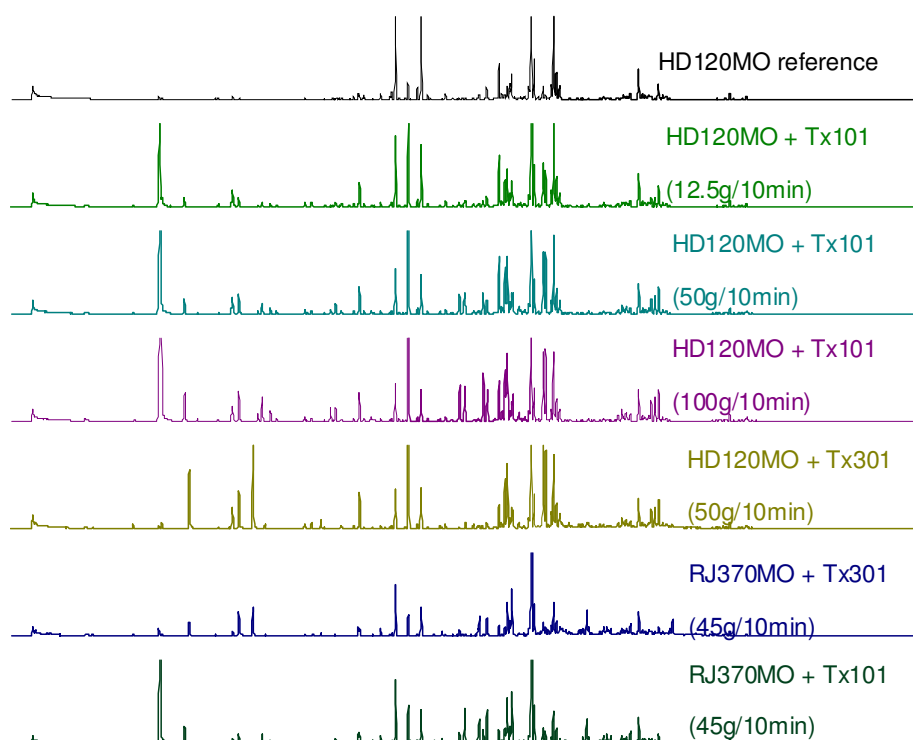


Figure 68. HS-SPME-GC-MS chromatograms of the analyzed data showing clear differences between the two peroxide systems Tx101 and Tx301.

Table 23. Differences in selected compounds representative for the use of Tx301 and Tx101. Tx101 was used as reference, values are expressed as difference to the use of Tx101.

Changes compared to the use of Tx101	RJ370MO + Tx301	HD120MO + Tx301
formaldehyde	+35%	+118%
acetaldehyde	+76%	-4%
methanol	+55%	only in Tx101
2-methyl-1-propene	only in Tx101	only in Tx101
ethanol	+343%	+162%
acetone	only in Tx101	only in Tx101
tert.-butanol	only in Tx101	only in Tx101
methyl acetate	only in Tx301	only in Tx301
methyl tert.-butyl ether	-79%	+22%
2-butanone	+185%	+90%
ethyl acetate	only in Tx301	only in Tx301
tert.-pentanol	only in Tx101	only in Tx101
pentanal	+11%	+71%

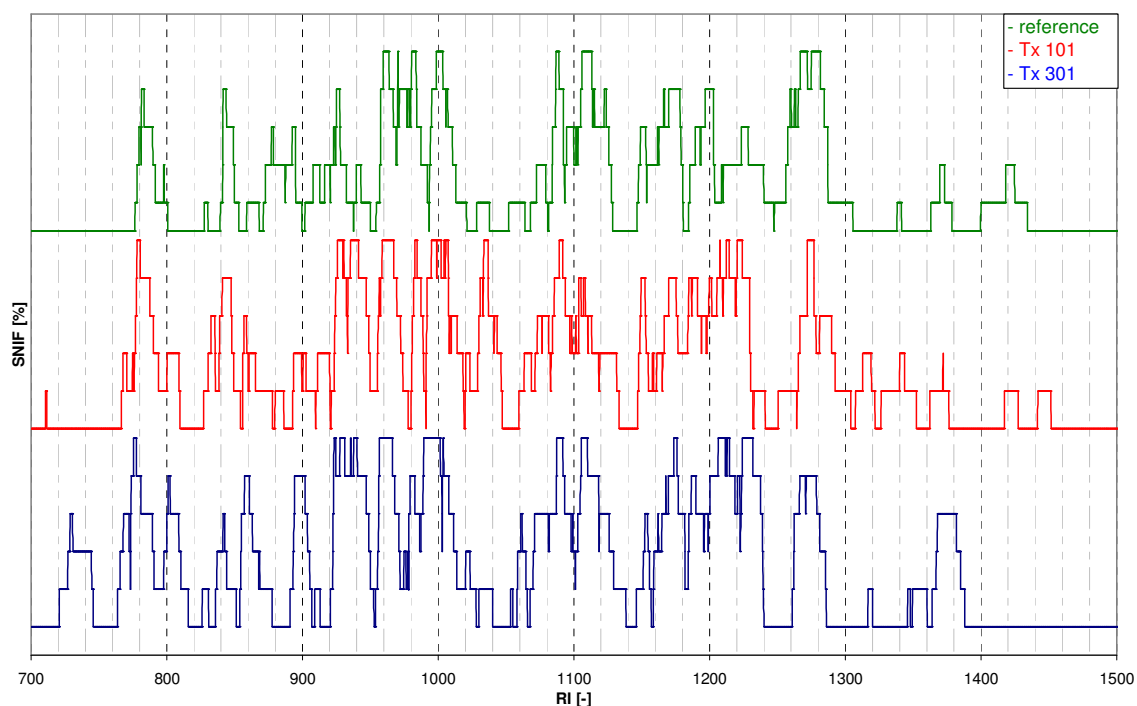


Figure 69. Summary of Detection Frequency (SNIF) diagrams for HD120MO without peroxide (in green), with Tx101 and a MFR of 50g/10min (in red) and with Tx301 and a MFR of 50g/10min (in blue).

#### 4.8. Autoxidation of PE and PP

During the first year of investigation the majority of odour-active compounds which were identified belong to the group of carbonyls. Carbonyls are known lipid oxidation products and are also generated in polyolefins during degradation and oxidation.

In a sub project we looked at the influence of autoxidation on the generation of odour-active compounds. Additionally, we investigated the effect of antioxidants.

The experimental set-up was as follows:

One PP (HD120MO) and one PE (ME3440) were screened (a) without or only small antioxidant addition (so called unstabilized samples taken right out of the polymerization reactor) and (b) with normal antioxidants level (stabilized). The samples were stored over a period of 1, 3 and 7 days at 80°C in either (a) a normal atmosphere (i.e. normal amount of oxygen) or (b) in a reduced oxygen atmosphere facilitated by blowing in N<sub>2</sub> to also study the effect of reduced oxygen amount on the generation of odour-active autoxidation products.

For this, we used 20 ml HS vials, filled them with the samples and either immediately capped them or blew out the vials with N<sub>2</sub> prior to the closing. Samples were analyzed with HS-SPME-GC-MS

and HS-SPME-GC-O. For a better use of the gained results samples were also analyzed using FTIR observing typical oxidation bands and calculating the Carbonyl Index (CI).

We received the samples in dark glass bottles intensely "aerated" with N<sub>2</sub> before filling and stored them in a freezer until use. As the non-stabilized samples were taken directly from the polymerization reactor in a powdery form, the stabilized samples were milled under liquid N<sub>2</sub> to get comparable surface as non-stabilised powder as autoxidation processes are surface-driven reactions.

#### **4.8.a. Results of the PP (HD120MO) samples**

In Figure 70 the MasStat© cluster of all PP samples is shown. As expected, unstabilized samples show a stronger answer to ageing as stabilized ones seen by larger differences between sampling points. In this cluster stabilised samples fall together in one cluster proving that stabilisation of samples works to a certain extent as also shown in Figure 71 and Figure 72, where HS-SPME-GC-MS chromatograms for unstabilized and stabilized PP samples are compared. A similar trend in volatile generation can be seen but in different amount e.g. by generation of acids with increasing storage time (i.e. "triangles") (3 and 7 days in unstabilized and stabilized samples). Reduction of oxygen by blowing in nitrogen (called "nitrogen" samples) results in only small changes as seen in the overall cluster where air and nitrogen samples are only little separated with a tendency of less oxidation than in the air sample.

In terms of odour following conclusions can be drawn and seen in Figure 73:

- With increasing oxidation time the number of odour-active compounds with high relevancy (SNIF value of 100 %) increased.
- No differences between stabilized and unstabilized samples in the odour pattern could be found, but in unstabilized samples much higher amounts of volatiles are generated especially acids (e.g. acetic acid) turn up after one day. This indicates similar oxidation processes in both samples regardless of the stabilization.
- A slightly smaller number of odour-active compounds with high SNIF values (100 %) was observed in nitrogen samples compared to air samples.
- Odour-active compounds (bold ones with high odour relevancy) include **1-hexen-3-one**, hexanal, **2,3-butandione**, **2,3-pentandione**, 2-methyl-2-pentenal, 1-hepten-3-one, heptanal, **2-acetyl-1-pyrroline**, 3-hepten-2-one, (E)-2-heptenal, **1-octen-3-one**, **octanal**, (E,E)-2,4-heptadienal, (E)-2-octenal, 3-octen-2-one, **1-nonen-3-one**, **6- / 8-nonenal**, (E,E)-2,4-octadienal, **(E)-2-nonenal**, **decanal**, **γ-octalactone**, (E)-2-decenal and (E)-2-undecenal.

We tried to use FTIR for reference measurements to determine after what period the FTIR is able to detect the degradation of the samples by using the Carbonyl Index (CI) as described in 3.4.a.

For the calculation of the CI we used both the area and the peak height, but in no case we were able to find a trend indicating an increase in degradation with FTIR and subsequent CI calculations. One possible explanation could be the heavy thermal treatment especially of the unstabilized samples during the film pressing at 220°C. But even for the stabilized samples no trend was observed. We then switched to NIR as alternative as described in 3.4.b and were able to achieve good correlation by partial least square regression as described in 3.4.b. The calibration curves are shown in Figure 77,

Using NIR measurements of the stabilized and unstabilized PP samples resulted in good correlation and multivariate calibration was possible.

Data was pre-treated with multiplicative scatter correction to minimise non-specific scatter phenomena. No outlier could be detected by Principal Component Analysis (PCA).

Distinct wavelengths responsible for Autoxidation could not be identified and so all wave numbers from 4000 – 10000<sup>-1</sup> were used for establishment of calibration model. Models shown are cross-validated, which is a proof that the established model describes well the happening. R-Square values are nearly 1 for both calibration and cross-validation curves.

However, a separation between samples stored in normal air and in a reduced oxygen atmosphere was not achieved.

The same was observed for the GC-O analyses indicating that after the oxygen reduction still enough oxygen was present for oxidative processes.

This is also important, as for preventing oxidation during processing or compounding very low amounts of oxygen are needed to achieve an effect as described by Epacher et al.<sup>15</sup>.

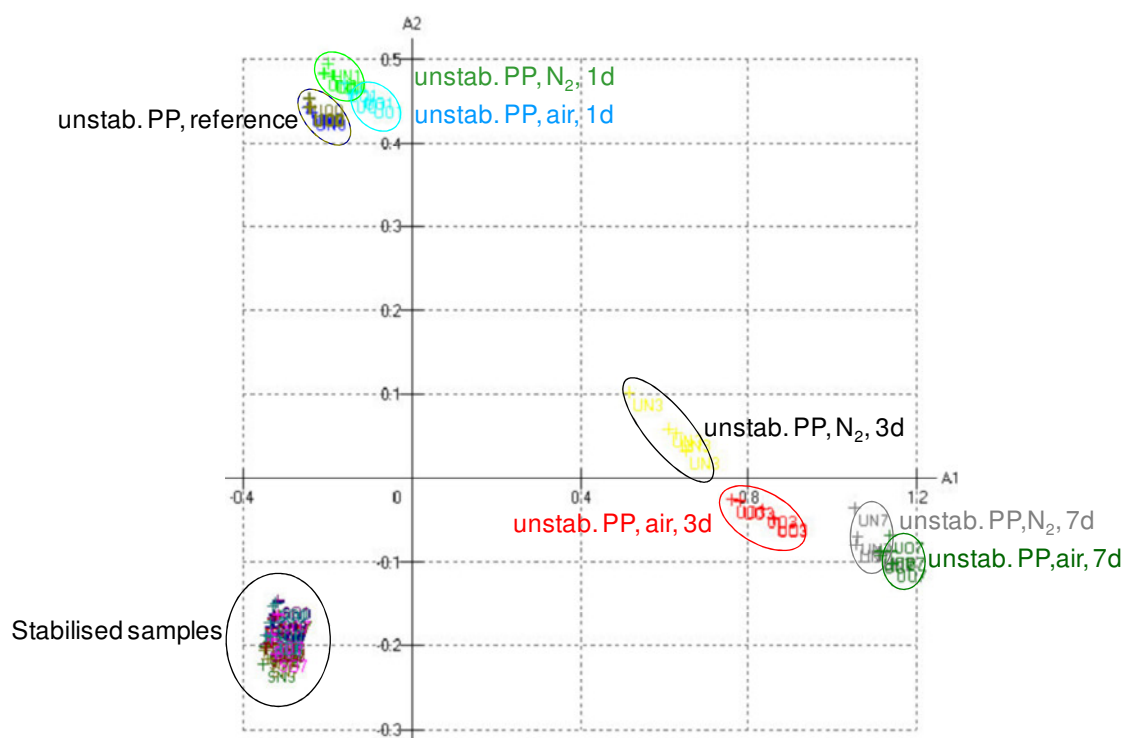


Figure 70. MasStat© Cluster obtained from the HS-SPME-GC-MS data of the unstabilized (unstab.) and stabilized PP samples stored for 0 (ref), 1 (1d), 3 (3d) and 7 (7d) days at 80 °C in normal atmosphere (air) or in reduced oxygen atmosphere (N<sub>2</sub>).

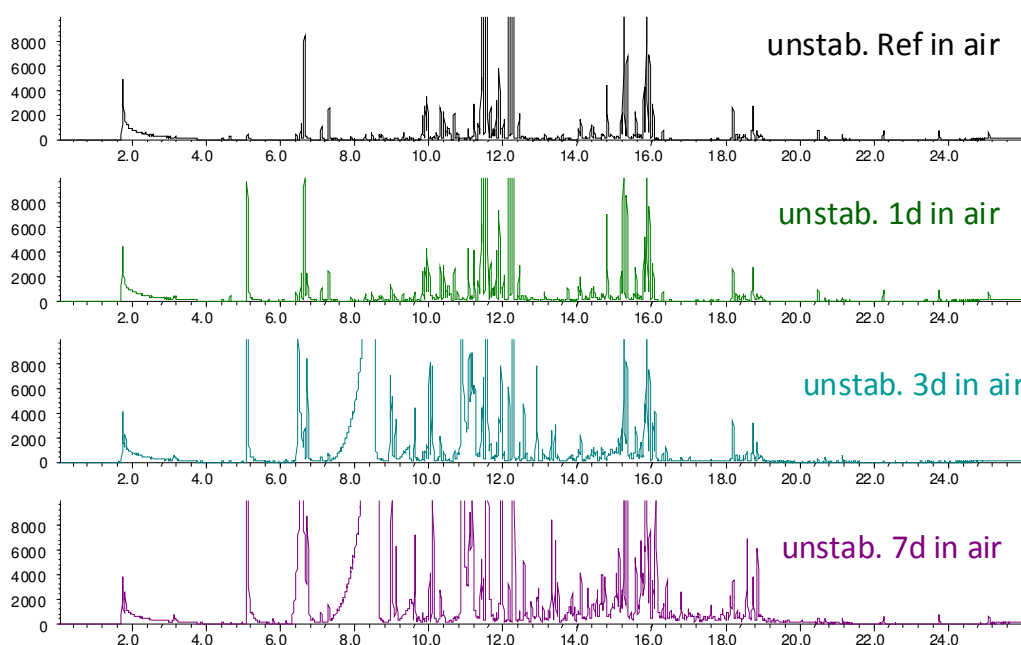


Figure 71. HS-SPME-GC-MS chromatograms of unstabilized PP samples stored @80 °C up to 7 days in normal atmosphere.

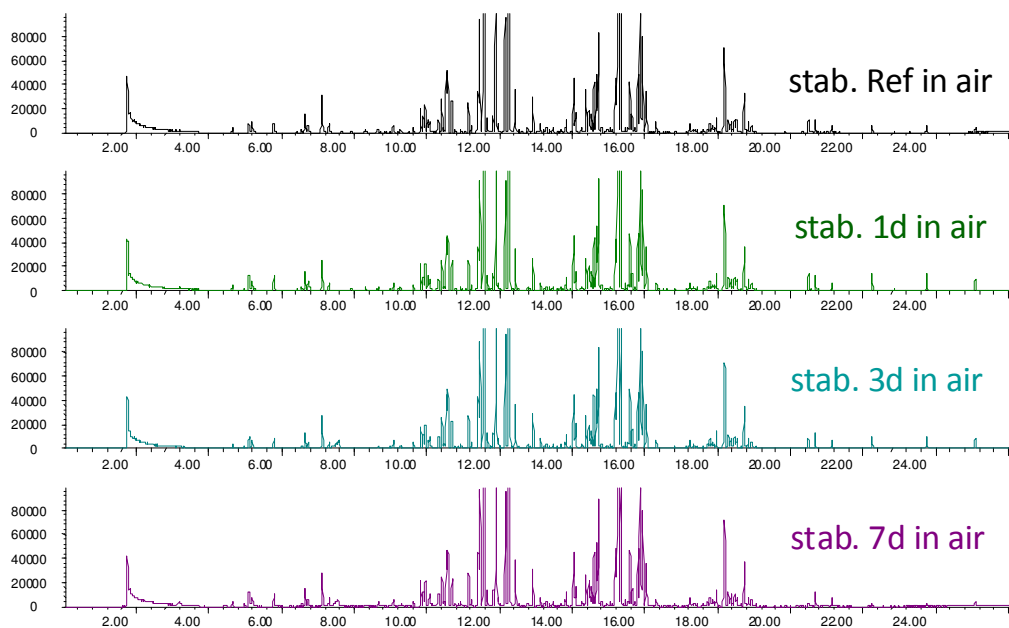


Figure 72. HS-SPME-GC-MS chromatograms of stabilized PP samples stored @80 °C up to 7 days in normal atmosphere.

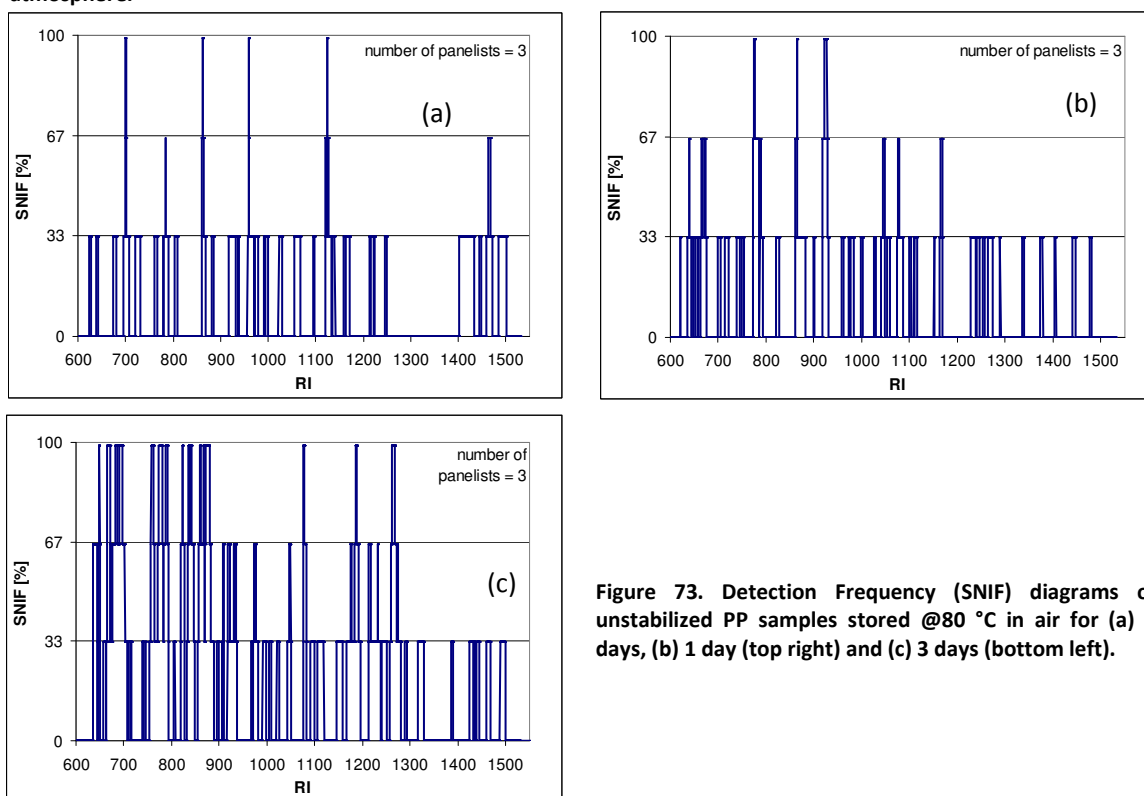


Figure 73. Detection Frequency (SNIF) diagrams of unstabilized PP samples stored @80 °C in air for (a) 0 days, (b) 1 day (top right) and (c) 3 days (bottom left).



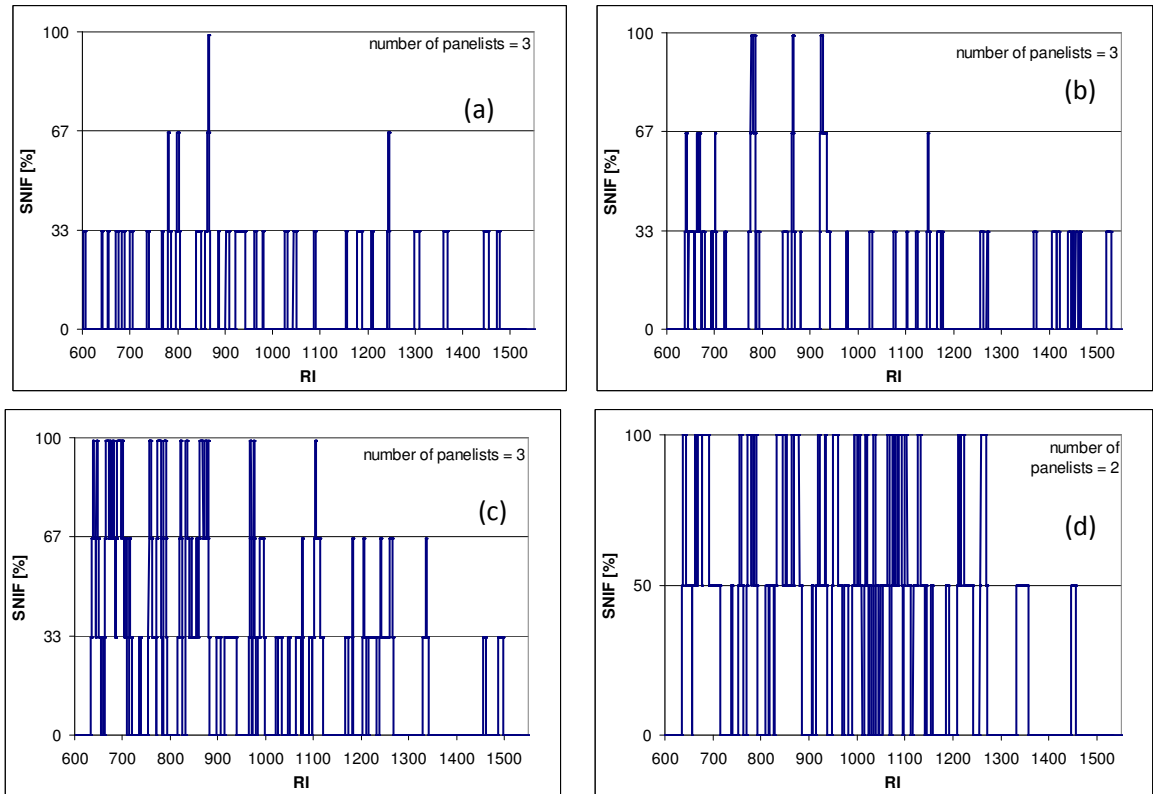


Figure 74. Detection Frequency (SNIF) diagrams of unstabilized PP samples stored @80 °C in reduced oxygen atmosphere for (a) 0 days, (b) 1 day, (c) 3 days and (d) 7 days.

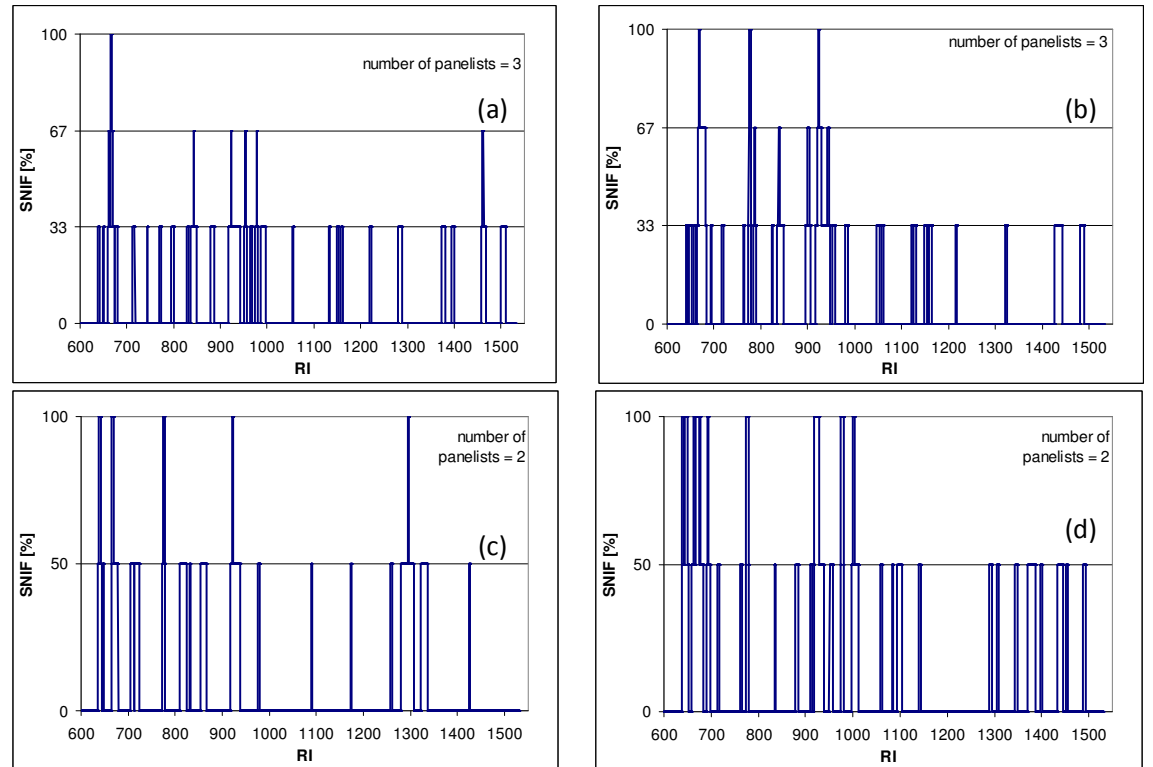


Figure 75. Detection Frequency (SNIF) diagrams of stabilized PP samples stored @ 80 °C in air for (a) 0 days, (b) 1 day, (c) 3 days and (d) 7 days.

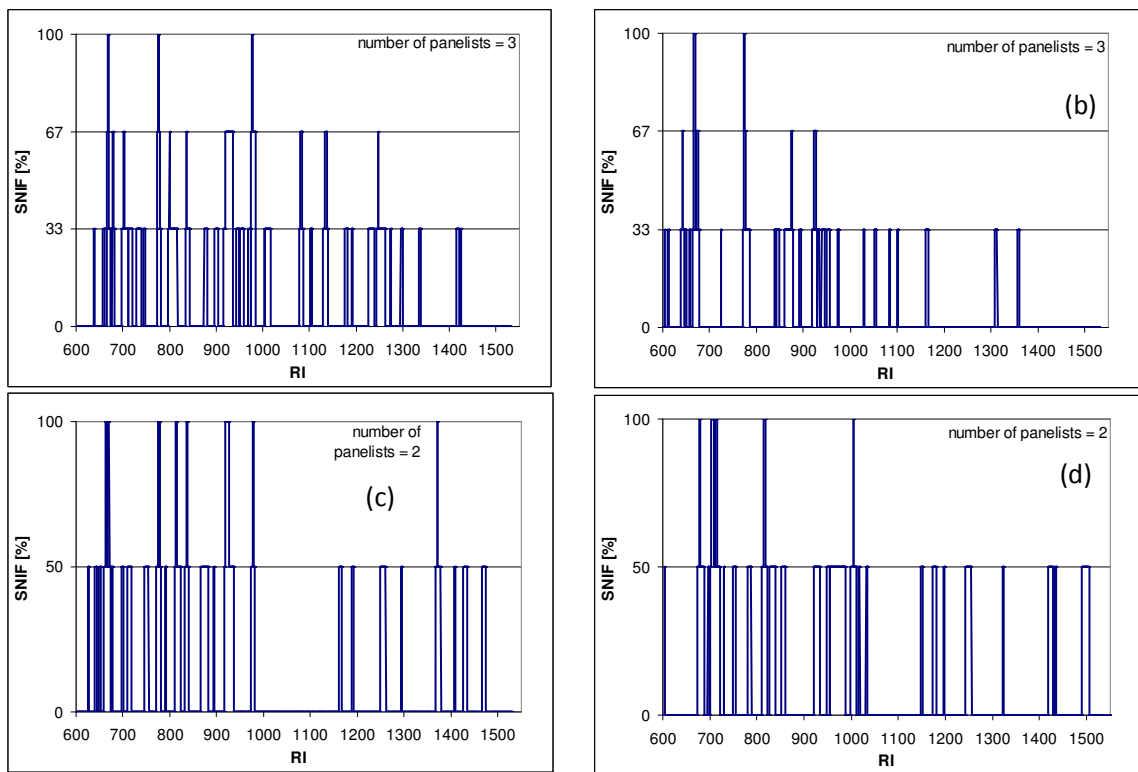


Figure 76. Detection Frequency (SNIF) diagrams of stabilized PP samples stored @ 80 °C in reduced oxygen atmosphere for (a) 0 days, (b) 1 day, (c) 3 days and (d) 7 days.

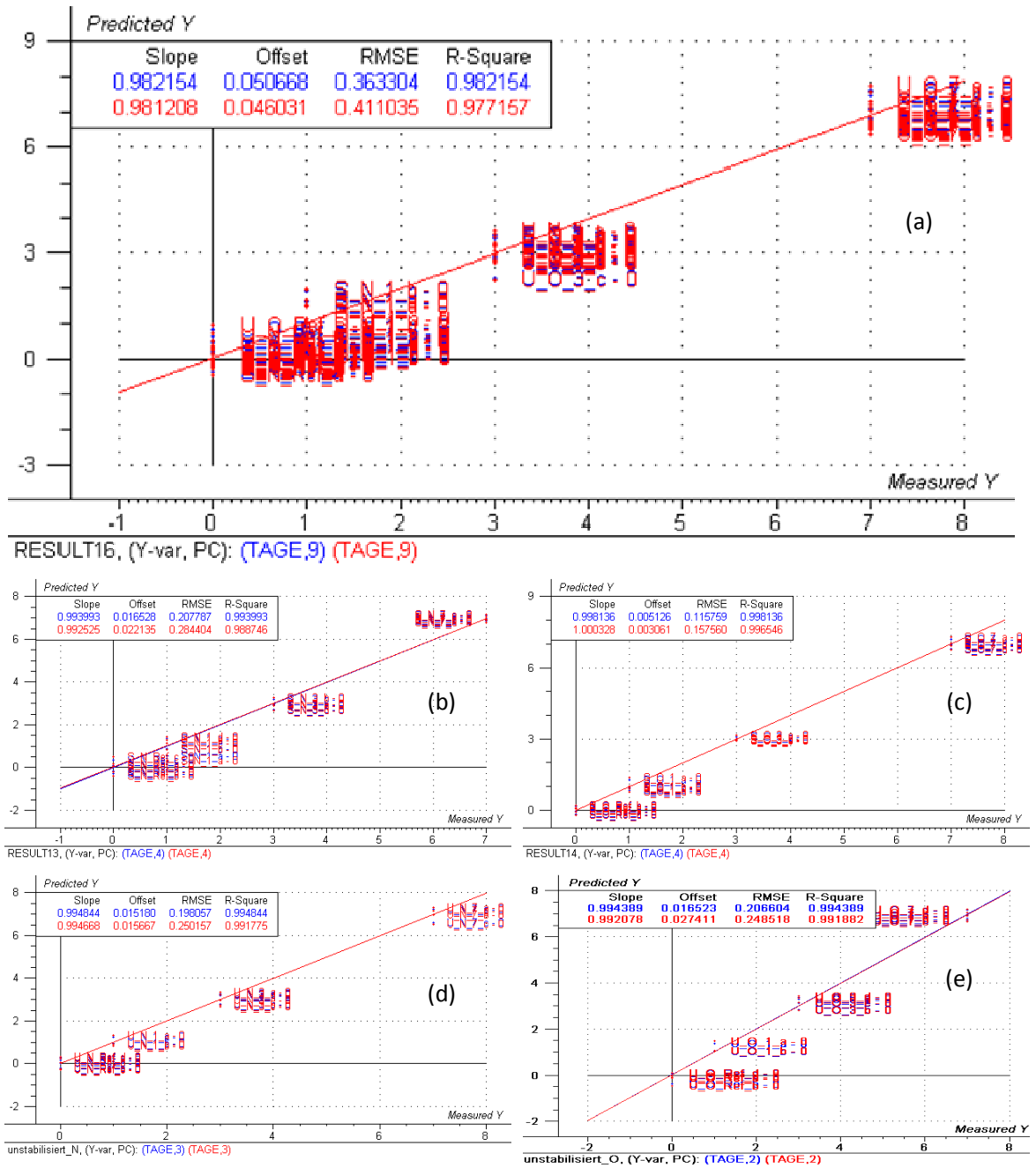


Figure 77. Multivariate calibration and cross-validation curves for (a) all PP (HD120MO) samples, (b) stabilized samples in a reduced oxygen atmosphere, (c) stabilized samples in air, (d) unstabilized samples in a reduced oxygen atmosphere and (e) unstabilized samples in air.

#### **4.8.b. Results of PE (ME3440) samples**

A different picture was observed for the PE samples. Here, not so clear conclusions could be drawn: In the MasStat© cluster the variation of the stabilized samples between the sampling points of 0, one, three and 7 days is larger than for the unstabilized samples. Additionally, a clear separation as in the PP samples between the air and the reduced oxygen atmosphere samples is not possible; only for the 7 days samples a differentiation can be made.

Looking into the GC-MS details for the reasons for these large deviations in the stabilized but not in the unstabilized samples, it is easy to see that the unstabilized samples are not as degraded as the PP samples; only after 7 days acetic acid at retention time 8 min is formed indicating oxidation. An explanation to this is that the PE samples are already addivated in the polymerization reactor. Due to the lack of the tertiary C-atom in the polymer chain PE is also less susceptible to oxidation. Differences between unstabilized and stabilized samples are pronounced in the early retention times: In the unstabilized samples higher amounts of highly volatiles are generated such as acetone, acetic acid and various alcohols.

For the Detection Frequency (SNIF) diagrams (shown in Figure 81 to Figure 84), one observes that for the unstabilized samples stored at 80 °C in air and for the stabilized samples stored in a reduced oxygen atmosphere the number of odour-active compounds with SNIF values of 100% triples or raises from the reference sample to the 7 days sample, while for the unstabilized samples stored in a reduced oxygen atmosphere and for the stabilized samples stored at air the highest number of odour-active compounds with SNIF values of 100% was detected after one day storage and decreased then.

All these observations might be an indicator that (1) in the ME3440 the oxidation was less pronounced for both the unstabilized and stabilized samples than in the PP and (2) the in-reactor-additivation prevents high degradation in the PE samples.

However, for some compounds an increase in the concentration during the oxidation period could be observed:

- 2,3-butandione was detected in the unstabilized samples and increased in the SNIF value from 67% to 100% after 7 days.
- $\gamma$ -octalactone was detected in both stabilized samples after three days with 67% SNIF value.
- 2-acetyl-1-pyrroline was detected in both unstabilized and stabilized samples with 67% SNIF value after one and 7 days.

These compounds could be detected with high SNIF values in all samples both stabilized and unstabilized and already in the reference samples:

- 1-hexen-3-one
- 1-octen-3-one
- octanal
- 1-nonen-3-one
- 6/8-nonenal

NIR measurements of the stabilized and unstabilized PE samples were carried out and the results used for a multivariate calibration. Good correlation was achieved and multivariate calibration was possible as shown in Figure 85.

Data was pre-treated with multiplicative scatter correction to minimise non-specific scatter phenomena. No outlier could be detected by Principal Component Analysis (PCA).

Distinct wavelengths responsible for Autoxidation could not be identified and so all wave numbers from 4000 – 10000<sup>-1</sup> were used for establishment of calibration model. Models shown are cross-validated, which is a proof that the established model describes well the happening. R-Square values are nearly 1 for both calibration and cross-validation curves, but are lower than those obtained for the PP samples.

Again, it was not possible to distinguish between samples stored in normal air and in a reduced oxygen atmosphere. For all plots the data points show a larger scattering than observed for the PP samples. For the stabilized samples in a reduced oxygen atmosphere the calibration points for 3 and 7 days could not be separated; for all other plots separation between the individual sampling days was achieved.

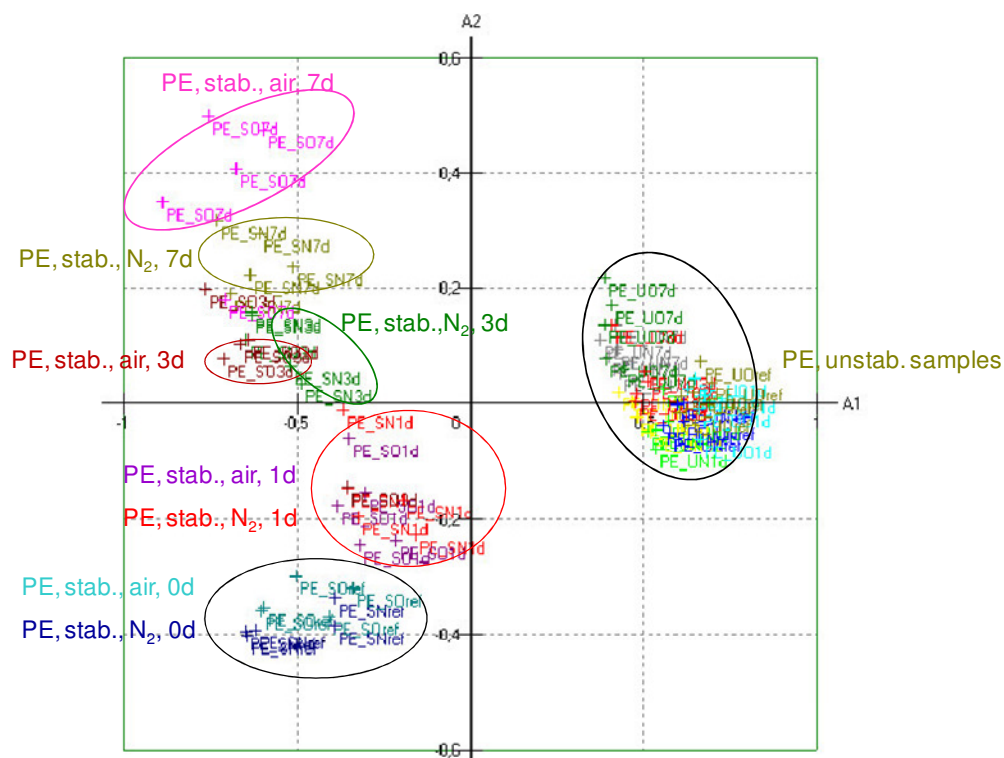


Figure 78. MasStat© Cluster obtained from the HS-SPME-GC-MS data of the unstabilized (unstab.) and stabilized (stab.) PE samples stored for 0 (ref), 1 (1d), 3 (3d) and 7 (7d) days at 80 °C in normal atmosphere (air) or in reduced oxygen atmosphere (N<sub>2</sub>).

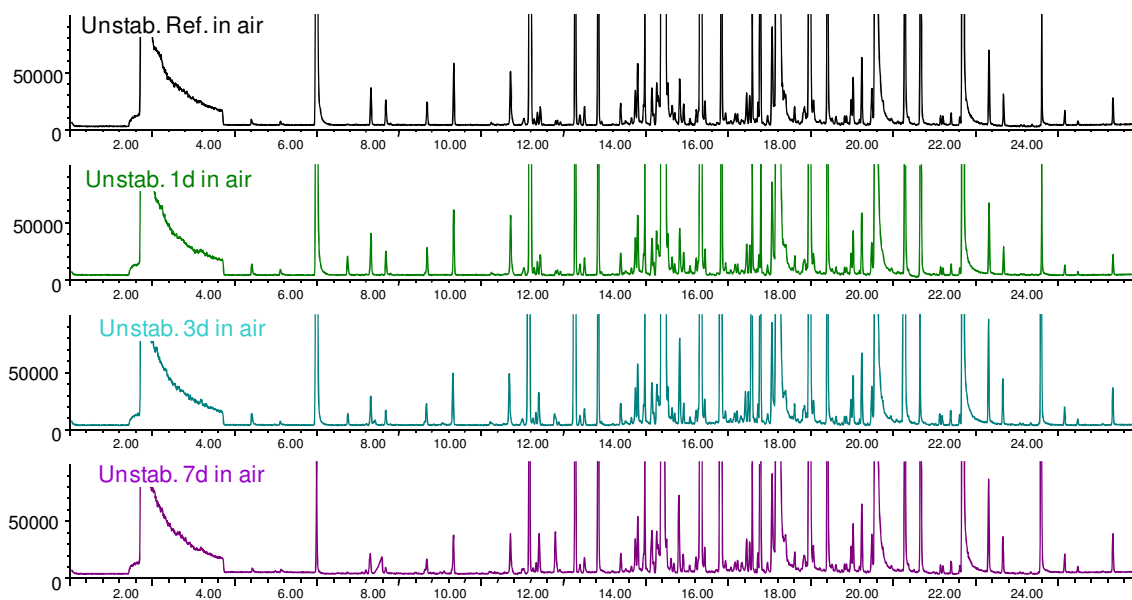


Figure 79. HS-SPME-GC-MS chromatograms of unstabilized PE samples stored @80 °C up to 7 days in normal atmosphere (air).

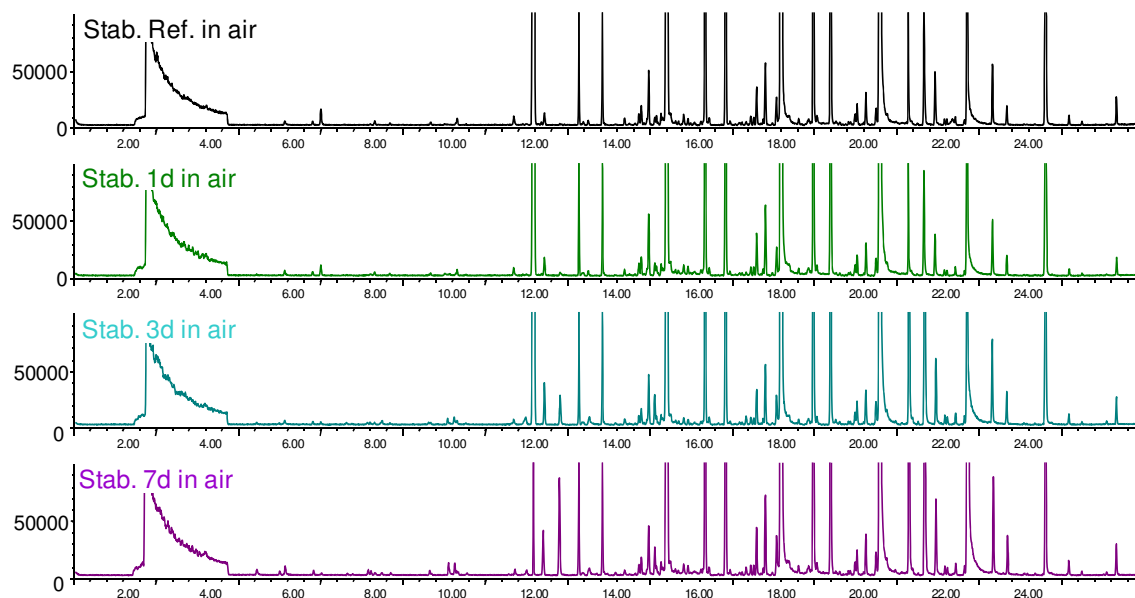


Figure 80. HS-SPME-GC-MS chromatograms of stabilized PE samples stored @80 °C up to 7 days in normal atmosphere (air).

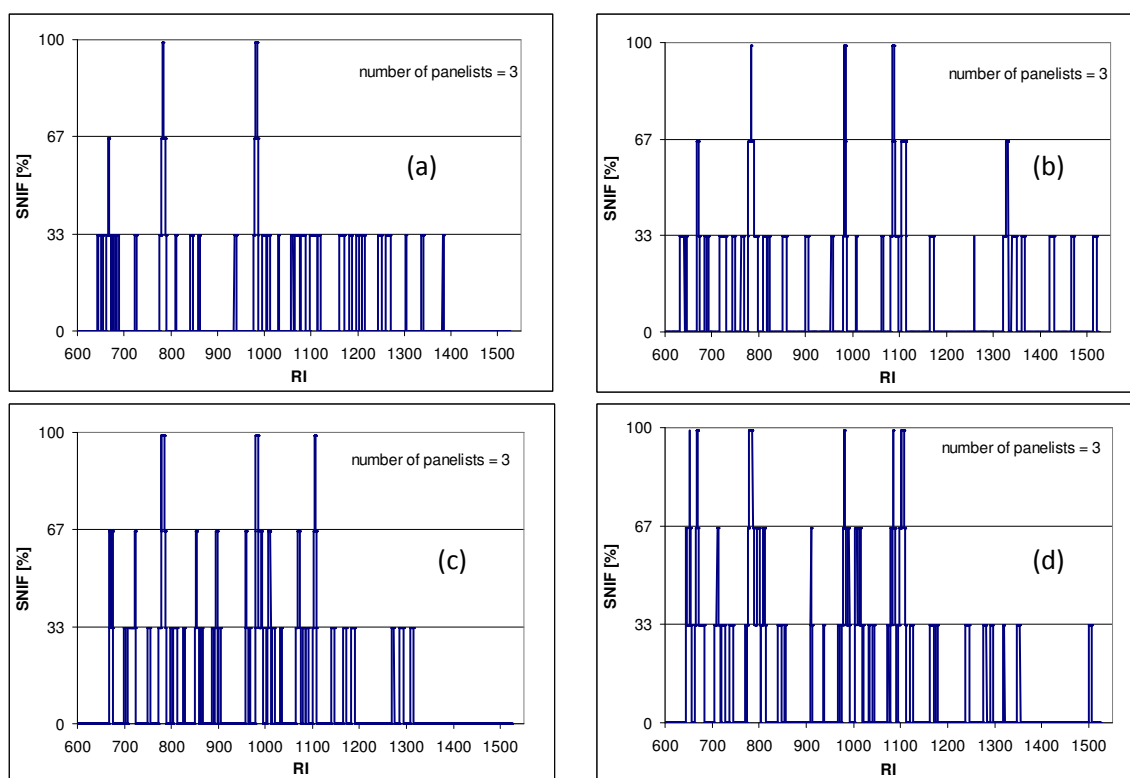


Figure 81. Detection Frequency (SNIF) diagrams of unstabilized PE samples stored @ 80 °C in air for (a) 0 days, (b) 1 day, (c) 3 days and (d) 7 days.

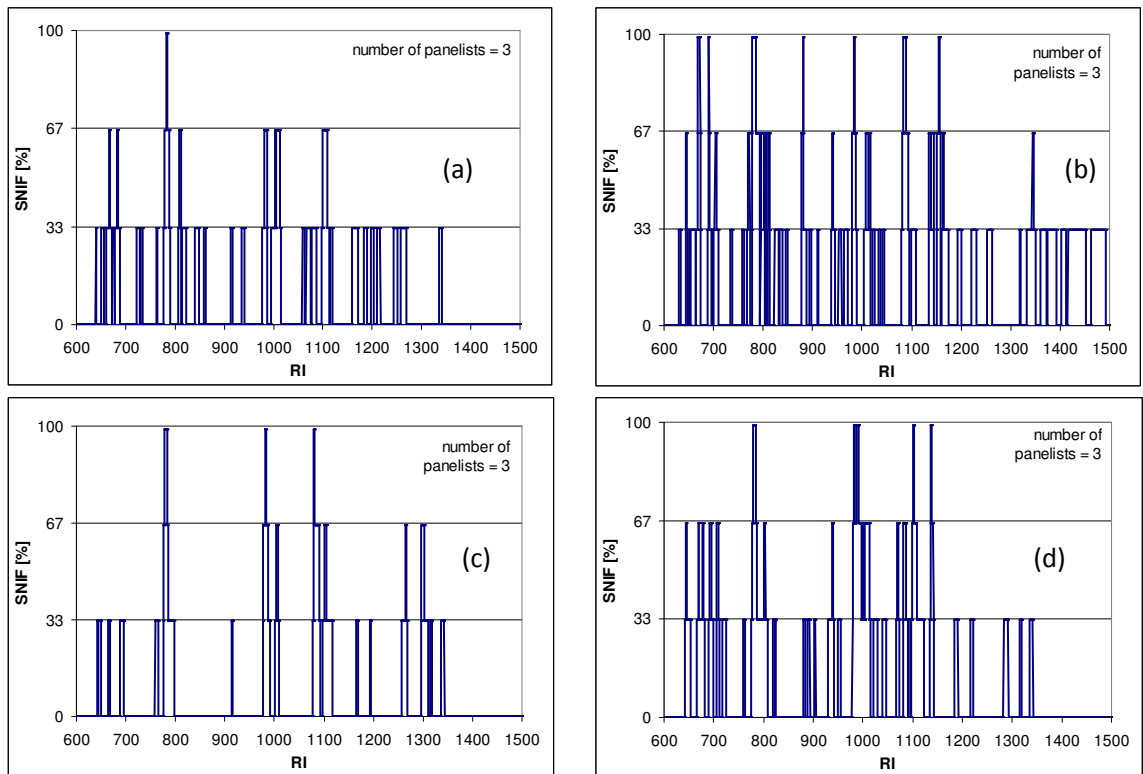


Figure 82. Detection Frequency (SNIF) diagrams of unstabilized PE samples stored @ 80 °C in a reduced oxygen atmosphere for (a) 0 days, (b) 1 day, (c) 3 days and (d) 7 days.

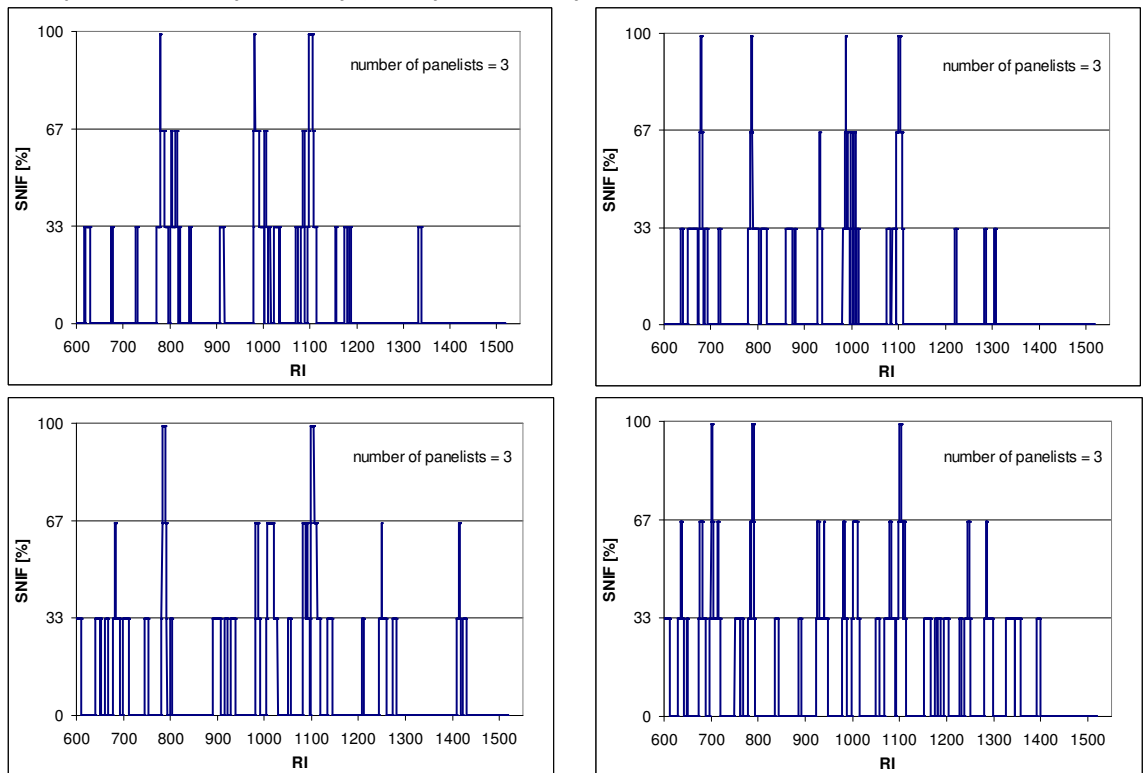


Figure 83. Detection Frequency (SNIF) diagrams of stabilized PE samples stored @ 80 °C in air for (a) 0 days, (b) 1 day, (c) 3 days and (d) 7 days.



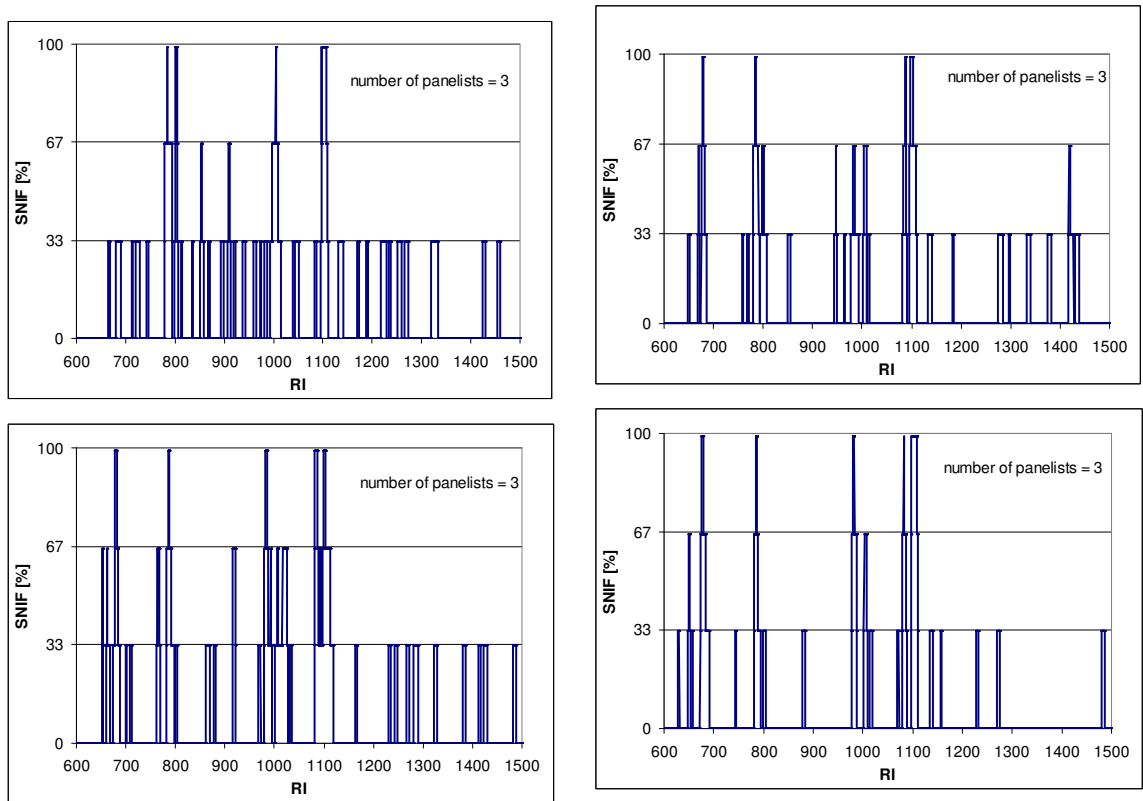


Figure 84. Detection Frequency (SNIF) diagrams of stabilized PE samples stored @ 80 °C in a reduced oxygen atmosphere for (a) 0 days, (b) 1 day, (c) 3 days and (d) 7 days.

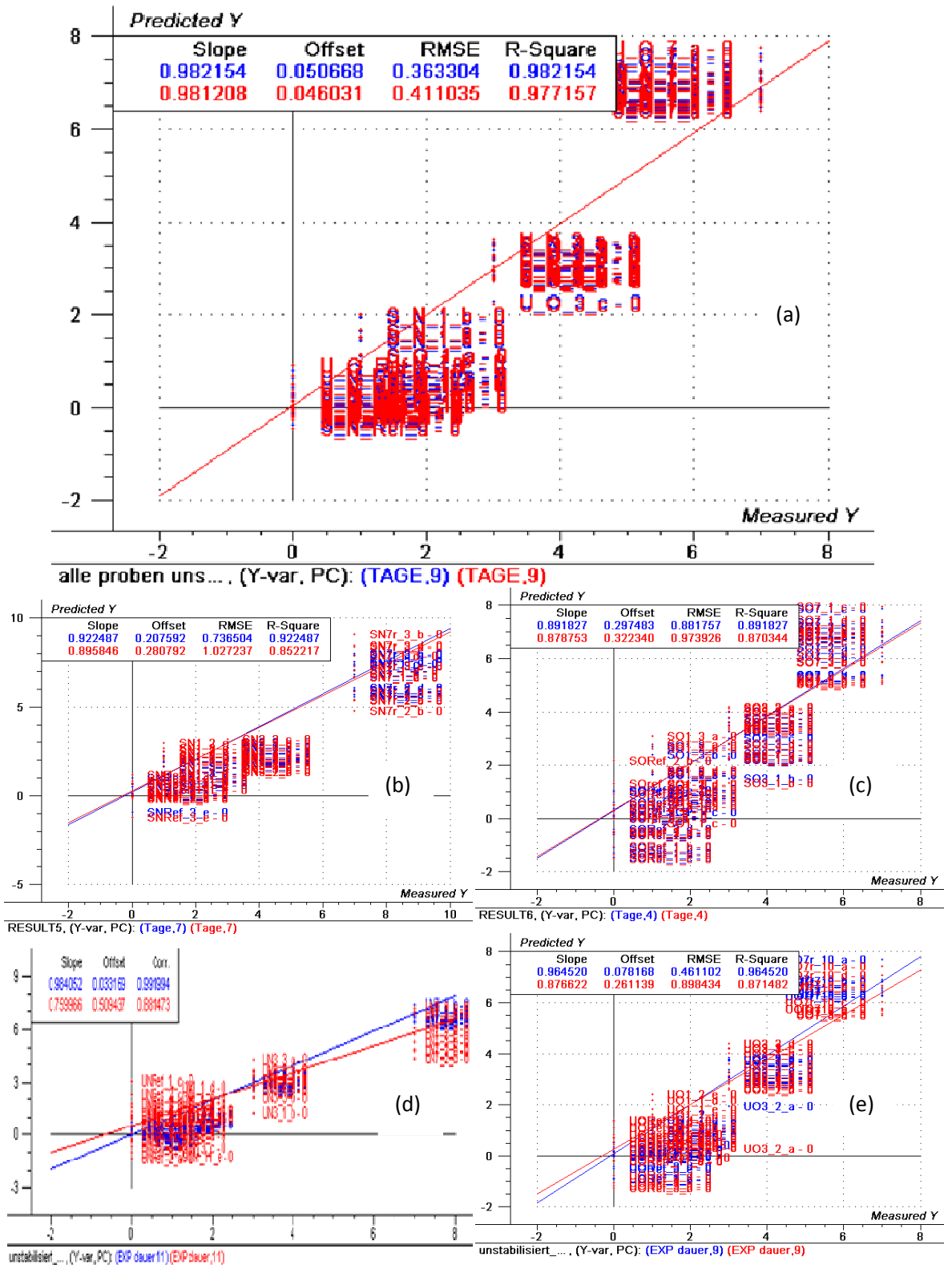


Figure 85. Multivariate calibration and cross-validation curves for (a) all PE (ME3440) samples, (b) stabilized samples in reduced oxygen atmosphere, (c) stabilized samples in air, (d) unstabilized samples in a reduced oxygen atmosphere and (e) unstabilized samples in air.

#### 4.9. QC method (HS-SPME-GC-PID)

Quality control (QC) is gaining more and more importance in the industry. For Borealis a QC system which is able to detect variations in the production of similar materials would be invaluable.

For this, the system should:

- work on- or at-line (i.e. directly in the plant)
- be able to detect production variations which might lead to problems in emissions and/or odour
- be self-learning
- be robust, reliable and easy to handle
- be able to detect odour-active compounds close to their sensory thresholds
- be able to deal with heavy interferences by non-odour-active compounds (alkanes, alkenes)

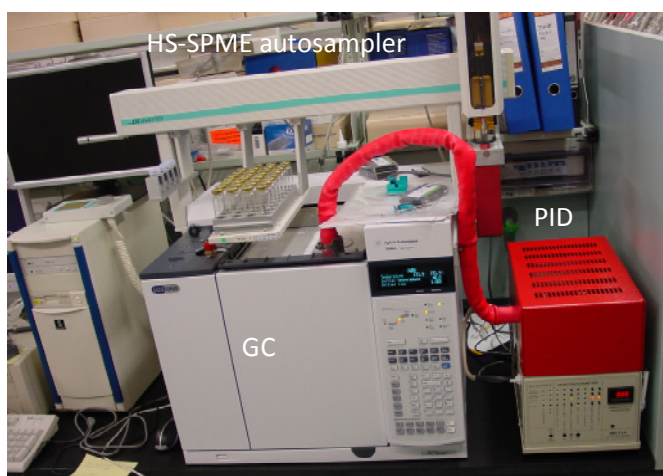


Figure 86. Proposed HS-SPME-GC-PID set-up.

Based on these assumptions and requirements an instrumentation depicted in Figure 86 including (a) an automated HS-SPME sampling unit, (b) a GC, (c) a photo ionization detector (PID) and (d) post data processing using MVDA. The PID was proposed as it is (i) more robust than an MS, (ii) is more selective than an FID due to different ionization potentials which could be of help for

suppressing the interfering alkanes and alkenes. In combination with the GC separation and the MVDA the system should be able to distinguish “good” and “bad” samples after an initial training and model establishment period.

In a first screening we analyzed 45 PE samples from Stenungsund listed in Table 3 using HS-SPME-GC-PID with subsequent cluster analysis with ChromStat© (Analyt, Germany) to evaluate the QC usability.

Similar to MasStat© Chromstat© also groups samples according to their similarities and/or differences, but in contrast to MasStat©, ChromStat© does not use the MS spectra but GC

integration results (i.e. peak areas or heights) from either the whole chromatogram or from selected retention time areas.

First screening results showed that the setup is able to differentiate between different materials (Figure 87) and different lots of the same material (Figure 88). It was proved that setup could be used as a QC tool, but further development and optimisation of whole setup is needed as each part of the system influences the results and has to be investigated. These influences include:

- sample amount in the HS vials
- type of SPME extraction (headspace vs. direct)
- extraction medium (air, water)
- SPME fibre
- SPME thermostating and extraction program
- GC oven program and flow parameter
- GC column
- PID lamps (i.e. ionization potential)
- PID setup (temperature, current, flow)
- data processing prior to cluster analysis (integration parameters, retention time areas)
- cluster analysis parameters
- robustness of the method to system deviations vs. sensitivity to real changes in production

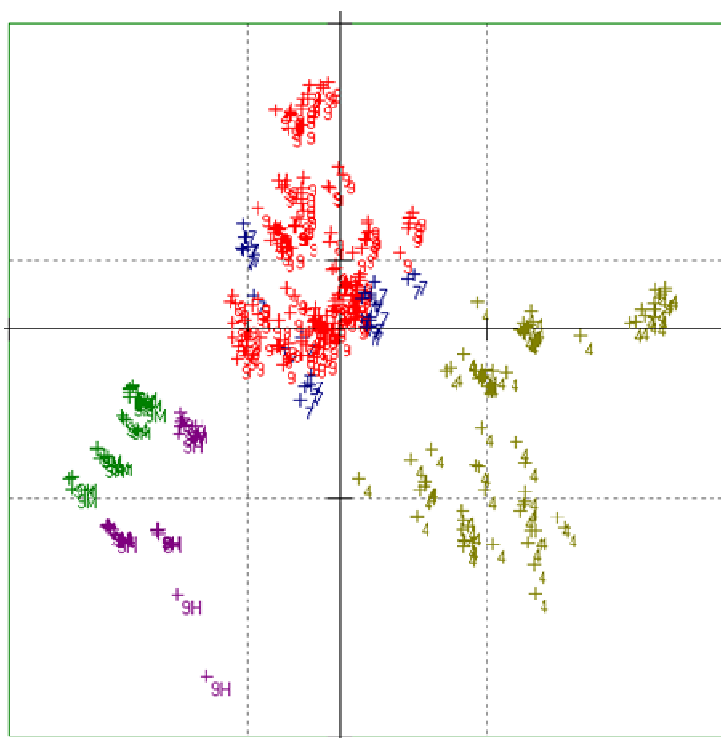


**Figure 87. ChromStat© Cluster of QC samples separated by the material**  
legend:  
9 ... ME3490,  
4 ... ME3440,  
7 ... ME3470,  
9H ... ME3490 H01,  
9M ... ME34901MO2

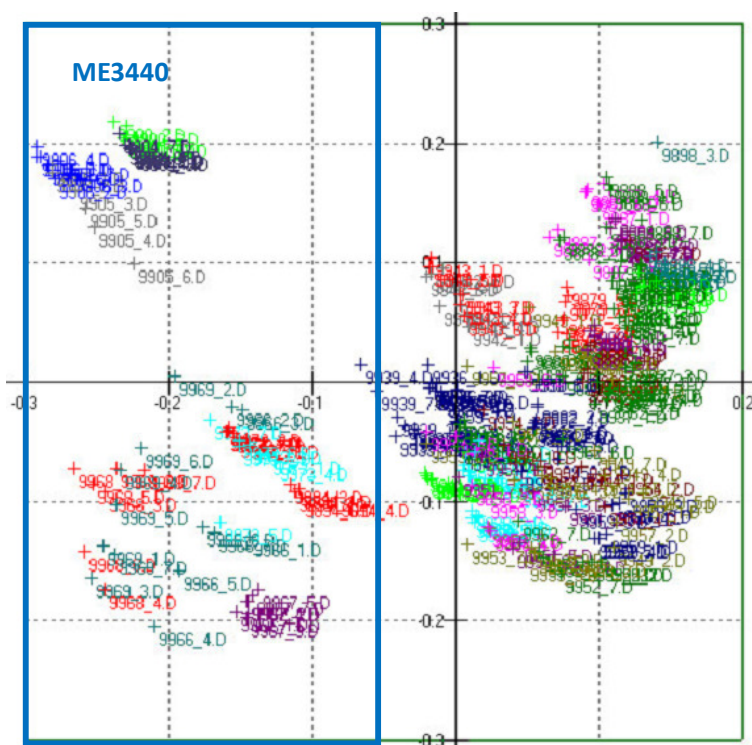


Figure 88. ChromStat© Cluster of QC samples showing separation of different lots of the same material ME3440-05.

#### 4.10. Sensory threshold determination applying the BET procedure

Sensory threshold values for selected odour-active compounds detected and identified in polyolefin samples were determined as described in section 3.6.a.

First, sensory threshold values were determined in water. Those compounds with sensory threshold values below  $1\mu\text{g}/\text{kg}$  in water were determined in an oil matrix in a second step. An oil matrix was chosen to determine values which are closer to the threshold values in polyolefins than the water values.

In Table 24 and Table 26 the determined group BET values are listed. For both matrices the standard  $\log_{10}$  deviation of the BET values is below 1 indicating valid results according to ASTM679<sup>6</sup>.

Generally, the water BET is lower than the miglyol value; the lowest values in the area of sub- $\mu\text{g}$  per kg range of all investigated compounds were found in both matrices for 1-octen-3-one and 1-hexen-3-one.

**Table 24. Sensory threshold values determined as group BET in water (s.d. ... standard deviation).**

Compound	BET <sup>a</sup> in water [µg/kg]	log <sub>10</sub> of BET [-]	log <sub>10</sub> s.d. [-]	upper limit BET [µg/kg]	lower limit BET [µg/kg]
(E)-2-heptenal	9.1	0.96	0.51	29.4	2.8
heptanal	2.8	0.44	0.33	5.9	1.3
octanal	2.1	0.32	0.87	15.4	0.3
decanal	2.1	0.33	0.86	15.3	0.3
nonanal	1.9	0.27	0.6	7.5	0.5
(E)-2-octenal	1.5	0.16	0.76	8.4	0.3
γ-octalactone	1.4	0.16	0.80	9.2	0.2
(E)-2-decenal	1.2	0.09	0.33	2.6	0.6
2,3-butandione	0.31	-0.51	0.55	1.10	0.09
(E)-2-nonenal	0.20	-0.70	0.42	0.52	0.08
1-octen-3-one	0.03	-1.60	0.68	0.12	0.005
1-hexen-3-one	0.0005	-3.30	0.47	0.0016	0.0002

<sup>a</sup> Values are given in terms of detection group BET. *n* = 10-13. The value for the detection threshold is the level at which the differing sample is selected correctly by the panel without being able to describe the sensory properties of the odour-active compound.

**Table 25. Sensory threshold values determined as group BET in miglyol (s.d. ... standard deviation).**

Compound	BET <sup>a</sup> in miglyol [µg/kg]	log <sub>10</sub> of BET [-]	log <sub>10</sub> s.d. [-]	upper limit BET [µg/kg]	lower limit BET [µg/kg]
(Z)-6-nonenal	2.01	3.31	0.51	6.55	0.630
(E)-2-nonenal	1.99	3.30	0.68	9.47	0.419
2,3-butandione	0.603	2.78	1.08	3.59	0.015
8-nonenal	0.371	2.57	0.70	1.85	0.075
1-octen-3-one	0.116	2.06	0.78	0.694	0.019
1-hexen-3-one	0.013	1.12	0.98	0.126	0.001

<sup>a</sup> Values are given in terms of detection group BET. *n* = 10-13. The value for the detection threshold is the level at which the differing sample is selected correctly by the panel without being able to describe the sensory properties of the odour-active compound.

#### **4.11. The influence of colour masterbatches (CMB) on the generation of odour-active compounds**

The influence of additives on the generation of odour-active compounds is strongly depending on the type of additive: In a first screening of additives used in a PP sample (see section 4.5) the filler (talc), UV stabilizers and colour masterbatches (CMB) were identified as strong contributor to odour in polyolefins. The influence of talc was investigated in section 4.4, and in the third year the influence of CMBs on the odour was evaluated.

Two PP materials were selected where the coloured samples are judged worse than the non-coloured ones by the Borealis sensory panel.

We analyzed (a) the coloured polymer (EE188HP-1048 (beige) and RA130E-8427 (grey)), (b) the uncoloured polymer (EE188HP natural and RA130E natural) and (c) the CMB (CMB347 for the EE188HP and CMB126 for the RA130E) itself. For the EE188HP samples we also analyzed injection moulded plaques.

Special attention was given, that both polymers (coloured and non-coloured) have the same processing history – the non-coloured polymers were compounded like the coloured ones but without the CMB.

HS-SPME-GC-MS and HS-SPME-GC-O with 5 trained panellists analyzing both 2 g and 500 mg of the samples in HS vials were applied. The resulting Detection Frequency (SNIF) diagrams are so called total SNIF diagrams including results of the 2 g and 500 mg analyses.

For the RA130E material all samples were separated in the cluster analysis using MasStat© from the HS-SPME-GC-MS data (see Figure 89). As expected, lays the coloured polymer in between the CMB and the natural polymer. For the RA130E material the differences between the three samples are mainly due to variations in alkane and alkene as well as in terpene ( $\alpha$ -pinene and limonene) concentrations.

The highest concentrations in terpenes can be found in the natural polymer, and the lowest in the CMB.

For the linear and branched alkanes and alkenes the highest amounts are present in the CMB. Also, toluene can be found in all samples with highest amounts in the CMB again. From the GC-MS chromatograms one can speculate that the CMB carrier polymer is also a PP due to the similar chromatographic pattern of all three samples; the highest number of peaks was found in the CMB as shown in Figure 90.

Comparing the Detection Frequency (SNIF) diagrams of the CMB, the natural RA130E pellets and the coloured RA130E pellets (see Figure 91) in the RI area between 900 and 1050 some compounds can be allocated being present either in the natural pellet or the CMB which turn up again in the coloured pellets:

- RI 935:  $\alpha$ -pinene or  $\alpha$ -thujene is present only in the natural pellets; most probably from the plant-derived additive GMS
- RI 960: benzaldehyde is present only in the CMB
- RI 978: 1-octen-3-one is present only in the natural pellets being a typical oxidation product with a very low sensory threshold
- RI 1005: octanal is present in highest amounts in the CMB being also a typical oxidation product

All these four compounds are present in the coloured RA130E pellets indicating that the odour-active compounds in the coloured sample (a) derive from the natural polymer, (b) are generated during the compounding step and (c) origin from the CMB.

Based on these data the CMB does contribute to the odour of the coloured pellets.

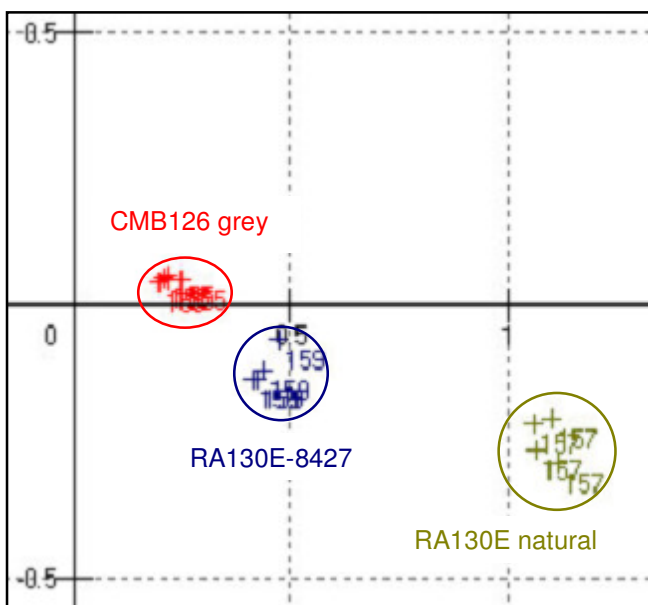


Figure 89. MasStat© cluster from the HS-SPME-GC-MS data of the coloured (RA130E-8427), the non-coloured (RA130E natural) and the CMB (CMB126 grey) samples.



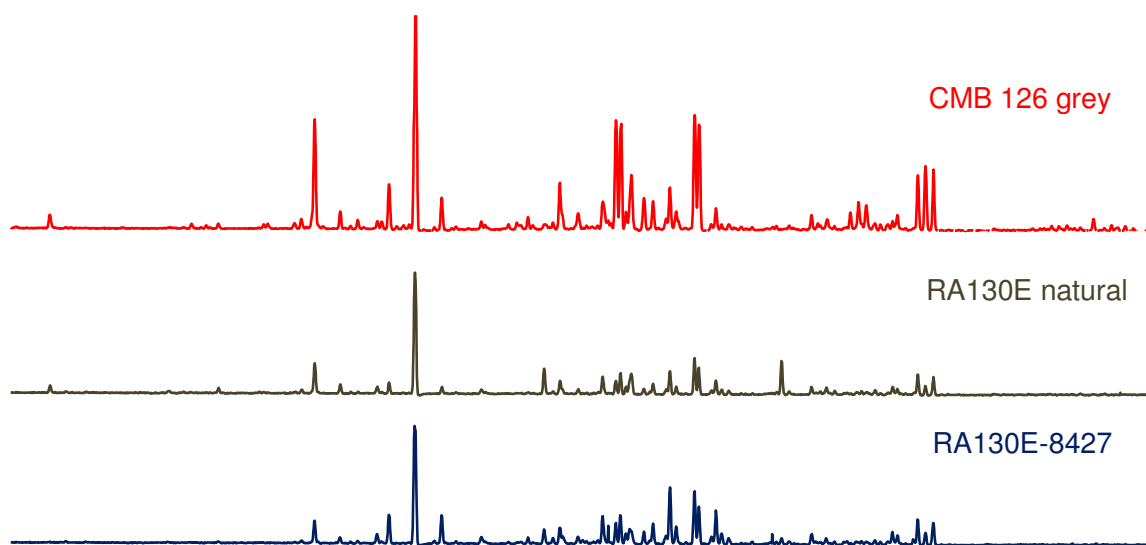


Figure 90. HS-SPME-GC-MS chromatograms of the coloured (RA130E-8427), the non-coloured (RA130E natural) and the CMB (CMB126 grey) samples.

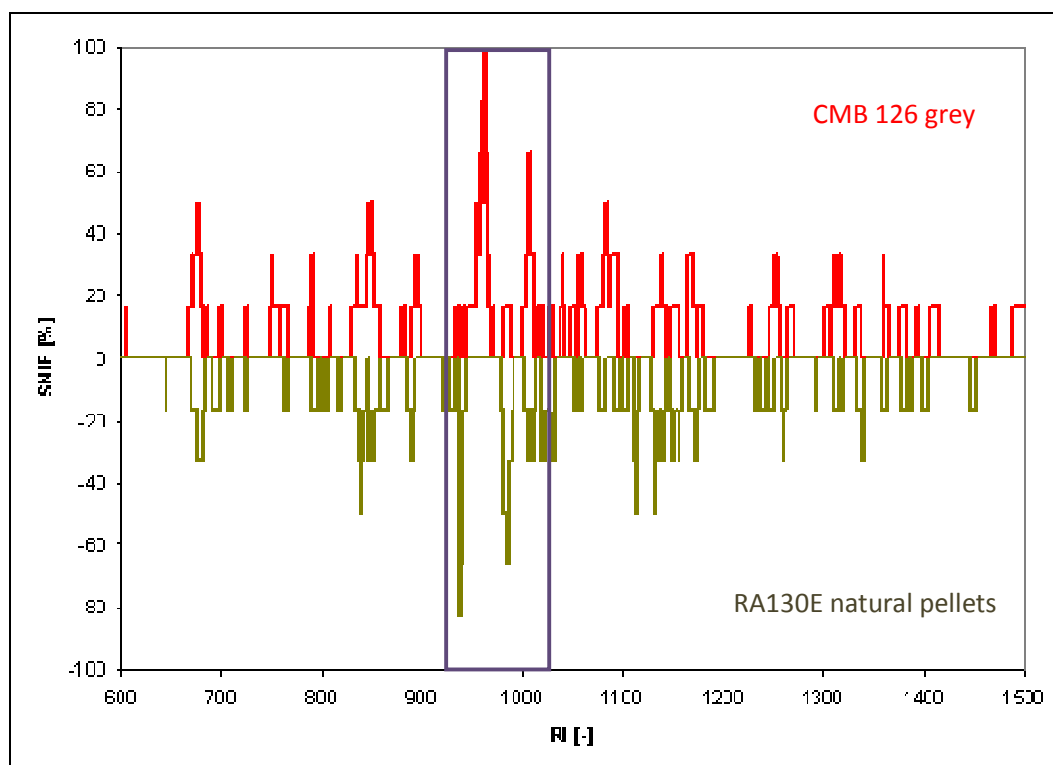


Figure 91. Detection Frequency (Total SNIF) diagrams of the CMB126 (in red) and the natural RA130E pellets (in brown) using the 2 g and the 500 mg GC-O results.

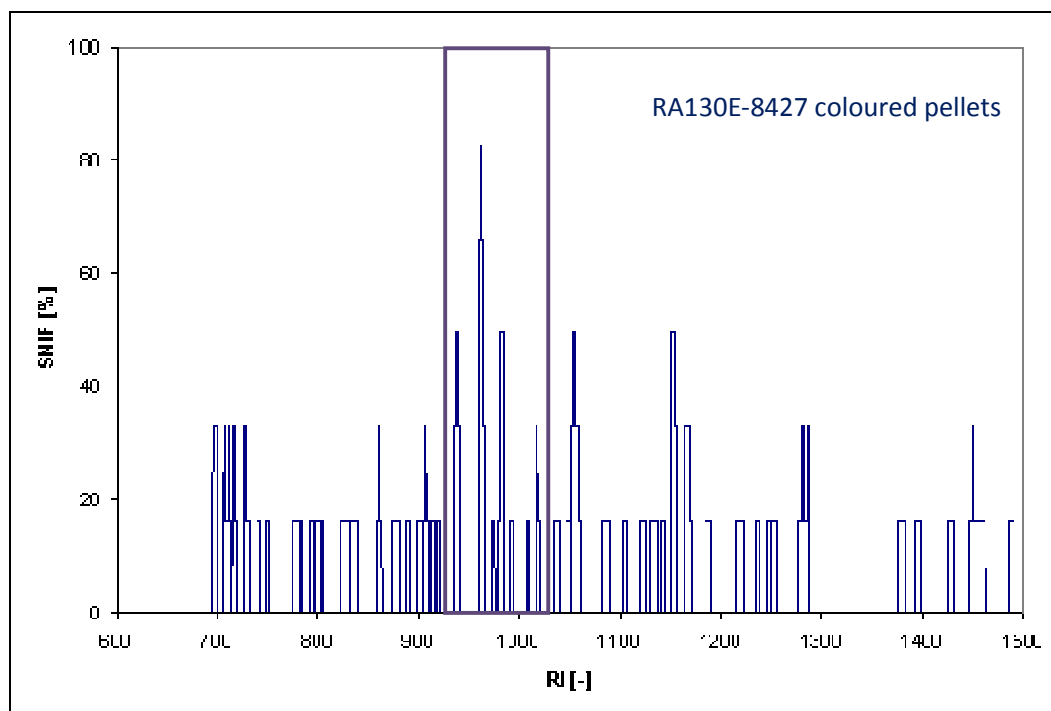


Figure 92. Detection Frequency (Total SNIF) diagrams of the coloured RA130E pellets (in blue) using the 2 g and the 500 mg GC-O results.

MasStat© analyses of the EE188HP samples gave a different picture (see Figure 93). As this material was already investigated in the first year in the screening of additives (section 4.5) we also analyzed injection moulded plaques besides the pellets and CMB. All pellets and plaques have the same history (i.e. storage time, lot number, ...).

An as clear linear effect by addition of the CMB as found in the RA130E samples was not observed for the EE188HP samples: It seems that the addition of the CMB and the injection moulding are running in opposite directions; injection moulding of the natural pellets moves the cluster of the natural plaques to the top left while for the coloured samples the inverse direction is found. Also, the differences between the coloured and non-coloured plaques are smaller than for the coloured and non-coloured pellets.

Comparing the HS-SPME-GC-MS chromatograms (see Figure 94) it is easy to see why the cluster looks like this: By addition of the CMB the number and the intensities of the peaks is dramatically reduced in the pellets. However, injection moulding of the coloured pellets diminish this effect and leads to a dramatic increase in the number and the amount of compounds ending with very similar chromatograms of coloured and natural plaques.

It seems that by addition of the CMB the emissions of the pellets are reduced, however, any further thermal treatment such as injection moulding completely destroys this effect and results in high emissions in the plaques.

MasStat© cluster differences are due to these compounds:

- pyrazines and methylpyrazines present only in the CMB
- aromatics (toluene, ethylbenzene, xylene) present in highest amounts in the natural pellets
- terpenes present only in the natural pellets and plaques

Comparing the total SNIF diagrams from the CMB and the natural EE188HP pellets (Figure 95) no significant differences could be identified which turn up also in the coloured pellets (Figure 96). For the coloured EE188HP-1048 no odour-active compounds coming only from the CMB could be identified. Comparing the CMB and the natural product similar odour pattern were found. No compound was detected by all panellists in both sample concentrations.

Those compounds with the highest SNIF values (66%) are:

- (E)-2-hexenal (RI 846) in the EE188HP natural pellets
- $\alpha$ -pinene (RI 938) in the EE188HP natural pellets
- 6-/8-nonenal in the CMB and the EE188HP-1048 coloured pellets
- unknown compound (RI 1340; described as sweet, intense, mouldy, dusty, warm elastomer) in the EE188HP-1048 coloured pellets

Based on the results from the two PP samples (RA130E and EE188HP) it is clear that (1) the CMB does influence the odour of the polyolefin product and (2) that the CMB either contributes with new odour-active compounds to the overall odour and/or increases the generation of odour-active compounds by influencing the thermal stability of the polymer or reacting with other species present in the polymer. For the RA130E sample it was possible to find odour-active compounds coming directly from the CMB; additionally, in the RA130E sample a linear relationship was found between the CMB, the natural and the coloured product.

In the EE188HP samples it was not possible to identify odour-active compounds coming only from the CMB, moreover, it seems that the CMB seems to have some kind of a suppressing effect in terms of emissions. Also, the odour pattern of the CMB and the natural polymer were very similar. For the EE188HP the natural polymer influences the odour of the coloured product mostly.

Based on these first results on the influence of CMBs on the odour of coloured products some questions arise and need to be addressed in the future:

- How do different CMBs contribute to the overall odour of coloured products?
- What are the ingredients of the CMBs?
- Which of those parts are responsible for the odour of the CMB? Which parts interact with the polymer and e.g. suppress the generation of emitting substances?
- Is it possible to extrapolate or estimate the overall odour of a coloured product when evaluating the odour of a CMB?

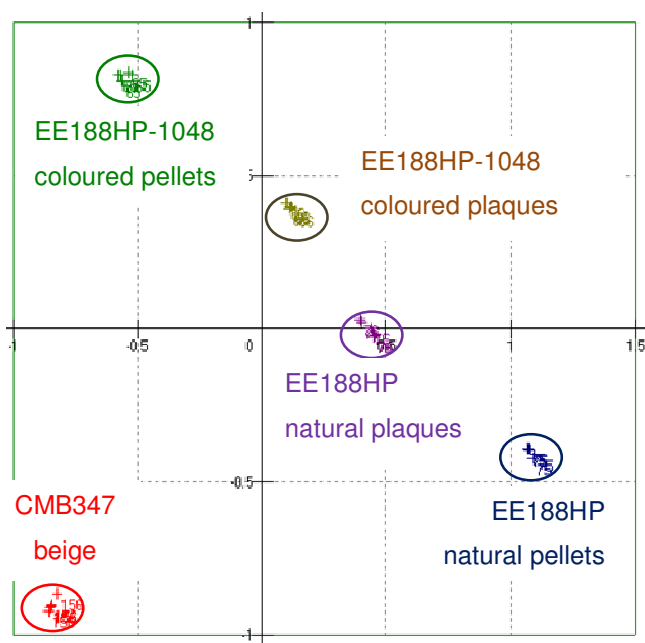


Figure 93. MasStat© cluster from the HS-SPME-GC-MS data of the coloured (EE188HP-1048), the non-coloured (EE188HP natural) and the CMB (CMB347 beige) pellet and plaque samples.

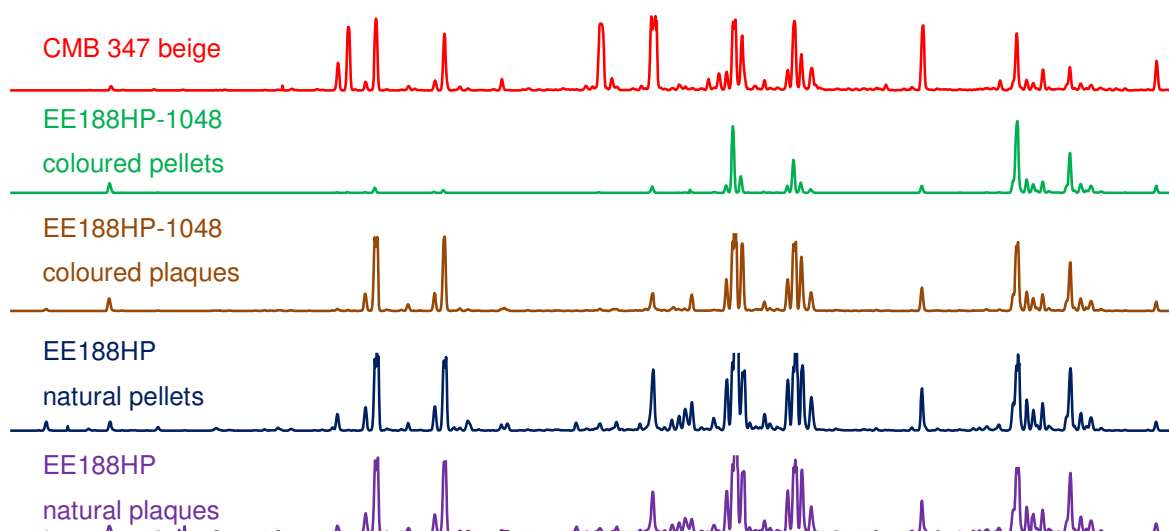


Figure 94. HS-SPME-GC-MS chromatograms of the coloured (EE188HP-1048), the non-coloured (EE188HP natural) and the CMB (CMB347 beige) pellets and plaque samples.

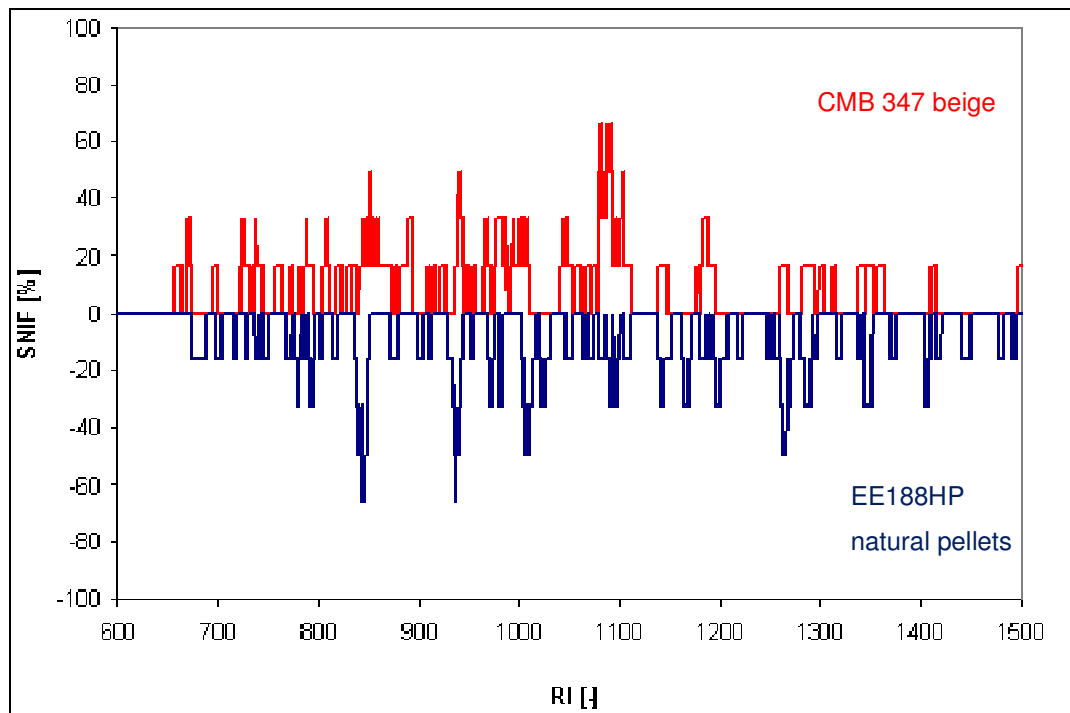


Figure 95. Detection Frequency (Total SNIF) diagrams of the CMB126 (in red) and the natural RA130E pellets (in brown) using the 2 g and the 500 mg GC-O results.

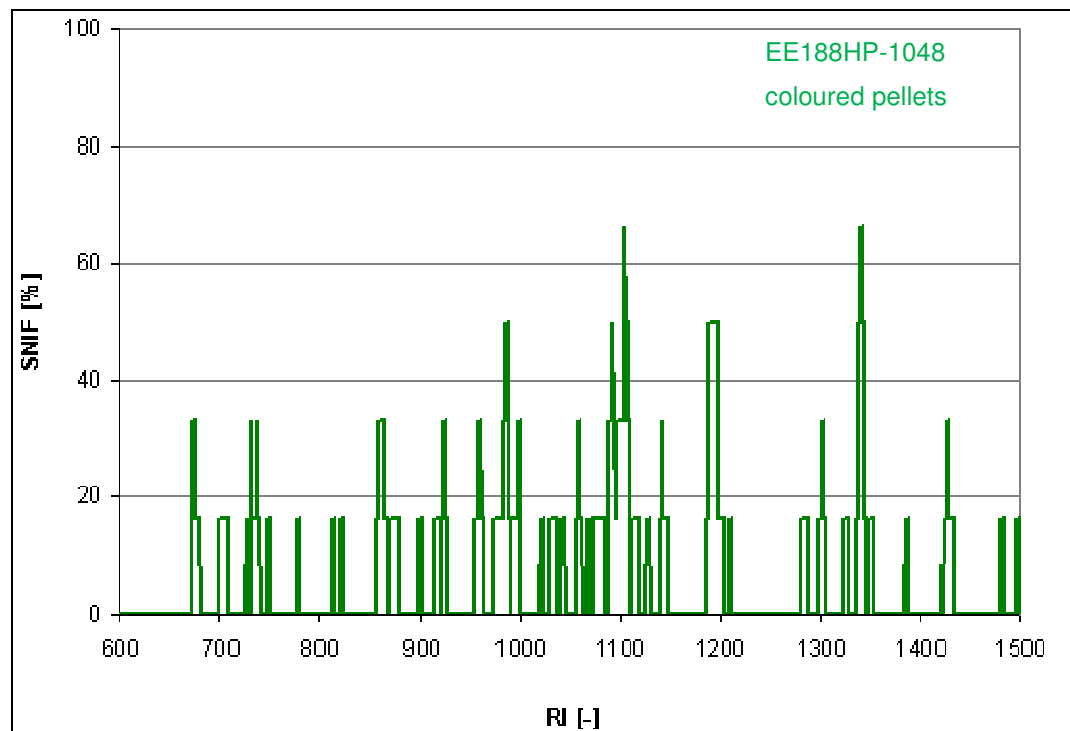


Figure 96. Detection Frequency (Total SNIF) diagrams of the coloured RA130E pellets (in blue) using the 2 g and the 500 mg GC-O results.

#### 4.12. Evaluation of the odour potential of Monomers

Looking at the process chain of polyolefins monomers at the beginning of the chain may also contribute to the overall odour of the polyolefin product.

In a master thesis by Edith Renöckl<sup>75</sup>, monomers (ethylene, propylene), comonomers (1-butene, 1-hexene) and diluents (propane) from different sources were screened for their odour potential applying HS-SPME-GC-MS and HS-SPME-GC-O.

In addition, after the thesis was finished some re-measurements were carried out applying the procedures as in the master thesis.

Propylene from Kallo sampled before (63001) and after dehydration (63103) used as purification was analyzed with HS-SPME-GC-MS and HS-SPME-GC-O. Air was sampled prior to filling in the lab in Linz to serve as blanks.

Due to difficulties with the originally used GC-MS system we switched another one with a different set-up as in Edith's work. We used an Agilent 7980 GC with a 5973 MS and an CTC CombiPal Autosampler. The used GC column was an HP-5-MS UI with 30mx0.25mm IDx0.25µm film thickness instead of the used 1µm film thickness in Edith's work.

However, as we ran all the samples on the same instrument and we only compare these samples to each other, this change in the set-up did not bother. Each sample was measured fivefold, the air only once.

For the comparison of the HS-SPME-GC-MS chromatograms (Figure 97) the sample with the highest number of peaks out of the five runs were taken. In Figure 98 we selected compounds which are contributing to the difference between samples 63001 and 63103. For each compound a selective m/z was selected, the area of the respective peak was integrated for all 5 runs and arithmetic mean and standard deviation were calculated.

Despite the huge deviation in sample amount, some aromatic compounds (toluene, phenol) are present in higher concentrations in the sample after the purification (63103) than in the one before (63001).

We were also able to detect some sulphur compounds by GC-MS such as dimethyl disulfide (higher conc. in 63103) and allyl propyl disulfide (present only in 63103).

---

<sup>75</sup> Renöckl E. (2010) *Monomer Purity concerning Odour and Taste*, Master Thesis, Graz University of Technology.

We extracted the  $m/z$  44, a typical  $m/z$  for the odour-active saturated aldehydes (Figure 99) to see that only a little to no effect of the purification on the concentration of the odour-active aldehydes was observed.

HS-SPME-GC with nitrogen sensitive detection and parallel PID detection was carried out and gave positive results for nitrogen compounds (Figure 100). However, the large peaks seen in the chromatogram originate from *n*-alkanes or siloxanes from the GC-column present in so high concentrations that the NPD also detects them. Those peaks are marked as “alkanes”.

For the remaining peaks some differences between the two samples can be observed. Peaks at 5.5 min and 8 min are only present in the 63001 sample.

Peaks at 5.4 min, 11.25 min and 14.4 min are present in both samples but in higher concentration in the 63103 sample.

The peak at 14.75 min is present in both samples but in higher concentration in the 63001 sample. Based on these NPD measurements the purification does seem to have an impact on nitrogen compounds.

HS-SPME-GC-O was carried out for analyzing the samples with one panellist. The resulting SNIF diagrams for both samples are shown in Figure 101.

In total, not many or strong odour-active compounds could be detected. In principal, the SNIF diagrams of both samples are similar except for the RI area around 1100 which gave a more intense odour impression in the 63103 sample as the odour lasts longer. This time area accounts to 6-/8-nonenal.

When comparing the SNIF diagrams to those obtained from the 1st monomer samples from Kallo shown in Figure 102, it can be seen that there were more and also more intense odour signals compared to the now evaluated samples 63001 and 63103.

Using the HS-SPME-GC-FID chromatogram in both “old” samples much more peaks are present while the propylene peak was bigger in the 2nd samples. Additionally, a so called “Ölberg” was observed only for the “old” samples. Based on this we assume that vials were equally filled and quality of Kallo monomer improved from the 1st to the 2nd measurements.

These measurements and the work of Renöckl prove that monomers do have an odour potential; however, it is not yet cleared if the odour-active compounds contribute to the odour of the polyolefins. As the in the monomer identified compounds are the same as those identified in the polyolefins, one can think of two possible ways: Either do these compounds survive the polymerization process or are destroyed and regenerated during the polymerization.

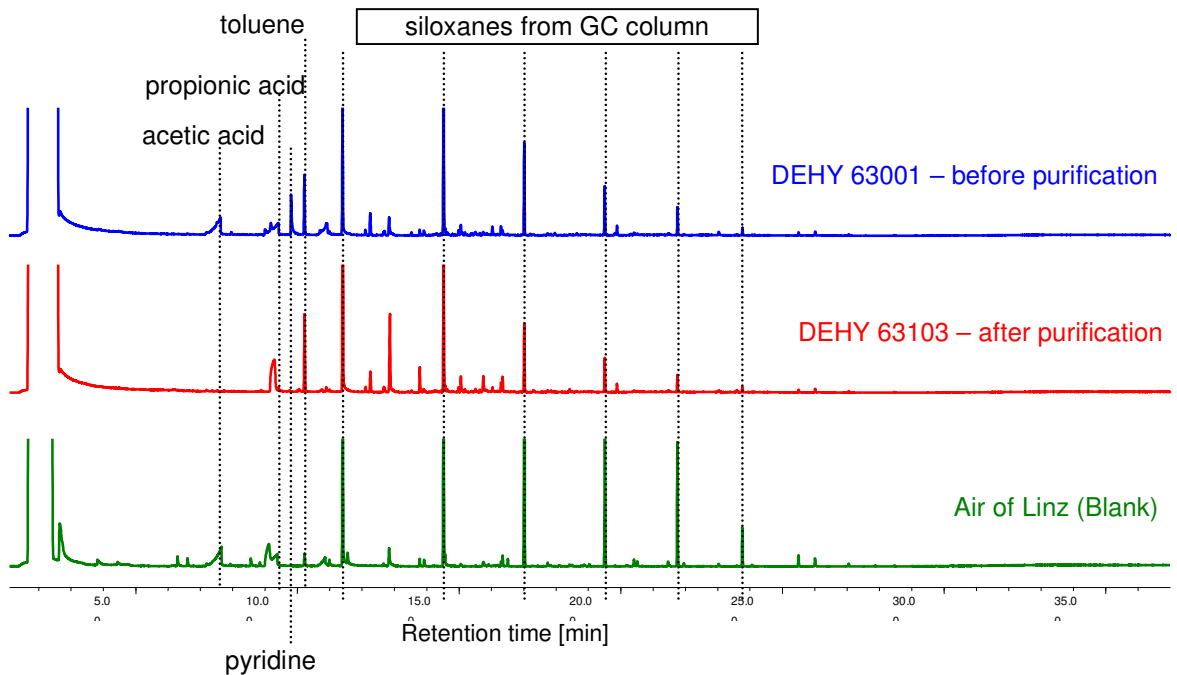


Figure 97. HS-SPME-GC-MS chromatograms of monomer sample 63001 (before purification) and 63103 (after purification) from Kallo and the air sample from Linz.

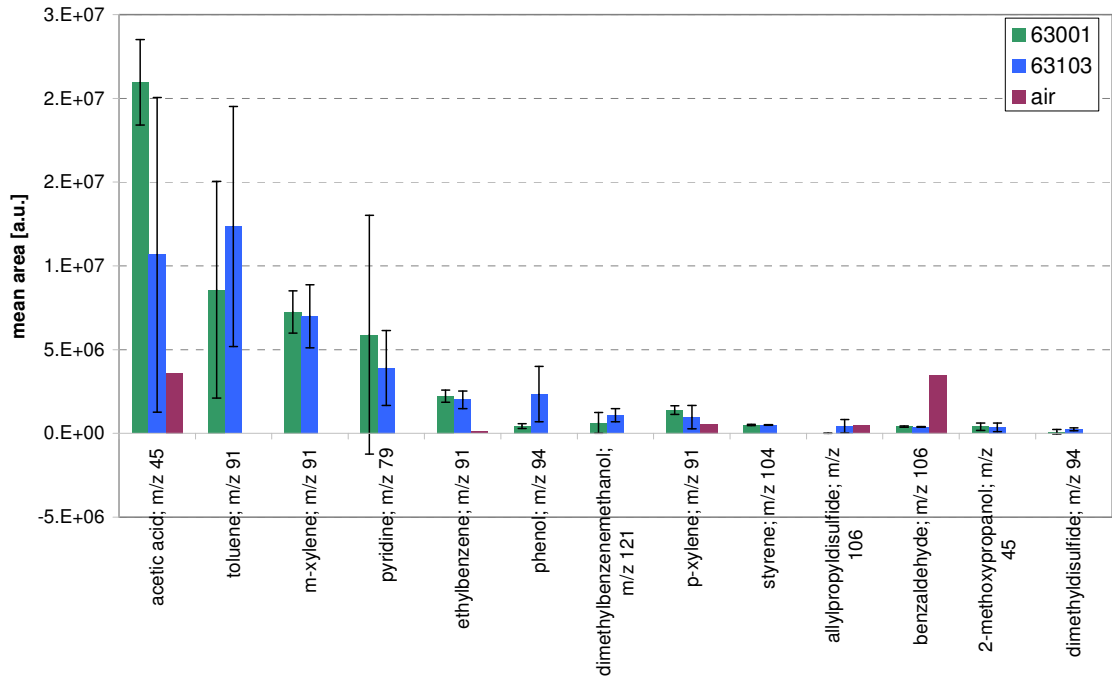


Figure 98. Mean areas and standard deviations for selected compounds calculated from 5 measurements for the 63001 and the 63103 samples.



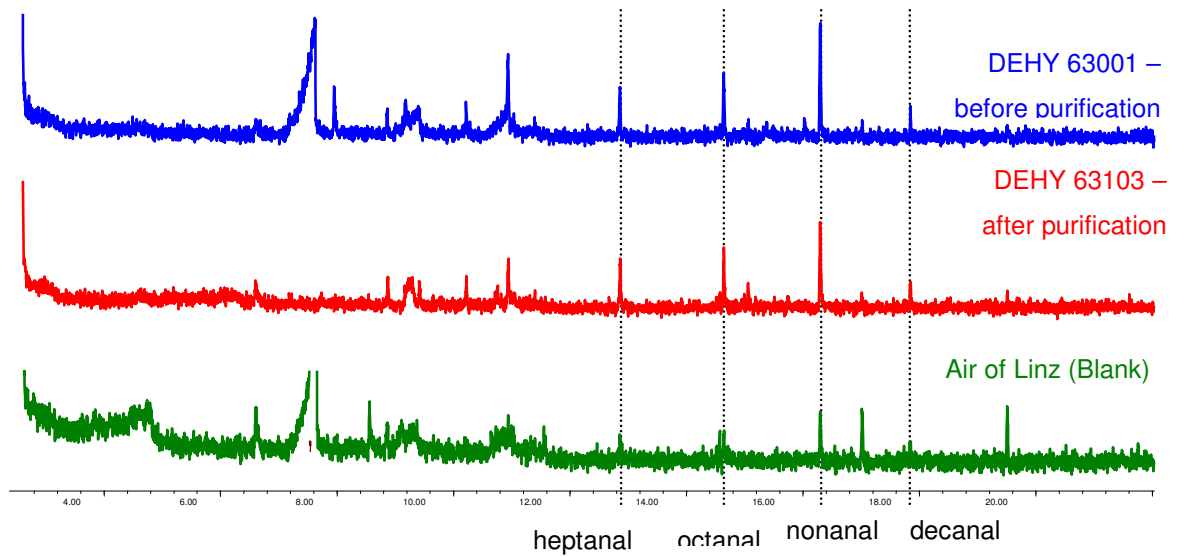


Figure 99. GC-MS measurements with extracted  $m/z$  44 typical for the odour-active saturated aldehydes for the 63001 and 63103 samples.

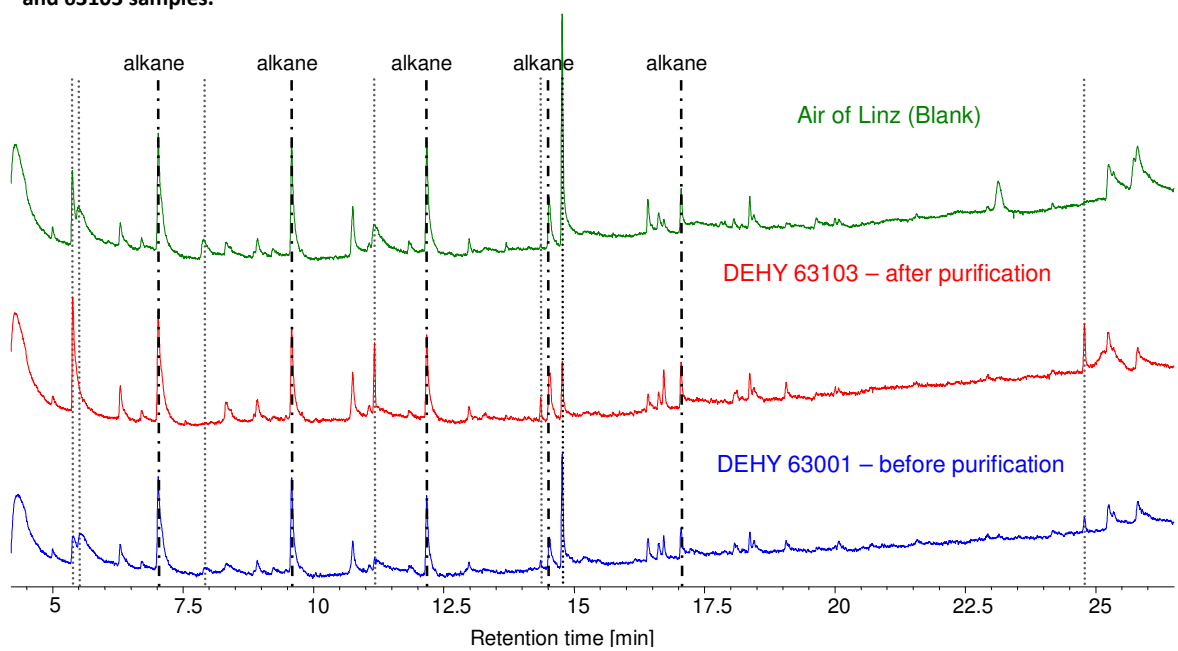


Figure 100. HS-SPME-GC-NPD chromatograms for the 63001 and 63103 samples.

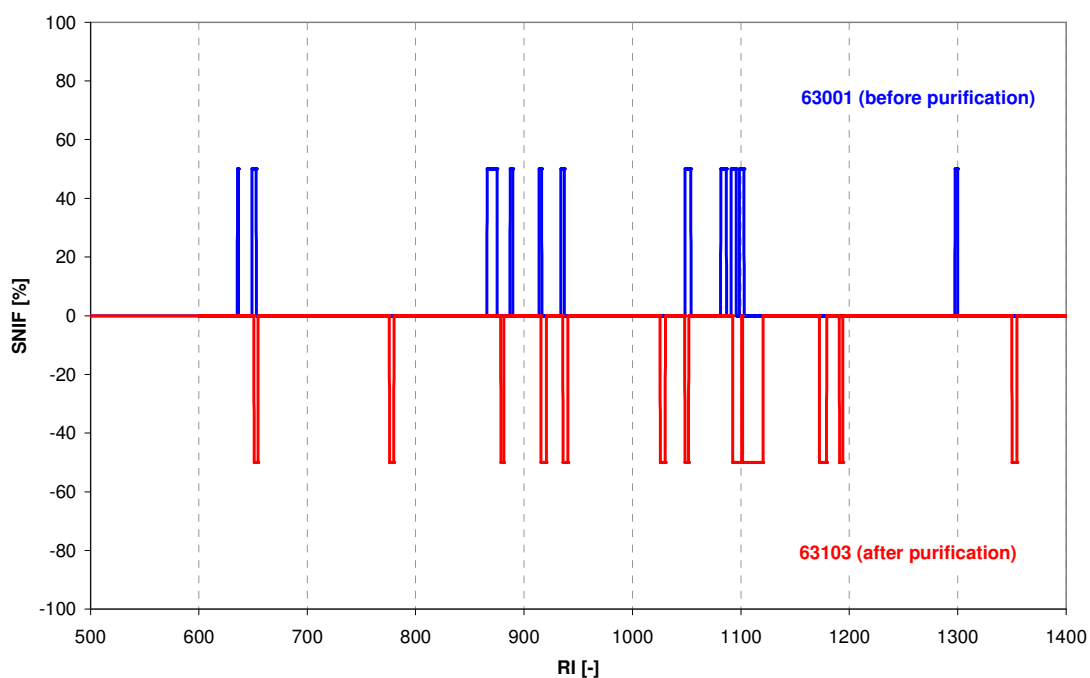


Figure 101. Detection Frequency (SNIF) diagram of the propylene monomer sample 63001 (before purification; in blue) and 63103 (after purification; in red) from Kallo.

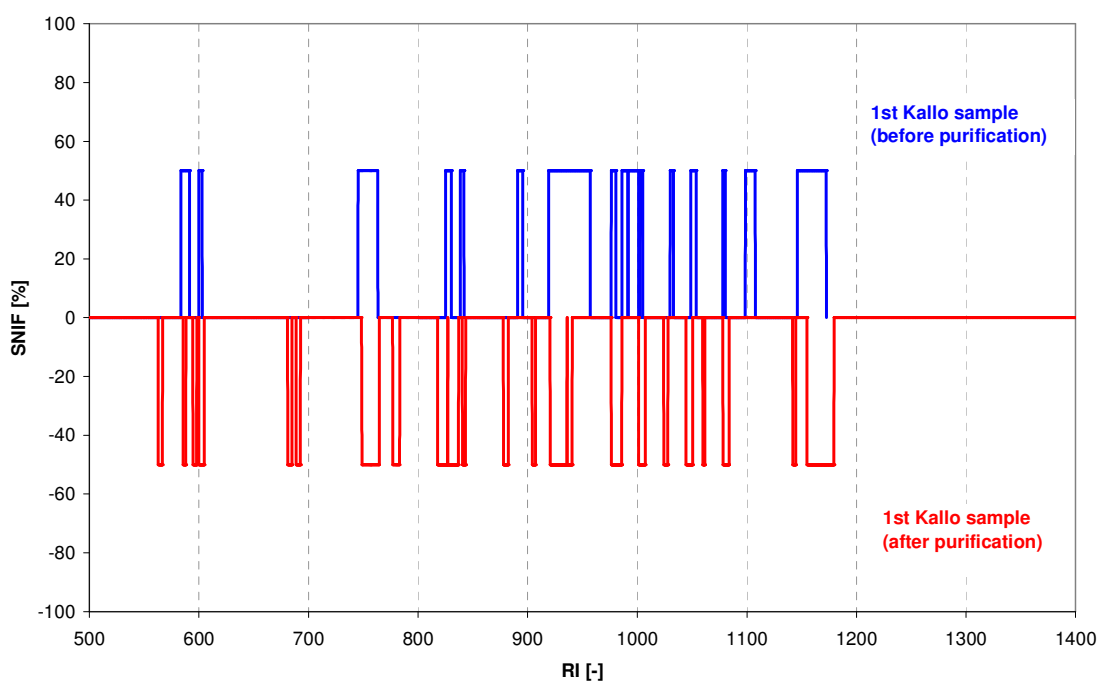


Figure 102. Detection Frequency (SNIF) diagram of the 1<sup>st</sup> propylene monomer sample before purification (in blue) and after purification (in red) from Kallo.

#### 4.13. 2-Acetyl-1-pyrroline in polyolefins

The odour of polyolefins is mostly composed of odour-active aldehydes and ketones. However, sometimes a highly odour-active compound described as “roasty, popcorn, cat-urine” was detected in the GC-O analyses and did not match with any known compound in the RI or odour quality.

Even in high diluted extracts the compound was still perceived and possible compounds were looked for in various data bases<sup>65-68</sup> based on the RI and the odour quality. The databases came up to the aromatic nitrogen compound 2-acetyl-1-pyrroline. This compound was previously identified in foods resulting from Maillard reactions in rice<sup>76</sup>, popcorn<sup>77</sup>, wheat and rye bread crusts<sup>78</sup> and cheddar cheese<sup>79</sup>, but also in tiger marking fluid<sup>80</sup> generated from enzymes.

A reference was synthesized according to Buechi<sup>81</sup> and Schieberle<sup>77</sup> and the unknown odour-active compound was positively identified as 2-acetyl-1-pyrroline.

This compound was detected either already in the pellets or in the injection moulded plaques indicating a thermal dependence of the formation:

- EE188AI-9524 and EE188AI-9530
- EE188HP-1048
- BE677AI
- EF015AE
- BF970MO
- ME3440
- FB2230
- BJ368MO

In the BJ368MO pellets and the injection moulded BJ368MO box labelled with an in-mould label from France a quantification of 2-acetyl-1-pyrroline by HS-SPME-GC-NPD applying a standard addition procedure<sup>54</sup> was carried out (see 3.3.f). In Table 26 the analytical parameter of the method are given, in Table 27 the concentrations are listed.

---

<sup>76</sup> Buttery R.G., Ling L.C., Juliano B.O., Turnbaugh J.G. (1983) *J. Agric. Food Chem.* 31:823-826.

<sup>77</sup> Schieberle P. (1991) *J. Agric. Food Chem.* 39:1141-1144.

<sup>78</sup> Schieberle P., Grosch W. (1985) *Z. Lebensm. Unters. Forsch.* 180:474-478.

<sup>79</sup> Avsar Y.K., Karagul-Yuceer Y., Drake M.A., Singh T.K., Yoon Y., Cadwallader K.R. (2004) *J. Dairy Sci.* 87: 1999-2010.

<sup>80</sup> Brahmachary R.L. (1996) *Curr. Sci.* 71:257-258.

<sup>81</sup> Büchi G., Wüest H. (1971) *J. Org. Chem.* 36:609-610.

**Table 26. Limits of Detection (LOD) and Limit of Quantification (LOQ) and the standard deviation of regression (SDR) for the 2-acetyl-1-pyrroline quantification with HS-SPME-GC-NPD and standard addition.**

	LOD [ng/kg]*	LOQ [ng/kg]	SDR [%]
2-acetyl-1-pyrroline	46.8	93.6	14.3

\* LOD/LOQ are calculated under consideration of 1g polyolefin sample.

**Table 27. 2-acetyl-1-pyrroline concentration in the BJ368MO pellets and the injection moulded box determined by standard addition and HS-SPME-GC-NPD (n=3).**

sample	2-acetyl-1-pyrroline concentration [ng/kg]
BJ368MO pellets	below LOD.
BJ368MO labelled and injection moulded box	119 ± 44

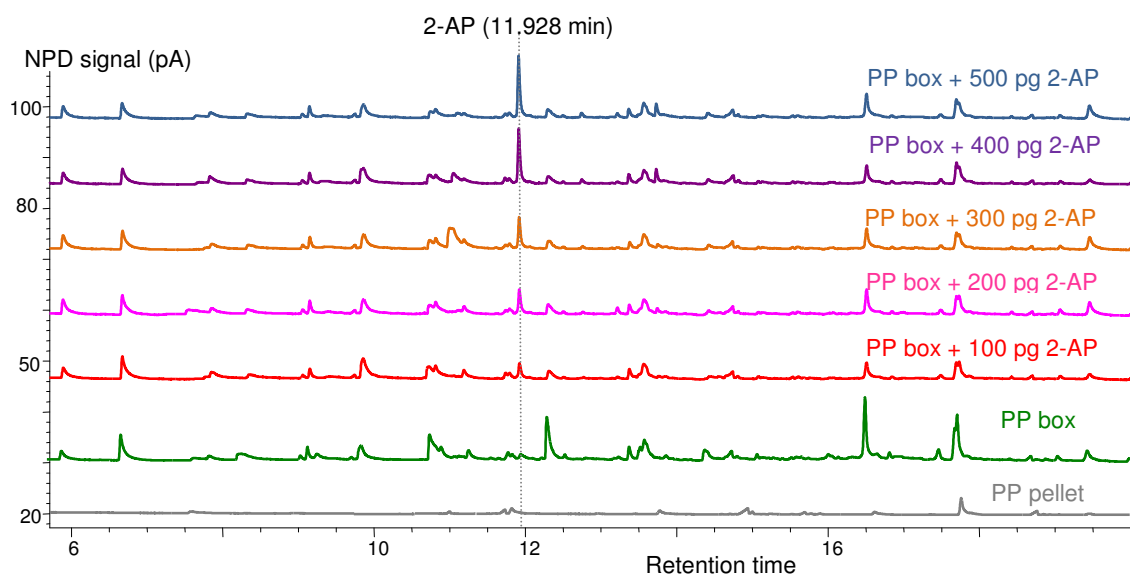


**Figure 103. HS-SPME-GC-NPD chromatograms of the PP pellet, the PP box and the standard addition samples.**

#### 4.14. BJ368MO claim

The business unit moulding had a customer claim for injection moulded BJ368MO boxes with in-mould labels concerning increased odour of the Borealis product compared to a competitor box.

The boxes having a strong popcorn-like odour and the corresponding pellets as well as the competitor's boxes arrived in Graz.

Additionally, test runs in Belgium with the same material but another label were done including volatile measurement during processing of the material. Last, we got additional pellets of Borealis internal test runs and plaques injection moulded at three temperatures (260, 280, 300°C). All samples were analyzed with HS-SPME-GC-MS and HS-SPME-GC-NPD, first samples were also analyzed with HS-SPME-GC-O. Additionally, processing was simulated by heating pellets for 10min at 200°C and 280°C and GC-MS analysis afterwards.

##### 4.14.a. Results of HS-SPME-GC-MS measurements

We ran HS-SPME-GC-MS analyses of all samples (5 repetitions) and analyzed the data with MasStat©. The cluster with all samples is shown in Figure 104.

A massive influence on the volatiles by the in-mould label (no BO175) can be seen for the labelled (no. BO173) and unlabelled (no BO172) boxes from Belgium. By analysis of the cluster the following conclusions were made:

- The application of an in-mould label has an impact on the number and concentration of volatiles. This can be seen by comparing the position of the labelled BJ368MO box (no. BO173) with that of the in-mould label (no. BO175) and that of the unlabelled BJ368MO box (no. BO172). The white colour MB (no. BO171a) does not have an impact on the volatile generation.
- Injection moulding of the pellets to the corresponding boxes moves the samples down to the left. This is outlined by comparing the BJ368MO pellets (no. BO168) with the unlabelled boxes (no. BO173) as well as comparing the 3 test run pellets (no. BO188, BO189, and BO190) with the produced plaques at various temperatures (no. BO179-BO187).
- Changing the MFR and/or leaving out the 1% talc does have an influence for the processed plaques, while no difference between the pellets can be seen (no. BO188-BO190) where the clusters fall together in one. With increasing injection moulding temperature differences become more prone esp. at 300°C plaques of sample 1 (no. BO181), which is

clearly separated from the other two samples. It can be assumed that changing the MFR by increasing  $H_2$  during polymerization to shorten chain length might also increase volatile generation at processing temperatures.

Observing the GC-MS data from the boxes made from BJ368MO and that made from the competitor's material in comparison to the pellets (BO168) reveals that BJ368MO seems to degrade more during processing (shown in Figure 105). The BJ368MO pellets have a small amount of volatiles, which is dramatically increased after injection moulding. The competitor material even with the in-mould label has a smaller number of peaks and also less intense peaks.

Air sampling around the injection moulding cavities with portable field samplers (PFS) from our institute was carried out in Belgium during the test runs for 45min during the runs with BJ368Mo and the competitor material.

A comparison between BJ368MO and the competitor material at the same cavity is shown in Figure 106. Much more volatiles can be found for BJ368MO, and also intensity of the peaks is higher.

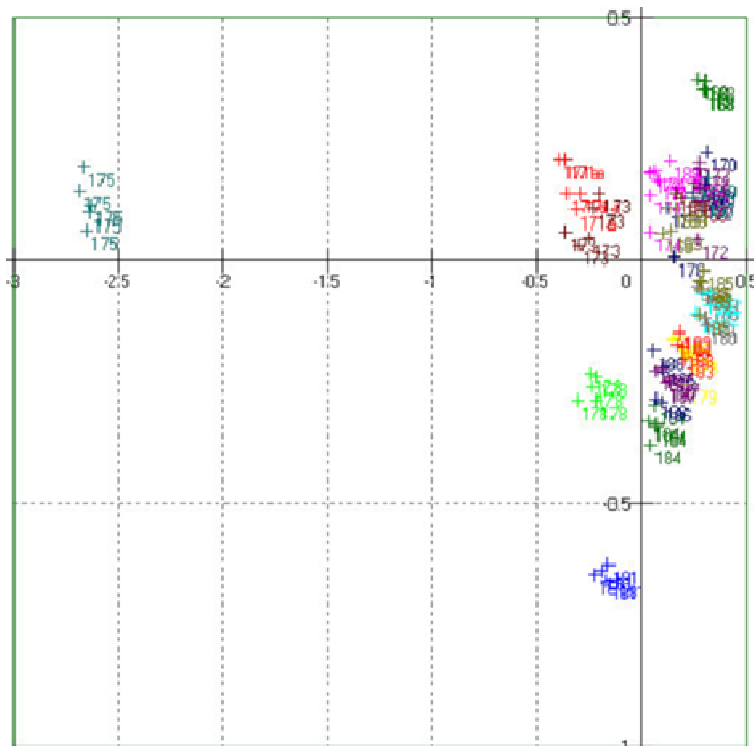


Figure 104. MasStat© cluster from all samples (labels as described in Table 3).

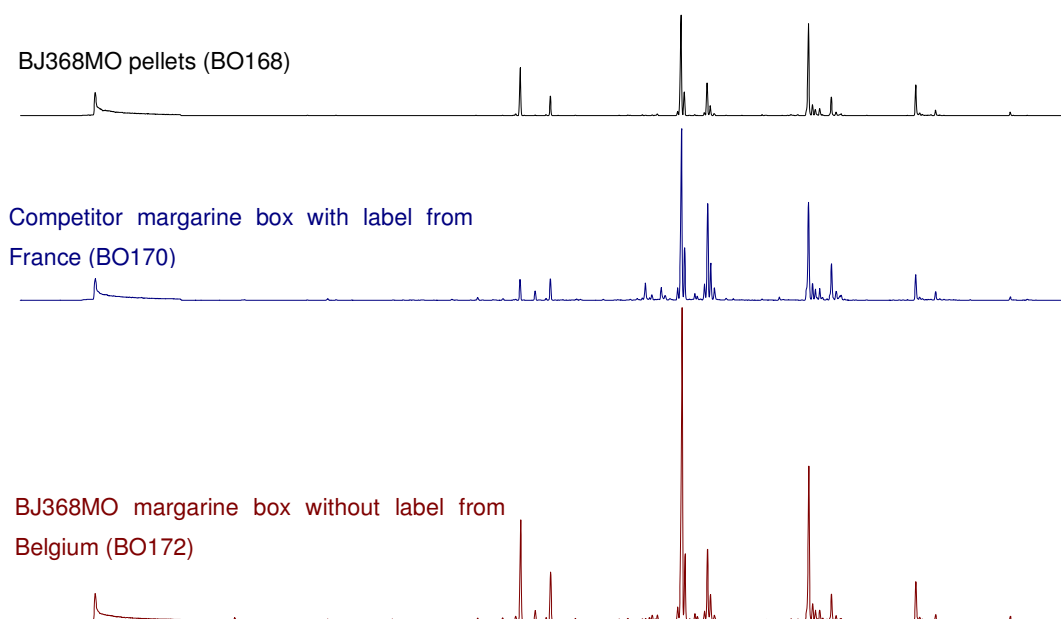


Figure 105. HS-SPME-GC-MS chromatograms of BJ368MO pellets (BO168) (in black), competitor box with label from France (BO170) (in blue) and BJ368MO box without label from Belgium (BO172) (in red).

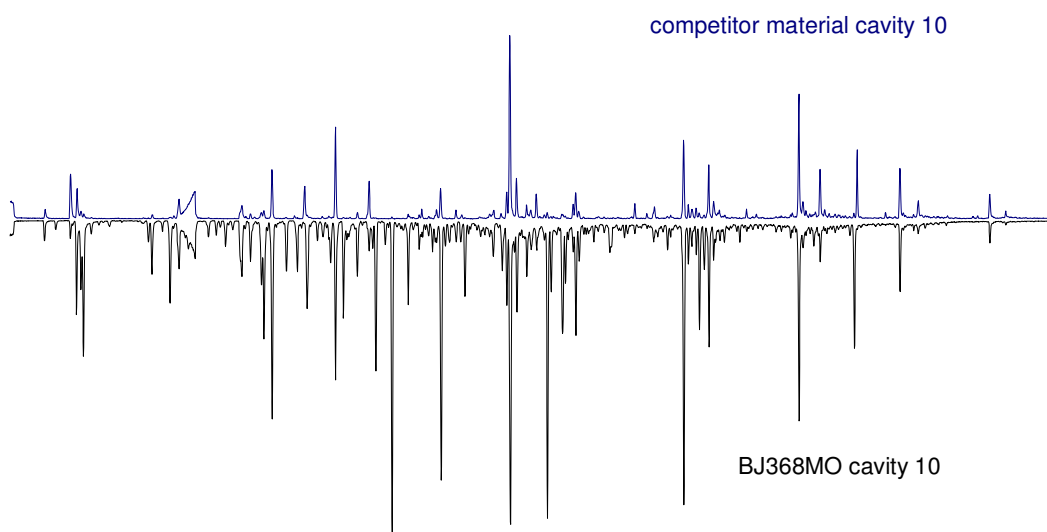


Figure 106. HS-SPME-GC-MS chromatograms of the air measurements during the injection moulding of the BJ368MO and the competitor material at cavity 10.

#### 4.14.b. Results of the HS-SPME-GC-O measurements

With HS-SPME-GC-O the BJ368MO pellets, the BJ368MO injection moulded and labelled box from France and the injection moulded and labelled competitor box from France were evaluated by two panellists (1 g sample in 20 mL headspace vials, with magnetic stir bar; 5 min thermostatising and 10 min extraction @40 °C to extract odour-active compounds on SPME fibre (DVB/CAR/PDMS)). In

Figure 107 a comparison of the SNIF diagrams of the BJ368MO pellets, the injection moulded and labelled BJ368MO boxes from France and the injection moulded and labelled competitor boxes from France are shown; the following conclusions can be drawn:

- For the BJ368MO pellets three major odour drivers (SNIF values of 100%) can be found, one of those is 2-acetyl-1-pyrroline (RT 6 min).
- For the BJ368MO margarine boxes from France 9 major odour-active compounds with SNIF values of 100% can be found with one compound showing a broad GC-O signal (= very intense odour) at RT 6 min retention time – 2-Acetylpyrroline.
- For the competitor margarine boxes from France (BO170) also 9 major odour-drivers detected with 100% can be found, again 2-acetyl-1-pyrroline but to a smaller extent.
- Injection moulding leads to an increase in number and intensity / concentration of odour-active compounds.
- Two differences in the odour profile between the two boxes can be found:
  - 2-acetyl-1-pyrroline at 6 min elutes in the BJ368MO box with a high odour intensity = high concentration, in the competitor boxes 2-acetyl-1-pyrroline is also present but to a much smaller extent.
  - 6-/8-Nonenal at 9 min turns up only in the Borealis material.

A quantification of the 2-acetyl-1-pyrroline was carried out by applying a standard addition procedure and HS-SPME-GC-NPD as described in 4.13.

Considering the obtained results it seems that the BJ368MO material is more sensitive to thermal oxidation than the competitor's material, although both materials show similar volatile pattern.

Again, leaving out the talc improves the emissions of the injection moulded plaques as was demonstrated with BJ368MO samples from test runs.

In contrast to that, it seems that changing the MFR by increasing  $H_2$  during polymerization to shorten chain length has a contrary effect on volatile generation at processing temperatures – especially at high  $T_M$  more volatiles were generated.



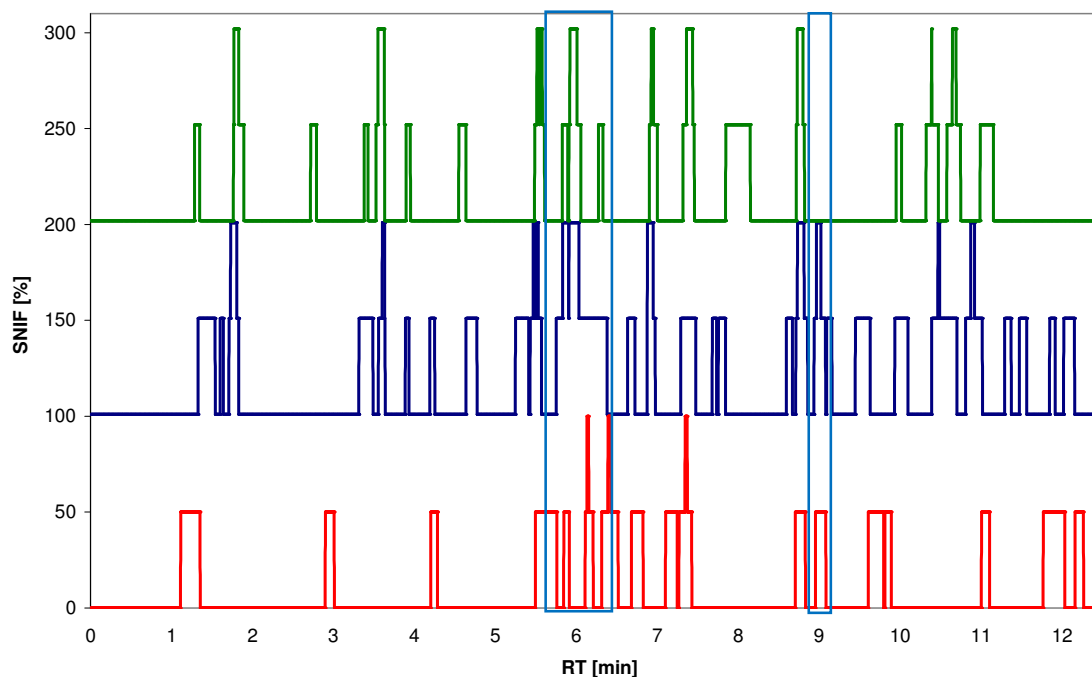


Figure 107. Detection Frequency (SNIF) diagrams of BJ368MO pellets (in red), BJ368MO injection moulded and labelled box from France (in blue) and the injection moulded and labelled competitor box from France (in green). Blue markings show differences in the odour pattern of the two boxes.

#### 4.15. The influence of the catalyst type - Metallocene-PP (m-PP) compared to conventional Ziegler-Natta-PP (ZN-PP)

A competitor PP produced with a metallocene catalyst instead of the conventional Ziegler-Natta type was evaluated in terms of odour.

Both the pellets and an injection moulded plaque were measured with HS-SPME-GC-MS and HS-SPME-GC-O; a similar PP from Borealis (EE188AI-9530) produced with the Ziegler-Natta catalyst was used as a reference.

In Figure 108 a SNIF comparison of the pellets and the plaques is given. Noteworthy is (1) the low odour intensity of the pellets (no compound with a SNIF value of 100%) and (2) the dramatic increase in the odour-active compounds with SNIF values of 100% after injection moulding (from 0 in the pellets to four in the plaques).

This trend is also observed with the HS-SPME-GC-MS data: When extracting the  $m/z$  44 a typical  $m/z$  for the odour-active saturated aldehydes (shown in Figure 109), it is easily seen that the amount of aldehydes after injection moulding is at least increased tenfold.

However, by comparing the HS-SPME-GC-MS chromatograms of the m-PP and the conventional ZN-PP, one is able to see the dramatic decrease in volatiles for the m-PP. Even if the amount of odour-active compounds is increased dramatically after injection moulding for the m-PP, the ZN-PP shows a higher amount of volatiles and odour-active compounds as shown in Figure 110.

The use of metallocene catalysts seems to be a significant step forward to the production of low emitting PP materials. However, the effect of injection moulding (i.e. increase in volatiles and odour-active compounds by thermal oxidation) is still present and needs to be addressed with other measures.

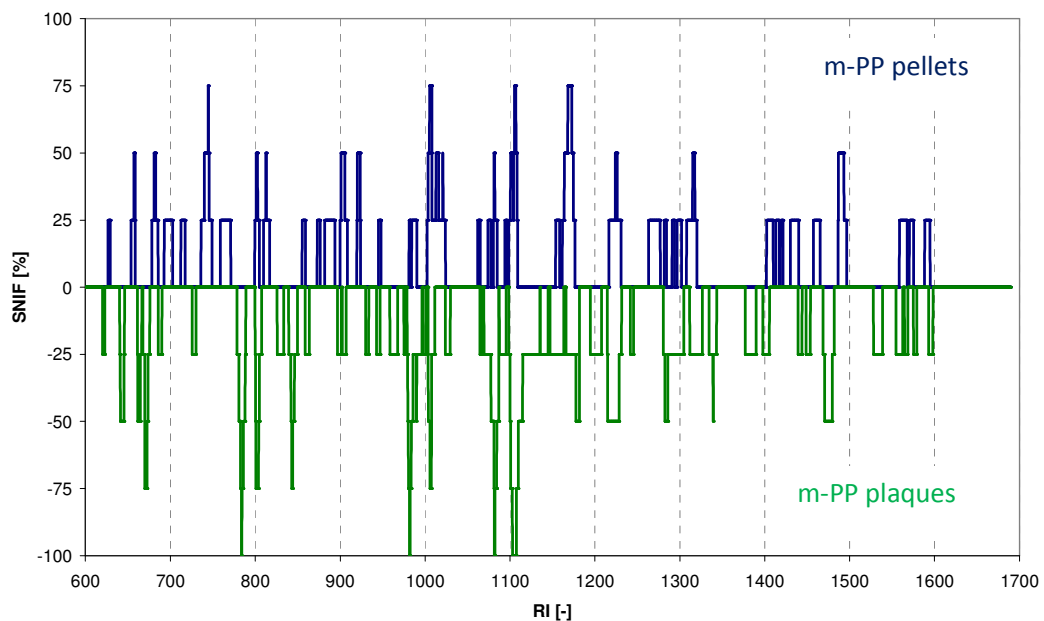


Figure 108. Detection Frequency (SNIF) diagram of the metallocene-PP (m-PP) pellets (in blue on top) and plaques (in green, at the bottom).

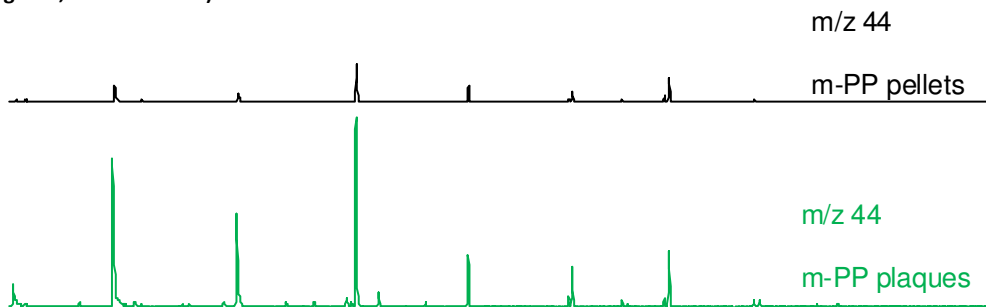


Figure 109. Extracted HS-SPME-GC-MS chromatogram with the  $m/z$  of 44, a typical  $m/z$  for saturated aldehydes of the metallocene-PP (m-PP) pellets (in black, on top) and plaques (in green, at the bottom).

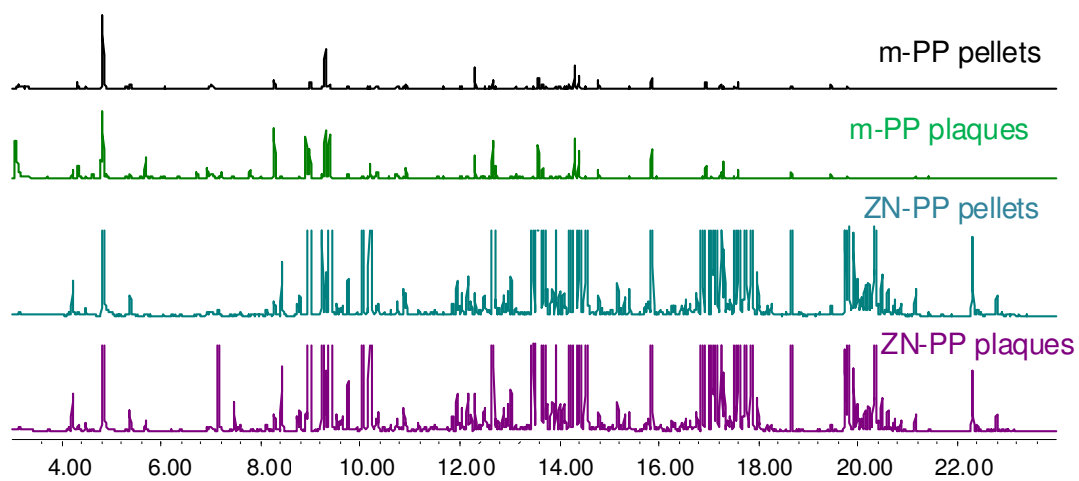


Figure 110. HS-SPME-GC-MS chromatograms of the metallocene-PP (m-PP) pellets (in black) and plaques (in green) compared to the Ziegler-Natta PP (ZN-PP) EE188AI-9530 pellets (in turquoise) and plaques (in lilac). .

## 5. Conclusion and Outlook

### 5.1. Identified odour-active compounds detected in PE and PP samples

In all investigated grades similar odour-active compounds could be detected.

Mainly aldehydes and ketones were identified as major odour contributors due to their low sensory thresholds which were also determined by the sensory panel in the lower and sub- $\mu\text{g}$  per kg range.

Especially carbonyls with 6 to 10 C-atoms could be detected with a high frequency; among these substances the unsaturated aliphatic aldehydes (E)-2-alkenals and the unsaturated aliphatic ketones 1-alken-3-ones were the most important ones including

- (E)-2-nonenal
- (E)-6-nonenal
- (Z)-6-nonenal
- 8-nonenal
- (E)-2-decenal
- 1-hexen-3-one
- 1-octen-3-one
- 1-nonen-3-one
- 2,3-butandione
- 2,3-pentandione

Regardless whether the investigated sample was a PE or a PP, the mentioned compounds were detected.

Comparing these compounds with those found in the literature (see Table 2) one is able to see that they match in most parts.

However, due to the majority of publications deal only with PE, in this work (E)-2-octenal, (E)-2-nonenal, 8-nonenal, 2,3-pentandione and 1-hexen-3-one were identified in PP for the first time.

The latter two compounds were also identified in PE-HD for the first time.

### 5.2. The influence of processing on the generation of odour-active compounds – Is an odour evaluation on pellets valid for the judgement of processed parts?

Processing such as injection moulding is a major influencing factor for the generation of odour-active compounds. In all investigations where pellets and injection moulded plaques were

analyzed a higher number of and more intense odour-active compounds were detected in the processed samples.

Based on these evaluations and separate investigations carried out on stabilized and unstabilized PE and PP materials autoxidation processes seem to take place leading to the increase in odour-active oxidation products such as aldehydes and ketones. It was observed that the investigated PP material was more affected by the oxidation than the investigated PE. This might result from the higher susceptibility of PP to oxidation in general.

Besides these carbonyls, other compounds such as 2-acetyl-1-pyrroline and the unknown substance from the talc and phenolic antioxidant interaction are present in higher amounts after injection moulding indicating as well a temperature-driven reaction.

Different degrees of autoxidation were observed depending on the polymer formulation (e.g. compound PP with high additivation compared to a PE pipe grade).

### **5.3. The influence of processing locations on the generation of odour-active compounds – Is there a typical plant smell?**

Various grades available from different plants were screened for the presence of a typical „plant smell“, i.e. identification of odour-active compounds specific for a plant / polymerization site / compounding site.

Three grades with at least two different origins were investigated (EE188AI from Schwechat and Beringen, FB2230 from Schwechat PE4 and Porvoo PE2, ME3440 from Porvoo PE2, Stenungsund PE3 and Borouge).

To summarize, there are differences in between the same grade from different plants. In all three screened grades similar odour-active compounds were detected including saturated and unsaturated aldehydes and ketones and the aromatic nitrogen compound 2-acetyl-1-pyrroline.

Of all three materials the compound PP EE188AI showed the highest number and amounts of odour-active compounds coming from (a) the use of different PE and PPs and additives in the formulation and (b) the additional compounding step inducing further thermally and mechanically induced oxidation.

Although different odour patterns of the PE and PP samples were obtained one is not able to specify typical compounds for PE or PP, mostly due to the low number of screened grades and therefore the lack of representativeness.

Although the methyl side chain in the PP should contribute to the generation of other types of oxidation compounds, these compounds were not exclusively identified.

Most probably this can be explained by (1) the use of both PE and PP in the investigated polyolefins and (2) the higher sensory threshold values for these methylated compounds compared to the thresholds of the mentioned substances.

#### **5.4. The influence of additives on the generation of odour-active compounds – What do talc, UV stabilization and colour contribute to the odour?**

In a screening program a compound PP containing numerous additives was analyzed for odour-active compounds originating from different additives. Here, talc, phenolic antioxidants and the colour masterbatch showed a massive impact on the generation of odour-active compounds by (a) an increase in odour-active oxidation products coming from the polymer and by (b) formation of new odour-active species coming most probably from the degradation of the additives and/or interactions between the additive and the polymer.

For the combination of talc and phenolic antioxidants the odour is dramatically increased by formation of one major odour contributor which is not yet identified. However, it is believed that this compound originates from the degradation of the phenolic antioxidants in the presence of talc.

Evaluations on stabilized and unstabilized PE and PP materials showed that the used additives are able to prevent the polymer from heavy degradation; however, the stabilizers are not able to prevent the formation of odour-active oxidation compounds during processing.

#### **5.5. The influence of the catalyst on the generation of odour-active compounds – What does 2-ethyl-1-hexanol contribute to the odour?**

The use of the new catalyst RCL50P leads to a massive increase in the 2-ethyl-1-hexanol concentration compared to the use of the old catalyst (BCF02P) by at least an order of 20. For the RCL50P samples concentrations of 2-ethyl-1-hexanol in the range of 3.5 mg/kg were determined with GC-MS and external calibration. For the BCF02P samples the concentrations were below 0.05 mg/kg.

No significant differences in the 2-ethyl-1-hexanol concentrations between the visbroken and non-visbroken samples neither with the new nor with the old catalyst were found.

The odour threshold of 2-ethyl-1-hexanol was determined with 1-2 mg/kg with GC-O using dilution analysis of fraction II until two panellists perceived no odour anymore.

Although the amount of 2-ethyl-1-hexanol is dramatically increased by the use of the new catalyst RCL50P, the odour contribution is not significantly increased due to the rather high odour threshold of 1-2 mg/kg which is in the range of the determined concentration of 3.5 mg/kg.

#### **5.6. The influence of visbreaking on the generation of odour-active compounds – Do peroxides always smell bad?**

The investigation of two different peroxide systems in two PP materials showed that the increased odour ratings of visbroken grades are originating (a) from an increase in odour-active degradation products coming from the polymer initiated by the peroxides and (b) from new species generated during the peroxide decomposition.

Although both peroxide systems showed diverse decomposition species, with no system it was possible to achieve as low odour values as with the non-visbroken grade.

#### **5.7. The crux with measuring “nothing” – How well do different methods measure the things we want to know?**

Analysis of odour-active compounds is not easy and despite a time-consuming and extensive sample preparation procedure it is for example still not possible to quantify the highly odour-active (E)-2-alkenales and 1-alken-3-ones with conventional GC systems, although they are clearly detected by the human nose.

For realising lower detection limits more sensitive detection systems are needed.

Second, often the needed information is highly interfered, and applying multivariate data analysis (MVDA) can help to filter all this data and get the essence out of it. It was shown that for trends and correlations the used HS-SPME-GC-MS procedure followed by multivariate data analysis (MVDA) can be applied to gain information about the contribution of various additives on the emissions of PP polymer in an easy and reliable way.

MVDA seems to be a valuable tool also for quality control issues as proposed with the HS-SPME-GC-PID system.

However, the gained information is still only qualitative. Even with high separation power provided by modern one-dimensional GC columns co-elution is happening.

For solving the problem of co-elution and interferences a higher degree of separation is needed.

There are systems on the market which can do both; using multi-dimensional GC (MDGC) or comprehensive GC in combination with a high resolution MS system such as time-of-flight (TOF) MS one is able to dramatically increase both the sensitivity and the selectivity. This is realised by coupling two GC columns of orthogonal behaviour. So, in the first column (also called first dimension) the analytes are separated e.g. according to their boiling points when using a non-polar column, and before going into the detector the analytes are separated in the second column (also called second dimension) e.g. according to their polarity when using a polar column.

MDGC and comprehensive GC are of enormous importance for material development and research, however, these systems are costly and require a lot of time and care. In most cases relative and qualitative answers are sufficient for ? as these information is easier and faster to obtain and to understand as MDGC and comprehensive GC data.



## References

- [1] Plastics Europe (2009): *The Compelling Facts About Plastics 2009 - An analysis of European plastics production, demand and recovery for 2008*. Available on [www.plasticseurope.org](http://www.plasticseurope.org). Accessed 12/14/2009.
- [2] Buck L.B., Axel R. (1991) *A novel multigene family may encode odorant receptors: A molecular basis for odor recognition*, Cell 65:175–187.
- [3] Vosshall L.B. (2004) *Olfaction: Attracting both sperm and the nose*, Curr. Biol. 14:R918-920.
- [4] Spehr M., Schwane K., Heilmann S., Gisselmann G., Hummel T., Hatt H. (2004) *Dual capacity of a human olfactory receptor*, Curr. Biol. 14:R832-833.
- [5] Starckenmann C., Le Calve B., Niclass Y., Cayeux I., Beccucci S., Troccaz M. (2008) *Olfactory Perception of Cysteine–S-Conjugates from Fruits and Vegetables*, J. Agric. Food Chem. 56:9575-9580.
- [6] ASTM E679 - 04 (2004) *Standard Practice for Determination of Odor and Taste Thresholds By a Forced-Choice Ascending Concentration Series Method of Limits*.
- [7] Brydson J.A. (1999) *Plastics Materials: 7th edition*, Elsevier Butterworth-Heinemann, Oxford, UK.
- [8] Oberbach K. (2001) *Saechtling Kunststoff Taschenbuch*, 28th edition, Hanser, Munich, Germany.
- [9] Imuta J.-I., Kashiwa N. (2000) *Recent Progress on single-site catalysts* in: Handbook of polyolefins (Vasile C., ed.) Marcel Dekker, New York, USA, 71-88.
- [10] Maier C., Haber T. (1998) *Polypropylene: The Definitive User's Guide and Databook* (Plastics Design Library), William Andrew, Norwich, USA.
- [11] Schneider B., Duskocilova D. (2000) *Structures of polyolefins*, in: Handbook of polyolefins (Vasile C., ed.) Marcel Dekker, New York, USA, 161-222.
- [12] Barret J., Gijsman P., Swagten J., Lange R.F.M. (2002) *A molecular study towards the interaction of phenolic anti-oxidants, aromatic amines and HALS stabilizers in a thermo-oxidative ageing process*, Polym. Degrad. Stab. 76:441–448.
- [13] Bertin D., Boutevin B., Rigal G., Fourty G. (1998) *Study of talc-additive interactions by combined TGA-FTIR system*, Eur. Polym. J. 34:163-170.
- [14] Sauer C. (2007) *Interaction of talc and phenolic antioxidants with respect to volatiles and odour*, Internal Technical report, Borealis Polyolefine GmbH.

- [15] Epacher E., Tolveth J., Kröhnke C., Pukansky B. (2000) *Processing stability of high density polyethylene: effect of absorbed and dissolved oxygen*, Polymer 41:8401-8409.
- [16] Andersson T., Stalbon B., Wesslen B. (2004) *Degradation of polyethylene during extrusion. II. Degradation of low-density polyethylene, linear low-density polyethylene and high-density polyethylene in film extrusion*, J. Appl. Polym. Sci. 91:1525-1537.
- [17] Tüdös F., Iring M. (1988) *Polyolefine oxidation: Rates and products*, Acta Polymerica 39:19-26.
- [18] Albertsson A.-C., Gröning M., Hakkarainen M. (2006) *Emission of volatiles from polymers – a new approach for understanding polymer degradation*, J. Polym. Environ. 14:9-13.
- [19] Bernstein R., Thornberg S.M., Assink R.A., Irwin A.N., Hochrein J.M., Brown J.R., Derzon D.K., Klamo S.B., Clough R.L. (2007) *The origins of volatile oxidation products in the thermal degradation of polypropylene, identified by selective isotopic labeling*, Polym. Degrad. Stab. 92:2076-2094.
- [20] Hoff A., Jacobsson S. (1981) *Thermo-Oxidative Degradation of Low-Density Polyethylene Close to Industrial Processing Conditions*, J. Appl. Polym. Sci. 26:3409-3423.
- [21] Frank H.P. (1976) *Some oxidation characteristics of polypropylene*, J. Polym. Sci. Symp. 57:311-318.
- [22] Hoff A., Jacobssen S. (1982) *Thermal Oxidation of Polypropylene Close to Industrial Processing Conditions*, J. Appl. Polym. Sci. 27:2539-2551.
- [23] Richaud E., Farcas F., Fayolle B., Audouin L., Verdu J. (2007) *Hydroperoxide build-up in the thermal oxidation of polypropylene- A kinetic study*, Polym. Degrad. Stab. 92:118-124.
- [24] Piringer O., Rüter M. (2000) *Sensory problems caused by food and packaging interactions in: Plastic Packaging Materials for Food* (Piringer O., Baner A.L., ed.), 407-426, Wiley-VCH, Weinheim, Germany.
- [25] Villberg K., Veijanen A. (2001) *Analysis of a GC/MS thermal desorption system with simultaneous sniffing for determination of off-odor compounds and VOCs in fumes formed during extrusion coating of low-density polyethylene*, Anal. Chem. 73:971-977.
- [26] Bravo A., Hotchkiss J.H., Acree T.E. (1992) *Identification of odor-active compounds resulting from thermal oxidation of PE*, J. Agric. Food Chem. 40:1881-1885.
- [27] Tyapkova O., Czerny M., Buettner A. (2009) *Characterization of flavour compounds formed by  $\gamma$ -irradiation of polypropylene*, Polym. Degrad. Stab. 94:757-769.
- [28] Villberg K., Veijanen A., Gustafsson I., Wickström K. (1997) *Analysis of odour and taste problems in high-density polyethylene*, J. Chromatogr., A 791:213-219.
- [29] Rebeyrolle-Bernard P., Etievant P. (1993) *Volatile compounds extracted from PP sheets by hot water: influence of temperature of sheets injection*, J. Appl. Polym. Sci. 49:1159-1164.

- [30] Skjervak I., Due A., Gjerstad K.O., Herikstad H. (2003) *Volatile organic components migrating from plastic pipes (HDPE, PEX, PVC) into drinking water*, Water Res 37:1912-1920.
- [31] Sanders R.A., Zyzak D.V., Morsch T.R., Zimmerman S.P., Searles P.M., Srothers M.A., Eberhart B.L., Woo A.K. (2005) *Identification of 8-Nonenal as an important contributor to "plastic" off-odor in PE packaging*, J. Agric. Food Chem. 53:1713-1716.
- [32] van Gemert L.J. (2003) *Compilations of odour threshold values in air, water and other media*; Oliemans Punter & Partner BV, Utrecht, The Netherlands.
- [33] Kovats E. (1958) *Gas-chromatographische Charakterisierung organischer Verbindungen. Teil 1: Retentionsindices aliphatischer Halogenide, Alkohole, Aldehyde und Ketone*, Helv. Chim. Acta 41:1915-1920.
- [34] Dool H, Kratz P.(1963) *A generalization of the retention index system including linear temperature programmed gas-liquid partition chromatography*, J Chromatogr. 11:463-471.
- [35] Farkas P., Le Quere J.L, Maarse H., Kovac M. (1994) *The standard GC retention index library of flavour compounds*, in: Maarse H., van der Heij D.G. (ed.), Trends in Flavour Research, Elsevier Science B.V., The Netherlands, 145-149.
- [36] Molyneux R.J., Schieberle P. (2007) *Compound Identification: A Journal of Agricultural and Food Chemistry Perspective*, J. Agric. Food Chem. 55:4625-4629.
- [37] Chaintreau A. (2001) *Simultaneous distillation-extraction: from birth to maturity*, Flav. Frag. 16:136-138.
- [38] Veith G.D., Kiwus L.M. (1977) *An exhaustive steam-distillation and solvent-extraction unit for pesticides and industrial chemicals*, Bull. Environ. Contam. Toxicol. 17:631-636.
- [39] Likens S.T., Nickerson G.B. (1964) *Detection of certain hop oil constituents in brewing products*, Am. Soc. Brew. Chem. Proc., 5-13.
- [40] Filek G., Bergamini M., Lindner W. (1995) *Steam distillation-solvent extraction, a selective sample enrichment technique for the gas chromatographic-electron-capture detection of organochlorine compounds in milk powder and other milk products*, J. Chromatogr., A, 712:355-364.
- [41] Repnegg F. (2001) *Geruchsaktive Verbindungen in Polyolefinen*, Dissertation Graz University of Technology.
- [42] Supelco (2009) *Normal Phase Solid Phase Extraction*, <http://www.sigmaaldrich.com/analytical-chromatography/sample-preparation/spe/normalphase-methodology.html> .accessed 01/12/2010.
- [43] Siegmund B. (1997) *Untersuchung und Optimierung der Aromaeigenschaften eines Convenience-Food Produkts*, Dissertation Graz University of Technology.

- [44] Pawliszyn J. (1997) *Solid Phase Microextraction Theory and Practise*, Wiley-VCH, New York, USA.
- [45] Supelco (2009) Product information, <http://www.sigmaaldrich.com/analytical-chromatography/analytical-products.html?TablePage=18156565>. Accessed 01/12/2010.
- [46] Supelco Technical note T397136A (1997) *Reduce Inlet Liner ID for Sharper Peaks by SPME/GC*, available on [www.sigmaaldrich.com](http://www.sigmaaldrich.com). Accessed 01/12/2010,
- [47] Knapp D.R. (1979) *Handbook of Analytical Derivatization reactions*, Wiley-Interscience, New York, USA.
- [48] Wood K.V., Schmidt C.E., Cooks R.G., Batts B.D. (1984) *Identification of Partially Hydrogenated Nitrogen-Containing Polycyclic Aromatic Hydrocarbons in Coal Liquids by Tandem Mass Spectrometry*, *Anal. Chem.* 56:1335-1338.
- [49] Schmarr H.G., Potouridis T., Ganß S., Sang W., Köpp B., Bokuz U., Fischer U. (2008) *Analysis of carbonyl compounds via HS SPME with onfibre derivatization and GC ion trap tandem mass spectrometric determination of their O-(2,3,4,5,6-pentafluorobenzyl)oxime derivatives*, *Anal. Chim. Acta* 617:119–131.
- [50] Hopfer, H.; Haar, N.; Koraimann C., Leitner, E. (2009) *Derivatization of odour-active carbonyls in trace amounts for determination with GC and various detectors* in: Food for the future – the contribution of chemistry to improvement of food quality (Sørensen H., Sørensen S., Sørensen A.D., Sørensen J.C., Andersen K.E., Bjerregaard C., Møller P.) Proceedings of the EURO FOOD CHEM XV, Copenhagen, University of Copenhagen: Copenhagen (2009) 100 – 103.
- [51] Tamura H., Shibamoto T. (1991) *Factors affecting cyclization of alkenal-N-methylhydrazones used for trace aldehyde determination*, *Anal Chim Acta* 248:619-623.
- [52] Agilent Technologies Inc. (2008) J&W GC Column Selection Guide.
- [53] Agilent Technologies Inc (2008) NEW Agilent J&W Ultra Inert Capillary GC Columns.
- [54] Hopfer H., Schrampf E., Leitner E. (2010) *Maillard Reactions in Polyolefins? - Identification of the odor-active Maillard product 2-Acetyl-1-pyrroline in polypropylene (PP)*, *J. Chromatogr., A.*, submitted.
- [55] Wegscheider W., Rohrer C., Neuböck R. (1997) *Validata - Excel 97 Makro zur Methodvalidierung*, Version 3.02.48.
- [56] Funk W., Damman V., Donnevert G. (1992) *Qualitätssicherung in der Analytischen Chemie*, VCH, Weinheim, Germany.
- [57] DIN 32645 (1994) *Chemical analysis - Decision limit, detection limit and determination limit under repeatability conditions - Terms, methods, evaluation*.

- [58] DIN 53383-2:1983-06 (1983) *Testing of plastics; testing of oxidation stability by means of ageing in an oven; polyethylene of high density (PE-HD), infra red spectroscopic (IR) determination of the carbonyl content.*
- [59] Kessler W. (2007) *Multivariate Datenanalyse für die Pharma-, Bio- und Prozessanalytik*, Wiley-VCH, Weinheim, Germany.
- [60] DIN 10961:1996-08 (1996) *Training of assessors for sensory analysis.*
- [61] O'Mahony M. (1995) *Who told you the triangle test was simple?*, Food Qual. Prefer. 6:227–238.
- [62] Pollien P., Ott A., Montigon F., Baumgartner M., Munoz-Box R., Chaintreau A. (1997) *Hyphenated headspace-gas chromatography-sniffing technique: Screening of impact odorants and quantitative aromagram comparisons* J. Agric. Food Chem.45:2630-2637.
- [63] Grosch W. (1994) *Review: Determination of potent odourants in foods by aroma extract dilution analysis (AEVA) and calculation of odour activity values (OAVs)*, Flav. Fragr. 9:147-158.
- [64] Linssen J.P.H., Janssens J.L.G.M., Roozen J.P., Posthumus M.A. (1993) *Combined gas chromatography and sniffing port analysis of volatile compounds of mineral water packed in polyethylene laminated packages*, Food Chem. 46:367-371.
- [65] Acree T., Arn H.(2004) *Flavornet and human odor space*, www.flavornet.org. Accessed 08/28/2009.
- [66] Mottram R., *The LRI and Odour Database*, www.odour.org.uk. Accessed 08/28/2009.
- [67] El-Sayed A.M. (2009) *The Pherobase: Database of Insect Pheromones and Semiochemicals*, [www.pherobase.com](http://www.pherobase.com). Accessed 08/28/2009.
- [68] Farkaš P., Sádecká J., Leitner E., Siegmund B., Petka J. (2001 ) *SKAF flavour database.*
- [69] CITAC/Eurachem Guide (2002) *Guide to Quality in Analytical Chemistry*, available on <http://www.eurachem.org/guides/CITAC%20EURACHEM%20GUIDE.pdf>. Accessed 12/19/2009.
- [70] Product data sheet Borstar © FB2230 (2008) Borealis AG, Vienna.
- [71] Product data sheet BorSafe™ ME3440 (2008) Borealis AG, Vienna.
- [72] Product data sheet Bormod™ BF970MO (2008) Borealis AG, Vienna.
- [73] Product data sheet Daplen™ EE188AI (2008) Borealis AG, Vienna.
- [74] Verband der Automobilindustrie, 1995, VDA 277 - *Nichtmetallische Werkstoffe der KFZ Innenausstattung-Bestimmung der Emission organischer Verbindungen.*

- 
- [75] Renöckl E. (2010) *Monomer Purity concerning Odour and Taste*, Master Thesis, Graz University of Technology.
- [76] Buttery R.G., Ling L.C., Juliano B.O., Turnbaugh J.G. (1983) *Cooked rice aroma and 2-acetyl-1-pyrroline*, J. Agric. Food Chem. 31:823-826.
- [77] Schieberle P. (1991) *Primary odorants in popcorn*, J. Agric. Food Chem. 39:1141-1144.
- [78] Schieberle P., Grosch W. (1985) *Identification of the volatile flavour compounds of wheat bread crust — comparison with rye bread crust*, Z. Lebensm. Unters. Forsch. 180:474-478.
- [79] Avsar Y.K., Karagul-Yuceer Y., Drake M.A., Singh T.K., Yoon Y., Cadwallader K.R. (2004) *Characterization of nutty flavour in cheddar cheese*, J. Dairy Sci. 87: 1999-2010.
- [80] Brahmachary R.L. (1996) *The expanding world of 2-acetyl-1-pyrroline*, Curr. Sci. 71:257-258.
- [81] Büchi G., Wüest H. (1971) *Synthesis of 2-acetyl-1,4,5,6-tetrahydropyridine, a constituent of bread aroma*, J. Org. Chem. 36:609-610.

## Appendix

### Retention indices

Compound	RI (HP-5)	RI (DB-WAX) <sup>(68)</sup>
2,3-butandione	596 <sup>(27)</sup>	981.7
pentanal	697.4 <sup>(68)</sup>	
2,3-pentandione	716 <sup>(27)</sup>	
3-penten-2-one	734.0 <sup>(68)</sup>	1126.9
4-methylcyclohexene	737	
(E)-2-pentenal	759.4	1129.4
1-Hexen-3-one	770.1	1103.6
(Z)-3-hexenal	788.1	1141.3
hexanal	790.6	1985.2
2-methyl-2-pentenal	823.3	1158.7
(E)-2-hexenal	849.5 <sup>(68)</sup>	1219.4
2-methyl-3-furanthiol	855.8	
1-Hepten-3-one	872.4	1204.1
heptanal	898.0	1188.7
methional	902.1	1456.0
(E,E)-2,4-hexadienal	907.2	1403.2
2-acetyl-1-pyrroline	926.0	
3-hepten-2-one	934.4	1303.9
(E)-2-heptenal	954.8	1325.2
1-Heptanol	968.4	1469.0
benzaldehyde	971.0	1520.9
1-octen-3-one	977.1	1306.5
octanal	1002.3	1293.0
(E,E)-2,4-heptadienal	1010.4	1494.5
2-ethylhexanol	1028.6	1503.1
3-octen-2-one	1039.2	1410.8
$\gamma$ -hexalactone		1698.8

(E)-2-octenal	1058.7	1431.2
1-nonen-3-one	1079.7	1409.4
furaneol	1087.4	2043.3
o-cresol	1092	
(E)-6-nonenal	1095.1	
(E)-4-nonenal	1096.0	1442.9
8-nonenal	1096.5	
(Z)-6-nonenal	1101.2	1454.4
nonanal	1104.6	1397.7
(E,E)-2,4-octadienal	1110.3	1590.8
3-nonen-2-one	1139.9 <sup>(68)</sup>	1515.3
$\gamma$ -heptalactone	1152.7	1800.0
(E)-2-nonenal	1161.4	1537.6
(Z)-4-decenal	1197.3	1544.4
decanal	1206.8	1502.9
(E,E)-2,4-nonadienal	1215.9	1702.5
$\gamma$ -octalactone	1258.8	1914.7
(E)-2-decenal	1264.1	1646.1
undecanal	1308.8	1608.6
(E,E)-2,4-decadienal	1319.4	1812.0
methyl anthranilate	1346.5	2240.0
$\gamma$ -nonalactone	1364.1 <sup>(68)</sup>	2028.3
(E)-2-undecenal	1366.5	1754.5
1-dodecen-3-one	1383	1724.9
$\delta$ -nonalactone	1392.7	2080.8
dodecanal	1409.7	1714.7
(E,E)-2,4-undecadienal	1423.1	1921.3
(E)-2-dodecenal	1467.6	1863.3
tridecanal	1511.7 <sup>(68)</sup>	1821.2



## Publications during PhD

### Peer-reviewed papers and proceedings

Hopfer, H., Schrampf, E.; Leitner, E. (2010) *Maillard Reactions in Polyolefins? - Identification of the odor-active Maillard product 2-Acetyl-1-pyrroline in polypropylene (PP)*, J. Chromatogr., A, submitted.

Hopfer, H.; Renöckl, E.; Stockreiter, W.; Sauer, C.; Leitner, E. (2010) *A rapid and simple screening method for polyolefin monomers*, Polym. Degrad. Stab., submitted.

Hopfer, H.; Sauer, C.; Haar, N.; Leitner, E. (2010) *Comparison of different analytical methods for volatile and odour-active substances in polyolefins*, Macromol. Symp., submitted.

Hopfer, H.; Haar, N.; Leitner, E.: *Analytical method for identification of odour-active compounds in polyolefins* - in: Expression of Multidisciplinary Flavour Science (Blank I., Wüst M., Yeretian C., eds.) Proceedings of the 12th Weurman Flavour Research Symposium, Interlaken; Zurich University: Zurich (2010) 561-564.

Hopfer, H.; Haar, N.; Koraimann C., Leitner, E.: *Derivatization of odour-active carbonyls in trace amounts for determination with GC and various detectors* – in: Food for the future – the contribution of chemistry to improvement of food quality (Sørensen H., Sørensen S., Sørensen A.D., Sørensen J.C., Andersen K.E., Bjerregaard C., Møller P.) Proceedings of the EURO FOOD CHEM XV, Copenhagen, University of Copenhagen: Copenhagen (2009) 100 – 103.

Hopfer, H.; Haar, N.; Leitner, E.: *Geruchsaktive Verbindungen in Polyethylen - Eine analytische Herausforderung* - in: Tagungsband Österreichische Lebensmittelchemietage 2008. (2008) 359 – 364.

### Talks

Hopfer, H.: *Odour of polyolefins* - in: DocDay – NAWI Graz Doctoral School Molecular Biosciences and Biotechnology, Graz, 03.07.2009.

Hopfer, H.: *Convenience Products* - in: 13. Österreichische Chemietage 2009, Wien, 24.08.2009.

Leitner, E.; Hopfer, H.: *Die Zusatzkomponente von GC-MS: Derivatisierung* - in: 26. Forum Analytik, Wien, 10.02.2009.

Hopfer, H.; Leitner, E.: *Identification and Determination of Off-Flavours in Water* - in: 12. Österreichische Chemietage 2007 - . Klagenfurt, 10.09.2007.

Hopfer, H.: *Odour-active substances in polyolefins* – in: 7th PhD Student Forum of the Key Research Area Life Science Technology, Graz University of Technology, Graz, 12.2007.

Hopfer, H.; Leitner, E.: *Methodik zur Bestimmung geruchsaktiver Verbindungen in Polyolefinen* - in: 3. ASAC JunganalytikerInnen Forum, Linz, 01.06.2007.

Hopfer, H.: *Technologie polymerbasierender Lebensmittelverpackungen* - in: Spezielle Kapitel der Lebensmittelchemie und -technologie II, Graz, 15.11.2006.

#### **Poster presentations**

Hopfer, H.; Leitner, E.: *Maillard reactions in polyolefins?* – in: HTC'11 Hyphenated Techniques in Chromatography. Bruges, Belgium, 2010.

Hopfer, H.; Sauer, C.; Haar, N.; Leitner, E.: *Comparison of different analytical methods for volatile and odour-active substances in polyolefins* – in: EPF'09 European Polymer Congress. Graz, Austria, 2009.

Hopfer, H.; Haar, N.; Koraimann, C.; Leitner, E.: *Derivatization of odour-active carbonyls in trace amounts for determination with GC and various detectors* – in: EURO FOOD CHEM XV, Copenhagen, Denmark, 2009.

Hopfer, H.; Haar, N.; Leitner, E.: *Analytical method for identification of odour-active compounds in polyolefins* - in: 12th Weurman Flavour Research Symposium. Interlaken, Switzerland, 2008.

Hopfer, H.; Haar, N.; Leitner, E.: *Geruchsaktive Verbindungen in Polyethylen - Eine analytische Herausforderung* - in: Österreichische Lebensmittelchemikertage 2008. Eisenstadt, Austria, 2008.

Hopfer, H.; Leitner, E.: *Evaluation of odorous compounds in a polyethylene food packaging material by Simultaneous Water Distillation/Extraction (SDE) and Solid Phase Micro Extraction (SPME)* - in: 3rd International Symposium on Recent Advances in Food Analysis. Prag, Czech Republic, 2007.

## Curriculum Vitae

### Personal Data

Name	Helene Hopfer
Date of birth	July, the 14 <sup>th</sup> , 1982
Place of birth	Graz
Nationality	Austria
Address	Niederschöcklstraße 66, A-8044 Weinitzen
Email	helene.hopfer@gmx.at

### Education

09/2006 – 03/2010	PhD thesis at the Institute of Analytical Chemistry and Food Chemistry, Graz University of Technology, “Identification of odour-active compounds in polyolefins”
06 – 07/2006	summer course <i>IIWE 2006 Women Engineers: Pushing for Sustainability</i> , EPF Ecole d’Ingénieurs Paris, France
06/29/2006	Final Examination; Master’s degree (M.Sc.) in Polymer Science and Engineering (passed with distinction)
11/2005 – 05/2006	Diploma thesis at the Institute for Chemistry of Polymers, University of Leoben, “Stabilization of UHMWE-PE with $\alpha$ -tocopherol below the melting point”
01/2005 – 06/2005	ERASMUS exchange semester at the Tampereen Teknillinen Yliopisto, Finland
12/15/2004	2 <sup>nd</sup> Diploma examination in Polymer Science and Engineering (equivalent to a BSc)
01/29/2003	1 <sup>st</sup> Diploma examination in Polymer Science and Engineering
2001 - 2006	Master studies in “Polymer Science and Engineering” at the University of Leoben.
2000 - 2001	Master studies in “Industrial Environmental Protection” at the University of Leoben.
1992 - 2000	High School, BG und BRG Kirchengasse, Graz
1989 - 1992	Elementary School, VS Weinitzen

**Research experience**

- 06 – 08/2005 IAESTE internship at the Queen Mary University London, UK, *New keratoprosthesis materials based on hydroxyapatite layered polymers.*
- 2002 - 2004 student worker at the Institute of Materials Science and Testing of Plastics, University of Leoben
- 07 – 08/2004 internship at DOW Europe GmbH, Horgen, Switzerland, *Noise reduction of adult diapers*
- 07 – 08/2003 internship at Roche Diagnostics, Near Patient Testing, Graz, Austria, *Materials Testing of plastics used in blood analyzer instruments*
- 07 – 08/2002 internship at the Joanneum Research, Institute for Polymer Engineering, Leoben, *Fracture mechanical characterization of PVDF films*

**Language and Other skills**

- Languages English (fluent), Italian (basic), Finnish (basic)
- PC skills MS Office, Agilent Chemstation, Java, Unscrambler, Matlab, Autocad

**Grants**

- 2009 GÖCH travel grant
- 2008 Weurman Symposium 2008 Scholarship
- 2008 GÖCH travel grant 2008